

Efficient valorization of biomass to biofuels with bifunctional solid catalytic materials



Hu Li ^{a,b,d}, Zhen Fang ^{a,d,*}, Richard L. Smith Jr. ^c, Song Yang ^b

^a Biomass Group, College of Engineering, Nanjing Agricultural University, 40 Dianjiangtai Road, Nanjing, Jiangsu 210031, China

^b State-Local Joint Engineering Laboratory for Comprehensive Utilization of Biomass, Center for R&D of Fine Chemicals, Guizhou University, Guiyang 550025, China

^c Research Center of Supercritical Fluid Technology, Graduate School of Environmental Studies, Tohoku University, Aramaki Aza Aoba 6-6-11, Aoba-ku, Sendai 980 8579, Japan

^d Chinese Academy of Sciences, Biomass Group, Key Laboratory of Tropical Plant Resources and Sustainable Use, Xishuangbanna Tropical Botanical Garden, 88 Xuefulu, Kunming, Yunnan Province 650223, China

ARTICLE INFO

Article history:

Received 29 July 2015

Accepted 20 April 2016

Available online 17 May 2016

Keywords:

Lignocellulose

Catalyst design

Catalysis

One-pot reaction

Platform chemicals

Nanotechnology

ABSTRACT

Mono-functional catalytic materials are used for many types of chemical transformations, but are tedious for delivering products from multiple-step reactions required for the valorization of biomass. An emerging trend is to integrate catalytic transformations, reaction engineering and product separation into a single operation, wherein catalyst design is considered as the key approach to develop efficient, low energy and environmentally-friendly reaction systems. Bifunctional solid catalysts open a door for carrying out domino/cascade- and tandem/sequential-type reactions in a single pot, for which the number of isolation or purification steps can be lessened or eliminated so that removal of unwanted by-products becomes unnecessary. This review introduces bifunctional materials used in one-pot multiple transformations of biomass into biofuels and related chemicals. Emphasis is placed on the assessment of the bifunctionality of catalytic materials, including Bronsted–Lewis acid, acid–base, and metal particles–acid or base bifunctional catalysts with some discussion being on combined catalytic systems with electrochemical, chemo-enzymatic and photochemical methods. Plausible reaction mechanisms for key pathways are shown. Relevant auxiliaries to boost catalytic activity and product selectivity, such as reaction media, heating modes and morphological properties of the catalytic materials are analyzed. Use of appropriate bifunctional catalytic materials provides many opportunities for design of highly efficient reaction systems and simplified processing for producing biofuels and chemicals from lignocellulosic biomass.

© 2016 Elsevier Ltd. All rights reserved.

Abbreviations: AC, activated carbon; AgSTA, silver exchanged silicotungstic acid; APPO, aqueous phase partial oxidation; ATP, attapulgite; 1,4-BDO, 1,4-butanediol; BG, 1,4-butylene glycol; BHMF, 2,5-bis(hydroxymethyl)furan; BHMTF, 2,5-bis(hydroxymethyl)tetrahydrofuran; BMF, 5-bromomethylfurfural; [BMIM]Cl, 1-butyl-3-methylimidazolium chloride; BS, benzene sulfonate; BV, Baeyer–Villiger; CFP, catalytic fast pyrolysis; CMF, 5-chloromethylfurfural; CNFs, carbon nanofibers; CNT, carbon nanotube; Coni, α -conidendrin; ConiA, α -conidendrin acid; CP, chloromethyl polystyrene; Cu-BTC, copper benzene-1,3,5-tricarboxylate; CVD, catalytic vapor deposition; DBU, 1,8-diazabicyclo[5.4.0]undec-7-ene; DFF, 2,5-diformylfuran; DFT, density functional theory; DHA, dihydroxyacetone; DHH, 2,5-dihydroxyhexane; DMA, *N,N*-dimethylacetamide; DMF, 2,5-dimethylfuran; DMSO, dimethylsulfoxide; DMTHF, 2,5-dimethyltetrahydrofuran; DS, dodecyl sulfate; DVB, divinylbenzene; EDX, energy-dispersive X-ray spectroscopy; EG, ethylene glycol; EL, ethyl levulinate; EMF, 5-ethoxymethylfurfural; [EMIM]Cl, 1-ethyl-3-methylimidazolium chloride; F₂Ac, 1,4-pentandien-3-on-1,5-di-2-furanyl; FAc, 4-(2-furyl)-3-buten-2-one; FAMEs, fatty acid methyl esters; FDCA, 2,5-furandicarboxylic acid; FDMC, 2,5-dimethylfuroate; Fe³⁺-POP-1, Fe³⁺-porous organic polymer; Fe-BTC, iron benzene-1,3,5-tricarboxylate; FFA, furfuryl alcohol; FFAs, free fatty acids; FFCA, 5-formyl-2-furancarboxylic acid; FT-IR, Fourier transform infrared spectroscopy; GC-MS, gas chromatography–mass spectrometry; GLY, glyceraldehyde; GO, graphene oxide; GVL, γ -valerolactone; HAA, hydroalkylation/alkylation; HAP, hydroxylapatite; HDO, hydrodeoxygenation; HHD, 5-hydroxy-2,5-hexanedione; HMF, 5-hydroxymethylfurfural; HMFCA, 5-hydroxymethyl-2-furancarboxylic acid; HMMF, 5-hydroxymethyl methylfuroate; HMR, hydroxymatairesinol; HNTs, halloysite nanotubes; HOAc, acetic acid; HPAs, heteropoly acids; HPLC, high-performance liquid chromatography; HT, hydrotalcite; HTFA, trifluoroacetic acid; ICP-AES, inductively coupled plasma–atomic emission spectroscopy; ILs, ionic liquids; LA, levulinic acid; LAS-OH, Lewis acid site-OH; MA, maleic anhydride; MC, mesoporous carbon; MF, 2-methylfuran; MFA, methyl furoate; MFFA, 5-methylfuryl alcohol; MFF, methyl 5-formyl-2-furoate; MFf, 5-methylfurfural; MIBK, methyl isobutyl ketone; [MIMPS]₃PW₁₂O₄₀, 1-(3-sulfonic acid)propyl-3-methyl imidazolium phosphotungstate; ML, methyl levulinate; MOF, metal organic framework; MSNs, mesoporous silica nanoparticles; MTHF, 2-methyltetrahydrofuran; NA-p, niobium hydroxide treated with 1 M phosphoric acid; NHC, *N*-heterocyclic carbene; oxoMAT, oxomatairesinol; P[BVIM]Cl, poly(3-butyl-1-vinylimidazolium chloride); PAL, pyruvic aldehyde; PBF, poly(butylene 2,5-furandicarboxylate); PMIM, propyl-3-methylimidazolium; POM, polyoxometalate; PON1, paraoxonase 1; PVP, polyvinyl pyrrolidone; ROP, ring opening products; SA, succinic acid; SAPO, silicoaluminophosphate; SC, supercritical; SZ, sulfated zirconia; TA-p, tantalum hydroxide treated with 1 M phosphoric acid; TBAC, tetrabutylammonium chloride; TEAB, tetraethylammonium bromide; TEMPO, 2,2,6,6-tetramethyl-piperidin-1-oxyl; TEOS, tetraethoxysilane; TGA, thermogravimetric; THF, tetrahydrofuran; THFA, tetrahydrofurfuryl alcohol; TiZ, titania zirconia; TRS, total reducing sugar; TS, TiO₂–SiO₂; VPO, vanadium phosphate; WC_x, tungsten carbide; WP, tungsten phosphide; WZ, tungstated zirconia; XPS, X-ray photoelectron spectroscopy; XRD, X-ray diffraction; ZrC, zirconium carbonate.

* Corresponding author. Biomass Group, College of Engineering, Nanjing Agricultural University, 40 Dianjiangtai Road, Nanjing, Jiangsu 210031, China. Tel.: +(86)025 58606570; Fax: +(86)025 58606570.

E-mail address: zhenfang@njau.edu.cn; zhen.fang@mail.mcgill.ca (Z. Fang).

Contents

1. Introduction	99
2. Bronsted–Lewis acid bifunctionalized materials	101
2.1. Synthesis of 5-hydroxymethylfurfural (HMF) from hexoses	101
2.1.1. Supported ionic liquids (ILs)	102
2.1.2. Metal oxides	106
2.1.3. Modified heteropoly acids	108
2.1.4. Zeolites	108
2.2. Synthesis of furfural from pentoses	110
2.2.1. Molecular sieves	110
2.2.2. Metal oxides	112
2.3. Synthesis of levulinic acid or levulinate esters	112
2.3.1. Molecular sieves	112
2.3.2. Resins and oxides	114
2.4. Other methods and products	115
2.4.1. Catalytic fast pyrolysis (CFP) for coke	115
2.4.2. Phthalic anhydride	116
2.4.3. 5-Ethoxymethylfurfural (EMF)	116
2.4.4. Alkyl lactates	117
2.4.5. Glycerol-derived chemicals	118
2.4.6. Oxygen-containing precursors for diesel and jet fuels	118
3. Acid–base bifunctionalized materials	119
3.1. HMF and furfural	120
3.2. HMF- and furfural-derivatives	123
3.3. Biodiesel	124
3.4. Other methods and biomass-derived chemicals	125
3.4.1. Nanosized mixed oxides for obtaining isobutene from bio-ethanol	125
4. Acid/base-metal bifunctionalized materials	125
4.1. Production of oxygenates	125
4.1.1. Oxidation of sugars and polyols	125
4.1.2. Oxidation of HMF and furfural	130
4.1.3. Oxidation of biomass derivatives to other oxygenates	139
4.2. Production of hydrogenates	142
4.2.1. Hydrolysis–hydrogenation of bio-polymers to polyols	142
4.2.2. Hydrodeoxygenation of biomass derivatives with HMF as an intermediate	148
4.2.3. Hydrodeoxygenation of biomass derivatives with furfural as an intermediate	152
4.2.4. (Hydrolysis)–hydrogenation–cyclization of biomass derivatives to γ -valerolactone (GVL)	157
4.2.5. Hydrogenation/hydrodeoxygenation of biomass derivatives to other hydrogenated products	165
5. Other bifunctional materials and catalytic routes	168
5.1. Metals (Au, Ag, Cd, Ru, Pt, Pd, Cu, Ni) dispersed into nano-sized particles	168
5.2. Cascade reactions with enzymes and electrocatalytic methods	169
6. Auxiliary processes to boost catalytic efficiency	170
6.1. Biomass pretreatment	171
6.1.1. Molten salt hydrates and dual metal salts	171
6.1.2. Preoxidation–hydrolysis	171
6.2. Reaction media	171
6.3. Control of functional materials	172
6.3.1. Porosity	172
6.3.2. Surface polarity	172
6.4. Heating modes including microwave and ultrasound	172
7. Conclusions and future outlook	173
Acknowledgments	174
References	174

1. Introduction

Lignocelluloses composed of chitosan, lipids, microalgae, macroalgae, polyols or polysaccharide and lignin units are the dominant biomass resources in the environment [1]. Microbial, thermochemical, and chemical/catalytic processes are three main approaches of converting biomass into energy, biofuels or chemicals [2]. Enzyme-mediated catalytic processes are the most common way to produce bioethanol, butanol and biodiesel, in which pre-treatment and post-treatment steps are used to remove compounds toxic to the microorganisms. Thermal processing of biomass gives syngas via steam gasification by partial oxidation at temperatures from ~800 to 1000 °C [3] or bio-oil via fast pyrolysis with or without catalyst at temperatures of ~500 °C [4,5]. Efficient processes for the

catalytic upgrading of both syngas and bio-oil to transportation fuels are in high demand [6,7]. At lower reaction temperatures (ca. 300 °C), thermal processing of biomass with catalytic methods offers the possibility of selectively yielding a narrow range of products and to reduce the energy requirements of the transformations [8–10]. Traditional catalytic strategies have relied mainly on mono-functional materials for chemical transformations and while they are able to deliver the desired products for a wide range of substrates, they lack efficiency when dealing with complex molecules [11–13]. Bifunctional solid catalysts provide a method for efficiently transforming complex substrates into products since they integrate sequential catalytic steps and avoid by-product formation and separation [14–16].

In organic synthesis, bifunctional catalysis denotes simultaneous activation of both partners of a bimolecular reaction [17].

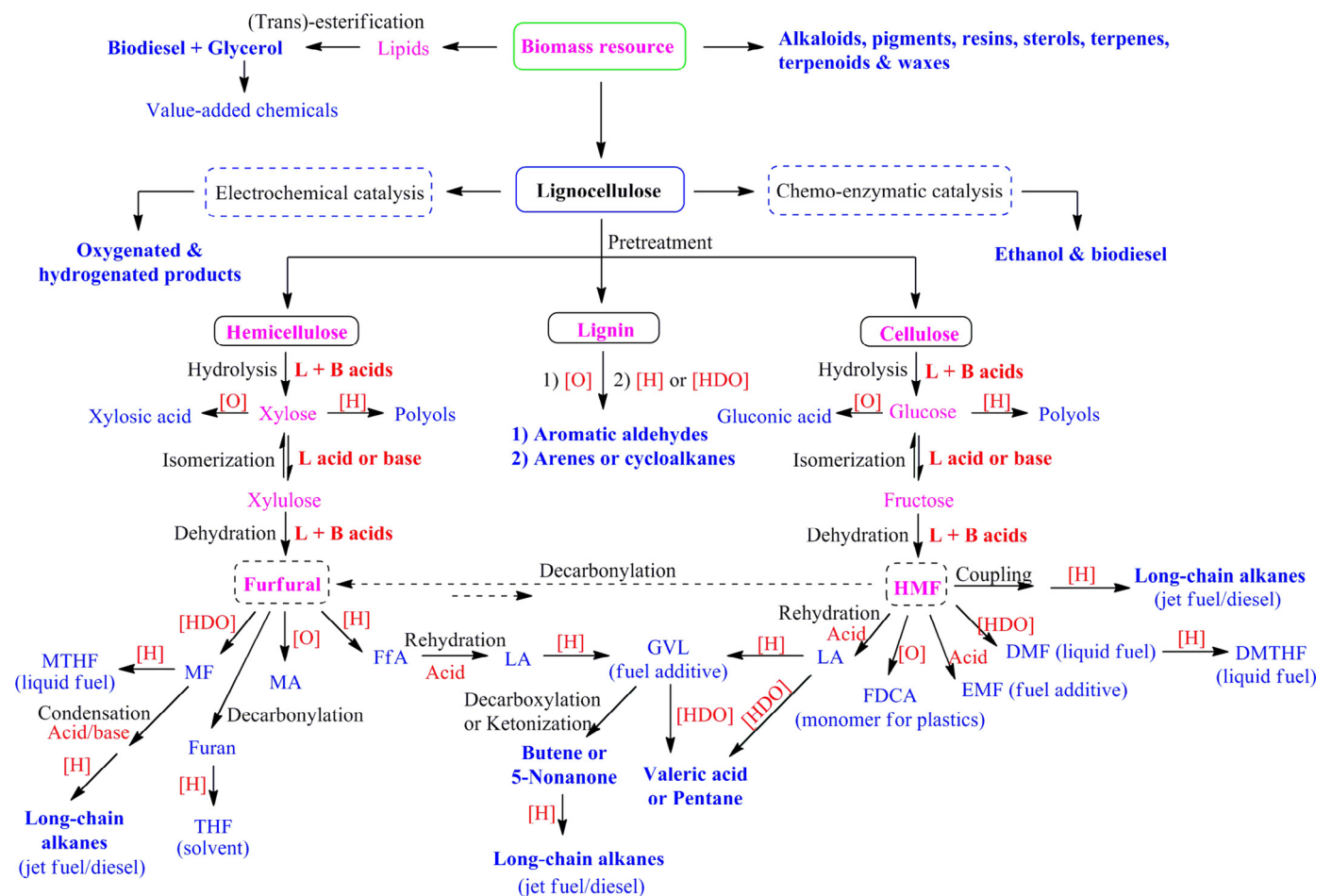


Fig. 1. Reaction routes for the valorization of biomass with catalytic methods (L: Lewis, B: Bronsted, [H]: hydrogenation, [O]: oxidation, [HDO]: hydrodeoxygenation, FDCA: 2,5-furandicarboxylic acid, HMF: 5-hydroxymethylfurfural, EMF: 5-ethoxymethylfurfural, DMTHF: 2,5-dimethyltetrahydrofuran, FfA: furfuryl alcohol, DMF: dimethylfuran, MF: 2-methylfuran, MTHF: 2-methyltetrahydrafuran, MA: maleic anhydride, THF: tetrahydrofuran, LA: levulinic acid, GVL: γ -valerolactone).

Bifunctionality of solid catalysts implies that the materials serve not only as activators for chemical species, but also that they can activate chemical species in a cascade of steps and possibly have synergistic characteristics depending on the multi-step process [18,19]. In other words, multiple catalytic steps are carried out in a single pot with bifunctional catalytic solid materials that are designed with the final product in mind. The combination of multiple synthetic, enzymatic, homogeneous/heterogeneous and electrochemical catalytic systems in single pot operations, proceeding through sequential/tandem- and cascade/domino-type reactions, can significantly eliminate the isolation and purification of intermediates and prevent the formation of unwanted by-products [20,21]. Bifunctional solid catalytic materials are designed to exploit enhanced selectivity of the target products so that processing is simplified.

In lignocellulosic biomass, the rigid structural backbone of the cell wall is formed by combination of cellulose microfibrils with hemicelluloses joined via hydrogen bonds, and this is surrounded by resistant lignin sheaths that provide chemical and physical integrity against stress and degradation [22–24]. Pretreatment of lignocellulosic biomass with a physical, physicochemical, chemical, biological and electrical methods alters its structure and allows release of sugars in polymeric or oligomeric forms so that catalytic transformations can proceed efficiently [25]. Fig. 1 illustrates representative reaction routes for catalytic valorization of lignocelluloses. The distribution of products varies and is closely associated with the type of catalysts applied. In the presence of acid catalysts,

cellulose and hemicellulose can be selectively converted into 5-hydroxymethylfurfural (HMF) and furfural, respectively [26]. The isomerization of sugars with a Lewis acid or a base catalyst acts as a vital bridge to connect polysaccharide hydrolysis and subsequent monosaccharide dehydration, both of which can be promoted by Bronsted and Lewis acids. The liquid fuel additive, 5-ethoxymethylfurfural (EMF), can be synthesized via acid-catalyzed etherification [27]. Hydrogenation or hydrodeoxygenation (HDO) and oxidation reactions are two major approaches to further upgrade biomass into biofuels and value-added chemicals. The introduction of metal particles into upstream acid-mediated catalytic processes, in some cases, is capable of realizing chain reactions in a single pot. For example, HDO and oxidation of in situ generated HMF from sugars are able to yield a liquid fuel 2,5-dimethylfuran (DMF) or 2,5-dimethyltetrahydrofuran (DMTHF) [28], and a potential monomer for plastics 2,5-furandicarboxylic acid (FDCA), respectively [29]. However, competing reactions between oxidation and dehydration such as glucose-to-gluconic acid oxidation versus glucose-to-HMF-to-FDCA conversion, as well as between hydrogenation/HDO and dehydration like glucose-to-polyols hydrogenation versus glucose-to-HMF-to-DMF transformation may proceed nonselectively. Likewise, the cascade production of four- or five-carbon furanic compounds such as furfuryl alcohol (FfA), 2-methylfuran (MF), 2-methyltetrahydrafuran (MTHF), maleic anhydride (MA), and tetrahydrofuran (THF) from xylose may also involve oxidation and hydrogenation of corresponding sugars. With levulinic acid (LA) as the key intermediate, both pentoses and hexoses

can be transformed into γ -valerolactone (GVL), which is considered to be a potential fuel additive [30]. Most importantly, some diesel fuels based on long-chain alkanes (C_8-C_{15}) are able to be produced from the integration of coupling, condensation, and ketonization with subsequent hydrogenation of biomass-derived molecules [31]. Catalytic oxidation, hydrogenation and HDO of pretreated lignin can correspondingly afford aromatic aldehydes, arenes and cycloalkanes [32]. Some other biomass-derived species, like microalgae and chitosan, can be used advantageously to produce biofuels [33,34]; in particular, the production of biodiesel can be achieved from simultaneous esterification and transesterification of lipids catalyzed by Lewis/Bronsted dual acids or acid/base bifunctionalized materials [35], and with some post-treatment steps, the major by-product glycerol can be used to produce carboxylic acids, esters, ethers, ketals/acetals, monohydric alcohols/diols, acrolein, and alkanes/syngas through corresponding reaction routes of oxidation, esterification, etherification/oligomerization, ketalation/acetalation, hydrogenolysis, dehydration, and pyrolysis/gasification [36].

Review articles on catalytic conversion of biomass report on reaction routes and potential substrates for the production of biofuels [37–40], catalytic performance for different catalysts [41,42], processing methods [43,44], heterogeneous catalysis [45–47], underlying mechanisms [48,49], and environmental and economic analyses [50,51]. An emerging trend for biomass valorization is to integrate the catalytic transformations, reaction engineering and product separation [52] processes into a single operation, wherein design of the catalytic materials is considered as one of the key points for establishing efficient and environmentally-friendly processing systems

[53]. In this review, examples of one-pot multiple transformation of biomass into biofuels and valuable chemicals over different types of functional catalysts are presented. Emphasis is given on assessing the bifunctionality of the catalytic materials and relevant auxiliaries such as reaction media, heating modes, catalyst compositions and texture/morphology properties, and compatibility of various reactions. Plausible reaction mechanisms and pathways are discussed for specific products and catalytic systems.

2. Bronsted–Lewis acid bifunctionalized materials

2.1. Synthesis of 5-hydroxymethylfurfural (HMF) from hexoses

Efficient routes to HMF from six-carbon carbohydrates are important for developing methods to process lignocellulosic biomass, since HMF is considered as a valuable precursor for the synthesis of biofuels (e.g. DMF and DMTHF) and value-added chemicals such as biopolymers [54–58]. Relatively high HMF yields can be achieved from fructose substrate catalyzed by Bronsted or Lewis acids. However, when glucose or glucose-derived bi-/polysaccharide is used as the substrate, either low HMF selectivity or low substrate conversion is observed in the presence of single Bronsted or Lewis acids [54,56,57]. Qian et al. [59–61] demonstrated that Bronsted acids have the capability to initiate both dehydration and isomerization reactions of glucose through protonating the C_2-OH to form a common 5-member ring intermediate, which implies that the formation of HMF occurs via a direct cyclic mechanism, rather than via the open chain mechanism that converts glucose to fructose and then to HMF (Fig. 2). HMF selectivities and yields from glucose are extremely

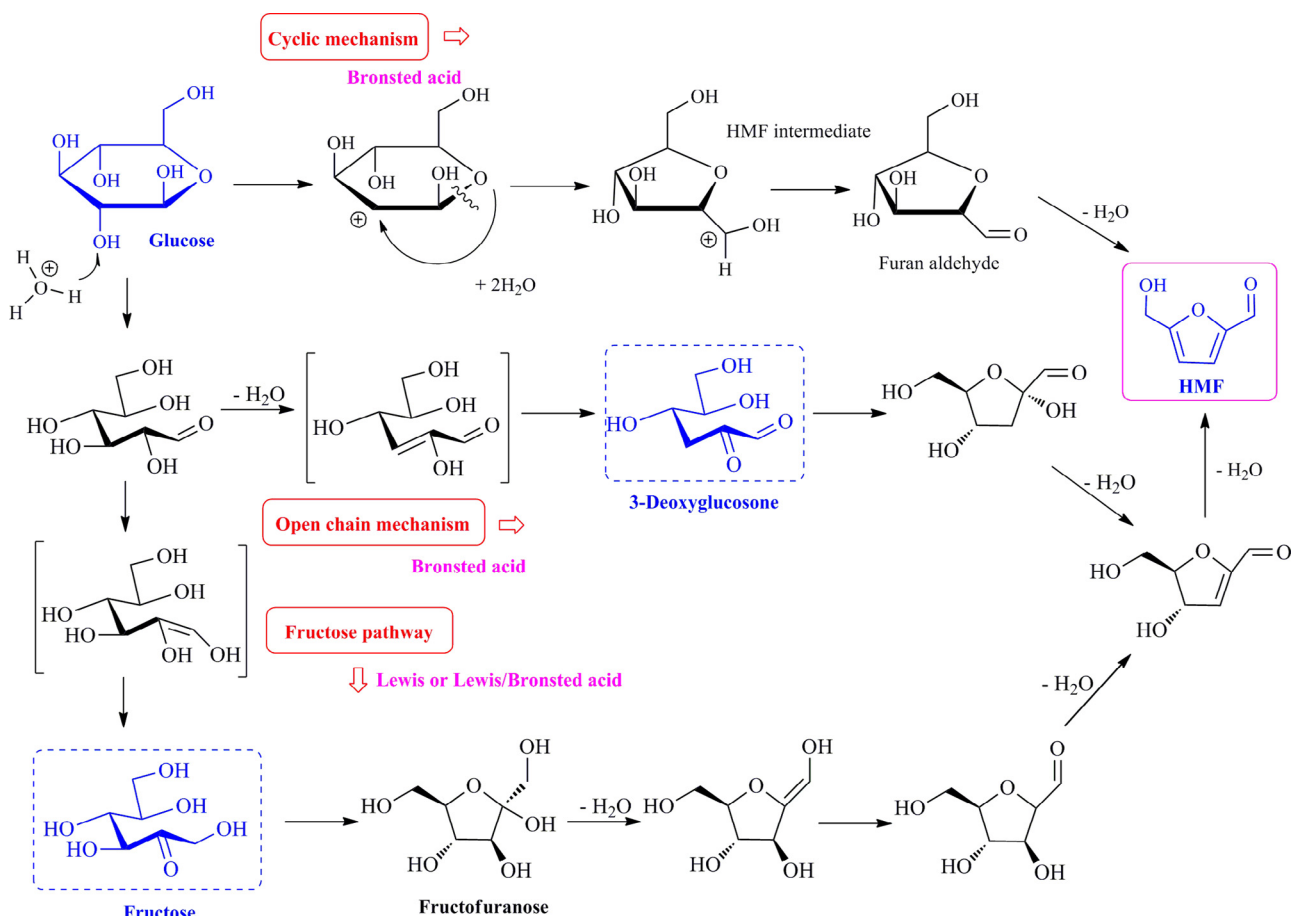


Fig. 2. Plausible pathways for glucose to 5-hydroxymethylfurfural (HMF) conversion mediated with Bronsted or Lewis acids.

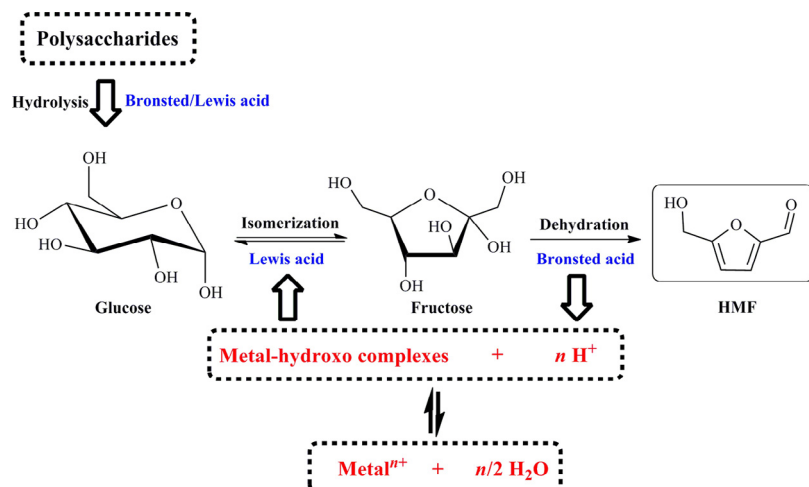


Fig. 3. Polysaccharide-to-HMF (5-hydroxymethylfurfural) conversion via sequential hydrolysis-isomerization-dehydration reactions.

sensitive to processing conditions using conventional Bronsted acid dehydration processes [59]. The dehydration of glucose to HMF begins from Lewis acid-catalyzed isomerization of glucopyranose to fructofuranose [62,63], which can be further dehydrated into HMF with Lewis or Bronsted acid catalysts (Fig. 2) [64–66]. The combined use of Lewis and Lewis/Bronsted acids is considered to be an improved approach for selective and efficient transformation of glucose and glucose-based biopolymers into HMF via one-pot sequential isomerization–dehydration reactions. Wrigstedt et al. [67] illustrated the role of Bronsted acids in Lewis acid-catalyzed aqueous-phase glucose dehydration to HMF, namely that the fructose dehydration step could be accelerated by the addition of a Bronsted acid (e.g. H₃PO₄, H₂SO₄, HNO₃, and HCl) into a Lewis acid (CrCl₃·6H₂O)-mediated system. A significant retardation of the glucose conversion rate was observed due to the restrained formation of the chromium–glucose chelate complex during reaction, which results in a substantial drop in the HMF yield. However, higher reaction temperatures with systematical adjustment of pH are able to obtain high HMF yields (ca. 50%) and efficient conversions (ca. 90%). Choudhary et al. [68] demonstrated that Bronsted acidity retards aldose-to-ketose isomerization, while Lewis acidity increases the overall rate of consumption of fructose and HMF by promoting side reactions. Furthermore, those authors indicated that it would be possible to maximize product yield by optimizing the concentrations of Lewis and Bronsted acids as well as catalyst structures/compositions in the cascade reactions.

Metal chlorides are considered as Lewis acids in 1-alkyl-3-methylimidazolium chloride ionic liquids (ILs) and have been found to be effective for the conversion of sugars to HMF [69–71], among which chromium (II) chloride (CrCl₂) is superior to others in the catalytic process of glucose-to-HMF transformation, affording an HMF yield of nearly 70% at 100 °C in 3 h [72]. For cellulose hydrolysis, CuCl₂ dissolved in 1-ethyl-3-methylimidazolium chloride ([EMIM]Cl) still displays high activity at 120 °C, but the product HMF yield is less than 10% [73]. In contrast, a pair of metal chlorides (CuCl₂ and CrCl₂) with CuCl₂ mole fraction of 0.83–0.95 or a combination of CrCl₂ and RuCl₃ (with a molar ratio of CrCl₂/RuCl₃ = 4/1) in [EMIM]Cl at temperatures of 80–120 °C could collectively catalyze the single-step process of converting cellulose to HMF in nearly 60% yield. The synergistic effect of two different metal chlorides on catalytic conversion of glucose units into HMF probably occurs due to the promotion of the cleavage of both α- and β-1,4-glucosidic bonds at comparable rates as well as glucose-to-fructose isomerization. Chloride ions of ionic liquids and metal chlorides are able to accept

hydrogen species from the hydroxyl groups of cellulose. Weak ion-paired halide ions promote disruption of the otherwise extensive network of intra and interchain hydrogen bonds of cellulose [74,75]. However, interaction of CrCl₂ with water results in the generation of stable and coordinative saturated [Cr(H₂O)₆]²⁺ complexes that significantly inhibit the catalytic activity of CrCl₂. It is still difficult to recycle the metal chlorides although solvent extraction, vacuum distillation, and N₂ stripping have been proposed [48,56]. Homogeneous catalysts require a recycle step that is time-consuming and energy-intensive so that their application in practical processes is limited.

Ionic liquids (e.g., [BMIM]Cl and [EMIM]Cl) are considered to act not only as a basic mediator, but also as a ligand for chromium that lessens the negative effect of water on HMF yield and promotes isomerization and dehydration of glucose into HMF [76]. Organic solvents (e.g., DMSO and DMA) can facilitate the formation of HMF by suppressing the degradation of the furan ring, but separation by evaporation and reuse of the solvent are problematic. Aqueous catalytic systems are preferable due to efficiency, since in situ generated metal ion hydroxo complexes (metal-hydroxo complexes + n H⁺ ⇌ metalⁿ⁺ + n/2 H₂O) seem to promote isomerization of glucose to fructose in the case of some metal salts (e.g., AlCl₃) [77]. The introduction of protonic acids not only increases the content of Bronsted acid sites to facilitate hydrolysis and dehydration reactions [78], but also promotes the formation of metalⁿ⁺ instead of metal-hydroxo complexes (Fig. 3), thus hindering glucose isomerization which is the key step of transformation [77]. Therefore, the ratio/distribution of Bronsted acid to Lewis acid sites must be adjusted to allow both the glucose-to-fructose isomerization and the hydrolysis/dehydration step to proceed smoothly.

2.1.1. Supported ionic liquids (ILs)

Polysaccharides (e.g., cellulose) are difficult to be degraded via simple heterogeneous catalysis that can be attributed to their strong intra- and intermolecular hydrogen bonds and the existence of crystalline and amorphous regions. Unlike neutral ionic liquids, acidic ILs such as 1-(4-sulfonic acid)butyl-3-methylimidazolium hydrogen sulfate ([SO₃H-BMIM]HSO₄) exhibit higher activity for the hydrolysis of cellulose than protonic acids such as HCl, HNO₃, H₃PO₄, and H₂SO₄ (70% vs. 40–60% conversion), and have improved catalytic performance (88–89% conversion) for producing HMF (37% yield) and furfural (18% yield) among different ILs with the addition of catalytic amounts of MnCl₂ in a biphasic system consisting of H₂O/MIBK (methyl isobutyl ketone) reaction system (Table 1, Entries 1–6) [79], in which the coordination effect of $-SO_3H/SO_4^{2-}$

Table 1

Bronsted–Lewis acid bifunctional solid catalysts used in the conversion of carbohydrate substrates into 5-hydroxymethylfurfural with summary of reaction conditions, maximum catalytic activity, catalyst reusability and catalyst preparation method.

Entry	Substrate	Catalyst ^a	Reaction condition			Catalytic activity		Reusability		Catalyst preparation			Ref.
			Solvent	Temp	Time	Conv	Yield/[Selc]	Cycles	Yield ^b	Method	Calcination	Waste	
1	Cellulose (25 wt%)	0.2 M MnCl ₂ + [SO ₃ H–BMIM]HSO ₄	MIBK	150 °C	5 h	89%	37%	5	>20%	Co-condensation	No	IL + Mn ²⁺	[79]
2	Cellulose (25 wt%)	0.2 M MnCl ₂ + [BMIM]BF ₄	MIBK	150 °C	5 h	5%	1%	–	–	Co-condensation	No	Mn ²⁺	[79]
3	Cellulose (25 wt%)	0.2 M MnCl ₂ + [BMIM]PF ₆	MIBK	150 °C	5 h	5%	1%	–	–	Co-condensation	No	Mn ²⁺	[79]
4	Cellulose (25 wt%)	0.2 M MnCl ₂ + [BMIM]Br	MIBK	150 °C	5 h	4%	<1%	–	–	Co-condensation	No	Mn ²⁺	[79]
5	Cellulose (25 wt%)	0.2 M MnCl ₂ + [BMIM]Cl	MIBK	150 °C	5 h	11%	2%	–	–	Co-condensation	No	Mn ²⁺	[79]
6	Cellulose (25 wt%)	0.2 M MnCl ₂ + [BMIM]H ₂ PO ₄	MIBK	150 °C	5 h	23%	8%	–	–	Co-condensation	No	Mn ²⁺	[79]
7	Glucose (10 wt%)	15 mol% GeCl ₄	[BMIM]Cl	100 °C	1 h	98%	38%	5	–	–	No	Ge ⁴⁺	[80]
8	Cellulose (50 wt%)	[SO ₃ H–BMIM]HSO ₄	MIBK	150 °C	5 h	70%	15%	–	–	Co-condensation	No	IL	[81]
9	Cellulose (50 wt%)	0.2 M FeCl ₂ + [SO ₃ H–BMIM]HSO ₄	MIBK	150 °C	5 h	34	84	5	26%	Co-condensation	No	IL + Fe ²⁺	[81]
10	Cellulose (25 wt%)	0.2 M CoSO ₄ + [SO ₃ H–BMIM]HSO ₄	MIBK	150 °C	5 h	84%	24%	5	~18%	Co-condensation	No	IL + Co ²⁺	[82]
11	Cellulose (5 wt%)	0.2 M CrCl ₃ ·6H ₂ O + [SO ₃ H–PMIM]HSO ₄	[BMIM]Cl	120 °C	5 h	95%	53%	8	~40%	Co-condensation	No	IL + Cr ³⁺	[83]
12	Cellulose (3.3 wt%)	[SO ₃ H–PMIM]HSO ₄	DMSO	160 °C	5 h	–	25%	–	–	Co-condensation	No	IL	[84]
13	Cellulose (3.3 wt%)	0.04 M InCl ₃ + [SO ₃ H–PMIM]HSO ₄	DMSO	160 °C	5 h	85%	45%	5	~30%	Co-condensation	No	IL + In ³⁺	[84]
14	Glucose (10 wt%)	10 mol% CrCl ₃ ·6H ₂ O	Et-DBUBS	110 °C	2 h	100%	83%	5	~80%	–	No	IL + Cr ³⁺	[85]
15	Glucose (3.3 wt%)	[CO ₂ H–PMIM]Cl	DMSO	120 °C	7 h	–	12%	–	–	Co-condensation	No	IL	[86]
16	Glucose (3.3 wt%)	0.2 M ZrOCl ₂ + [CO ₂ H–PMIM]Cl	DMSO	120 °C	7 h	–	51%	6	–	Co-condensation	No	IL + Zr ⁴⁺	[86]
17	Glucose (4 wt%)	10 mol% CrCl ₂	DMF	120 °C	3 h	–	50%	–	–	–	–	Cr ²⁺	[87]
18	Glucose (4 wt%)	10 mol% P[BVIM]Cl–CrCl ₂	DMF	120 °C	3 h	–	66%	6	~38%	Polymerization, immobilization	No	Cr ²⁺	[87]
19	Glucose (4 wt%)	10 mol% P[BVIM]Cl–AlCl ₃	DMF	120 °C	3 h	–	49%	6	~38%	Polymerization, immobilization	No	NM ^c	[87]
20	Glucose (5 wt%)	30 wt% SO ₃ H–PIL–PW	DMSO	150 °C	2 h	–	18%	–	–	Polymerization, protonation	No	NM	[88]
21	Glucose (5 wt%)	30 wt% SO ₃ H–PIL–PW/CrCl ₃	DMSO	150 °C	2 h	–	34%	–	–	Polymerization, protonation, immobilization	No	Cr ³⁺	[88]
22	Glucose (10 wt%)	10 mg CrCl ₂ –Im–SBA-15	H ₂ O:DMSO/2-BuOH:MIBK	150 °C	3 h	50%	35%[70%]	–	–	Post-grafting	No	Cr ²⁺	[89]
23	Fructose (30 wt%)	3.3 wt% Taa–SBA-15	H ₂ O/2-BuOH:MIBK	180 °C	0.5 h	66%	49%[74%]	–	–	Co-condensation, protonation	No	NM	[90]
24	Glucose (6.7 wt%)	100 wt% H ⁺ –D001-cc resin	[BMIM]Cl	110 °C	0.5 h	–	10%	–	–	Ion exchange	No	NM	[91]
25	Glucose (6.7 wt%)	100 wt% Cr ³⁺ –D001-cc resin	[BMIM]Cl	110 °C	0.5 h	–	61%	6	40%, ~70% (2nd)	Ion exchange	No	Cr ³⁺	[91]
26	Fructose (3 wt%)	26.7 wt% MSN	DMSO	90 °C	3 h	27%	0	–	–	Co-condensation	No	NM	[92]
27	Fructose (3 wt%)	26.7 wt% [HSO ₃ + (ILs/CrCl ₂)]–MSN	DMSO	90 °C	3 h	98%	73%[75%]	5	60%, 73% (4 th)	Co-condensation, post-grafting	No	NM	[92]
28	Glucose (5 wt%)	60 wt% Cr–HAP	[BMIM]Cl	400 W ^d	150 s	78%	40%	5	~40%	Impregnation	500 °C	NM	[93]
29	Glucose (5 wt%)	Sn-Mont	THF-DMSO (7:3, v/v)	160 °C	3 h	98%	54%	6	~53%	Ion-exchange	600 °C, 4 h	NM	[94]
30	Cellulose (5 wt%)	Sn-Mont	THF/H ₂ O–NaCl (5:1, v/v)	160 °C	3 h	–	39%	–	–	Ion-exchange	600 °C, 4 h	NM	[94]
31	Cellulose (5 wt%)	100 wt% ATP–SO ₃ H–Cr(III)	[EMIM]Cl	120 °C	2 h	–	31%	5	22%	Post-grafting, impregnation	No	Cr ³⁺	[95]

(continued on next page)

Table 1 (continued)

Entry	Substrate	Catalyst ^a	Reaction condition			Catalytic activity		Reusability		Catalyst preparation			Ref.
			Solvent	Temp	Time	Conv	Yield/ [Selc]	Cycles	Yield ^b	Method	Calcination	Waste	
32	Cellulose (5 wt%)	100 wt% HNTs–SO ₃ H–Cr(III)	[EMIM]Cl	120 °C	2 h	–	41%	5	22%	Post-grafting, impregnation	No	Cr ³⁺	[95]
33	Cellulose (10 wt%)	100 wt% ZrO ₂	H ₂ O	250 °C	5 min	~20%	~6%	–	–	Precipitation	550 °C, 6 h	NM	[96]
34	Cellulose (10 wt%)	100 wt% SO ₄ /ZrO ₂	H ₂ O	250 °C	5 min	~30%	~11%	–	–	Precipitation	550 °C, 6 h	Sulfur	[96]
35	Fructose (0.3 wt%)	90 wt% SO ₄ /ZrO ₂ hollow nanoshells	DMSO	120 °C	1 h	–	64%	–	–	Impregnation	550 °C, 3 h	Sulfur	[97]
36	Fructose (5 wt%)	50 wt% porous PO ₄ /TiO ₂ nanoparticles	DMA–LiCl	140 °C ^d	5 min	–	44%	6	~35%	Etching SiO ₂ , impregnation	650 °C, 6 h	Sulfur	[97]
37	Glucose (5 wt%)	20 wt% porous H ₃ PO ₄ /TiO ₂ nanoparticles	DMA–LiCl	140 °C ^d	5 min	–	22%	–	–	Slow evaporation	400 °C, 6 h	NM	[98]
38	Sugarcane bagasse (5 wt%)	20 wt% porous PO ₄ /TiO ₂ nanoparticles	DMA–LiCl	140 °C ^d	5 min	–	26%	–	–	Slow evaporation	400 °C, 6 h	NM	[98]
39	Fructose (1 wt%)	13.3 wt% 9.8WO ₃ /ZrO ₂	H ₂ O	130 °C	4 h	–	[40%]	–	–	Impregnation	700 °C, 4 h	NM	[99]
40	Glucose (5 wt%)	2 wt% Zr–Mo–SA	[BMIM]Cl/H ₂ O	150 °C	3 h	–	27%	–	–	Sol-gel	600 °C, 5 h	NM	[100]
41	Glucose (5 wt%)	50 wt% mesoporous TiO ₂ nanospheres	DMA–LiCl	130 °C ^d	2 min	–	30%	–	–	Self-assembly	500 °C, 4 h	NM	[101]
42	Glucose (5 wt%)	50 wt% mesoporous TiO ₂ nanospheres	DMSO	140 °C ^d	5 min	–	36%	–	–	Self-assembly	500 °C, 6 h	NM	[102]
43	Cellulose (8.8 wt%)	26.7 wt% mesoporous TiO ₂ nanocatalyst	[EMIM]Cl/H ₂ O	120 °C	3 h	–	18%	–	–	Self-assembly, hydrothermal treatment	550 °C, 6 h	NM	[103]
44	Cellulose (8.8 %)	26.7 wt% mesoporous ZrO ₂ nanocatalyst	[EMIM]Cl/H ₂ O	120 °C	3 h	–	29%	–	–	Self-assembly, hydrothermal treatment	550 °C, 6 h	NM	[103]
45	Glucose (2 wt%)	30 wt% nanosized PO ₄ /TiO ₂	H ₂ O/n-BuOH	175 °C	3 h	97%	81%	6	~70%	Sol-gel, impregnation	600 °C, 4 h	NM	[104]
46	Fructose (6 wt%)	71 wt% PO ₄ /Nb ₂ O ₅ (P/Nb = 2, w/w)	H ₂ O	100 °C	0.5 h	29%	[100%]	–	–	Impregnation	255 °C, 6 h	NM	[105]
47	Fructose (8 wt%)	100 wt% mesoporous PO ₄ /Nb ₂ O ₅	H ₂ O	130 °C	0.5 h	58%	45%	5	32%	Sol-gel, hydrothermal treatment	500 °C, 5 h	NM	[106]
48	Glucose (1 wt%)	100 wt% PO ₄ /Nb ₂ O ₅	H ₂ O	120 °C	3 h	92%	[52%]	–	–	Precipitation, impregnation	100 °C, 12 h	NM	[107]
49	Inulin (6 wt%)	8.3 wt% PO ₄ /Nb ₂ O ₅ (NA-p)	H ₂ O/2–BuOH (2:3, v/v)	160 °C	80 min	76%	74%	–	–	Impregnation	300 °C, 3 h	NM	[108]
50	Glucose (10 wt%)	33.3 wt% PO ₄ /Ta ₂ O ₅	H ₂ O/MIBK (3:7, v/v)	175 °C	1.5 h	69%	23%	–	–	Sol-gel	550 °C, 3 h	NM	[109]
51	Glucose (6 wt%)	8.3 wt% PO ₄ /Ta ₂ O ₅ (TA-p)	H ₂ O/2–BuOH (2:3, v/v)	160 °C	180 min	99%	90%	15	85%	Impregnation	300 °C, 3 h	NM	[110]
52	Glucose (6 wt%)	8.3 wt% PO ₄ /Ta ₂ O ₅ (TA-p)	H ₂ O/2–BuOH (2:3, v/v)	160 °C	140 min	70%	57%	–	–	Impregnation	300 °C, 3 h	NM	[110]
53	Glucose (10 wt%)	33.3 wt% mesoporous PO ₄ /Ta ₂ O ₅	H ₂ O/MIBK (3:7, v/v)	170 °C	1 h	56%	33%	3	22%	Sol-gel, impregnation	550 °C, 6 h	NM	[111]
54	Glucose (18 wt%)	55.6 wt% Sn–W oxide	THF/H ₂ O (5/1, v/v)	120 °C	18 h	–	48%	–	–	Co-precipitation	800 °C, 3 h	NM	[112]
55	Glucose (10 wt%)	500 wt% Sn–VPO	DMSO	110 °C	6 h	100%	74%	4	~70%	Impregnation	450 °C, 6 h	NM	[113]
56	Glucose (10 wt%)	10 wt% α-Sr(PO ₃) ₂	H ₂ O	220 °C	5 min	60%	21%	–	–	Precipitation	900 °C, 3 h	NM	[114]
57	Glucose (10 wt%)	10 wt% CaP ₂ O ₆	H ₂ O	220 °C	5 min	70%	20%	–	–	Precipitation	900 °C, 3 h	NM	[114]
58	Glucose (10 wt%)	33.3 wt% SO ₄ /Zr–MCM-550	H ₂ O/MIBK (3:7, v/v)	175 °C	2.5 h	82%	23%	4	~15%	Sol-gel, impregnation	500 °C, 6 h	NM	[115]
											750 °C, 2 h;		

(continued on next page)

Table 1 (continued)

Entry	Substrate	Catalyst ^a	Reaction condition			Catalytic activity		Reusability		Catalyst preparation			Ref.
			Solvent	Temp	Time	Conv	Yield/[Selec]	Cycles	Yield ^b	Method	Calcination	Waste	
59	Glucose (10 wt%)	33.3 wt% Al-MCM-550	20 wt% NaCl–H ₂ O/MIBK (3:7, v/v)	195 °C	0.5 h	98%	63%	3	~45%	Sol-gel	500 °C, 3 h	NM	[116]
60	Glucose (30 wt%)	3.3 wt% Ag ₃ PW ₁₂ O ₄₀	H ₂ O/MIBK (1:2.25, v/v)	130 °C	4 h	89%	76%	6	~70%	Precipitation	200 °C, 12 h	NM	[117]
61	Sucrose (10 wt%)	10 wt% AgSTA	H ₂ O	120 °C	160 min	92%	63%	8	~60%	Precipitation	120 °C, 12 h	NM	[118]
62	Fructose (30 wt%)	21.3 wt% Cs ₂ H _{0.5} PW	H ₂ O/MIBK (1:3, v/v)	115 °C	1 h	95%	74%	6	~67%	Precipitation	No	NM	[119]
63	Cellulose (5 wt%)	5 mol% Cr[(DS)H ₂ PW ₁₂ O ₄₀] ₃	H ₂ O	150 °C	2 h	77%	53%	–	–	Precipitation	No	NM	[120]
64	Glucose (15 wt%)	5.9 mol% C ₁₆ H ₃ PW ₁₁ CrO ₃₉	H ₂ O	130 °C	2 h	84%	35%	6	~34%	Precipitation	No	NM	[121]
65	Glucose (2.5 wt%)	83 wt% H-Beta (Si/Al: 15)-750	H ₂ O–DMSO (9:1)/THF (1:3)	180 °C	3 h	78%	[55%]	5	40%	Dealumination	750 °C, 1 h	NM	[122]
66	Glucose (10 wt%)	40 wt% H-Beta (Si/Al: 25)	[BMIM]Cl	180 °C	50 min	81%	50%	6	36%	Dealumination	550 °C, 5 h	NM	[123]
67	Cellulose (2.5 wt%)	200 wt% H-ZSM-5 (Si/Al: 37)	H ₂ O	190 °C	4 h	67%	46%	5	~40%	Desilication	550 °C, 5 h	NM	[124]
68	Glucose (10 wt%)	0.5 mol% Sn-Beta	1-Butanol + H ₂ O + 35 wt% NaCl	160 °C	1.5 h	75%	14%/[18%]	–	–	Dealumination	550 °C, 5 h	NM	[125]
69	Glucose (10 wt%)	HCl (pH = 1)	1-Butanol + H ₂ O + 35 wt% NaCl	160 °C	1.5 h	26%	10%/[40%]	–	–	–	No	Acid	[125]
70	Glucose (10 wt%)	HCl (pH = 1) 0.5 mol% Sn-Beta	1-Butanol + H ₂ O + 35 wt% NaCl	160 °C	1.5 h	75%	41%/[55%]	–	–	Dealumination	550 °C, 5 h	Acid	[125]
71	Glucose (10 wt%)	HCl (pH = 1) 0.5 mol% Sn-Beta	H ₂ O	160 °C	1.5 h	45%	2.7%/[6%]	–	–	Dealumination	550 °C, 5 h	Acid	[125]
72	Glucose (10 wt%)	HCl (pH = 1) 0.5 mol% Sn-Beta	1-Butanol + H ₂ O	160 °C	1.5 h	77%	20%/[26%]	–	–	Dealumination	550 °C, 5 h	Acid	[125]
73	Glucose (10 wt%)	HCl (pH = 1) 0.5 mol% Sn-Beta	THF + H ₂ O + 35 wt% NaCl	160 °C	1.5 h	79%	57%/[72%]	–	–	Dealumination	550 °C, 5 h	Acid	[125]
74	Glucose (2 wt%)	3.3 wt% Amberlyst-70 3.3 wt% Sn-Beta	GVL/H ₂ O (9:1, w/w)	130 °C	0.33 h	92%	59%/[64%]	–	–	Dealumination	550 °C, 5 h	NM	[126]
75	Glucose (2 wt%)	3.3 wt% Amberlyst-70 3.3 wt% Sn-SBA-15	GVL/H ₂ O (9:1, w/w)	130 °C	0.25 h	90%	46%/[51%]	–	–	Dealumination	550 °C, 5 h	NM	[126]
76	Glucose (2 wt%)	3.3 wt% Amberlyst-70 3.3 wt% Sn-Beta	THF/H ₂ O (9:1, w/w)	130 °C	0.5 h	90%	63%/[70%]	–	–	Dealumination	550 °C, 5 h	NM	[126]
77	Glucose (2 wt%)	3.3 wt% Amberlyst-70 3.3 wt% Sn-SBA-15	THF/H ₂ O (9:1, w/w)	130 °C	0.33 h	90%	36%/[40%]	–	–	Dealumination	550 °C, 5 h	NM	[126]
78	Glucose (2 wt%)	3.3 wt% Amberlyst-70 3.3 wt% Sn-Beta	MTHF:THF/H ₂ O (9:1, w/w)	130 °C	0.67 h	90%	59%/[66%]	–	–	Dealumination	550 °C, 5 h	NM	[126]

^a Catalyst dosage relative to substrate.^b Yield of 5-HMF in the last cycle.

c NM: not mentioned.

d Microwave heating. SA: succinic acid, DS: dodecyl sulfate, NA-p: niobium hydroxide treated with 1 M phosphoric acid and calcined at 300 °C, TA-p: tantalum hydroxide treated with 1 M phosphoric acid and calcined at 300 °C, VPO: vanadium phosphate, Al-MCM-550: aluminum containing MCM-41 molecular sieve calcined at 550 °C, STA: silicotungstic acid, H-ZSM-5: a protonic zeolite, Amberlyst 70: a macroporous polymer catalyst, Sn-Beta: a modified zeolite, Sn-SBA-15: a mesoporous molecular sieve, PMIM: propyl-3-methylimidazolium; MIBK: methyl isobutyl ketone, DMSO: dimethylsulfoxide, DBUBS: DBU-based (DBU: 1,8-diazabicyclo[5.4.0]undec-7-ene) ILs with the benzene sulfonate (BS) anion.

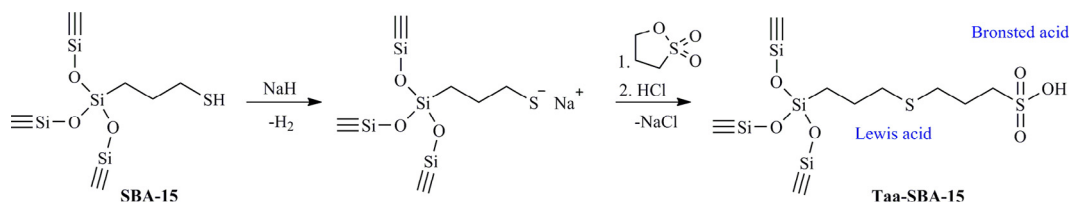


Fig. 4. Synthetic route for preparation of SBA-15 supported bifunctional acid catalyst. Adapted with permission from Refs. 90 and 127, Copyright © 2011, American Chemical Society; Copyright © 2010, Springer.

with moderate acidity and MnCl_2 occurs to promote cascade cellulose hydrolysis and glucose dehydration reactions efficiently. By employing $-\text{SO}_3\text{H}$ or COOH -functionalized IL as the Bronsted acid counterpart, a series of other related metal chlorides including GeCl_4 , FeCl_2 , FeCl_3 , CoCl_2 , ZnCl_2 , CuCl_2 , NiCl_2 , InCl_3 and CrCl_3 catalyze the transformation of carbohydrates especially cellulose to HMF with high yields (Table 1, Entries 7–16) [80–86]. Strong Bronsted acid ILs seem to be necessary for the hydrolysis of cellulose, while metal chlorides are active for the subsequent dehydration of glucose to HMF. However, the recycle of acidic ILs tends to be complicated, since water remains in the IL phase that leads to rehydration of HMF and the formation of LA.

To improve the recyclability of IL-based catalytic systems, a series of heterogeneous Bronsted–Lewis acid bifunctional materials have been proposed (Table 1). Liu and Chen [87] used a polymeric IL (PIL) as a catalyst support for catalyst recovery as well as biomass conversion, and found that poly(3-butyl-1-vinylimidazolium chloride) ($\text{P}[\text{BVIM}]\text{Cl}$) is effective for glucose-to-HMF conversion with up to 66% yields being obtained at 120 °C for 3 h when combined with CrCl_2 in situ or used as the prebuilt PIL metolate $\text{P}[\text{BVIM}]^+[\text{CrCl}_3]^-$ in DMF (Table 1, Entries 17–19). The $\text{P}[\text{BVIM}]\text{Cl}$ – CrCl_2 catalyst remains effective for the two-step transformation of cellulose into HMF covering cellulose-to-glucose conversion through controlled hydrolysis in $[\text{EMIM}]\text{Cl}$, and then by adding the PIL-based catalyst for subsequent dehydration of glucose, achieves 50% HMF yield at 120 °C. The analogous $\text{P}[\text{BVIM}]\text{Cl}$ – AlCl_3 catalyst is less effective than the PIL–Cr system in glucose-to-HMF conversion (HMF yield: 49% vs. 66%), but recycle tests show that the PIL–Al system is more robust because less metal leaching occurs that allow an HMF yield of 42% to be obtained for an average of 6 cycles. Immobilizing Cr^{3+} with SO_3H -functionalized solid PILs bearing counter anions such as Cl^- and $\text{PW}_{12}\text{O}_{40}^{3-}$ (i.e., SO_3H –PIL– Cl/CrCl_3 and SO_3H –PIL– PW/CrCl_3) is found to be effective for selective transformation of carbohydrates especially glucose into HMF [88]. In comparison to chloridion, the presence of the heteropoly anion is able to enhance the hydrophobicity of the PIL catalyst and the relatively low activation energy (22.02 kJ mol⁻¹) demonstrates its high catalytic performance in the production of HMF from carbohydrates (Table 1, Entries 20 and 21). Providing a local reaction microenvironment via immobilization on a solid porous support is thought to allow coordination in the IL medium. For example, Degirmenci et al. [89] introduced CrCl_2 into an IL propyl-3-methylimidazolium chloride ($[\text{PMIM}]\text{Cl}$) supported on the surface of SBA-15 that lead to the formation of loosely bound, catalytically active Cr^{2+} species. The resulting high mobility of these complexes (CrCl_2 –Im–SBA-15; Im refers to immobilized imidazolium-based IL) is found to be beneficial for selective glucose dehydration, and affords an HMF selectivity of 70% for a glucose conversion of 50% in H_2O :dimethylsulfoxide (DMSO)/2-BuOH:MIBK at 150 °C for 3 h (Table 1, Entry 22). The stability of CrCl_2 –Im–SBA-15 strongly depends on the actual composition of the reaction medium, in particular, DMA used as solvent reduces the Cr leaching to 30%. Complexing of DMA with Cr is likely to relieve the interaction of Cr^{2+} chloride with water to form coordinatively saturated $[\text{Cr}(\text{H}_2\text{O})_6]^{2+}$ complexes that are inactive for HMF production from glucose. By

choosing an appropriate solvent, the degree of ion exchange and swelling of the support can be lessened that is helpful to some extent in lowering the leaching of active sites to a few percent. In the aqueous phase, the leaching of IL in small amounts is detected, but it does not seem to perturb the reaction (Table 1, Entry 22) [89].

By using a co-condensation method [90,127], a Lewis/Bronsted acid bifunctional mesoporous catalyst (Taa-SBA-15) can be prepared by incorporating 3-((3-(trimethoxysilyl)propyl)thio) propane-1-sulfonic acid into SBA-15-type silica (Fig. 4) that shows good activity in the dehydration of aqueous fructose after a short time of 0.5 h (Table 1, Entry 23), which is capable of affording a higher selectivity to HMF (71%, with 84% conversion) than its sulfone derivative at 130 °C after 141 min. The superior catalytic performance might be due to the hydrophobic nature as well as the promoting effect of Lewis acid thioether groups of Taa-SBA-15 on the tautomerization of fructose to its furanose [90,127]. As evidence for this, it has been reported that D001-cc resin having Bronsted acid-rich sites is favored for the dehydration of fructose but it lacks Lewis acid sites for conversion of glucose to HMF [128]. As an improved approach, the D001-cc resin modified with Cr^{3+} can be obtained by simple ion-exchange, in which it is found that the material converts glucose into HMF with a yield of 61% in $[\text{BMIM}]\text{Cl}$ at 110 °C in 30 min (Table 1, Entries 24 and 25) [91]. In that work [91], the HMF yields in two recycle tests were higher than that in the first run, which might be the result of formation of CrCl_4^- with the IL or incomplete washing of residual substrate from the catalyst. Although ICP-AES (inductively coupled plasma-atomic emission spectroscopy) shows the existence of leached elemental Cr in the solution, examination of solids with TGA (thermogravimetric analysis) and EDX (energy-dispersive X-ray spectroscopy) for adsorbed chemical species and surface complexes show that some species cannot be simply washed off so that method development is needed to allow reliable assessment of catalyst reusability.

Other porous solids supported Bronsted–Lewis acid bifunctional catalysts such as mesoporous silica nanoparticles (MSNs) functionalized with both sulfonic acid and IL ($[\text{HSO}_3^+](\text{ILs}/\text{CrCl}_2)$ –MSN) (Table 1, Entries 26 and 27) [92], hydroxyapatite supported chromium chloride (Cr-HAP) (Table 1, Entry 28) [93], tin hydroxide nanoparticles-embedded montmorillonite (Sn-Mont) (Table 1, Entries 29 and 30) [94], and acid-chromic chloride functionalized natural clay particles including treated attapulgite (ATP) and halloysite nanotubes (HNTs) (ATP– SO_3H –Cr(III) and HNTs– SO_3H –Cr(III)) (Table 1, Entries 31 and 32) [95], as well as porous polymerized solid acids [129,130] and bio-carbon-based solid acids [131,132] have been explored for the carbohydrate-to-HMF transformation (Table 1). Auxiliary weak acidic groups like $-\text{OH}$ and $-\text{COOH}$ along with robust Lewis/Bronsted acid sites of functionalized materials are responsible for the enhanced catalytic activities shown in Table 1.

2.1.2. Metal oxides

From the point of view of cost, metal oxides, such as ZrO_2 - and TiO_2 -solid catalysts, are good candidates for biomass conversion (Table 1). Nevertheless, only low to moderate HMF yields have been achieved from saccharides for unmodified ZrO_2 and TiO_2 catalysts

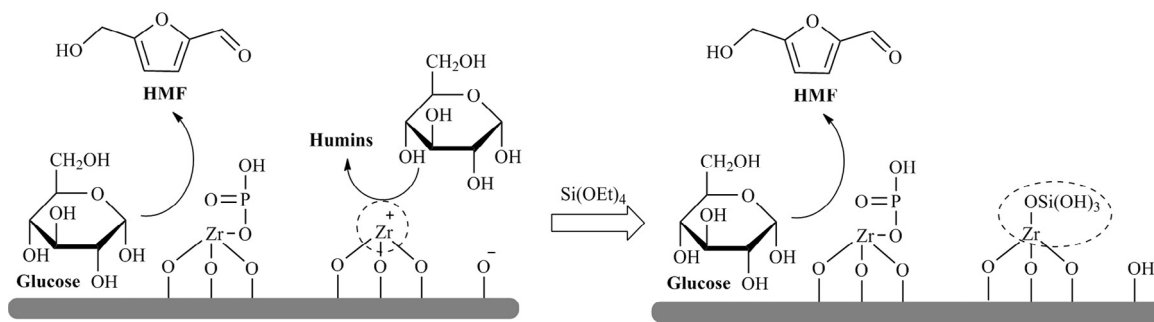


Fig. 5. A silylation procedure leading to deactivation of unselective Lewis acid sites in conversion of glucose to 5-hydroxymethylfurfural (HMF). Adapted with permission from Ref. [40], Copyright © 2013, Elsevier.

[133]. Three major routes have been developed to enhance the catalytic performance of ZrO_2 and TiO_2 catalysts for carbohydrate-to-HMF conversion (Table 1, Entries 33–44): (1) modification of ZrO_2 and TiO_2 with strong Bronsted acids such as H_2SO_4 and H_3PO_4 to incorporate Bronsted acid sites [96–98,134], (2) deposition of Zr or Ti together with other metals like W and Mo bearing strong acidity [99,100,135,136], (3) creation of porous and nano-sized ZrO_2 and TiO_2 materials to make the sites more accessible to substrates [101–103]. Thermal stability of the materials can be enhanced by the metal–O–P bond formation (Table 1, Entry 45) [104].

Due to strong acidic properties and high stability for acid catalytic reactions in aqueous solution, Ta_2O_5 and Nb_2O_5 derived catalysts have been investigated to produce HMF from various substrates including monosaccharides and polysaccharides in water, however, the HMF yields obtained have not been very encouraging (Table 1, Entries 46 and 47) [105,106,137,138]. Nakajima et al. [107] illustrated that Lewis acid sites (NbO_4 tetrahedra) on the $\text{Nb}_2\text{O}_5\text{-nH}_2\text{O}$ surface immediately form $\text{NbO}_4\text{-H}_2\text{O}$ adducts in the presence of water and a part of the adducts are able to function as effective Lewis acid sites that promote HMF formation from glucose (Table 1, Entry 48) but simultaneously giving the formation of complex polymers that could not be readily analyzed by HPLC (high-performance liquid chromatography) or GC-MS (gas chromatography–mass spectrometry) [139]. H_3PO_4 -treated $\text{Nb}_2\text{O}_5\text{-nH}_2\text{O}$ ($\text{H}_3\text{PO}_4/\text{Nb}_2\text{O}_5\text{-nH}_2\text{O}$) leads to a large decrease in undetectable products and an increase in HMF yield from 12% to 52% for the case of glucose-to-HMF transformation. It was speculated that most of the phosphate ions are fixed as neutral –OH groups on $\text{Nb}_2\text{O}_5\text{-nH}_2\text{O}$ without covering Lewis acid sites, which might reduce undesirable side reactions [107]. Another possibility is that NbO_4 tetrahedra species having effective positive charges as Lewis acid sites are still active in water even after the formation of $\text{NbO}_4\text{-H}_2\text{O}$ adducts.

In the water-2-butanol (2:3, v/v) biphasic system, niobic acid treated with 1 M phosphoric acid and calcinated at 300 °C (abbreviated as NA-p) gives materials with large surface area and strong acidic properties providing effective activity for dehydration of monosaccharides to HMF as well as hydrolysis of polysaccharides to give HMF yields of 89% and 74% successively from fructose and inulin via a one-pot reaction (Table 1, Entry 49) [108]. Several modified tantalum oxide catalysts including mesoporous tantalum oxide prepared by acid hydrolysis of tantalum penta-ethoxide in the presence of a triblock co-polymer Pluronic L-121 (a non-ionic surfactant) at room temperature and subsequent calcination at 550 °C for 6 h (Table 1, Entry 50) [109], hydrated tantalum oxide treated with 1 M H_3PO_4 and calcined at 300 °C for 3 h (Table 1, Entries 51 and 52) [110], and mesoporous tantalum phosphate prepared from tantalum tartrate and ammonium phosphate monobasic in the presence of an ionic surfactant at room temperature followed by calcination at 550 °C (Table 1, Entry 53) [111] exhibits high specific surface area, strong acidity and remarkable stability, as well as high catalytic

activity (90%, 58%, 87% and 50–79% HMF yields obtained from fructose, glucose, inulin and juice of Jerusalem artichoke tuber, respectively) in aqueous biphasic systems (e.g. $\text{H}_2\text{O}/\text{MIBK}$, H_2O -2-butanol). Ordovsky et al. [140] demonstrated that the reactivity of glucose conversion decreases in the order of niobium phosphate (NbPO) > zirconium phosphate (ZrPO) > titanium phosphate (TiPO) > aluminum phosphate (AlPO), corresponding to the amount of strong acid sites on these catalysts. It was found that the selectivity to HMF varies in the range of 30–60% and increases with the decrease in the ratio of Lewis to Bronsted acid sites and the density of isolated Lewis acid sites. Treatment of the catalyst with tetraethoxysilane (TEOS) decreased the content of isolated Lewis acidity (Fig. 5), leading to a drastic increase in the selectivity toward HMF owing to the coverage of Lewis acid sites that is non-selective for the desired reaction process. The reaction mechanism was proposed to occur via the adsorption of the carbohydrate substrate (e.g., glucose) onto the Lewis acid site for isomerization, followed by dehydration over an adjacent phosphate group to give HMF.

After screening a series of heterogeneous and homogeneous catalysts including SnO_2 , WO_3 , $\text{SO}_2 + \text{WO}_3$, Sn–W oxide, Amberlyst-15, Nafion NR-50, sulfated zirconia, H-mordenite, H–Y, H_2SO_4 , $\text{H}_3\text{PW}_{12}\text{O}_{40}$, and hydrotalcite (HT), Yamaguchi et al. [112] found that only Sn–W oxide bearing both strong Bronsted (97 $\mu\text{mol g}^{-1}$) and Lewis acid sites (37 $\mu\text{mol g}^{-1}$) [141,142] are active for both glucose isomerization and fructose dehydration, such that HMF yields of 48%, 39%, 42%, and 41% are achieved in $\text{THF}/\text{H}_2\text{O}$ (5/1, v/v) at 120 °C after 18 h from glucose, cellobiose, sucrose, and starch, respectively (Table 1, Entry 54). Behera and Parida [113] prepared different weight percentages (wt.%) of Sn-promoted vanadium phosphate (VPO) catalysts by a wet-impregnation method using water as the solvent, and the 20 wt% Sn–VPO afforded an HMF yield of 74% from glucose in DMSO at 110 °C for 6 h (Table 1, Entry 55). The presence of both Lewis and Bronsted acid sites in Sn–VPO plays an important role in the two reaction processes involving isomerization and dehydration in the one-pot reaction system. Without regeneration at high temperatures, the Sn–VPO catalyst separated by centrifugation and thoroughly washed with acetone could be reused four times with almost constant HMF yields of ~70%. Alkaline earth phosphates including calcium and strontium (i.e., CaP_2O_6 and $\alpha\text{-Sr}(\text{PO}_3)_2$) with same acid strength in the range of $+3.3 \leq \text{H}_0 \leq +4.8$ prepared through a modified co-precipitation method have been employed as heterogeneous catalysts for the transformation of sugars (e.g., fructose, glucose, and cellulose) to HMF in hot compressed water (200–230 °C) [114]. In the hydrothermal system, both phosphate catalysts show similar catalytic reactivity toward the dehydration of monosaccharides after reacting for 5 min, providing HMF yields of 34–39% and 20–21% from fructose at 200 °C and glucose at 220 °C (Table 1, Entries 56 and 57), respectively, whereas the total yield of HMF and glucose from the catalytic hydrolysis and dehydration of cellulose at 230 °C for 5 min with $\alpha\text{-Sr}(\text{PO}_3)_2$ (34%) is higher than

that with CaP_2O_6 (17%). Incorporation of metals such as Zr and Al into mesoporous acidic solid supports like MCM-41 and TUD-1 can give bifunctional solid catalysts that possess both Bronsted and Lewis acid sites that have high surface areas, for which approximately 30% HMF yields have been obtained (Table 1, Entries 58 and 59) [115,116,143].

2.1.3. Modified heteropoly acids

Modification of heteropoly acids (HPAs) with large monovalent cations such as Cs^+ and Ag^+ can overcome their limitations such as high solubility in water and in polar solvents, low surface area and poor thermal stability to allow the design of a range of insoluble, microporous solid Lewis acid catalysts [144]. Shimizu et al. [145] reported on the use of $\text{FePW}_{12}\text{O}_{40}$ and $\text{Cs}_{2.5}\text{H}_{0.5}\text{PW}_{12}\text{O}_{40}$ for fructose conversion in DMSO to give HMF yields of 100% and 91–97%, respectively at conditions of 120 °C and 2 h. Water was removed during the process, which apparently suppresses undesired reactions including the hydrolysis of HMF to LA and partial dehydration of intermediates to condensation products. The removal of adsorbed water from the surface and near-surface of the catalyst can possibly be enhanced by decreasing the catalyst particle size. Fan et al. [117] found $\text{Ag}_3\text{PW}_{12}\text{O}_{40}$ exhibits both Bronsted and Lewis acidities by pyridine adsorption infrared spectroscopy. Using water/MIBK (1/2.25, v/v) as reaction medium, this bifunctional catalyst proved to be suitable for the dehydration of glucose into HMF with a yield of 76% at 130 °C for 4 h, and could be reused for up to six reaction cycles with low leaching (5.1%) of $\text{Ag}_3\text{PW}_{12}\text{O}_{40}$ (Table 1, Entry 60). Acidity modified silver exchanged silicotungstic acid (AgSTA) catalyst catalyzes sucrose degradation (92%) in superheated water to afford HMF in a yield of 63% at 120 °C in 160 min (Table 1, Entry 61) [118] and an HMF yield of 74% with a selectivity of 95% for fructose in the presence of $\text{Cs}_{2.5}\text{H}_{0.5}\text{PW}_{12}\text{O}_{40}$ catalyst in a biphasic system consisting of water and MIBK in 60 min at 115 °C (Table 1, Entry 62) [119]. Notably, only trace amounts of metal leaching determined by UV-vis spectrometry and constant HMF yields are detected for these polyoxometalates after being reused for several times. The high durability of the catalyst can be ascribed to its negligible solubility in water and organic solvents as well as to the stable structure of Keggin-type $\text{PW}_{12}\text{O}_{40}^{3-}$ ions.

An HPA salt of an IL-forming cation functionalized with propanesulfonate, 1-(3-sulfonic acid)propyl-3-methyl imidazolium phosphotungstate ($[\text{MIMPS}]_3\text{PW}_{12}\text{O}_{40}$), was synthesized, and used as a “reaction-induced self-separating catalyst” in the conversion of fructose to HMF [146]. An HMF yield of 99% is realized when the reaction is conducted in 2-butanol for 2 h at 120 °C. Phosphotungstic acid, $\text{H}_3\text{PW}_{12}\text{O}_{40}$ (PTA), encapsulated in MIL-101 (a chromium terephthalate-based mesoscopic metal-organic framework) was also evaluated as an efficient heterogeneous catalyst for the selective dehydration of fructose to HMF (63% yield within 60 min) in $[\text{EMIM}]Cl$ at 80 °C, although the catalytic system was ineffective for glucose-to-HMF conversion [147]. Other catalytic functionalities like Lewis acid or base sites are likely to be required for the achievement of high HMF yields from glucose.

Zhao et al. [120] prepared a Bronsted–Lewis–surfactant-combined HPA $\text{Cr}[(\text{DS})_2\text{PW}_{12}\text{O}_{40}]_3$ (DS: dodecyl sulfate) as a heterogeneous catalyst for the one-pot conversion of cellulose to HMF. The Lewis

acidity of $\text{Cr}[(\text{DS})_2\text{PW}_{12}\text{O}_{40}]_3$ was considered to stem from the electron pair acceptor metal cation (Cr^{3+}), and Bronsted acidity was generated from some protons of PTA molecules. The addition of surfactant DS to the Cr–HPA-based solid acid helps the assemble of micelles in water solutions, by providing a hydrophobic environment sufficient for protecting HMF from further decomposition and by restricting formation of by-products. It was shown that 53% HMF yield with 77% conversion is obtained directly from cellulose in aqueous medium at 150 °C in 2 h (Table 1, Entry 63). The $\text{Cr}[(\text{DS})_2\text{PW}_{12}\text{O}_{40}]_3$ had remarkable stability for approximately six cycles after being subjected to hot CH_2Cl_2 extraction prior to each recycle trial. The same research group designed an analogous Bronsted–Lewis–surfactant-combined cetyltrimethyl ammonium salt of polyoxometalate substituted with a transition metal (Cr^{3+}) [$\text{C}_{16}\text{H}_3\text{PW}_{11}\text{CrO}_{39}$ (C_{16} : cetyltrimethyl ammonium)] [121]. Owing to the formation of micellar assemblies with favorable hydrophobic surroundings, a high concentration of substrate could exist around the catalytic sites, although lower conversions of HMF were observed. In the process of catalytic transformation of glucose and fructose into HMF, $\text{C}_{16}\text{H}_3\text{PW}_{11}\text{CrO}_{39}$ shows high conversion rates (84% and 90%, respectively) and good yields (35% and 41%, respectively) in water at 130 °C (Table 1, Entry 64). Furthermore, the catalyst is able to be recovered by centrifugation from the reaction mixture with a leaching rate of 0.4% as measured by ICP-AES, and it can be reused for six times with fructose conversion rates and HMF yields for all runs remaining around 90% and 40%, respectively. Several factors including the coexistence of both Lewis and Bronsted acid sites in the catalyst and the micellar structure containing hydrophobic groups in coordination contribute to the high catalytic activity.

2.1.4. Zeolites

With respect to sulfated zirconia supported over mesoporous silica (SBA-15) and homogeneous HPAs, Lanzafame et al. [148] demonstrated that microporous materials exhibited higher selectivity/yields of glucose and HMF from cellulose because of the presence of shape-selectivity effects that limit the polymerization of products that form humic-type species. As an example, zeolites composed of SiO_4 and $[\text{AlO}_4]$ tetrahedral are generally covered with micropores, in which the negative charge of $[\text{AlO}_4]$ tetrahedral compensated with H^+ gives zeolites high acidity [149]. An IL/zeolite/ CrCl_2 system was reported to be efficient for selectively producing HMF (48% yield) from cellulose at 120 °C via sequential hydrolysis and dehydration (Fig. 6) [150]. Nevertheless, the imidazolium based ILs are expensive and CrCl_2 is hazardous to the environment. Jadhav et al. [151] replaced the chromium salt with H-ZSM-5 zeolite to achieve a 45% yield of HMF from glucose in $[\text{BMIM}]Cl$ at 110 °C after 8 h. Moreover, the IL solvent could be substituted with a non-toxic ammonium salt, tetrabutylammonium chloride (TBAC), to give an even higher HMF yield of 56% at 110 °C within 4 h.

To improve the catalytic performance of Beta zeolite for the direct transformation of glucose into HMF, Otomo et al. [122] examined the effects of calcination and steam treatment on the structure of Al atoms in the framework and its acidic properties. It was found that the amount of Lewis acid sites increases at the expense of Bronsted acid sites by partial cleavage of Si–O–Al bonds in the framework to form Al species out of the *BEA framework, when the

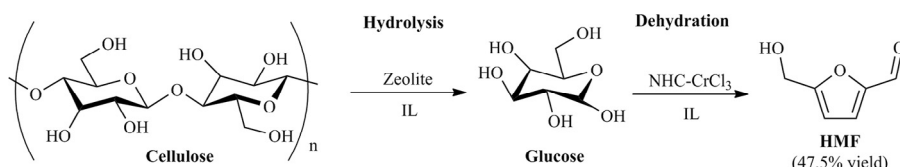


Fig. 6. Conversion of cellulose to HMF (5-hydroxymethylfurfural) over NHC–metal/zeolite catalysts in IL. Adapted with permission from Ref. 150, Copyright © 2011, Elsevier.

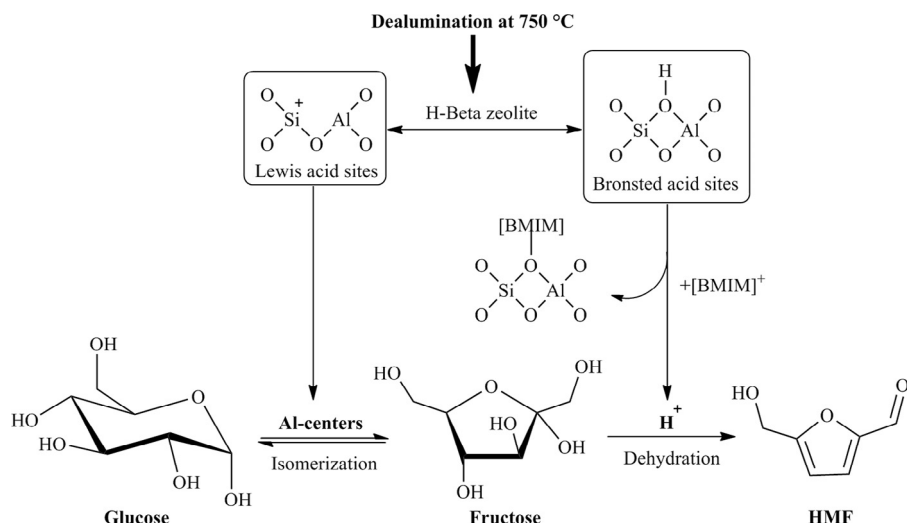


Fig. 7. Schematic of glucose-to-HMF (5-hydroxymethylfurfural) dehydration over H-Beta zeolite calcined at 750 °C. Adapted with permission from Ref. 126, Copyright © 2014, Elsevier.

ammonium-type Beta is calcined at temperatures greater than 700 °C or is treated with steam (50 kPa in N_2 balance) at temperatures more than 500 °C. These bifunctional catalysts bearing Lewis acid sites are effective for the production of HMF from glucose, and H-Beta (Si/Al: 15) prepared by calcination at 750 °C shows a high HMF selectivity (55%) at 78% conversion of glucose in $\text{H}_2\text{O}-\text{DMSO}/\text{THF}$ reacting at 180 °C for 3 h (Table 1, Entry 65). With ^{13}C NMR, the authors clarified that glucose molecule are first isomerized to fructose through an intramolecular hydride transfer, and the generated intermediate is subsequently dehydrated to HMF over Bronsted acid sites (Fig. 7). The Beta zeolite catalyst could be recovered by filtration and regenerated by simple calcination and the HMF yield varied from 43% to 40% for five consecutive runs. Employing [BMIM]Cl as the reaction medium, H-Beta zeolite with a moderate Si/Al ratio of 25 has high catalytic activity due to the presence of Bronsted and Lewis acid sites of the material that are in a suitable ratio (1.03), leading to 50% HMF yield with 81% glucose conversion (Table 1, Entry 66) [123]. Furthermore, the combined use of H-Beta (Si/Al: 25) and [BMIM]Cl allows multiple recycle with non-varying HMF yields after calcination at moderate conditions and is efficient for transformation of other di- and poly-carbohydrates such as sucrose, cellobiose, starch and cellulose into HMF with consistent yields (ca. 45%). Apart from dealumination of zeolites, bimodal-HZ-5 zeolite (Si/Al: 30.15) with a Bronsted/Lewis acid ratio of 0.817 fabricated by modification of H-ZSM-5 (Si/Al: 37.00) with desilication is also efficient for the hydrolysis of microcrystalline cellulose to HMF [124]. The post-synthesized heterogeneous catalyst exhibits improvement in total surface area, total pore volume and total acidity as compared with the parent H-ZSM-5, and enhanced HMF yields of 46% for a cellulose conversion of 67% can be obtained (Table 1, Entry 67). It is clear that the modification of commercial zeolites through either dealumination or desilication allow improvement of material

properties such as total surface area, pore volume/size and acidity, and allow the development of robust catalysts for producing HMF.

Sn-Beta zeolite has been reported to facilitate the isomerization of glucose to fructose in aqueous media even at low pH [152,153]. Nikolla et al. [125] described the combination of Sn-Beta with a Bronsted acid HCl in a biphasic reactor system ($\text{H}_2\text{O}/\text{THF}$ or $\text{H}_2\text{O}/1\text{-butanol}$) to synthesize HMF from carbohydrates such as glucose (Fig. 8), cellobiose, and starch with HMF selectivities over 70% at sugar conversions of around 75% at 180 °C. For Sn-Beta, the addition of HCl to give a solution pH to 1 affords an improved HMF yield (Table 1, Entries 68–70). The addition of inorganic salts (especially NaCl) results in efficient extraction of HMF from the aqueous phase to the organic phase, thus improving HMF selectivity (Table 1, Entries 70–73). Combination of a solid Bronsted acid Amberlyst-70 (a macroporous polymeric catalyst) with a Lewis acid Sn-SBA-15 (a mesoporous molecular sieve) or Sn-Beta for HMF synthesis from sugars in a monophasic system using γ -lactones, THF or THF/MTHF with water in a weight ratio of 9:1 affords high selectivity for HMF (up to 70%) at glucose conversions of ~90% at 130 °C in 15–60 min (Table 1, Entries 74–78) [126]. Although water is known to promote side reactions in the dehydration of carbohydrates, it can be beneficial at low concentrations for increasing the solubility of sugars in the reaction phase. The effectiveness of glucose isomerization by the catalyst can be speculated to control the HMF selectivity, which is determined by the extent of fructose formation in different solvents (i.e., THF > THF/MTHF \approx GVL) [126]. Although Sn-Beta predominantly isomerizes glucose to fructose via 1,2-intramolecular hydride shift in both water and alcohol (e.g., methanol), Lewis acidic open Sn sites with Na-exchanged silanol groups instead of proximal silanol groups are active for glucose-mannose epimerization [154]. Therefore, an appropriate choice of

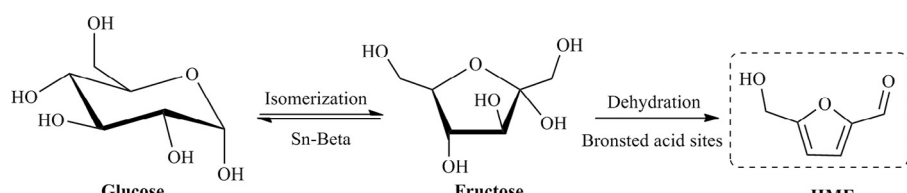


Fig. 8. Sn-Beta combined with Bronsted acid sites for glucose-to-HMF (5-hydroxymethylfurfural) dehydration.

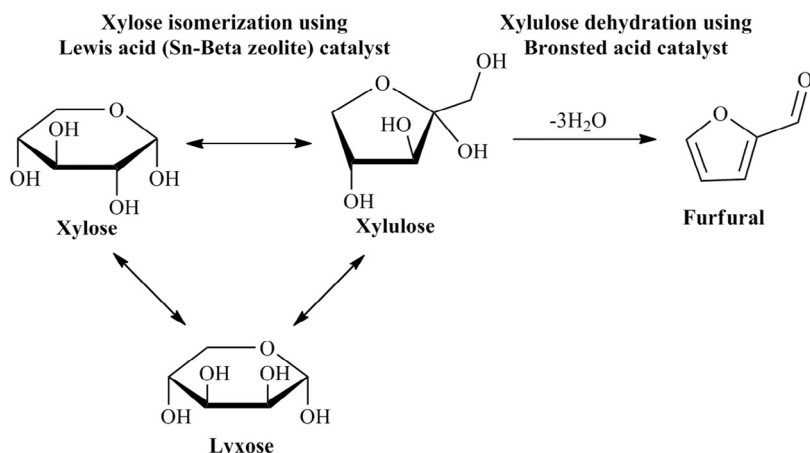


Fig. 9. Lewis/Bronsted acid catalyst mediated xylose-to-furfural conversion. Adapted with permission from Ref. 158, Copyright © 2011, American Chemical Society.

solvents and catalytic materials with well-controlled functional groups/sites are crucial to obtain desired products in high yields.

2.2. Synthesis of furfural from pentoses

Among various bio-derived furan-type compounds, furfural is a building-block chemical since its derivatives like MF, MTHF, THF, and FFa are potential biofuel components, industrial solvents, and key feedstocks [155–157]. Furfural produced from pentosan-rich biomass by xylose cyclodehydration seems to proceed through a sequence of cascade reactions involving Lewis acid-catalyzed isomerization of xylose to xylulose and Bronsted acid-catalyzed dehydration of xylulose to furfural (Fig. 9) [159,160]. In a non-enzymatic route for xylose isomerization with the presence of a single Lewis acid catalyst Sn-Beta zeolite in an aqueous solution, xylulose and lyxose are the primary and secondary products, respectively [158]. At ~60% xylose conversion, a maximum xylulose yield of 27% with an 11% yield to lyxose is attained at 100 °C in 15 min. Analysis shows that xylulose was thermodynamically and kinetically favored over lyxose [161]. Thus, Bronsted-acid-catalyzed dehydration of xylulose to furfural is faster than that of xylose to furfural, and the combined use of Sn-Beta with a Bronsted acid catalyst (HCl or Amberlyst-15) can produce furfural from xylose in a single pot at temperatures (~110 °C) that are typically lower than those required for this reaction [158]. A furfural yield of ~38% is obtained using a combination of Lewis (CrCl₃) and Bronsted (HCl) acids compared with ~29% using HCl alone at moderate temperatures (145 °C) in a single aqueous phase, and a 76% yield of furfural is obtained with the same combination of catalysts in a biphasic system using toluene as extractant (Table 2, Entries 1–3) [162].

2.2.1. Molecular sieves

The isomerization of xylose to xylulose allows formation of furfural by facilitating the process of dehydration. Lewis acid sites promote xylose isomerization, but lower furfural selectivity by catalyzing side reactions between xylose and furfural to form humins (insoluble degradation products) [181,182]. Bronsted acids such as H₂SO₄, Amberlyst-15, MCM-SO₃H, and SBA-15-SO₃H protonate the hydroxyl groups on the xylose to promote furfural formation [183–188], but at a lower rate than Lewis acids [189,190]. To design efficient aqueous-phase dehydration catalysts, it is necessary to have an appropriate distribution of Bronsted to Lewis acid sites (Table 2). As an example, MCM-41 (Table 2, Entry 4) provides furfural in 44% yield from xylose (97% conversion) at 170 °C after 3 h in *n*-BuOH/H₂O (3:2, v/v) solvent probably due to its high specific surface area (800 m²/g), good adsorption capacity (average pore diameter = 3 nm),

sufficient pore volume (0.70 cm³/g) and acidity (10 μmol/g surface acidity with a high Lewis/Bronsted acid sites ratio of ~15/1) [163]. Incorporation of niobium into MCM-41 with Si/Nb molar ratios of either 25 or 50 (Lewis/Bronsted acid sites ratio: ~1/5–8) has higher reactivity for xylose conversion (up to 99%) but lower selectivity to furfural (39%) in toluene/H₂O (7:3, v/v) (Table 2, Entry 5), the formed terminal Nb—OH protons or Bronsted acidic protons associated with Si—O—Nb bridges may be responsible for the enhanced substrate conversion, but lead to the occurrence of side reactions (e.g., condensation) to lower the selectivity of product [164]. Microporous AM-11 crystalline niobium silicate prepared from a gel with molar compositions of 11.5Na₂O:8.2SiO₂:Nb₂O₅:418.6H₂O gives a xylose conversion of 90% and a significantly increased furfural yield of 50% under identical reaction conditions (Table 2, Entry 6) [164]. The microporous AM-11 catalyst is more active than HY zeolite (39% yield at 94% conversion) and mordenite (28% yield at 79% conversion). Appropriate concentration of niobium species (Si/Nb molar ratio: 2.3/1) is important to fix the distribution of Lewis-Bronsted acid sites (molar ratio: ~1/2–3) to obtain high furfural yields. Impregnation, rather than incorporation of niobium into the siliceous network of MCM-41 materials, is another effective method for the dehydration of xylose to furfural (Table 2, Entry 7), for which a significant increase in the furfural yield from 37 to 60% is obtained in the absence and presence of 0.5 g NaCl/g_{aq.sol.}⁻¹ (0.5 g NaCl per gram aqueous solution) when using MCM-Nb16 catalyst with nominal 16 wt% of Nb₂O₅ [165]. The combination of the highly distorted NbO₆ octahedra sites corresponding to Lewis acidic sites with the slightly distorted surface NbO₆, NbO₇ and NbO₈ sites associated with Bronsted acidic sites on MCM-41 [191], as well as the promoting effect of Cl⁻ ions might be the reason for the superior results (Table 2, Entry 7). Among the various supports (i.e., commercial fumed silica, γ-Al₂O₃, MCM-41, and SBA-15 silica) those with different amounts of Nb₂O₅ (4, 12 and 20 wt%), the Al-12Nb catalyst with γ-Al₂O₃ support apparently promotes secondary reactions, as compared with silica supported catalysts, while SBA-12Nb and MCM-12Nb bearing both Bronsted and Lewis acid sites as well as micro-mesoporous structure provide high xylose dehydration rates compared with commercial silica. A xylose conversion of 84% and furfural selectivity of 93% in water/toluene can be obtained with the SBA-12Nb catalyst (Table 2, Entry 8) [166].

To modify the Lewis and Bronsted acid functionality and morphological structure of zeolites, dealumination, desilication, and incorporation of other species have been used and the resulting materials are effective for the isomerization of xylose and subsequent dehydration to yield furfural [192–194]. Under batch conditions, H-MCM-22 zeolite and its delaminated counterpart (ITQ-2),

Table 2

Bronsted-Lewis acid bifunctional solid catalysts used in the conversion of carbohydrate substrates into furfural with summary of reaction conditions, maximum catalytic activity, catalyst reuse and catalyst preparation method.

Entry	Substrate	Catalyst ^a	Reaction condition			Catalytic activity		Reusability		Catalyst preparation		Ref.
			Solvent	Temp	Time	Conv	Yield	Cycles	Yield ^b	Method	Calcination	
1	Xylose (1 wt%)	0.1 M HCl	H ₂ O	145 °C	300 min	–	29%	–	–	–	No	Acid [162]
2	Xylose (1 wt%)	0.1 M HCl + 6 mM CrCl ₃	H ₂ O	145 °C	90 min	–	38%	–	–	–	No	Acid/Cr ³⁺ [162]
3	Xylose (1 wt%)	0.1 M HCl + 6 mM CrCl ₃	H ₂ O	140 °C	120 min	96%	76%	–	–	–	No	Acid/Cr ³⁺ [162]
4	Xylose (15 wt%)	66.7 wt% acidic MCM-41	<i>n</i> -BuOH/H ₂ O (3:2, v/v)	170 °C	3 h	97%	44%	–	–	Activation	560 °C, 6 h	NM ^c [163]
5	Xylose (10 wt%)	100 wt% Nb/MCM-41	Toluene/H ₂ O (7:3, v/v)	160 °C	6 h	99%	39%	3	34%	Sol-gel	400 °C, 4 h	NM [164]
6	Xylose (10 wt%)	100 wt% AM-11 niobium silicate	Toluene/H ₂ O (7:3, v/v)	160 °C	6 h	90%	50%	3	43%	Sol-gel	400 °C, 4 h	NM [164]
7	Xylose (10 wt%)	33.3 wt% Nb ₂ O ₅ /MCM-41	Toluene/H ₂ O -NaCl (7:5, v/v)	170 °C	3 h	~98%	60%	3	~56%	Impregnation	550 °C, 6 h	NM [165]
8	Xylose (20 g/L)	20 wt% SBA-12Nb	Toluene/H ₂ O (1:1, v/v)	160 °C	24 h	84%	93%	–	–	Impregnation	550 °C, 6 h	NM [166]
9	Xylose (3 wt%)	66.7 wt% H-MCM-22 (Si/Al: 24) zeolite	Toluene/H ₂ O (7:3, v/v)	170 °C	16 h	98%	71%	4	~60%	Sol-gel, ion-exchange	540 °C, 6 h	NM [167]
10	Xylose (10 wt%)	66.7 wt% Beta/TUD-1	Toluene/H ₂ O (7:3, v/v)	170 °C	8 h	98%	74%	4	~69%	Sol-gel	600 °C, 10 h	NM [168]
11	Xylose (10 wt%)	del-Nu-6(1)	Toluene/H ₂ O (7:3, v/v)	170 °C	4 h	90%	47%	3	~45%	Swelling ultrasonication	580 °C, 7 h	NM [169]
12	Glucose (0.5 wt%)	H-Beta	GVL-H ₂ O (9:1, v/v)	175 °C	40 min	99%	37%	–	–	Activation	450 °C, 6 h	NM [170]
13	Xylose (10 wt%)	66.7 wt% SAPO-11 silicoaluminophosphate	Toluene/H ₂ O (7:3, v/v)	175 °C	4 h	69%	38%	3	~42%	Sol-gel	550 °C, 6 h	NM [171]
14	Hemicellulose (1 wt%)	25 wt% SAPO-44	Toluene/H ₂ O (1:1, v/v)	170 °C	8 h	–	63%	8	64%	Sol-gel	550 °C, 6 h	NM [172]
15	Hemicellulose (1 wt%)	25 wt% SAPO-11	Toluene/H ₂ O (1:1, v/v)	170 °C	8 h	–	35%	–	–	Sol-gel	550 °C, 6 h	NM [172]
16	Xylose (10 wt%)	66.7 wt% eHTiNbO ₅ –MgO	Toluene/H ₂ O (7:3, v/v)	160 °C	4 h	92%	55%	3	~35%	Exfoliation	No	NM [173]
17	Xylose (10 wt%)	100 wt% TiO ₂ –ZrO ₂	H ₂ O	250 °C	5 min	80%	~35%	–	–	Precipitation	600 °C, 6 h	NM [174]
18	Xylose (10 wt%)	66.7 wt% SO ₄ /ZrO ₂ –Al ₂ O ₃	Toluene/H ₂ O (7:3, v/v)	160 °C	4 h	>90%	50%	3	~40%	Impregnation	650 °C, 5 h	NM [175]
19	Corn cob (10 wt%)	20 wt% SO ₄ /TiO ₂ –ZrO ₂ /La ³⁺	H ₂ O	180 °C	2 h	–	7%	–	–	Precipitation, impregnation	550 °C, 4 h	NM [176]
20	Xylose (10 wt%)	66.7 wt% ZrAlW-MP	Toluene/H ₂ O (7:3, v/v)	170 °C	4 h	98%	51%	4	~42%	Precipitation	630 °C, 5 h	NM [177]
21	Xylose (10 wt%)	66.7 wt% (VO) ₂ P ₂ O ₇	Toluene/H ₂ O (7:3, v/v)	170 °C	4 h	91%	53%	4	~50%	Evaporation	550 °C, 2 h	NM [178]
22	Xylose (10 wt%)	66.7 wt% SO ₄ /ZrO ₂ –Al ₂ O ₃ /SBA-15	Toluene/H ₂ O (7:3, v/v)	160 °C	4 h	99%	53%	3	39%	Impregnation	650 °C, 3 h	NM [179]
23	Xylose (20 wt%)	20 wt% MgF ₂ –PF	Toluene/H ₂ O (1:1, v/v)	160 °C	20 h	79%	71%	–	–	Sol-gel, post-grafting	No	NM [180]

^a Catalyst dosage relative to the substrate.

^b The yield of furfural in the last cycle.

^c NM: not mentioned. TUD-1: a siliceous mesoporous matrix, del-Nu-6(1): a delaminated zeolite, SAPO-11: silicoaluminophosphate, ZrAlW-MP: mixed zirconium tungsten oxides impregnated with aluminum on mesophases (MP) of zirconia, MgF₂-PF: MgF₂ prepared from Mg and perfluorosulfonic (PF) precursor.

furfural yields of up to 71% and 54% are obtained at more than 96% xylose conversion with a water/toluene (3/7, v/v) and a water solvent system, respectively (**Table 2**, Entry 9) [167]. A decrease in the Si/Al ratio from 38 to 24 for H-MCM-22 increases the total amount of Lewis plus Bronsted acid sites and improves catalytic performance without significantly affecting furfural selectivity. With the same Si/Al molar ratio of 24, the ITQ-2 catalyst exhibits comparable catalytic activity to its counterpart H-MCM-22 and correlates with the like total amounts of Lewis and Bronsted acid sites of these materials. The structure of the catalysts can be regenerated by thermal treatment to remove organic residues, and furfural yields in consecutive uses remain approximately constant [167]. In a similar manner, a composite material consisting of commercial nanocrystalline zeolite Beta (Si/Al: 12) in the protonic form incorporated in a purely siliceous TUD-1 mesoporous matrix (denoted Beta/TUD-1) is an effective catalyst for the acid-catalyzed conversion of xylose into furfural and gives a higher furfural yield than bulk Beta (74% vs 54%) at xylose conversions of 98% in H₂O/toluene (3/7, v/v) (**Table 2**, Entry 10) [168]. Delaminated zeolite del-Nu-6(1) with Si/Al: 29, obtained by swelling and ultrasonication of a laminar precursor of Nu-6(2) (i.e., Nu-6(1) with Si/Al: 38) [195], which has a specific surface area about seven times higher than that for proton-exchanged Nu-6(2), promotes the reaction to have a rate of about two times higher than that for H-Nu-6(2), affording a relatively furfural yield of 47% in a water-toluene (3/7, v/v) biphasic reactor system (**Table 2**, Entry 11), compared with 34% in the presence of an H-mordenite sample with Si/Al of ~6 [169]. The yield of furfural from C6 sugar was low with Bronsted acids such as mineral acids (H₂SO₄ and HCl) and A70 (with –SO₃H), Lewis acids (γ -Al₂O₃), and combined Bronsted and Lewis acids (a mixture of γ -Al₂O₃ and A70); whereas the furfural yield was significant when zeolites (H-mordenite and H-Beta) were used, and yields of furfural (>30%) could be produced from glucose by cascade dehydration and decarbonylation using GVL as the solvent (**Table 2**, Entry 12) [170]. Both C₆ and C₅ sugars have the potential to be converted into furfural with zeolite catalysts.

2.2.2. Metal oxides

Despite the advantages of zeolites, many forms are not stable in aqueous solutions under hydrothermal conditions (ca. ~150 °C) [196,197] so that their use requires careful consideration of the reaction system. Silicoaluminophosphate catalysts (SAPO) containing bifunctional Lewis and Bronsted properties are found to have good stability under hydrothermal conditions (**Table 2**, Entry 13) [171], of which SAPO-44 with a Si/P ratio of 44 gives 63% furfural yields for a one-pot conversion with hemicellulose substrate and has constant activity for multiple cycles (**Table 2**, Entry 14) [172]. The catalytic performance of SAPO-11 with a Lewis/Bronsted acid ratio of 0.48 (total acid content: 111 μ mol/g) is superior to its counterpart SAPO-44 with a ratio of 1.3 (total acid content: 119 μ mol/g) in xylose-to-furfural conversions (35% furfural yield; **Table 2**, Entries 14 and 15), indicating the importance of the distribution of Bronsted and Lewis acid sites [171]. Metal oxide-based Bronsted–Lewis acid bifunctional solid catalysts such as exfoliated titanate, niobate and titanoniobate nanosheets (**Table 2**, Entry 16) [173], mixed-oxide TiO₂–ZrO₂ (**Table 2**, Entry 17) [174], sulfated zirconia/titania (**Table 2**, Entries 18 and 19) [175,176], tin–tungsten mixed oxide [198], and Zr–(W,Al) mixed oxides (**Table 2**, Entry 20) [177] are effective solid catalysts in the aqueous-phase dehydration of xylose to furfural. Nevertheless, active water soluble species leach metal oxides and affect the dehydration activity of these catalysts (**Table 2**, Entry 21) [178,199]. Regeneration of the catalysts can be realized by the removal of residual species through the use of H₂O₂ as oxidant or calcinations at certain temperatures (**Table 2**, Entries 22 and 23) [179,180]. To meet the specifications of a clean, renewable, and economical facility for producing furfural from sugars on the industrial

scale, development of robust and stable Bronsted/Lewis acid bifunctionalized solid zeolite-like materials is urgently needed.

2.3. Synthesis of levulinic acid or levulinate esters

Reactions producing LA and levulinate esters (LEs) from sugar molecules represent important pathways for the transformation of biomass to chemicals and biofuels [200–202]. LEs such as methyl levulinate (ML) and ethyl levulinate (EL) have numerous potential applications in the fragrance and flavoring industry and can be used as additives for diesel and biodiesel transportation fuels [203–206], as well as preferred substrates for chemical conversion to many other products [207].

Under relatively harsh conditions (ca. 200 °C) at low sulfuric acid concentrations (\leq 0.01 mol L⁻¹) in methanol solvent, glucose can be rapidly (ca. 10 min) and almost quantitatively converted into a key and stable intermediate product methyl glucoside, which when allowed to react to completion (150 min) provides methyl levulinate in yields of 50% (**Table 3**, Entry 1) [228]. The formation of LA and LEs (24–65% yields) from glucose or cellulose can be obtained with other –SO₃H mono-functionalized homogeneous and heterogeneous materials [e.g., SO₃H–SBA-15, sulfonated chloromethyl polystyrene, 1-(1-propylsulfonic)-3-methylimidazolium chloride ([PSMI]Cl), and [C₄H₆N₂(CH₂)₃SO₃H]_{3-n}H_nPW₁₂O₄₀ (*n*: 1, 2 and 3; HPA ILs)] in various reaction systems (**Table 3**, Entries 2–5) [208–211]. Relatively long reaction times and high temperatures are generally required for high yields of LA and LEs, otherwise alkyl glucopyranosides are likely to be the major products in alcohols at low temperatures (<140 °C) [211].

2.3.1. Molecular sieves

The combination of Lewis and Bronsted acids has a strong synergistic effect on catalytic activity for the direct decomposition of glucose to LA [229–231] as shown in **Table 3**. With respect to the CrCl₃–H₃PO₄ mixed acids, catalytic systems with a CrCl₃/H₃PO₄ ratio of 0.4–0.5 show superior reactivity (**Table 3**, Entries 6–8) [212]. Bronsted acids can increase the H⁺ concentration, facilitating the Lewis acid-mediated glucose-to-fructose isomerization thus enhancing selectivity [232]. In the subsequent dehydration reaction, CrCl₃ and H₂PO₄²⁻/HPO₄²⁻ combine with 2,5-dioxohex-3-enal to form a complex, promoting the decomposition of the intermediates like HMF to LA. In this scenario, zeolites and mesoporous materials offer efficient conversion routes from crude biomass due to their high concentration of active sites, high thermal/hydrothermal stability and enhanced shape selectivity (i.e., the selective accessibility of reactant, intermediate, or product to zeolite pores) [233]. In general, aluminum-free Lewis acidic zeotype materials and mesoporous molecular sieves containing Sn, Ti, or Zr are able to isomerize hexoses, pentoses and trioses, and convert them into desirable chemicals [234–238]. Saravanamurugan and Riisager [213] show that glucose efficiently isomerizes glucose to form fructose in alcoholic media over zeolites such as HY(2.6), HUSY(6), HUSY(30), H β (12.5), H β (19) and HZSM(15) without auxiliary Lewis acid metals (e.g. Sn, Ti and Zr) other than Al. As compared with other zeolites, HUSY(6) containing more Lewis acid sites [239] as well as a certain amount of Bronsted acid sites facilitate the isomerization of (methylated) glucose to fructose and the succeeding dehydration and rehydration to ML in methanol provides relatively high yields (ca. 50%) (**Table 3**, Entry 9).

Metal halides, especially chromium chloride, facilitate mutarotation and isomerization of glucose to fructose with simultaneous dehydration to HMF, and the subsequent rehydration with hydroxium ions affords LA [240,241]. An alternative method is to modify the HY zeolite structure by combining the zeolite and metal halide (CrCl₃) to form a hybrid catalyst for improving the catalytic properties and enhancing LA yields [214]. The catalytic reaction of the

Table 3

Bronsted-Lewis acid bifunctional solid catalysts used in the conversion of carbohydrate or furfuryl alcohol substrates into levulinic acid or its esters with summary of reaction conditions, maximum catalytic activity, catalyst reusability and catalyst preparation method.

Entry	Substrate	Catalyst ^a	Reaction condition			Product	Catalytic activity		Reusability		Catalyst preparation		Ref.
			Solvent	Temp	Time		Conv	Yield	Cycles	Yield ^b	Method	Calcination	
1	Glucose (5.4 wt%)	0.01 mol/L H ₂ SO ₄	MeOH	200 °C	2.5 h	ML	100%	50%	–	–	–	–	Acid [208]
2	Cellulose (21.0 wt%)	33 wt% [PSMI]Cl	54 wt% H ₂ O/EtOH	150 °C	48 h	LA	100%	24%	–	–	Condensation + acidification	–	NM [208]
3	Cellulose (20.0 wt%)	200 wt% HPA ILs	10 wt% H ₂ O/MIBK	140 °C	12 h	LA	100%	63%	6	60%	Condensation + acidification	–	NM [209]
4	Cellulose (5 wt%)	300 wt% CP-SO ₃ H	10 wt% H ₂ O/GVL	170 °C	10 h	LA	100%	65%	3	43%	Sulfonation	–	NM [210]
5	Cellulose (2.8 wt%)	SO ₃ H-SBA-15 (7.1%)	EtOH	140 °C	24 h	EDGP (EL)	94%	80% (0)	–	–	–	–	NM [211]
6	Glucose (1.0 wt%)	72 mol% CrCl ₃	H ₂ O	170 °C	4.5 h	LA	100%	10%	–	–	–	–	Cr ³⁺ [212]
7	Glucose (1.0 wt%)	72 mol% H ₃ PO ₄	H ₂ O	170 °C	4.5 h	LA	37%	8%	–	–	–	–	Acid [212]
8	Glucose (1.0 wt%)	36 mol% CrCl ₃ -H ₃ PO ₄	H ₂ O	170 °C	4.5 h	LA	100%	50%	–	–	–	–	Acid, Cr ³⁺ [212]
9	Glucose (2.5 wt%)	60 wt% HUSY(6)	MeOH	160 °C	20 h	ML	–	50%	5	45%	Activation	550 °C, 6 h	NM ^c [213]
10	Glucose (1.0 wt%)	100 wt% Cr/HY(15) (1:1, w/w)	H ₂ O	160 °C	3 h	LA	100%	62%	–	–	Impregnation	400 °C, 24 h	NM [214]
11	Glucose (2.0 wt%)	100 wt% Fe/HY(2.5) (10 wt% Fe loading)	H ₂ O	180 °C	3 h	LA	100%	62%	5	47%	Impregnation	400 °C, 5 h	NM [215]
12	Cellulose (5.0 wt%)	Fe/HY(2.5) (10 wt% Fe loading)	[BMIM]Br	120 °C	3 h	TRS	–	61%	5	46%	Impregnation	500 °C, 5 h	NM [216]
13	FfA (2.9 wt%)	34 wt% Al-TUD-1	EtOH	140 °C	24 h	EL	100%	80%	–	–	–	–	NM [217]
14	FfA (2.9 wt%)	34 wt% Beta/TUD-1	EtOH	140 °C	24 h	EL	100%	63%	–	–	–	–	NM [217]
15	FfA (2.9 wt%)	34 wt% H-Beta	EtOH	140 °C	24 h	EL	100%	60%	–	–	–	–	NM [217]
16	FfA (2.9 wt%)	34 wt% ITQ-2	EtOH	140 °C	24 h	EL	100%	60%	–	–	Delamination	–	NM [217]
17	FfA (2.9 wt%)	34 wt% H-MCM-22	EtOH	140 °C	24 h	EL	100%	47%	–	–	–	–	NM [217]
18	Glucose (15.0 wt%)	20wt% Ru/HZSM-5	H ₂ O	200 °C	1 h	LA	86%	38%	–	–	Impregnation	500 °C, 4 h	NM [218]
19	Glucose (15.0 wt%)	20wt% Ru/Al-SBA-15	H ₂ O	200 °C	1 h	LA	85%	29%	–	–	Impregnation	500 °C, 4 h	NM [218]
20	Glucose (15.0 wt%)	10wt% Ru/Al-SBA-15	H ₂ O	200 °C	1 h	LA	85%	28%	–	–	Impregnation	500 °C, 4 h	NM [218]
21	Glucose (15.0 wt%)	10wt% Ni/Al-SBA-15	H ₂ O	200 °C	1 h	LA	91%	29%	–	–	Impregnation	500 °C, 4 h	NM [218]
22	Starch (10 wt%)	20wt% Ru/HZSM-5	H ₂ O	200 °C	1 h	LA	81%	25%	–	–	Impregnation	500 °C, 4 h	NM [218]
23	Starch (10 wt%)	20wt% Ru/Al-SBA-15	H ₂ O	200 °C	1 h	LA	82%	32%	–	–	Impregnation	500 °C, 4 h	NM [218]
24	Cellulose (1.25 wt%)	60% H-resin	5 wt% NaCl-H ₂ O	200 °C	5 h	LA	97%	20%	–	–	Ion-exchange	No	NM [219]
25	Cellulose (1.25 wt%)	60% Fe/H-resin	5 wt% NaCl-H ₂ O	200 °C	5 h	LA	91%	33%	–	–	Impregnation	No	NM [219]
26	Glucose (15 wt%)	1.7 wt% GO-SO ₃ H (Lewis type S:O)	H ₂ O	200 °C	2 h	LA	89%	79%	5	45%	Post-grafting	No	NM [220]
27	Glucose (5.0 wt%)	2.5 wt% SO ₄ /ZrO ₂	EtOH	200 °C	3 h	EL	98%	30%	5	27%	Precipitation, impregnation	550 °C, 3 h	NM [221]
28	Sucrose (5.0 wt%)	2.5 wt% SO ₄ /TiO ₂	MeOH	200 °C	2 h	ML	–	43%	–	–	Precipitation, impregnation	550 °C, 3 h	NM [222]
29	Glucose (5.0 wt%)	2.5 wt% SO ₄ /TiO ₂	MeOH	200 °C	2 h	ML	–	33%	5	20%	Precipitation, impregnation	550 °C, 3 h	NM [222]
30	Glucose (5.6 wt%)	50 wt% SO ₄ /ZrO ₂ /SBA-15	MeOH	140 °C	24 h	ML	–	25%	–	–	Post-grafting, impregnation	550 °C, 3 h	NM [223]
31	Glucose (3.9 wt%)	50 wt% SO ₄ /ZrO ₂ /SBA-15	EtOH	140 °C	24 h	EL	–	24%	3	25%	Post-grafting, impregnation	550 °C, 3 h	NM [223]
32	Rice straw (6.7 wt%)	13.3 wt% S ₂ O ₈ /ZrO ₂ -SiO ₂ -Sm ₂ O ₃	H ₂ O	200 °C	10 min	LA	–	70%	3	67%	Precipitation	110 °C, 12 h	NM [224]
33	Cellulose (2 wt%)	100 wt% ZrO ₂	H ₂ O	180 °C	3 h	LA	100%	54%	5	55%	–	No	NM [225]
34	Celllobiose (12.5 wt%)	5 mol% [PyBS] ₅ PV ₂ Mo ₁₀ O ₄₀	H ₂ O	150 °C	3 h	LA	100%	46%	4	45%	Hybridization	No	NM [226]
35	Cellulose (10 wt%)	50 wt% ZrO ₂	H ₂ O	240 °C	20 min	LA	87%	52%	5	40%	Activation	250 °C, 1 h	NM [227]

^a Catalyst dosage relative to the substrate.

^b Yield of LA or esters in the last cycle.

^c NM: not mentioned.

LA: levulinic acid, ML: methyl levulinate, EL: ethyl levulinate, MeOH: methanol, EtOH: ethanol, [PSMI]Cl: 1-(1-propylsulfonic)-3-methylimidazolium chloride, HPA ILs: [C₄H₆N₂(CH₂)₃SO₃H]_{3-n}H_nPW₁₂O₄₀ (n: 1, 2 and 3), MIBK: methyl isobutyl ketone, CP-SO₃H: sulfonated chloromethyl polystyrene, GVL: γ-valerolactone, EDGP: ethyl-D-glucopyranoside, HY/HUSY: Y type zeolites, [BMIM]Br: 1-butyl-3-methylimidazolium bromide, TRS: total reducing sugars, FfA: furfuryl alcohol, GO: graphene oxide, PyBS: a zwitter-ion prepared from pyridine and 1,4-butane sulfone.

hybrid catalysts is predominantly influenced by the type of acid sites (Lewis acidity enhanced by Cr^{3+}), amount of acid sites and strength surface area, hierarchical porous structures and shape selectivity so that high LA yields (ca. 62%) are achieved with the 1:1 weight ratio of CrCl_3 and HY (**Table 3**, Entry 10). A series of Fe/HY zeolite catalysts was composed of HY zeolite and FeCl_3 prepared by wet impregnation method exhibit high acid site density and increased number of Lewis acid sites, in which Fe/HY catalyst with 10% Fe loading provides high catalytic performance with 62% LA yields being obtained from glucose (**Table 3**, Entry 11) [215] with a total reducing sugar (TRS) yield of 61% being obtained from cellulose in [BMIM]Br (**Table 3**, Entry 12) [216]. Those authors [215] show that Lewis acid sites promote isomerization of glucose into fructose and that the combination of Bronsted and Lewis acidity favors the dehydration/rehydration reaction, while the increase in the number of Lewis acid sites might also decrease the yields of LA by promoting the decomposition of glucose and reaction between glucose and furfural to form humins. LA can also be synthesized from xylose conversion involving an intermediate hydrogenation of furfural to FFA assisted by co-produced formic acid under hot-compressed water [242].

Zeolites commonly encounter drawbacks associated with their microporosity including limited accessibility of active sites to the substrate and the existence of strong internal diffusion limitations in the liquid-phase conversion of biomass or biomass-related chemicals. Aluminosilicate catalysts with improved texture properties have been achieved through: (1) use of an organic template for introducing mesopores and obtaining relatively narrow pore-size distributions [243–245], (2) reducing the crystallite sizes of zeolites to the nano-scale and embedding nanocrystalline zeolites into mesoporous silica matrices [246], and (3) delaminating lamellar precursors of zeolites [247,248]. Neves et al. [217] found that several aluminosilicates including mesoporous Al-TUD-1, composite Beta/TUD-1 and nanocrystalline zeolite H-Beta, as well as ITQ-2 and the zeolite counterpart H-MCM-22 are active to transform Ffa into EL in ethanol solvent (**Table 3**, Entries 13–17). Among these catalysts (**Table 3**, Entries 13–17), Al-TUD-1 gives high EL yields (ca. 80%) despite its relatively weak acidity that is essentially of the Lewis type, which might be attributed to its high specific surface area that enhances active site accessibility along with its inhibition of by-products. SBA-15 incorporated with Al by the post-synthesis method with a nominal Si/Al molar ratio of 30:1 and the Ni- or Ru-doped Al-SBA-15 and ZSM-5 catalysts prepared by wetness impregnation have characteristic properties of mesoporous materials (9.23 nm) and an increased acidity (SBA-15: 0.23 mmol/g < Al-SBA-15: 0.45 mmol/g < 10 wt% Ni/Al-SBA-15: 0.53 mmol/g < 10 wt% Ru/Al-SBA-15: 0.64 mmol/g < 20 wt% Ru/Al-SBA-15: 0.81 mmol/g; ZSM-5: 0.51 mmol/g < 20 wt% Ru/ZSM-5: 0.70 mmol/g) [218]. The moderate increase of Ru amount in ZSM-5 and Al-SBA-15 catalysts increases the levels of LA, and provides LA selectivities as high as 44% for glucose for a 20 wt% Ru/ZSM-5 catalyst (**Table 3**, Entries 18–21) [218]. The acid content and porous properties proved to be important keys to control yield and selectivity of LA, wherein the MFI structure of ZSM-5 is suitable for glucose monosaccharide hydrothermolysis while the hexagonal mesoporous structure of Al-SBA-15 is preferable for hydrothermolysis of starch polysaccharide (**Table 3**, Entries 18, 19, 22 and 23).

2.3.2. Resins and oxides

For polymer based acid ion-exchange resins with Bronsted acid, the incorporation of Lewis acid sites enhances their reactivity for carbohydrate-to-LA transformations. Fe-resin prepared by modification of Dowex 50 with Fe^{3+} through cation exchange shows both Bronsted and Lewis acidity, and gives 91% conversion of cellulose and ~80% total selectivity of glucose (39% yield) and LA (33% yield) in 5 wt% NaCl aqueous solution (**Table 3**, Entries 24 and 25) [219].

Graphene oxide (GO)-based solid catalysts with SO_3H functional groups (GO– SO_3H) are efficient for the selective decomposition of glucose into LA giving a yield of 78% for glucose conversions of 89% (**Table 3**, Entry 26) [220]. Lewis acid sites caused by the electron inductive effect of the S=O double bonds in the surface sulfate complex [249], together with the presence of other functional groups such as carboxyl and hydroxyl play positive roles in enhancing the isomerization and adsorption of glucose for the reaction. The layered morphology of GO– SO_3H allows rapid diffusion of the reactants and products, and the SO_3H groups are thermally stable and do not cause leaching into the reaction mixture. Introduction of Bronsted acid sites such as phosphate [250,251], sulfate [221–223], and superacid groups [224] into metal oxides (e.g., ZrO_2 , SnO_2 and TiO_2) bearing Lewis acid or Lewis base sites responsible for glucose-to-fructose isomerization [225] gives moderate to good catalytic performance for sugar-to-LA/LE transformations (**Table 3**, Entries 27–33).

To identify the dominant reaction routes for the synthesis of LA from sugars, Yang et al. [252] studied acid-mediated conversion of glucose and fructose in aqueous solutions with density functional theory (DFT). The dehydration of fructose catalyzed by a Bronsted acid catalyst is preferential for protonating –O2H hydroxyl group, thus there are a number of potential reaction paths to HMF. The succedent rehydration of HMF to give LA is difficult and competes with polymerization or condensation processes that result in the formation of humins. When glucose is the reactant, the –O1H group is the preferred protonation site. In this case, HMF is unable to be formed in the relevant reaction paths, which leads to humin precursors and reversion products. However, in the DFT simulations, LA can be produced from glucose through a reaction mechanism possibly without forming fructose and HMF intermediates, since protonation of other sites including –O2H, –O3H and –O5 positions is able to activate glucose at a lower rate. Nevertheless, these simulation results are in contradiction with the known reaction pathway to some extent, since fructose and HMF are key intermediates for LA formation from sugars containing glucose units. Hence, an alternate route can be hypothesized for sugar-to-LA transformation, in which five-membered ring carbocations are initially generated by direct activation of the –O1H, –O2H, –O3H and –O5 sites, followed by a sequence of acid-catalyzed isomerization reactions to some specific intermediates that are dependent on catalytic systems and that ultimately lead to LA by decarboxylation.

Li et al. [226] reported one-pot transformation of cellobiose into LA and formic acid via an aqueous phase partial oxidation (APPO) process illustrated in **Fig. 10**, wherein both the Bronsted-acidic sites in the IL cations and the redox catalytic sites in the polyoxometalate (POM) anions of $[\text{PyBS}]_5\text{PV}_2\text{Mo}_{10}\text{O}_{40}$ catalyst are involved. At an oxygen partial pressure of 3 MPa, 100% cellobiose conversion with 46% selectivity to LA and 26% selectivity to formic acid is obtained (**Table 3**, Entry 34). The prepared $[\text{PyBS}]_5\text{PV}_2\text{Mo}_{10}\text{O}_{40}$ is remarkably stable and gives LA selectivities of about 45% for multiple uses. Examination of the spent catalyst with ^{51}V NMR spectroscopy of the spent catalyst did not reveal any evidence of impurities or degradation. In contrast, the simple catalytic material ZrO_2 provides LA yields of 52% through catalytic partial oxidation of cellulose in aqueous media under lean air pressure of 2.4 MPa with 2.8% O_2 at 240 °C in 20 min (**Table 3**, Entry 35) [227]. In this catalytic process, gluconic acid rather than HMF is the key intermediate to produce LA (**Fig. 10**), thus this shows the importance of redox over acid–base properties for the ZrO_2 catalyzed oxidative deconstruction of cellulose. Recycle of the ZrO_2 catalyst gave yields of LA that slightly decreased from ~50% to ~40% over five uses, for which the ZrO_2 catalyst was only regenerated once by facile calcination at 250 °C after the first cycle.

It can be deduced that the isomerization of glucose into fructose promoted by Lewis acid sites is a key step for transforming glucose units into LA or its esters and the hydrolysis/dehydration/rehydration reactions are favorable with combination of Bronsted

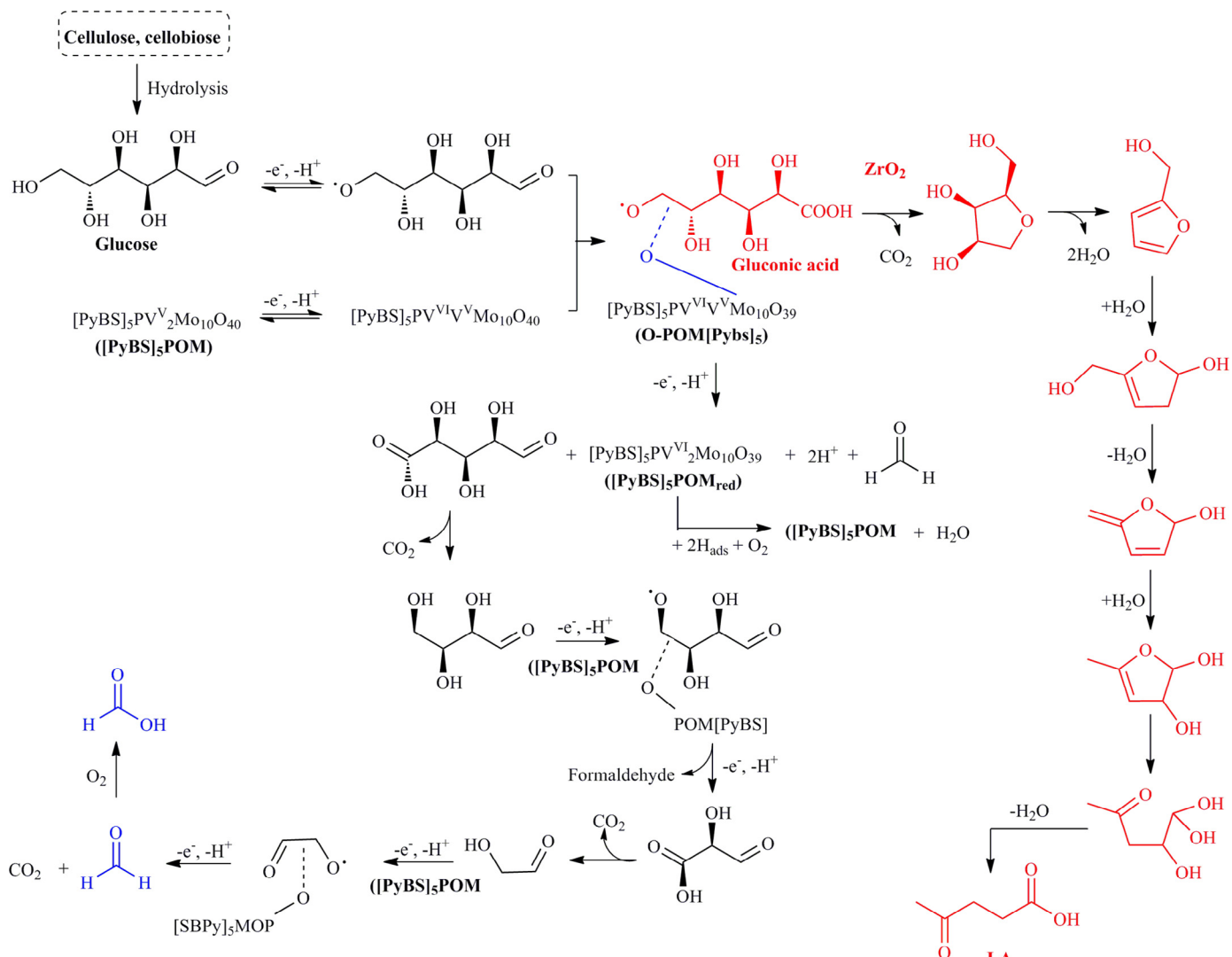


Fig. 10. Pathways for the transformation of cellulose/cellobiose into levulinic acid (LA) and formic acid via an aqueous phase partial oxidation (APPO) process. Adapted with permission from Refs. 226 and 227, Copyright © 2014 Wiley-VCH; Copyright © 2012 Royal Society of Chemistry.

and Lewis acid sites. Nevertheless, the increase in Lewis acidity may also decrease the yield of LA or its esters by promoting nonselective decomposition of glucose units and the reactions among substrates, intermediates (e.g., fructose and HMF) and products to form soluble polymers and humins [253]. The integration of acidic sites with redox properties allow catalysis of the partial oxidation of glucose or cellulose to gluconic acid other than HMF, followed by decarboxylation to yield LA. Therefore, the development of functional catalytic materials containing acidic sites appropriately combined with other active species that can promote different reaction pathways shows great potential for efficient valorization of biomass to LA and other biorefinery products.

2.4. Other methods and products

2.4.1. Catalytic fast pyrolysis (CFP) for coke

The ideal process for conversion of solid biomass into liquid fuels would be one that could occur in a single step at short reaction times. Catalytic fast pyrolysis (CFP) is a promising candidate for converting oxygenated compounds generated from pyrolysis into gasoline range aromatics in the presence of a zeolite catalyst (Fig. 11) [254–257]. Among the various zeolites such as silicalite, Beta,

Y-zeolite and silica–alumina, HZSM-5 (Si/Al: 600) has superior aromatic yields and gives the least amount of coke with more than 30 molar carbon% of aromatics being obtained from glucose, xylitol, cellobiose, and cellulose at a reaction temperature of 600 °C and a reaction time of 240 s [258]. In pyrolysis, HZSM-5 zeolites with high silica-to-alumina ratios, which correlate with a large separation of acid sites, are effective for eliminating methoxyl groups, cleaving ether and aliphatic C–C bonds, and dehydrating aliphatic hydroxyl groups [259]. Bronsted acid sites have a critical role in the upgrading reactions in consideration of HZSM-5 more active than silicalite-1 [260,261]. Lewis acid sites play an important role in hydrogen atom transfer that is a major factor in aromatization [262,263]. For example, Zn-doped HZSM-5 improves furan conversion (100% vs. 80%), yielding more benzene (72% vs. 29%), carbon oxides (6% vs. 3%), and alkenes (>6% vs. ~6%) than native HZSM-5 catalyst at 500 °C within 13 min [264]. H-atom transfer activity, possibly correlated to the Lewis acid sites offered by exchanged Zn cations, is important for high aromatic yields, and probably suppresses the alkylation of benzene to toluene. Cheng et al. [265] report that Ga-promoted HZSM-5 catalysts increase the yield of aromatics through CFP process by 40% compared with that of standard HZSM-5 catalysts, in which Ga catalyzes both the desired

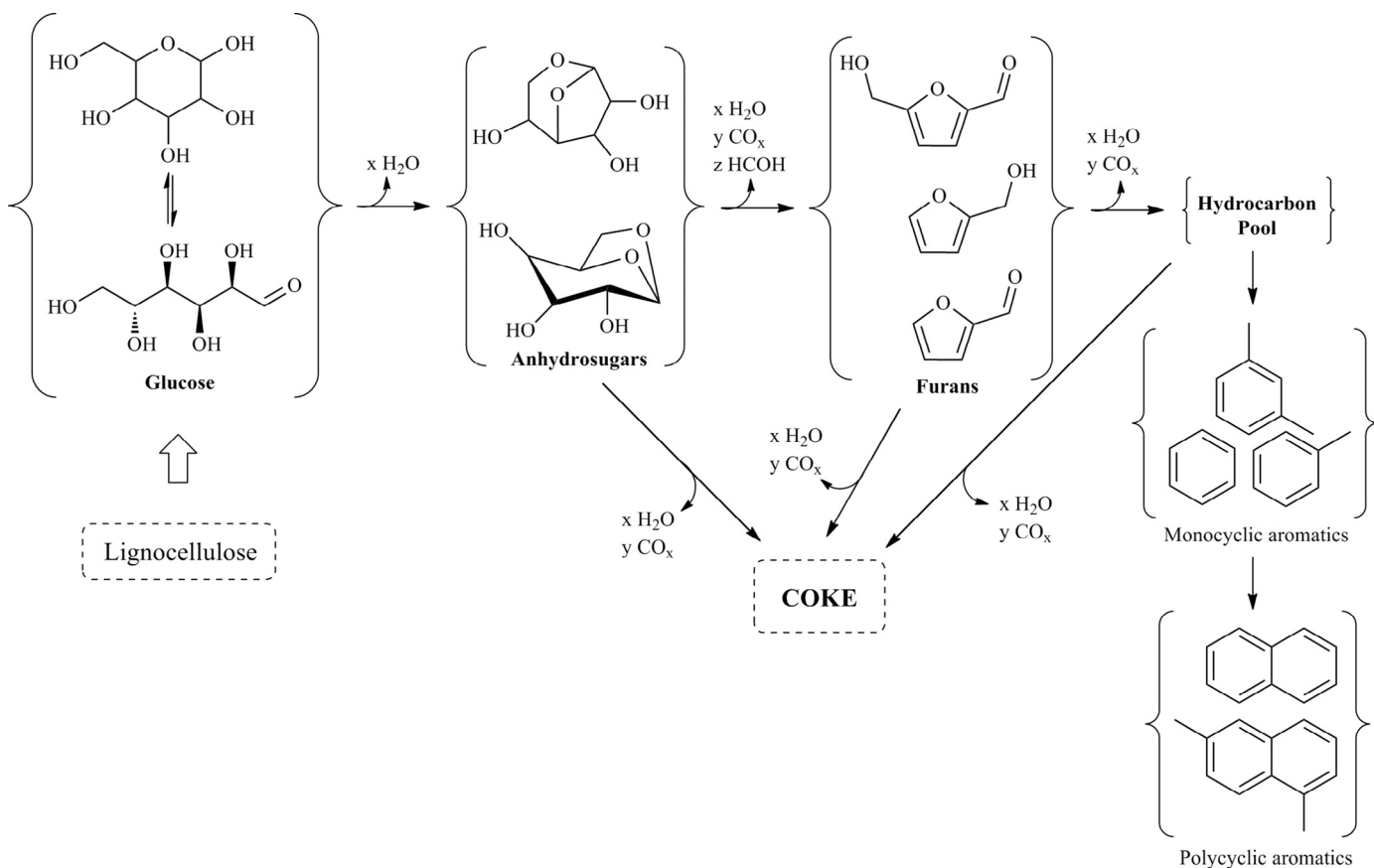


Fig. 11. Possible routes for catalytic fast pyrolysis (CFP) of glucose over a zeolite. Adapted with permission from Ref. 254, Copyright © 2010 Elsevier.

decarbonylation reactions and olefin aromatization, while the ZSM-5 portion of the catalyst promotes the remaining reactions such as oligomerization and cracking to produce aromatics.

The micropore openings in ZSM-5 used in that study had a size in the range of 5.2–5.9 Å which is close to the optimum required for conversion of glucose toward aromatic species [266]. It was shown that the aromatic yield was a function of the pore size of the zeolite catalyst, that is, the majority of aromatics and oxygenated species present during reaction are accessible to the pores of most medium and large-pore zeolites but are excluded from entering small pores. Desilication of HZSM-5 zeolite with 0.5 M NaOH solution creates intraparticle mesopores in the microporous zeolite, producing more aromatic hydrocarbons (carbon yields of 26–30%) and less coke (40–41%) in CFP of beech wood than the parent microporous HZSM-5 (23% aromatics and 44% coke) [267]. Acid dealuminated HZSM-5 (leaching agent of H₃PO₄, H⁺ concentration of 2 mol/L, temperature of 20 °C, and time of 4 h) decreases the coke yield from 44% with original HZSM-5 to 27%, and affords increased yields of target chemicals (14% olefins and 32% aromatics) compared with the original HZSM-5 catalyst (10% olefins and 25% aromatics) [268]. Zeolites with small pores severely hinder the diffusion of both reactants and products and are unable to produce aromatics from glucose, instead yielding a mixture of oxygenates, CO, CO₂ and coke, while zeolites with large pores allow for fast reactant diffusion and lead not only to the formation of larger amounts of polyaromatics, but also to significant coke formation [269]. Several oxygenates such as HMF, furfural and guaiacol might also be formed in relatively high yields [270–273], which would contribute to rapid coke formation and catalyst deactivation on HZSM-5 during pyrolysis oil upgrading [274].

2.4.2. Phthalic anhydride

As discussed above, furanic compounds (e.g., benzofuran) generated in HZSM-5 nanopores are important intermediates in producing aromatic-range biofuels [275,276]. In the CFP of biomass, a Diels–Aldol reaction followed by a ring-opening process involving dehydration reaction has been reported as the key reaction pathway [277]. Lewis acidity is more effective than Bronsted acidity at catalyzing Diels–Alder cycloaddition among different types of acid catalysts [278,279]. The WO_x–ZrO₂ and zeolite-based catalysts such as HY, H β and Sn β bearing both Bronsted and Lewis acid sites, however, are active for conversion of biomass-derived furans to aromatics under relatively mild conditions (around 200 °C) [280–283]. This dehydration process is inherently difficult, because the formed intermediates are sensitive to heat and readily undergo retro-Diels–Alder reaction [284]. For this issue, mixed sulfonic carboxylic anhydrides used as strong acylating agents rapidly cleave the ether rings with high selectivity to their ring-opened products [285], and an 80% selectivity to phthalic anhydride is obtained from biomass-derived furan and MA after running the reaction for 2 h at 25 °C to form a stable intermediate from the Diels–Aldol product assisted by acetyl methanesulfonate (Fig. 12), followed by dehydration at 80 °C for 4 h to drive the reaction to completion [286].

2.4.3. 5-Ethoxymethylfurfural (EMF)

The compound EMF, which has an energy density of 8.7 kW h L⁻¹, is a promising second generation biofuel [287]. Generally, Bronsted acids catalyze HMF, fructose and fructose-based sugars to produce EMF in high yields, but are inactive for glucose-to-EMF transformation [288–295]. To explore the possibility of directly converting glucose to EMF, Lew et al. [296] developed a catalytic system by

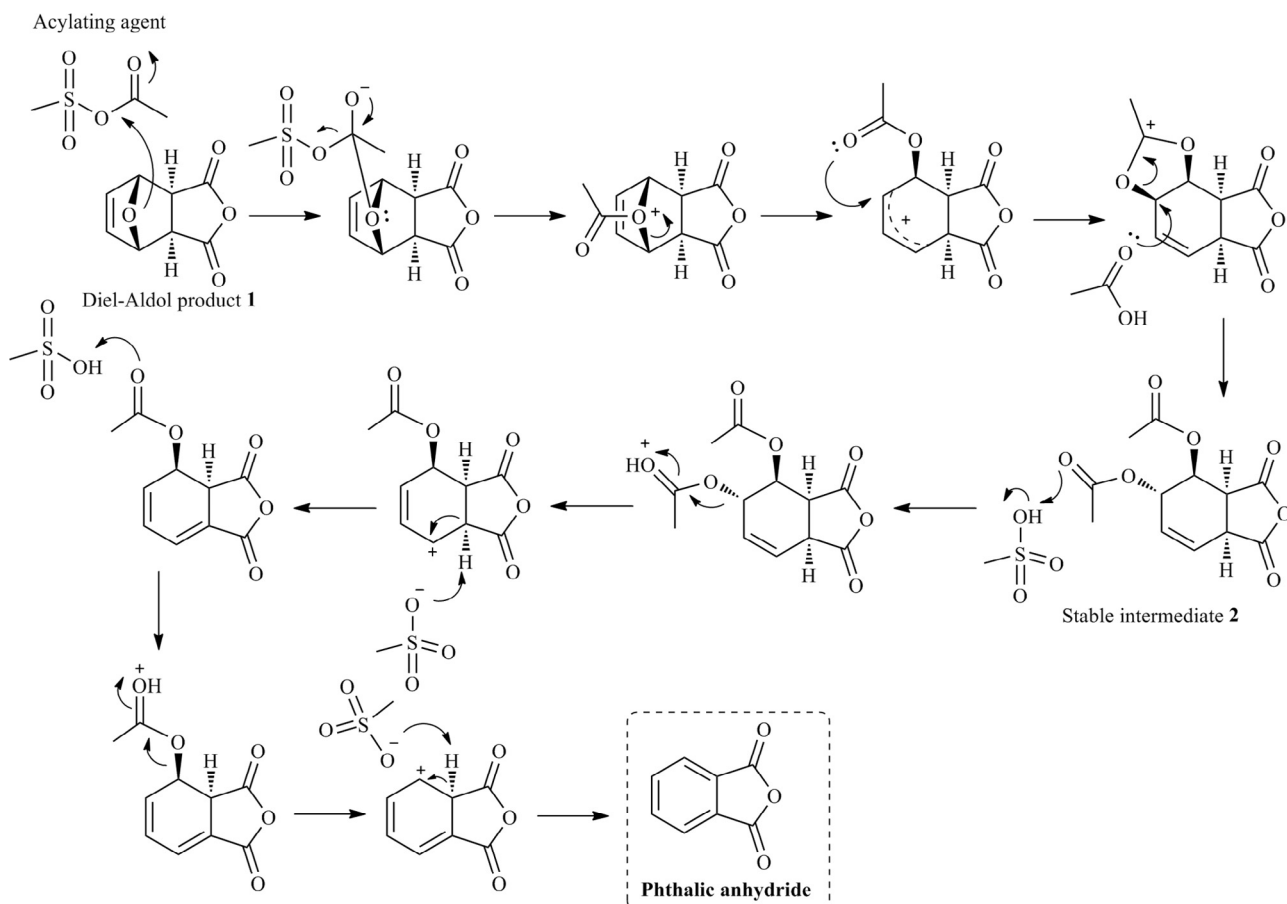


Fig. 12. Synthesis of phthalic anhydride from dehydration of a Diel-Aldol product **1** proceeding through a stable intermediate **2** by using mixed sulfonic carboxylic anhydrides as strong acylating agents. Adapted with permission from Ref. 286, Copyright © 2014 Royal Society of Chemistry.

combining the Lewis acid zeolite Sn-Beta with Bronsted acid Amberlyst 131 in a single pot. In this catalytic system, the isomerization of glucose to fructose proceeds with zeolite Sn-Beta, and the resulting fructose is dehydrated to HMF followed by etherification to afford EMF using Amberlyst 131 (Fig. 13). After reacting at 90 °C for 24 h, an EMF yield of 31% is obtained from glucose in ethanol. EL is readily formed during synthesis of EMF from HMF and fructose in the presence of strong Bronsted acid catalysts at high temperatures [297–299].

2.4.4. Alkyl lactates

In contrast, Lewis acids, especially Sn-Beta, might facilitate the direct conversion of hexoses such as glucose, fructose, and sucrose into alkyl lactates [300–302]. In the catalytic process of sugar-to-alkyl lactate conversion, it is generally accepted that the conversion involves initial isomerization of aldose into ketose, followed by retro-aldol to the corresponding trioses, glyceraldehyde (GLY) and dihydroxyacetone (DHA),

while the use of disaccharides and polysaccharides would entail an additional cleavage to glucose or fructose that could be promoted by Bronsted and Lewis acids [303] before the retro-aldol cleavage (Fig. 14). Various mechanisms have been proposed to explain the conversion of GLY and DHA to alkyl lactates [305–308]. In one reaction pathway, both Lewis acids and weak Bronsted acids such as acetic acid catalyze sequential dehydration and rearrangement of GLY in equilibrium with DHA [309] into pyruvic aldehyde (PAL) [310,311], and the resulting PAL is further converted into the desired alkyl lactates in the presence of a Lewis acid in alcoholic solvents, otherwise an undesirable acetal by-product would be generated in a parallel reaction path under the action of strong Bronsted acid groups (Fig. 14) [304]. A Lewis acid in combination with a weak Bronsted acid is not only effective for the formation of HMF and furfural [312–314], but also plays an important role in catalyzing glucose into fructose [315,316] and retro-aldol reaction of hexoses into trioses to facilitate the formation of alkyl lactates [317–319].

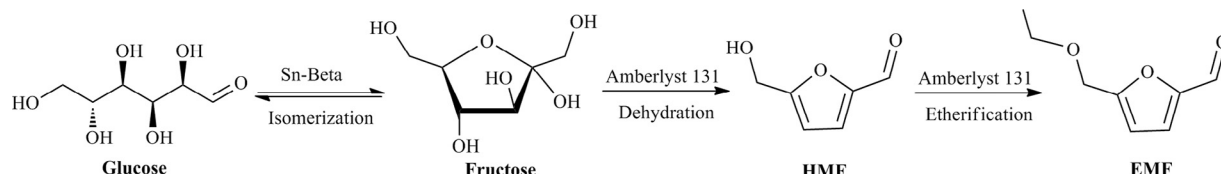


Fig. 13. Combination of Sn-Beta and Amberlyst-15 for glucose-to-EMF (5-ethoxymethylfurfural) transformation involving HMF (5-hydroxymethylfurfural) as intermediate. Adapted with permission from Ref. 296, Copyright © 2012 American Chemical Society.

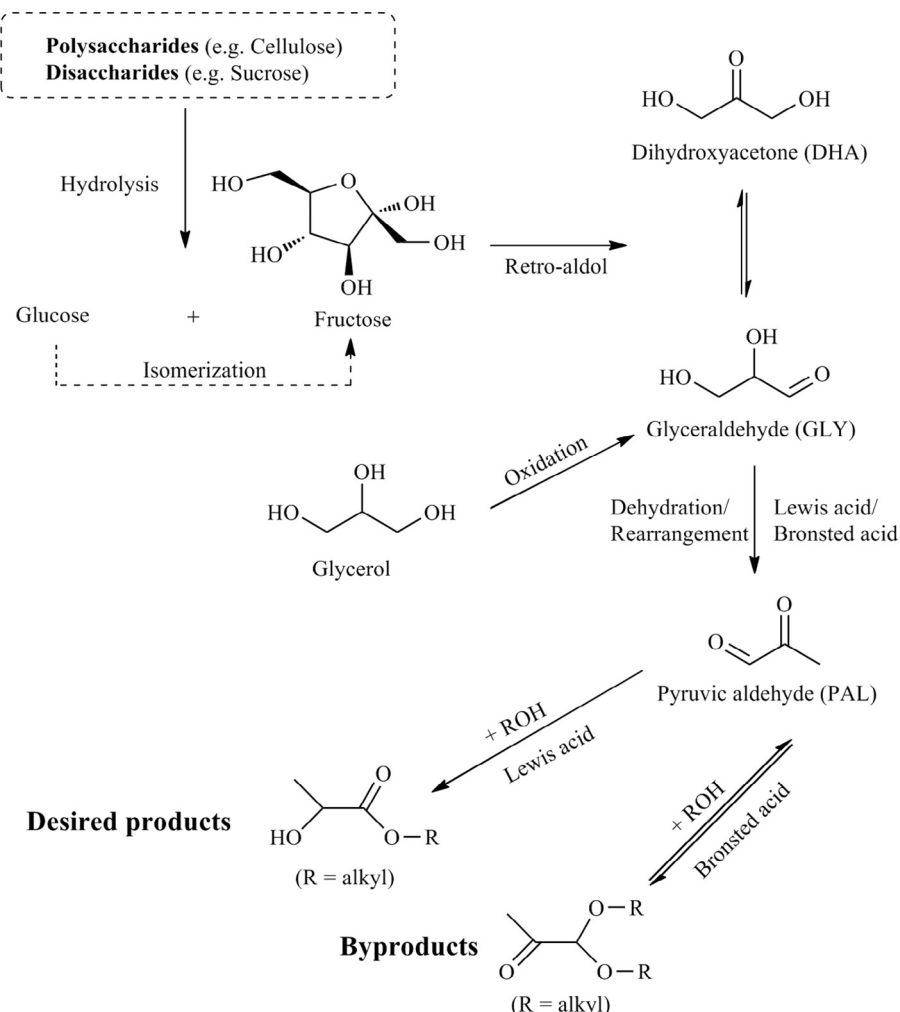


Fig. 14. Plausible pathway for converting sugars into alkyl lactates in alcoholic solvents. Adapted with permission from Ref. 304, Copyright © 2012 American Chemical Society.

Acid catalysts are generally preferable for raw oils containing moisture and free fatty acids (FFAs) in the simultaneous esterification of FFAs and transesterification of triglycerides to produce biodiesel [320,321]. At a reaction temperature (ca. 200 °C), esterification and transesterification steps can be both promoted by a Bronsted catalyst such as 12-tungstophosphoric acid [322,323]. Introduction of Lewis acid sites into the catalytic process can lower the reaction temperature [324–326], implying a synergic effect between Bronsted and Lewis acid sites on simultaneous esterification and transesterification reactions in biodiesel production.

2.4.5. Glycerol-derived chemicals

A significant surge in biodiesel production will cause a surplus of glycerol to exist, and thus glycerol is expected to be among the top 12 most important bio-based chemicals in the world [327]. Selected value-added chemicals that can be obtained from glycerol through various pathways are shown in Fig. 15 [328]. Among these pathways, the glycerol-to-acrolein dehydration is a typical acid-catalyzed reaction.

Two different reaction pathways for glycerol dehydration have been proposed on the basis of the type of acid sites: (1) Bronsted acid sites sequentially promote dehydration of the internal secondary hydroxyl groups and primary hydroxyl groups of glycerol to afford acrolein (Fig. 16a), while (2) Lewis acid sites exclusively catalyze one step dehydration of the primary hydroxyl group of glycerol to produce acetol (Fig. 16b) [329–331]. Foo et al. [332] investigated the

role of Lewis and Bronsted acid sites in the dehydration of glycerol on niobium oxide and Na⁺-exchanged niobium oxide using FT-IR (Fourier transform infrared spectroscopy) supported by DFT calculations. It was found that Lewis acid sites activate primary C–O bonds of glycerol to form 2-propene-1,2-diol, but Bronsted acid sites are involved in the formation of acrolein. Wang et al. [333] demonstrated that exclusively tuning Lewis or Bronsted acid sites does not promote acrolein production from glycerol, and that Bronsted acid sites with neighboring Lewis acid sites in a bifunctional catalyst like zeolite ZSM-5 are necessary for two-step dehydration of glycerol to acrolein. The two-step catalytic process might consist of Bronsted acid sites initiating the reaction via dehydration of the secondary hydroxyl groups of glycerol, and Lewis acid sites completing the reaction in a second reaction step through the dehydration of the primary hydroxyl groups to form acrolein (Fig. 17).

2.4.6. Oxygen-containing precursors for diesel and jet fuels

To form oxygen-containing precursors with carbon chain lengths in the range of the diesel (C₉–C₂₁) [334] and jet fuel (C₈–C₁₆) [335,336], C–C coupling reaction of biomass-derived platform molecules with carbon atoms no more than six is considered to be a promising approach. The groups of Dumesic [337,338] and Huber [339] initially proposed the idea of making C₈–C₁₅ alkanes with furfural as the feedstock by successive aldol condensation, hydrogenation and HDO. In this catalytic process, the aldol condensation is efficiently catalyzed by homogeneous and heterogeneous bases

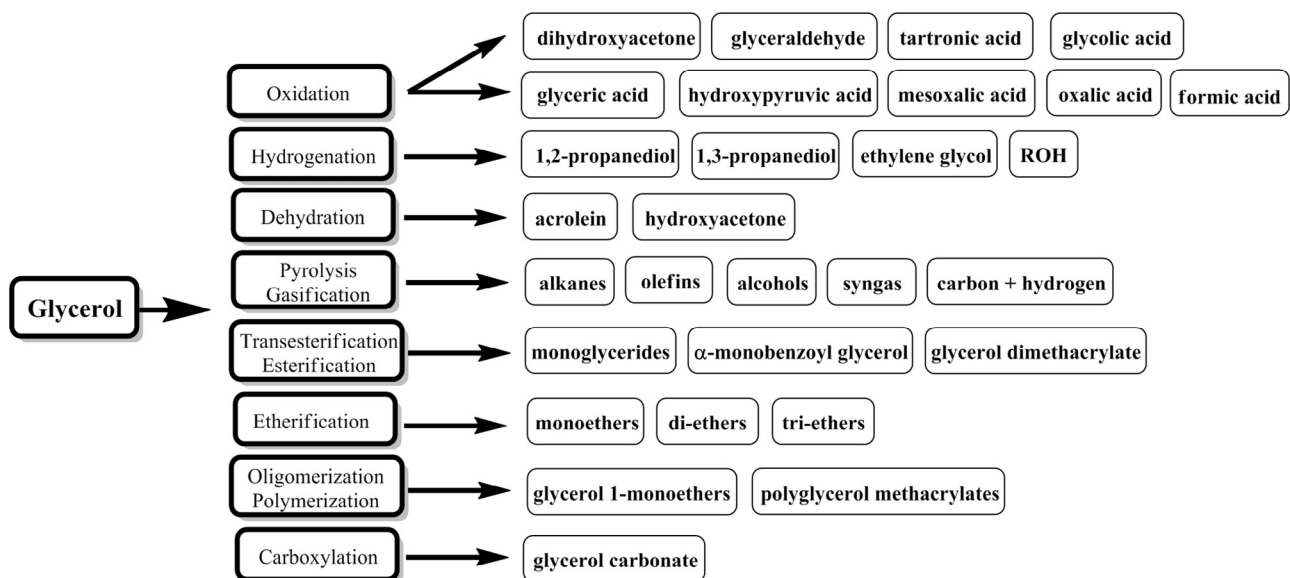


Fig. 15. Value-added chemicals that can be produced from glycerol via catalytic pathways. Adapted with permission from Ref. 328, Copyright © 2014 Elsevier.

[340–343], however, solid acids are seldom employed. Kikhtyanin et al. [344,345] showed that both Lewis and Bronsted acid sites of zeolites (e.g., H-ZSM-5, H-Beta, H-MOR, H-USY and MWW) might be involved in aldol condensation of furfural with acetone to yield 4-(2-furyl)-3-but-en-2-one (FAc) as well as a certain amount of 1,4-pentandien-3-one-1,5-di-2-furanyl (F₂Ac). Unlike base catalysts, an additional product (FAc)₂ was formed as a result of FAc dimerization over Bronsted acid sites (Fig. 18). To determine the role of Lewis and Bronsted acidity in aldol condensation of furfural and acetone, a number of metal organic framework (MOF) materials possessing Lewis acidity have been investigated. Bronsted acidity, lead by structural defects, rather than Lewis acidity of Cu–BTC (copper benzene-1,3,5-tricarboxylate) or Fe–BTC (iron benzene-1,3,5-tricarboxylate) seems to be primarily responsible for the high catalytic performance [346]. Likewise, hydroalkylation/alkylation (HAA) of MF with biomass-derived aldehydes or ketones to carbon-chain increased oxygenates could also be efficiently catalyzed by Bronsted acids [347–352]. Pt-loaded ZrP bearing Bronsted and Lewis acidity showed enhanced catalytic performance for the subsequent hydrogenolysis reaction as compared with Pt-loaded SiO₂–Al₂O₃, TiO₂, and Nb₂O₅ catalysts [353]. In general, the specific activity of small metal particles is superior to large particle counterparts, while the coordinatively unsaturated metal atoms

present in the small particles are prone to cleave C–C bonds as compared with the low index planes that dominates in large particles. In this respect, one more reason for the higher selectivity to C₁₅ alkanes over the Pt/ZrP catalyst can be the result of the larger Pt particle size in the Pt/ZrP catalyst that is helpful to prevent the undesirable C–C cleavage reactions. Both the acidity of solid support and the characteristics of the metal particles are two important factors for improving catalytic activity for multiple-step reactions.

Variation of reaction systems with Bronsted–Lewis acid bifunctional catalytic materials allows a wide range of products to be formed. Further, by adjusting Bronsted–Lewis acid sites, use of active metals or supports along with relevant morphological structures, control of product distributions and reaction pathways is possible. Bifunctional acidic materials are broadening the spectrum of biorefinery products and accelerating practical methods for transforming biomass resources.

3. Acid–base bifunctionalized materials

Acids and bases can be used effectively in solid catalytic materials by spatially isolating acidic and basic sites [354]. Acid–base bifunctionality of a catalyst promotes chemical transformations via active site isolation so that a wide range of biomass conversions are

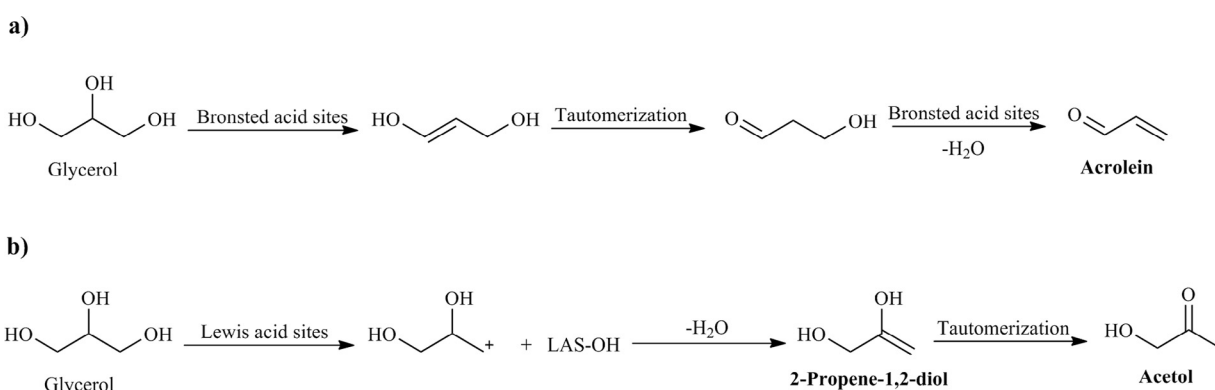


Fig. 16. Proposed reaction pathways of glycerol dehydration on Bronsted acid sites (a) and Lewis acid sites (b). LAS-OH: Lewis acid site -OH. Adapted with permission from Refs. 329 and 330, Copyright © 2010; 2014 Elsevier.

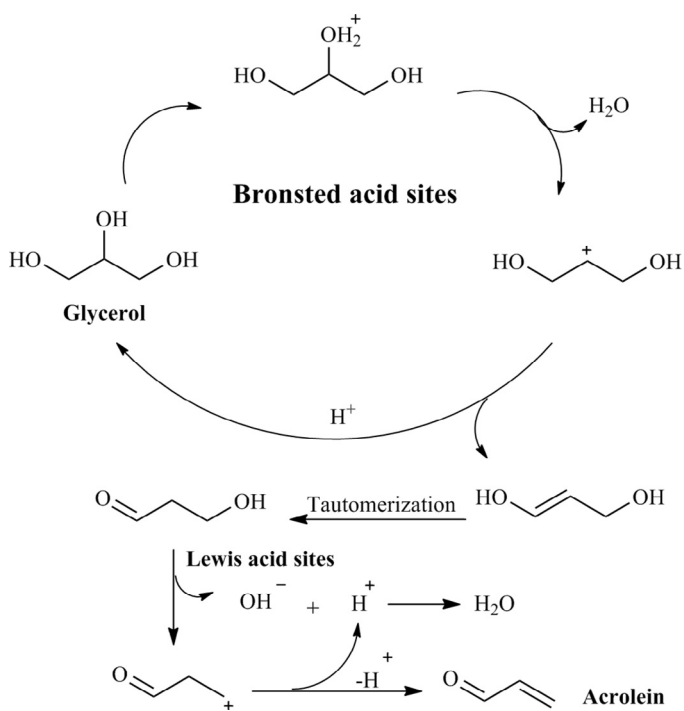


Fig. 17. Proposed reaction pathway for the cooperativity of Bronsted and Lewis acid sites in glycerol dehydration. Adapted with permission from Ref. 333, Copyright © 2014 American Chemical Society.

possible when one considers acid-catalyzed and base-catalyzed routes to a product [355]. Representative studies on catalytic transformation of biomass and its derivatives to selected chemicals are discussed in the following sections.

3.1. HMF and furfural

In hydrothermal systems, homogeneous alkali catalysts are efficient for promoting glucose isomerization to fructose and homogeneous acid catalysts are active for facilitating fructose dehydration to HMF (Table 4, Entries 1–3) [356,357]. Solid acid-base catalysts, namely, metal oxides, anatase TiO₂ (a-TiO₂), rutile TiO₂ (r-TiO₂) and monoclinic/tetragonal mixture ZrO₂ (m/c-ZrO₂) have been employed for the glucose-to-HMF transformation. The metal oxide,

m/c-ZrO₂ has the highest amount of acid sites (0.67 mmol/g) and base sites (0.55 mmol/g), whereas a-TiO₂ has the highest density of acid sites (0.08 mmol/m²) and base sites (0.04 mmol/m²) among these compounds. The a-TiO₂ has superior catalytic activity for the glucose-to-HMF transformation (Table 4, Entries 4–6) [358]. In a study of TiO₂ and ZrO₂ for glucose and fructose conversion in water under microwave irradiation, Qi et al. [359] reported that solid base ZrO₂ could promote isomerization of glucose to 1,2-enediol (fructose), and HMF would be formed by an additional acidic condition (Table 4, Entries 7 and 8). In this regards, ZrO₂ in combination with a solid acid SO₄²⁻/TiO₂–SiO₂ (3:4, w/w) catalyzes the degradation of corn starch hydrolyzate (glucose solution) to attain HMF in a yield of 48% (Table 4, Entry 9) [360].

To enhance the acidity of metal oxides, mineral acids such as H₃PO₄ and H₂SO₄ can be introduced by impregnation [387,388]. Acid-modified oxides show enhanced reactivity in the dehydration of fructose and glucose units to HMF (Table 4, Entries 10–22). For example, sulfated zirconia (SO₄²⁻/ZrO₂) prepared by mixing zirconium hydroxide with 1M H₂SO₄ and subsequent calcination gives a fructose conversion of 94% with an HMF yield of 73% in acetone–DMSO mixtures (Table 4, Entry 10) [361]. Investigation on the bifunctionality of SO₄²⁻/ZrO₂ by further incorporation of aluminum species in varied loadings was carried by Yan et al. (Table 4, Entry 11–13) [362]. Yang et al. found that with an increase in Al content, the number of acid sites decrease while the number of base sites increase so that an optimized HMF yield of 55% could be obtained from starch over SO₄²⁻/ZrO₂–Al₂O₃ catalyst having a Zr/Al molar ratio of 1:1 (acidity: 1.55 mmol/g, basicity: 0.52 mmol/g) (Table 4, Entries 14–16) [363]. Submonolayer SO₄ coverages in sulfated catalysts (SO₄/ZrO₂) with a suitable SO₄ content (~1.5 wt% SO₄) offer an ideal balance of basic and Lewis–Bronsted acid sites (with a molar ratio of ~1/3.55) and promote isomerization of glucose to fructose and subsequent dehydration of fructose to HMF (Table 4, Entries 17–22) [364].

Hydrotalcite (HT), which shares some similar catalytic properties as ZrO₂, is active for promoting isomerization of glucose to fructose, as well as xylose to xylulose [365,389], but HT is inactive for hydrolysis/dehydration reactions (Table 4, Entries 23–28) [366]. In the presence of both HT and Amberlyst-15, HMF is produced in moderate yields (up to ~54%) from glucose, sucrose, and cellobiose in a polar aprotic solvent such as DMSO, N,N-dimethylformamide, and DMA (Table 4, Entries 29–36) [367,368]. Glucose/fructose and xylose/xylulose, galactose/tagatose and arabinose/ribulose are converted into HMF and furfural, respectively, and 5-methyl-2-furaldehyde is produced from rhamnose/rhamnulose under the

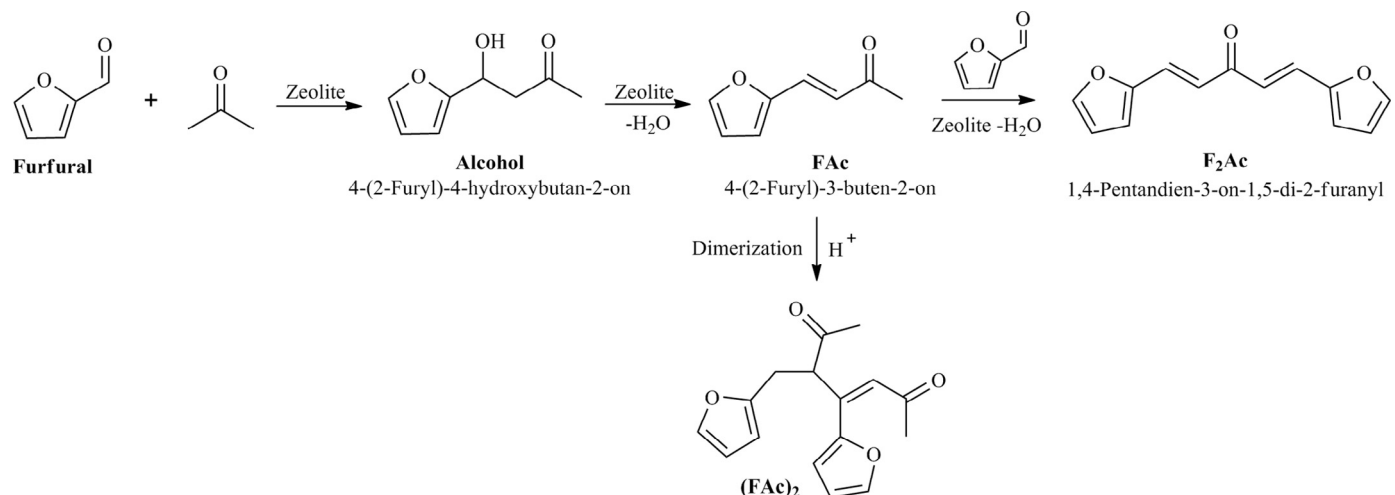


Fig. 18. Reaction pathways for Aldol condensation between furfural and acetone. Adapted with permission from Ref. 344, Copyright © 2014 Elsevier.

Table 4

Acid-base bifunctional materials and selected homogeneous catalytic systems used in the conversion of biomass-related substrates into value-added products with summary of reaction conditions, maximum catalytic activity and catalyst reusability.

Entry	Substrate	Catalyst ^a	Acid/base ratio	Reaction conditions			Main product	Catalytic activity		Reusability		Ref.
				Solvent	Temp.	Time		Conv.	Yield	Cycles	Yield ^b	
1	Glucose (10 wt%)	1 mmol/g H ₂ SO ₄	1/0	H ₂ O	220 °C	5 min	HMF [Fructose]	30%	2% [3%]	NM	NM	[356]
2	Glucose (10 wt%)	1 mmol/g NaOH	0/1	H ₂ O	220 °C	5 min	HMF [Fructose]	30%	2% [11%]	NM	NM	[356]
3	Glucose (10 wt%)	1 mmol/g H ₃ PO ₄	1/0	H ₂ O	200 °C	5 min	HMF	40%	4% [13%]	NM	NM	[357]
4	Glucose (10 wt%)	100 wt% m/c-ZrO ₂	1.22/1	H ₂ O	200 °C	5 min	HMF [Fructose]	50%	6% [13%]	NM	NM	[358]
5	Glucose (10 wt%)	100 wt% a-TiO ₂	2/1	H ₂ O	200 °C	5 min	HMF [Fructose]	82%	20% [2%]	NM	NM	[358]
6	Glucose (10 wt%)	100 wt% r-TiO ₂	0.88/1	H ₂ O	200 °C	5 min	HMF [Fructose]	22%	3% [5%]	NM	NM	[358]
7	Glucose (2 wt%)	50 wt% ZrO ₂	-	H ₂ O	200 °C	3 min	HMF [Fructose]	48%	5% [26%]	NM	NM	[359]
8	Glucose (2 wt%)	50 wt% TiO ₂	-	H ₂ O	200 °C	3 min	HMF [Fructose]	42%	8% [17%]	NM	NM	[359]
9	Glucose (50 wt%)	10 wt% ZrO ₂ + SO ₄ ²⁻ /TiO ₂ –SiO ₂	3/4	H ₂ O/DMSO (1:2, v/v)	120 °C	12 h	HMF	-	48% [48%]	NM	NM	[360]
10	Fructose (2 wt%)	20 wt% SO ₄ ²⁻ /ZrO ₂	-	Acetone/DMSO (7:3)	180 °C	20 min	HMF	94%	73% [73%]	NM	NM	[361]
11	Glucose (7.6 wt%)	16.7 wt% SO ₄ ²⁻ /ZrO ₂ –Al ₂ O ₃ (Zr/Al : 1/1)	2.98/1	DMSO	130 °C	4 h	HMF	72%	48% [5%]	5	35%	[362]
12	Glucose (7.6 wt%)	16.7 wt% SO ₄ ²⁻ /ZrO ₂ –Al ₂ O ₃ (Zr/Al : 9/1)	5.11/1	DMSO	130 °C	4 h	HMF	97%	27% [27%]	NM	NM	[362]
13	Glucose (7.6 wt%)	16.7 wt% SO ₄ ²⁻ /ZrO ₂ –Al ₂ O ₃ (Zr/Al : 1/9)	0.97/1	DMSO	130 °C	4 h	HMF	95%	37% [37%]	NM	NM	[362]
14	Starch (4.5 wt%)	5.3 wt% SO ₄ ²⁻ /ZrO ₂ –Al ₂ O ₃ (Zr/Al : 1/1)	2.98/1	H ₂ O/DMSO (1:5, v/v)	150 °C	6 h	HMF	-	55% [55%]	NM	NM	[363]
15	Starch (4.5 wt%)	16.7 wt% SO ₄ ²⁻ /ZrO ₂ –Al ₂ O ₃ (Zr/Al : 9/1)	5.11/1	H ₂ O/DMSO (1:5, v/v)	150 °C	6 h	HMF	-	38% [38%]	NM	NM	[363]
16	Starch (4.5 wt%)	16.7 wt% SO ₄ ²⁻ /ZrO ₂ –Al ₂ O ₃ (Zr/Al : 1/9)	0.97/1	H ₂ O/DMSO (1:5, v/v)	150 °C	6 h	HMF	-	45% [45%]	NM	NM	[363]
17	Glucose (0.5 wt%)	100 wt% ZrO ₂	1/1	H ₂ O	100 °C	6 h	HMF [Fructose]	21%	<1% [18%]	NM	NM	[364]
18	Glucose (0.5 wt%)	100 wt% SO ₄ /ZrO ₂ (1 wt% SO ₄)	3.25/1	H ₂ O	100 °C	6 h	HMF [Fructose]	23%	1% [19%]	NM	NM	[364]
19	Glucose (0.5 wt%)	100 wt% SO ₄ /ZrO ₂ (1 wt% SO ₄)	3.25/1	H ₂ O	120 °C	6 h	HMF [Fructose]	42%	5% [30%]	NM	NM	[364]
20	Glucose (0.5 wt%)	100 wt% SO ₄ /ZrO ₂ (1.5 wt% SO ₄)	3.55/1	H ₂ O	100 °C	6 h	HMF [Fructose]	21%	1% [16%]	NM	NM	[364]
21	Glucose (0.5 wt%)	100 wt% SO ₄ /ZrO ₂ (5 wt% SO ₄)	10.33/1	H ₂ O	100 °C	6 h	HMF [Fructose]	12%	1% [8%]	NM	NM	[364]
22	Glucose (0.5 wt%)	100 wt% SO ₄ /ZrO ₂ (5 wt% SO ₄)	10.33/1	H ₂ O	120 °C	6 h	HMF [Fructose]	37%	7% [15%]	NM	NM	[364]
23	Xylose (3.3 wt%)	100 wt% Amberlyst-15	1/0	N,N-dimethylformamide	100 °C	3 h	Furfural	51%	<1% [51%]	NM	NM	[365]
24	Xylose (3.3 wt%)	100 wt% HT	0/1	N,N-dimethylformamide	100 °C	3 h	Furfural	60%	0 [60%]	NM	NM	[365]
25	Xylose (3.3 wt%)	100 wt% Amberlyst-15 + 100 wt% HT	1/1	N,N-dimethylformamide	100 °C	3 h	Furfural	57%	24% [57%]	NM	NM	[365]
26	Xylose (3.3 wt%)	100 wt% Amberlyst-15 + 200 wt% HT	1/2	N,N-dimethylformamide	100 °C	3 h	Furfural	72%	37% [72%]	NM	NM	[365]
27	Cellulose (0.3 wt%)	111.1 wt% HT	0.50/1	H ₂ O	150 °C	24 h	Glucose	27%	11% [27%]	NM	NM	[366]
28	Cellulose (0.3 wt%)	111.1 wt% HT–OH _{Ca} (3.38 mg/L Ca)	0.66/1	H ₂ O	150 °C	24 h	Glucose	47%	40% [47%]	NM	NM	[366]
29	Glucose (3.3 wt%)	100 wt% Amberlyst-15 + 200 wt% HT	1/2	N,N-dimethylformamide	80 °C	9 h	HMF	73%	42% [42%]	NM	NM	[367]
30	Sucrose (3.3 wt%)	100 wt% Amberlyst-15 + 100 wt% HT	1/1	N,N-dimethylformamide	120 °C	3 h	HMF	58%	54% [58%]	NM	NM	[367]
31	Celllobiose (3.3 wt%)	100 wt% Amberlyst-15 + 100 wt% HT	1/1	N,N-dimethylformamide	120 °C	3 h	HMF	52%	35% [52%]	NM	NM	[367]
32	Glucose (3.3 wt%)	100 wt% Amberlyst-15	1/0	N,N-dimethylformamide	100 °C	3 h	AHG	69%	32% [69%]	NM	NM	[368]
33	Glucose (3.3 wt%)	100 wt% HT	0/1	N,N-dimethylformamide	100 °C	3 h	Fructose	62%	38% [62%]	NM	NM	[368]
34	Glucose (3.3 wt%)	100 wt% Amberlyst-15 + 200 wt% HT	1/2	N,N-dimethylformamide	100 °C	3 h	HMF [Fructose]	72%	41% [41%]	(AHG)	(41%)	[368]
35	Glucose (3.3 wt%)	100 wt% Amberlyst-15 + 200 wt% HT	1/2	DMA	100 °C	3 h	HMF [Fructose] (AHG)	97%	14% [14%]	NM	NM	[368]

(continued on next page)

Table 4 (continued)

Entry	Substrate	Catalyst ^a	Acid/base ratio	Reaction conditions			Main product	Catalytic activity		Reusability		Ref.
				Solvent	Temp.	Time		Conv.	Yield	Cycles	Yield ^b	
36	Glucose (3.3 wt%)	100 wt% Amberlyst-15 + 200 wt% HT	1/2	DMSO	100 °C	3 h	HMF [Fructose] (AHG)	94%	12% [0] (<1%)	NM	NM	[368]
37	Xylose (3.3 wt%)	100 wt% Amberlyst-15 + 200 wt% Al ₂ O ₃ –Ni–Al	1/2	N,N-dimethylformamide	100 °C	8 h	Furfural	–	46%	NM	NM	[369]
38	Arabinose/rhamnose/lactose (3.3 wt%)	100 wt% Amberlyst-15 + 200 wt% HT	1/2	N,N-dimethylformamide	110 °C	6 h	Furfural [MFD] (HMF)	97%	31% [29%] (32%)	NM	NM	[370]
39	Glucose (50 wt%)	66.7 wt% Amberlyst-15 + 266.7 wt% Na ₂ ZrSi ₄ O ₁₁	1/4	H ₂ O/THF (1/10, v/v)	180 °C	1.5 h	HMF	87%	39%	NM	NM	[371]
40	Glucose (10 wt%)	100 wt% ZrC	0/1	H ₂ O	120 °C	20 min	Fructose	45%	34%	6	29%	[372]
41	Glucose (10 wt%)	100 wt% Amberlyst-15 + 50 wt% ZrC	2/1	H ₂ O/toluene (1/1, v/v)	120 °C	12 h	LA	41%	17%	NM	NM	[372]
42	Sucrose (1.3 wt%)	~50 wt% Amberlite IR120 (H ⁺) + ~300 wt% Amberlite IRA-400 (OH ⁻)	~1/6	H ₂ O or DMF	100 °C	65 h for 4 steps	HMF	~100%	50%	NM	NM	[373]
43	Cellulose (1.3 wt%)	~26.7 wt% LPMSN-both	0.81/1	[EMIM]Cl/H ₂ O (9:1, v/v)	120 °C	3 h	HMF [Glucose]	–	15% [36%]	NM	NM	[374]
44	Cellulose (1.3 wt%)	~26.7 wt% LPMSN–SO ₃ H + LPMSN–NH ₂	1/1	[EMIM]Cl/H ₂ O (9:1, v/v)	120 °C	3 h	HMF [Glucose]	–	19% [39%]	NM	NM	[374]
45	Glucose (6.7 wt%)	100 wt% P-VI-0	0/1	THF/DMSO (1.5/1, w/w)	100 °C	10 h	HMF	–	0	NM	NM	[375]
46	Glucose (6.7 wt%)	50 wt% P–SO ₃ H-154	1/0	THF/DMSO (1.5/1, w/w)	100 °C	10 h	HMF	–	0	NM	NM	[375]
47	Glucose (6.7 wt%)	50 wt% P–SO ₃ H-154 + 100 wt% P-VI-0	1/2	THF/DMSO (1.5/1, w/w)	100 °C	10 h	HMF	–	95%	NM	NM	[375]
48	Fructose (4.5 wt%)	27.8 wt% Lys/PW(2)	6.1/1	EtOH/DMSO (7:3, v/v)	120 °C	15 h	EMF [HMF]	100%	77% [9%]	6	~70%	[376]
49	HMF (2.5 wt%)	50 wt% ZrO(OH) ₂	–	EtOH	150 °C	2.5 h	BHMF	94%	84%	6	47%	[377]
50	HMF (1.2 wt%)	1 mol % Sn-Beta (Sn/HMF molar ratio)	–	2-PrOH	180 °C	6 h	BHMF bis-ether	92%	80%	2	55%	[378]
51	HMF (8.0 wt%)	1 mol % Sn-Beta (Sn/HMF molar ratio)	–	2-PrOH	180 °C	6 h	BHMF bis-ether	83%	48%	–	–	[378]
52	HMF (1.0 wt%)	3 mol % Hf-Beta (Sn/HMF molar ratio)	–	EtOH	120 °C	24 h	BHMF bis-ether	87%	67%	–	–	[379]
53	HMF (1.0 wt%)	3 mol % Zr-Beta (Sn/HMF molar ratio)	–	EtOH	120 °C	24 h	BHMF bis-ether	81%	54%	–	–	[379]
54	Furfural (2.4 wt%)	208.3 wt% Zr–PhyA	0.39/1	2-PrOH	100 °C	2 h	FFA	99%	99%	5	98%	[380]
55	FfA (2.9 wt%)	28.2 wt% SBA-15-SO ₃ H	1/0	1-BuOH	110 °C	4 h	Butyl levulinate	100%	96%	–	–	[381]
56	FfA (3.6 wt%)	1.5 wt% (12.5% SO ₃ H) ArSO ₃ H–Et/Ph–HNS	1/0	EtOH	120 °C	2 h	Ethyl levulinate	–	85%	–	–	[382]
57	Vegetable oil (8.3 wt%) + FFA (4.7 wt%)	5 wt% Li/ZrO ₂	–	MeOH	65 °C	1.25 h	FAME	–	99%	9	90%	[383]
58	Rapeseed oil (5 wt%) + FFA (10 wt%)	3 wt% SO ₄ /ZrO ₂	–	MeOH	200 °C	1 h	FAME	–	86%	5	42%	[384]
59	Waste oil (70 wt%) + FFA (5.2 wt%)	2.4 wt% ZnO–La ₂ O ₃	–	MeOH	200 °C	3 h	FAME	–	96%	NM	NM	[385]
60	Jatropha oil (4 wt%) + FFA (9 wt%)	3 wt% CaO–La ₂ O ₃	–	MeOH	160 °C	3 h	FAME	–	99%	5	75%	[386]
61	Jatropha oil (4 wt%) + FFA (9 wt%)	3 wt% CaO	–	MeOH	120 °C	3 h	FAME	–	96%	5	60%	[386]
62	Jatropha oil (4 wt%) + FFA (9 wt%)	3 wt% La ₂ O ₃	–	MeOH	160 °C	3 h	FAME	–	23%	NM	NM	[386]

^a Catalyst dosage relative to the substrate.^b Product yield in the last cycle.

c NM: not mentioned.

HMf: 5-hydroxymethylfurfural, EMF: 5-ethoxymethylfurfural, HT: hydrotalcite, AHG: anhydroglucosamine: sum of 1,6-anhydro- β -D-glucopyranose and 1,6-anhydro- β -D-glucofuranose, DMA: N,N-dimethylacetamide, DMSO: dimethyl sulfoxide, MFD: 5-methyl-2-furaldehyde, THF: tetrahydrofuran, ZrC: zirconium carbonate, LA: levulinic acid, LPMSN: mesoporous silica nanoparticles with large pores, [EMIM]Cl: 1-ethyl-3-methylimidazolium chloride, P-VI-0 is synthesized from copolymerization of divinylbenzene, 1-vinylimidazole and N,N-methylenebisacrylamide with water contact angle of 0°, P–SO₃H-154: SO₃H functionalized polymers with water contact angle of 154°, EMF: 5-ethoxymethylfurfural, BHMF: 2,5-bishydroxymethyl furan, PhyA: phytic acid, FfA: furfural alcohol, ArSO₃H–Et–HNS: arenesulfonic acid functionalized ethane-bridged organosilica hollow nanospheres, FAME: fatty acid methyl esters, FFA: free fatty acid.

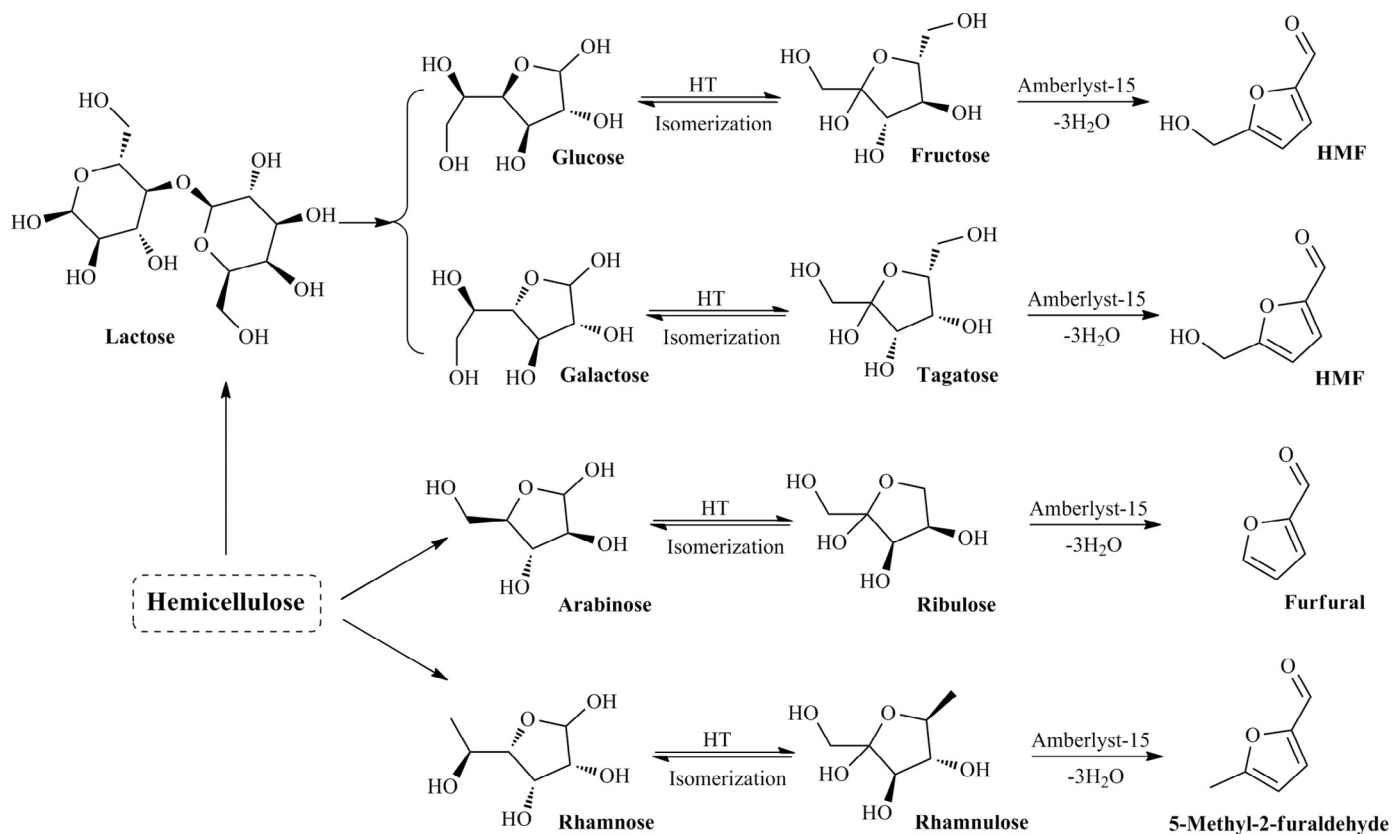


Fig. 19. Schematic of the conversion of various sugars to the corresponding furans: 5-hydroxymethylfurfural (HMF), fufural, and 5-methyl-2-furaldehyde.

combined action of HT and Amberlyst-15 (Fig. 19; Table 4, Entry 37) [369,370]. This catalytic system promotes mixtures of carbohydrates containing arabinose, rhamnose, and lactose to produce fufural (31% yield), 5-methyl-2-furaldehyde (MFD, 29% yield), and HMF (32% yield), respectively, in *N,N*-dimethylformamide (Table 4, Entry 38). Combined with the strongly acidic polymer resin Amberlyst-15, a layered basic zirconosilicate Na₂ZrSi₄O₁₁ is capable of catalyzing glucose transformations to give HMF at 45% selectivity and 87% glucose conversion (Table 4, Entry 39) [371]. A solid base catalyst zirconium carbonate (ZrC) applied to the same reaction affords 17% yield of LA after 12 h reaction in water–toluene biphasic solvent (Table 4, Entries 40 and 41) [372]. The product distribution depends on the types of substrates, the reaction media, and the catalyst type.

Other combined solid acid–base catalysts have been developed for sugar-to-HMF conversions. Pérez-Maqueda et al. [373] reported an efficient catalytic process for the preparation of HMF from sucrose following a sequence of four steps (hydrolysis, dehydration, glucose/fructose isomerization and dehydration) catalyzed by reusable cation- and anion-exchange resins, Amberlite IR120 (H^+) and Amberlite IRA-400 (OH^-) to give an isolated HMF yield of 50% (Table 4, Entry 42). Peng et al. [374] synthesized a series of mesoporous silica nanoparticles (MSNs) with large pore sizes (ca. 30 nm) functionalized with acid ($-SO_3H$, denoted as LPMSN– SO_3H), base (NH_2 , LPMSN– NH_2) and both acid–base ($-SO_3H$ and NH_2 , LPMSN-both) functional groups with a grafting method. A mixture of LPMSN– SO_3H and LPMSN– NH_2 (1:1, w/w), and LPMSN-both exhibits comparable efficacy for one-pot cellulose-to-HMF conversion in an IL [EMIM]Cl in the presence of a trace amount of water (Table 4, Entries 43 and 44), and good yields of glucose and HMF are obtained for LPMSN– SO_3H and LPMSN– NH_2 mixed catalyst (~39 and 19%, respectively) and LPMSN-both (36 and 15%, respectively).

Side-reactions of HMF hydration occurring on acidic sites with water molecules are likely to be inhibited by the basic sites [390,391]. Wang et al. [375] designed and synthesized mesoporous acid catalysts ($P-SO_3H-x$, x stands for the water contact angle on the surface of solid catalyst) with different water wettabilities including superhydrophobic $P-SO_3H-154$, hydrophobic $P-SO_3H-125$ and $P-SO_3H-105$, and hydrophilic $P-SO_3H-44$ [392]. Among these solid acids, PSO_3H-154 with superhydrophobic character is more favorable for isolating water molecules from the acidic sites and for suppressing further hydration of HMF to LA. To realize one-pot transformation of glucose to HMF, solid bases with controllable wettability ($P-VI-x$) synthesized from copolymerization of divinylbenzene, 1-vinylimidazole and *N,N*-methylenediacrylamide have been proposed [375]. Although, the pure base catalyst ($P-VI-0$) or pure acid catalyst ($P-SO_3H-154$) is practically inactive for the formation of HMF, the combined catalysts, superhydrophobic $P-SO_3H-154$ and superhydrophilic $P-VI-0$ give HMF with yields as high as 95% in DMSO–THF (3:2, w/w) (Table 4, Entries 45–47). The superhydrophobicity of the solid acid $P-SO_3H-154$ facilitates the isolation of the acidic sites from water molecules and inhibits the hydration of HMF while the superhydrophilic base $P-VI-0$ promotes glucose-to-fructose isomerization, thus, their combination gives superior catalytic performance.

3.2. HMF- and fufural-derivatives

As discussed in Section 2.4, catalytic sequential dehydration and etherification of carbohydrates into EMF proceeds in the presence of both homogeneous and heterogeneous catalysts with Bronsted acidic sites and Lewis acidic sites (Fig. 13). Nevertheless, relatively low yields of EMF are always observed, owing to the lack of catalytic sites for etherification of HMF with ethanol as well as the low

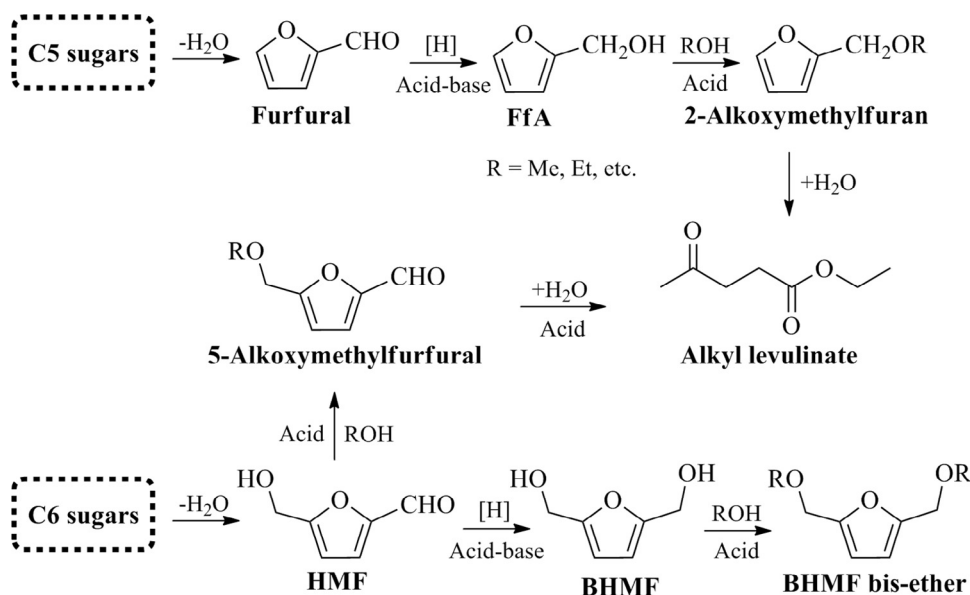


Fig. 20. Catalytic routes for conversion of 5-hydroxymethylfurfural (HMF) and furfural into value-added products with acid–base bifunctional materials. FfA: furfuryl alcohol, BHMF: 2,5-bis(hydroxymethyl)furan.

stability of EMF that tends to be converted into EL [393]. Considering that the catalytic activity of etherification can be controlled by both the surface basicity and Lewis acidity [394–396], a series of nanocatalysts functionalized with both acidic and basic sites was synthesized from the self-assembly of the corresponding basic amino acids with PTA [376]. These obtained acid–base bifunctional hybrid nanospheres that act as heterogeneous catalysts are effective for the conversion of fructose, sucrose and inulin to EMF and give an EMF yield of 77% through sequential dehydration–etherification reaction over Lys/PW(2) in EtOH/DMSO (Table 4, Entry 48). The nanocatalyst Lys/PW(2) functionalized with acid (1.28 mmol/g) and base (0.21 mmol/g) sites is able to be reused six times with EMF yields slightly decreasing from 77% to ~70%. In this cascade catalytic process, solid acid sites promote the dehydration of fructose to HMF in ethanol, and the subsequent etherification is promoted by both surface basicity through deprotonation of alcohol and Lewis acidity by facilitating the elimination of the OH group.

Catalytic transfer hydrogenation between –OH of alcohols and –C:O of furan aldehydes can be facilitated by acid–base pair sites through Meerwein–Ponndorf–Verley (MPV) reduction [397]. Hao et al. [377] demonstrated that ethanol could be used as hydrogen donor and solvent for catalytic transfer hydrogenation of biomass-derived HMF to 2,5-bishydroxymethyl furan (BHMF) over low-cost ZrO(OH)₂, with a maximum BHMF yield of 89% at HMF conversion of 94% being obtained (Table 4, Entry 49). The –OH groups and Zr–O species of ZrO(OH)₂ successively contribute to weak basic and Lewis acidic sites, which are important for the activity of the MPV reaction. However, the presence of excess acid sites catalyzes BHMF to its ether counterparts (Fig. 20). The increase of substrate concentration accelerates the self-etherification of HMF, thus directly leads to a decrease in selectivity toward BHMF and its bis-ether product (Table 4, Entries 50–53) [378,379]. Therefore, appropriate substrate concentration and number of acid–base sites are important for obtaining desired yields of etherified products.

When furfural is used as substrate, Song et al. [380] demonstrated that zirconium phosphonate (Zr–PhyA) synthesized from phytic acid (PhyA) reacting with ZrCl₄ is active for the selective MPV reduction in 2-propanol, affording furfuryl alcohol (FfA) with a yield of 99% (Table 4, Entry 54). The good performance of Zr–PhyA is due to the formation of in situ basic sites (O²⁻ in phosphate groups,

1.32 mmol/g) and Lewis acidic sites (Zr⁴⁺, 0.51 mmol/g). In the catalytic process, 2-propanol is adsorbed onto Zr–PhyA, followed by dissociation to the corresponding alkoxide and H species by the acid–basic sites (Zr⁴⁺–O²⁻), thus increasing the reaction rate of the MPV reaction. As a downstream product of furfural, alkyl levulinates can be synthesized through cascade hydrogenation (with Lewis acid–base sites) and alcoholysis (with Bronsted acid sites) in alcohols (Table 4, Entries 55 and 56) [381,382]. It can be concluded that the distribution of products derived from HMF and furfural can be adjusted by controlling the content and type of acid–base sites in a bifunctional solid catalyst.

3.3. Biodiesel

Apart from enzymatic and Bronsted/Lewis acid-mediated catalytic processes [398–402], biodiesel can be efficiently produced through simultaneous esterification and transesterification reactions promoted by acid–base bifunctional catalysts. As compared with acid-catalyzed transesterification of vegetable oils, base-catalyzed reactions proceed faster and are less corrosive, therefore, industrial processes usually favor base catalysts [403,404]. The traditional homogeneous base-mediated catalytic process is simple and fast, but the neutralization/washing step requires the consumption of acids, and generates acid/base wastes [405]. Moreover, soap formation occurs under homogeneous alkaline catalysis when the raw oils contain more than 1 wt% of total FFAs [406,407]. A two-step process of acid-catalyzed esterification followed by base-catalyzed transesterification is commonly employed to resolve the problems of saponification, slow reaction rate and biodiesel stability in biodiesel production with high FFA content for which the process involves multiple reactions, washing, and separation stages [408,409]. Impregnation of extra active sites (i.e., Al₂O₃ and KOH) into ZrO₂ possessing both acidity and basicity [410] is an efficient approach for catalyzing simultaneous esterification and transesterification of raw oils containing high FFAs (Table 4, Entries 57 and 58) [383,384]. Through investigating the catalytic performance of three thermally robust ZrO₂-based catalysts including titania zirconia (TiZ), sulfated zirconia (SZ), and tungstated zirconia (WZ) for esterification and transesterification, López et al. [411] found that TiZ bearing relatively higher basicity has the lowest

activity for esterification but is more active than WZ for transesterification. Sulfated zirconia is the most active catalyst (on a weight basis) for both transesterification and esterification reactions examined by López et al. [411], although it exhibits significant sulfur loss that greatly reduces its long-term activity.

Lanthanum can affect zinc oxide distribution, as well as increase the surface acid and base sites, because of the strong interaction between Zn and La species [385]. Among possible Zn/La catalysts, Zn_3La_1 was found to simultaneously catalyze oil transesterification and FFA esterification reactions in a single-step, while minimizing oil and biodiesel hydrolysis. High yields (up to 96%) of fatty acid methyl esters (FAMEs) are obtained even using unrefined or waste oils (Table 4, Entry 59). Integration of Ca and La metal oxides enhance their catalytic activity in simultaneous transesterification and esterification reactions as compared with sole bulk CaO and La_2O_3 (Table 4, Entries 60–62) [386,412], which may be attributed to the increased surface acidic and basic sites that become activated by dispersed CaO on the composite surface. During esterification, the interaction of the carbonyl oxygen of FFAs with the Lewis acidic site of the catalyst is speculated to assist in the formation of carbocation and the subsequent nucleophilic attack of the alcohol that produces FAMEs via elimination of water molecule from a tetrahedral intermediate. In a parallel reaction of transesterification, methanol is adsorbed onto the Lewis base site of the catalyst to form oxygen anion, followed by nucleophilic attack to the esters producing two kinds of esters through the break of hydroxyl groups of a tetrahedral intermediate. Therefore, appropriate control of acid-base site distribution can facilitate one-pot production of biodiesel from triglycerides with high content of FFAs through concurrent transesterification and esterification reactions.

3.4. Other methods and biomass-derived chemicals

Acid/base catalysis plays an important role in most practical biofuel processes such as esterification and transesterification of plant oils containing FFAs with alcohols to produce biodiesel, and pretreatment/hydrolysis of lignocellulose to fermentable sugars for bioethanol production [413]. However, shortcomings of catalysts with single acid or single base sites are encountered. In the case of biodiesel production over a basic catalyst, the presence of FFAs and water always leads to the formation of soaps and the difficulty in the catalyst and product separation.

3.4.1. Nanosized mixed oxides for obtaining isobutene from bio-ethanol

A range of related reaction pathways for upgrading biomass-derived molecules with high efficiency have been realized by acid-base catalysis. Nanosized $Zn_xZr_yO_z$ mixed oxides with balanced acid and base sites can directly catalyze the conversion of bio-ethanol to isobutene in yields as high as ~83% at 450 °C with a steam to carbon ratio (S/C) of 5 and residence time of 0.11 s·g·mL⁻¹ (Fig. 21) [414]. The addition of ZnO into ZrO_2 selectively passivates strong Lewis acidic sites and weakens Bronsted acidic sites of zirconia, but enhances the basicity [414]. Basic catalysts such as $ZnO-CaO$ and $ZnO-Fe_2O_3$ are effective for the conversion of ethanol to acetone [415], although the selective transformation of acetone into isobutene requires microporous acidic zeolites [416]. A specific microporous environment in zeolites does not appear to be a critical factor in the Zn/Zr materials for selectively producing isobutene from acetone, possibly due to the moderate Bronsted acidity of $Zn_xZr_yO_z$ catalysts [416]. Acetone can be formed from gas-phase dehydration of 1,2-propanediol in the presence of basic catalyst such as CeO_2 and MgO , while strongly acidic catalysts ($-8.2 < H_0 \leq -3.0$) show high selectivity for propanol as compared with basic ($H_0 \geq +7.2$) and acidic catalysts with either weaker ($-3.0 < H_0 \leq +6.8$) or stronger acidity ($H_0 \leq -8.2$) [417]. In contrast, a wide range of products are

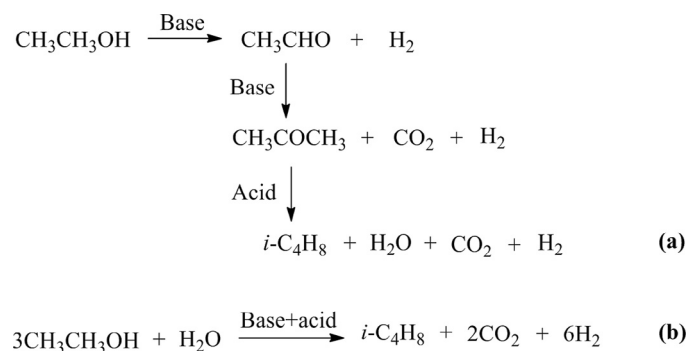


Fig. 21. Schematic of ethanol-to-isobutene transformation: (a) reaction pathway, (b) overall reaction. Adapted with permission from Ref. 414, Copyright © 2011 American Chemical Society.

obtained from 1,3-propanediol dehydration over these acid–base catalysts, owing to the absence of a secondary –OH group. For the case of glycerol-to-acrolein dehydration, the reactivity is controlled by the strength, type and the amount of the acidic sites and hindering as much as possible the number, strength and action of the basic sites [418]. The combined use of acid–base catalysis favors glycerol transesterification and carbonylation with urea to give glycerol carbonate [419], etherification to short-chain polyglycerols [420], and steam reforming to hydrogen [421]. Some reactions such as cascade isomerization–dehydration–Knoevenagel condensation [422], tandem deacetalization–nitroaldol [423], and cooperative aldol condensation [424] can be implemented with acid–base bifunctional catalysts. Co-existence of acid–base sites in a single catalyst at some level provides a degree of cooperative catalysis that have enhanced catalytic performance compared with physical mixtures of monofunctional catalysts. Acid–base bifunctional catalytic materials greatly expand the scope of development for biomass transformations.

4. Acid/base–metal bifunctionalized materials

Biomass refineries deal with highly-oxygenated compounds that are upgraded to moderately-oxygenated and deoxygenated platform molecules. Dehydration, etherification, C–C coupling reactions including aldol-condensation, ketonization, oligomerization and hydroxyalkylation over acid and base catalysts are capable of removing oxygen functionalities and increasing carbon number of the feedstock compounds [425]. Some of the challenges for converting biomass into products are related to the efficient cleavage of alcoholic C–O linkages within the feedstock molecules to reduce both degree of polymerization and oxygen content, as well as the selective oxidation of –OH into specific functional groups. Precious metal catalysts (e.g., Au, Pd, Pt and Ru) and non-precious metal catalysts (e.g., Fe, Cu and Ni) with the presence of acid/base additives or supports exhibit good activities for hydrogenation/hydrogenolysis and oxidation reactions [426–428]. Synthetic procedures for these supported metal nanoparticles, impregnation, calcination and subsequent reduction of metal ions with H_2 , $NaBH_4$, carbon/CO, and alcohols are frequently adopted. This section introduces advances in metal nanoparticles combined with acid/base catalysis for transformation of biomass derivatives into chemical products.

4.1. Production of oxygenates

4.1.1. Oxidation of sugars and polyols

The selective oxidation of alcohols in aqueous solution over supported metal catalysts is facilitated by high-pH conditions. Oxygen

atoms originating from hydroxide ions formed via catalytic decomposition of a peroxide intermediate instead of molecular oxygen are incorporated into the alcohol during the oxidation reaction [429] so that the acidity of the support can play a role in the activity and selectivity of the catalysts [430]. In this regard, acid or base properties are essential for metal-catalyzed oxidation processes with high conversion rates and selectivities. Cooperative effects between metal particles and solid support related to structure and textural characteristics influence the selective oxidation of alcohols [431]. Anaerobic and aerobic conversions of carbohydrates promoted by bi- or multifunctional catalysts are two important renewable routes to produce organic acids and aldehydes/ketones [432]. In these catalytic processes, conversions and selectivities to target products depend on oxidants, pH values, catalysts, and reactor operating conditions [433–436]. When the pH of the reaction solution is unregulated, strong adsorption of acids onto a metal surface occurs, causing the poisoning of metal catalysts during oxidation of sugars [437]. To prevent inactivation of metal particles, buffering of reaction solutions is necessary when using this approach for selective conversion of biomass derivatives that involve oxidation.

Selective oxidation of sugars could produce commercially relevant polyoxy-acids, such as gluconic acid, which is widely used in the chemical, food, pharmaceutical and textile industries. Gluconic acid is produced via selective oxidation of glucose in the C1 position [438]. Much attention has been paid to the production of gluconic acid via liquid phase oxidation catalyzed by metal particles such as Pd and Au (Table 5, Entries 1–3) [439–441]. In comparison to monometallic systems, bimetallic catalysts are capable of enhancing reactivity, but typically exhibit low stability because of metal leaching that occurs during reaction (Table 5, Entries 4–8) [442,443]. Metal oxide supported catalysts are more active for glucose-to-gluconic acid transformation than supported or free metal colloids (Table 5, Entry 9) [444], and they have relatively higher stability over the long-term than other solid supports such as carbon [464,465]. Table 5 shows that base sites resulting from solvents, solid supports, or co-existent metal oxides are helpful to increase the selectivity toward gluconic acid from glucose oxidation. When biopolymers (e.g., cellobiose and cellulose) are used as substrate, acidity is necessary for hydrolysis to occur before intermediate products can be oxidized.

Acid-base pairs combined with metal particles (Table 5) seem to be exclusively used for the oxidation of saccharides. Under base-free conditions, Rautiainen et al. [445] demonstrated that microwave heating could provide an efficient catalytic system for the oxidation of glucose to gluconic acid (76 % yield) in the presence of supported Au nanoparticles (Table 5, Entry 10). In contrast, Wojcieszak et al. [446] reported that glucuronic acid, except gluconic acid, is the dominant oxidized product from glucose over Au/CeO₂ and AuCs/CeO₂ under oil heating and base-free conditions (Table 5, Entries 11 and 12). The improved activity of the Au catalyst after being doped with Cs may be the result of an increase in local surface basicity caused by CsOH species. However, many reaction mechanisms involving acid-base properties of the catalysts are not well understood yet, so that detailed studies on this topic are needed.

Formic acid is a promising medium for both hydrogen storage and production, and it is also an important commodity chemical. By using a Keggin-type polyoxometalate (H₅PV₂Mo₁₀O₄₀) as homogeneous catalyst, *p*-toluenesulfonic acid as additive, oxygen as oxidant and water as solvent, water-insoluble biomass such as wood, waste paper, cyanobacteria and xylan can be transformed into formic acid with up to 53% yield (Table 5, Entry 13) [447]. Without the addition of strong acid, water-soluble glucose is oxidized into formic acid in yields of up to 49% with molecular oxygen (Table 5, Entry 14) [448] and up to 52% with air (Table 5, Entry 15) [449] over H₅PV₂Mo₁₀O₄₀. The H₅PV₂Mo₁₀O₄₀ has been used as a bifunctional catalyst for the

degradation of cellulose to formic acid with 35% yield (Table 5, Entry 16), where it was speculated that cellulose was first hydrolyzed into glucose, followed by oxidation involving electron and oxygen transfer processes to produce formic acid (Fig. 22) [449]. In this process, catalytic oxidation to formic acid and deep hydrolysis to byproducts proceeds in a competitive way that can be adjusted by changing O₂ partial pressure, reaction temperature and acid concentration (Table 5, Entries 17–21) [450–453]. Together with formic acid, some other organic acids such as lactic acid, acetic acid, and glycolic acid are also formed from sugars via sequential reactions (Table 5, Entries 22–29) [454–456].

Starting from polyols, formic acid can be generated via oxidation processes. For instance, Zhang et al. [457] reported that V-substituted phosphomolybdc acids were active for oxidation of glycerol to formic acid in highly concentrated aqueous solutions with molecular oxygen, and 3.64 g formic acid was produced from 10 g glycerol/water (50/50, w/w) solution (Table 5, Entries 30 and 31). In an aqueous solution of Lewis acid (e.g., FeCl₃, ZnCl₂, CrCl₃ or AlCl₃), Ru(OH)₄/r-GO catalyst prepared via refluxing, RuCl₃ aqueous solution containing graphite oxide (GO) promotes the oxidation of glycerol to formic acid (Table 5, Entries 32–35) [458]. A synergistic effect between Ru(OH)₄/r-GO and FeCl₃ is observed for glycerol oxidation such that high formic acid yields (ca. 60%) are obtained. The oxidation of C₃ oxygenates to C₁ oxygenates might simultaneously yield the C₂ (C₃→C₂+C₁) products. For the case of glycerol oxidation, Kapkowski et al. [459] detected that sol-gel SiO₂-supported Au affords high acetic acid yields (up to 90%) besides single carbonaceous products with glycerol conversion of 100% in a dilute and viscous H₂O₂/H₂O liquid phase (Table 5, Entry 36). Bimetallic Au/Cu and Au/Ni catalysts obtained by nano-Au transfer show comparable performance, while Cu or Ni leaching results in deactivation of these catalysts during the reaction. A large number of oxidized chemicals including dihydroxyacetone, glyceric acid, lactic acid, hydroxypyruvic acid, dihydroxymalonic acid, glycolaldehyde, glyoxylic acid, glycolic acid, oxalic acid, tartronic acid, mesoxalic acid and other unstable intermediates can be produced via chemoselective oxidation of glycerol (Fig. 23) by controlling the type of the support, the size of the metal particles, and the acid/base properties of the reaction medium [466–468]. Control of product selectivity is necessary for efficient valorization of glycerol in consideration of its wide product distribution for different catalytic processes. Nanoparticles promoted by acid/base solid supports or reaction media, in most cases, show good selectivity for the desired products in the chemoselective oxidation of glycerol, but lead to relatively low glycerol conversions owing to three hydroxyl groups that have similar reactivity. Therefore, the development of robust nanosized bifunctional catalysts is necessary for practical glycerol oxidation. Moreover, the use of bifunctional catalysts for biodiesel production as well as for subsequent glycerol conversion will improve process efficiency and economics.

Lactic acid is produced mainly by anaerobic conversion of sugars with fermentation [469]. Lactic acid can also be produced by Lewis acid-mediated catalytic processes involving successive hydrolysis of polysaccharides to glucose, glucose-to-fructose isomerization, retro-aldol fragmentation to trioses (i.e., dihydroxyacetone and glyceraldehydes), and dehydration and 1,2-hydride shift reactions [470,471]. In an aerobic process, the catalytic dehydrogenation of sorbitol, mannitol, xylitol and erythritol to lactic acid can be achieved with a series of Ir–NHC complexes under basic conditions, affording a maximum lactic acid yield of ~50% (Table 5, Entries 37–40) [460]. Catalytic dehydrogenation of mannitol and xylitol, mannose and xylose gives similar oxidized product mixtures as those of sorbitol aerobic transformation; base-driven isomerization and dehydration of simple sugars account for the catalyst selectivity. In light of these observations, it has been speculated that the conversion of sorbitol to lactic acid occurs as shown in Fig. 24 [460]. Initially,

Table 5

Acid/base catalytic systems used in the conversion of carbohydrates into organic acids with summary of reaction conditions, oxidant, maximum catalytic activity and catalyst reusability.

Entry	Substrate	Catalyst ^a	Reaction conditions			Oxidant	Main product	Catalytic activity		Reusability		Ref.
			Solvent	Temp.	Time			Conv.	Yield	Cycles	Yield ^b	
1	Glucose (10 wt%)	5.0 wt% PdBi/C	Basic H ₂ O	40 °C	155 min	0.1 MPa Air	Gluconic acid	100%	99%	5	99%	[439]
2	Celllobiose (0.5 wt%)	1.0 wt% Au/Amberlyst-15	H ₂ O	100 °C	24 h	0.1 MPa Air	Gluconic acid	–	45%	4	40%	[440]
3	Glucose (1.8 wt%)	0.94 wt% Au/CMK-3	H ₂ O	110 °C	2 h	0.3 MPa O ₂	Gluconic acid	92%	80%	NM ^c	NM	[441]
4	Glucose (4.5 wt%)	5 wt% PdTe/SiO ₂	H ₂ O	60 °C	2 h	0.1 MPa Air	Gluconic acid	100%	100%	10	86%	[442]
5	Glucose (4.5 wt%)	5 wt% Pd/SiO ₂	H ₂ O	60 °C	2 h	0.1 MPa Air	Gluconic acid	59%	44%	10	22%	[442]
6	Celllobiose (1.0 wt%)	0.5 wt% AuCu/TiO ₂	H ₂ O	145 °C	3 h	1 MPa O ₂	Gluconic acid	100%	89%	4	~70%	[443]
7	Celllobiose (1.0 wt%)	0.5 wt% Cu/TiO ₂	H ₂ O	145 °C	3 h	1 MPa O ₂	Gluconic acid	98%	62%	NM	NM	[443]
8	Celllobiose (1.0 wt%)	0.5 wt% Au/TiO ₂	H ₂ O	145 °C	3 h	1 MPa O ₂	Gluconic acid	98%	74%	NM	NM	[443]
9	Glucose (20.0 wt%)	0.3% Au/A ₁₂ O ₃	Basic H ₂ O	40 °C	5190 mmol min ⁻¹ g _{Au} ⁻¹	0.9 MPa O ₂	Gluconic acid	100%	99%	NM	NM	[444]
10	Glucose (2.2 wt%)	1.8 wt% Au/A ₁₂ O ₃	H ₂ O	120 °C	10 min ^d	2.2 equiv. H ₂ O ₂	Gluconic acid	87%	76%	4	>60%	[445]
11	Glucose (9.9 wt%)	1.7 wt% Au/CeO ₂	H ₂ O	70 °C	4 h	1.5 MPa O ₂	Glucuronic acid	12%	11%	NM	NM	[446]
12	Glucose (9.9 wt%)	2.5 wt% AuCs/CeO ₂	H ₂ O	70 °C	4 h	1.5 MPa O ₂	Glucuronic acid	55%	54%	NM	NM	[446]
13	Xylan (2.7 wt%)	TSA + 4.2 mol% H ₅ PV ₂ Mo ₁₀ O ₄₀	H ₂ O	90 °C	24 h	3.0 MPa O ₂	Formic acid	97%	53%	NM	NM	[447]
14	Glucose (3.0 wt%)	4.4 mol% H ₅ PV ₂ Mo ₁₀ O ₄₀	H ₂ O	80 °C	7 h	3.0 MPa O ₂	Formic acid	100%	49%	NM	NM	[448]
15	Glucose (2.5 wt%)	5 mol% H ₅ PV ₂ Mo ₁₀ O ₄₀	H ₂ O	100 °C	3 h	5.0 MPa Air	Formic acid	100%	52%	NM	NM	[449]
16	Cellulose (1.0 wt%)	5 mol% H ₅ PV ₂ Mo ₁₀ O ₄₀	H ₂ O	170 °C	9 h	5.0 MPa Air	Formic acid	100%	35%	NM	NM	[449]
17	Cellulose (1.7 wt%)	0.35 wt% NaVO ₃ + 2 wt% H ₂ SO ₄	H ₂ O	160 °C	10 min	3.0 MPa O ₂	Formic acid	–	58%	NM	NM	[450]
18	Wheat straw (0.8 wt%)	0.35 wt% NaVO ₃ + 2 wt% H ₂ SO ₄	H ₂ O	160 °C	5 min	3.0 MPa O ₂	Formic acid	100%	47%	4	46%	[451]
19	Xylan (1.7 wt%)	0.35 wt% NaVO ₃ + 0.7 wt% H ₂ SO ₄	H ₂ O	160 °C	30 min	3.0 MPa O ₂	Formic acid	100%	64%	5	63%	[452]
20	Cellulose (6.7 wt%)	38.8 wt% H ₄ PMo ₁₁ O ₄₀	H ₂ O	180 °C	1 h	1.0 MPa O ₂	Formic acid	100%	36%	NM	NM	[453]
21	Cellulose (6.7 wt%)	38.8 wt% IL-PMo	H ₂ O	180 °C	1 h	1.0 MPa O ₂	Formic acid	100%	51%	3	50%	[453]
22	Cellulose (0.9 wt%)	10 mol% VOSO ₄	H ₂ O	160 °C	2 h	2.0 MPa O ₂	Formic acid	–	39%	NM	NM	[448]
23	Cellulose (0.9 wt%)	5 mol% VOSO ₄	H ₂ O	180 °C	2 h	2.0 MPa N ₂	Formic acid	–	4%	NM	NM	[454]
24	Cellulose (1.0 wt%)	10 mol% H ₄ PVMo ₁₁ O ₄₀	H ₂ O	180 °C	3 h	0.6 MPa O ₂	Formic acid	100%	68%	4	65%	[455]
25	Cellulose (5.0 wt%)	10 mol% H ₄ PVMo ₁₁ O ₄₀	H ₂ O	180 °C	3 h	2.0 MPa O ₂	Formic acid	–	35%	NM	NM	[455]
26	Glucose (1 wt%)	24.3 mol% H ₃ PMo ₁₂ O ₄₀	H ₂ O	180 °C	1 h	0.6 MPa O ₂	Glycolic acid [Formic acid] (Acetic acid)	96%	42%	NM	NM	[456]
27	Cellulose (1 wt%)	24.3 mol% H ₃ PMo ₁₂ O ₄₀	H ₂ O	180 °C	1 h	0.6 MPa O ₂	Glycolic acid [Formic acid] (Acetic acid)	–	49%	9	50%	[456]
28	Bagasse (1 wt%)	24.3 mol% H ₃ PMo ₁₂ O ₄₀	H ₂ O	180 °C	1 h	0.6 MPa O ₂	Glycolic acid [Formic acid] (Acetic acid)	–	32%	NM	NM	[456]

(continued on next page)

Table 5 (continued)

Entry	Substrate	Catalyst ^a	Reaction conditions			Oxidant	Main product	Catalytic activity		Reusability		Ref.
			Solvent	Temp.	Time			Conv.	Yield	Cycles	Yield ^b	
29	Hay (1 wt%)	24.3 mol% H ₃ PMo ₁₂ O ₄₀	H ₂ O	180 °C	1 h	0.6 MPa O ₂	Glycolic acid [Formic acid] (Acetic acid)	–	28% [8%] (7%)	NM	NM	[456]
30	Glycerol (50 wt%)	0.2 mol% H ₆ PV ₃ Mo ₉ O ₄₀	H ₂ O	150 °C	3 h	4.0 MPa O ₂	Formic acid [Acetic acid]	95%	51% [11%]	NM	NM	[457]
31	Glycerol (1.0 wt%)	10 mol% H ₆ PV ₃ Mo ₉ O ₄₀	H ₂ O	150 °C	3 h	2.0 MPa O ₂	Formic acid [Acetic acid]	100%	60% [3%]	NM	NM	[457]
32	Glycerol (1.9 wt%)	FeCl ₃ + 0.1 mol% Ru(OH) ₄ /r-GO	H ₂ O	160 °C	1 h	0.5 MPa O ₂	Formic acid [Acetic acid]	96%	~60% [1%]	NM	NM	[458]
33	Glycerol (1.9 wt%)	AlCl ₃ + 0.1 mol% Ru(OH) ₄ /r-GO	H ₂ O	160 °C	1 h	0.5 MPa O ₂	Formic acid [Acetic acid]	92%	39% [3%]	NM	NM	[458]
34	Glycerol (1.9 wt%)	CrCl ₃ + 0.1 mol% Ru(OH) ₄ /r-GO	H ₂ O	160 °C	1 h	0.5 MPa O ₂	Formic acid [Acetic acid]	80%	18% [7%]	NM	NM	[458]
35	Glycerol (1.9 wt%)	ZnCl ₂ + 0.1 mol% Ru(OH) ₄ /r-GO	H ₂ O	160 °C	1 h	0.5 MPa O ₂	Formic acid [Acetic acid]	30%	10% [5%]	NM	NM	[458]
36	Glycerol (1.9 wt%)	0.1 wt% Au/SiO ₂	H ₂ O	80 °C	24 h	37 equiv. H ₂ O ₂	Acetic acid	100%	90%	4	60%	[459]
37	Sorbitol (3.5 wt%)	0.1 mol% [(η ⁵ -C ₅ Me ₅)Ir(IME) ₂ Cl]BF ₄	–	160 °C	24 h	Atmospheric N ₂	Lactic acid	49%	40% [42%]	NM	NM	[460]
38	Mannitol (3.5 wt%)	0.1 mol% [(η ⁵ -C ₅ Me ₅)Ir(IME) ₂ Cl]BF ₄	–	160 °C	24 h	Atmospheric N ₂	Lactic acid	54%	43% [36%]	NM	NM	[460]
39	Xylitol (3.5 wt%)	0.1 mol% [(η ⁵ -C ₅ Me ₅)Ir(IME) ₂ Cl]BF ₄	–	160 °C	24 h	Atmospheric N ₂	Lactic acid	56%	49% [21%]	NM	NM	[460]
40	Erythritol (3.5 wt%)	0.1 mol% [(η ⁵ -C ₅ Me ₅)Ir(IME) ₂ Cl]BF ₄	–	160 °C	24 h	Atmospheric N ₂	Lactic acid	16%	12% [18%]	NM	NM	[460]
41	Glycerol (1.0 wt%)	5 wt% Ru/C	H ₂ O + NaOH	200 °C	5 h	4.0 MPa O ₂	Lactic acid [Propylene glycol]	100%	34% [18%]	NM	NM	[461]
42	Glycerol (1.0 wt%)	3 wt% Pt/C	H ₂ O + NaOH	200 °C	5 h	4.0 MPa O ₂	Lactic acid [Propylene glycol]	92%	44% [42%]	NM	NM	[461]
43	Glycerol (1.0 wt%)	3 wt% Pt/C	H ₂ O + CaO	200 °C	5 h	4.0 MPa O ₂	Lactic acid [Propylene glycol]	100%	58% [36%]	NM	NM	[461]
44	Glycerol (1.0 wt%)	3 wt% PtRu/C	H ₂ O	200 °C	5 h	4.0 MPa O ₂	Lactic acid [Propylene glycol] (Ethylene glycol)	42%	0% [18%]	NM	NM	[462]
45	Glycerol (1.0 wt%)	3 wt% PtRu/C	H ₂ O + NaOH	200 °C	5 h	4.0 MPa O ₂	Lactic acid [propylene glycol] (ethylene glycol)	100%	37% [2%]	NM	NM	[462]
46	Glucose (0.45 wt%)	400 mol% [IMEP]Cl	H ₂ O + NaOH	100 °C	30 min	0.1 MPa N ₂	Lactic acid	99%	63% [54%]	6	54%	[463]

^a Metal loading of the catalyst or catalyst dosage relative to the substrate.^b Product yield in the last cycle.

c NM: not mentioned.

d Microwave irradiation.

CMK-3: an ordered mesoporous carbon, TSA: *p*-toluenesulfonic acid, IL-PMo: ionic liquids composed of HPMo₁₁O₄₀³⁻ and –SO₃H functionalized methylimidazole cations, [IMEP]Cl: polymerization of imidazole and epichlorohydrin.

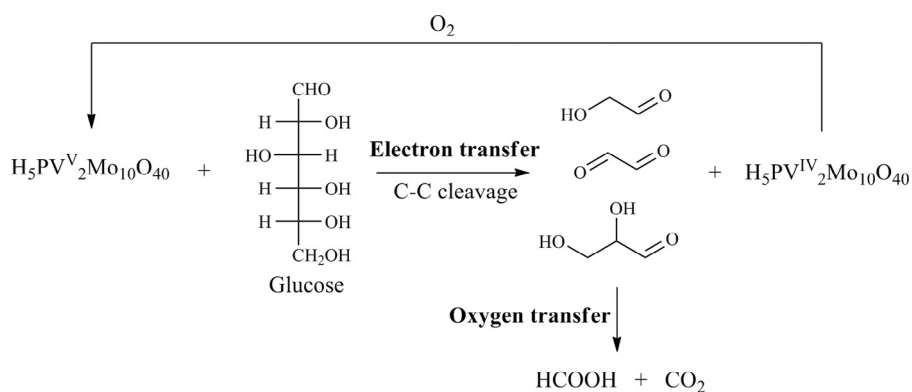


Fig. 22. Possible reaction pathway for catalytic oxidation of glucose with $\text{H}_5\text{PV}_2\text{Mo}_{10}\text{O}_{40}$ through electron and oxygen transfer processes. Adapted with permission from Ref. 449, Copyright © 2012 Wiley-VCH.

iridium-catalyzed dehydrogenation of sorbitol to a tautomeric mixture containing glucose, fructose and galactose occurs under basic conditions ($\text{KOH}-\text{H}_2\text{O}$) [472], followed by a retro-aldol condensation, cleaving C–C bonds, to form two different C_3 molecules

depending on the type of C_6 sugar. Dihydroxyacetone and glyceraldehyde from fructose could act as direct precursors to lactate via an intramolecular Cannizzaro reaction (Table 5, Entries 41–45) [461,462]. In the case of glucose, two potential enol molecules formed

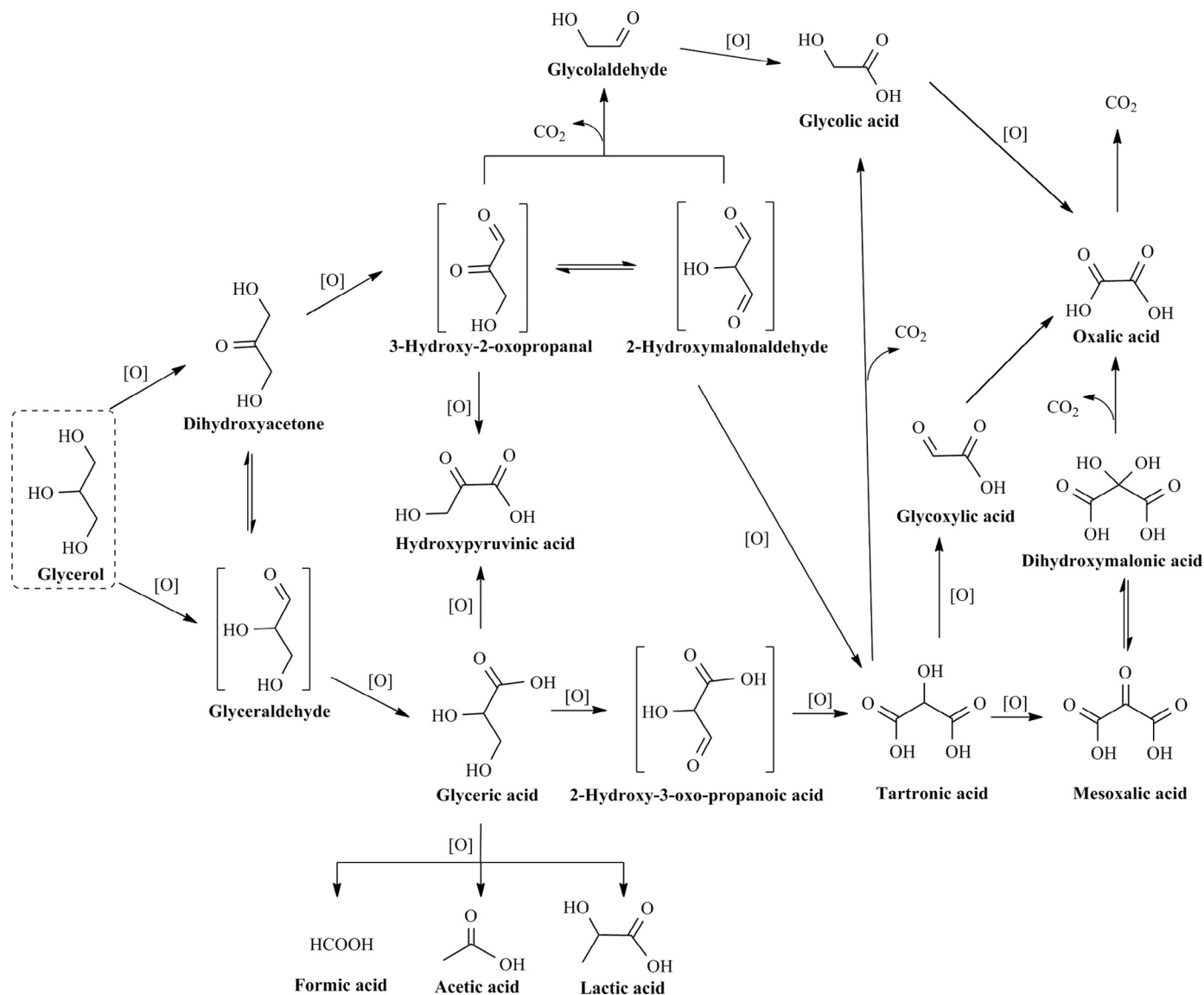


Fig. 23. Catalytic oxidation of glycerol to various fine chemicals. Adapted with permission from Ref. 466, Copyright © 2011 Royal Society of Chemistry.

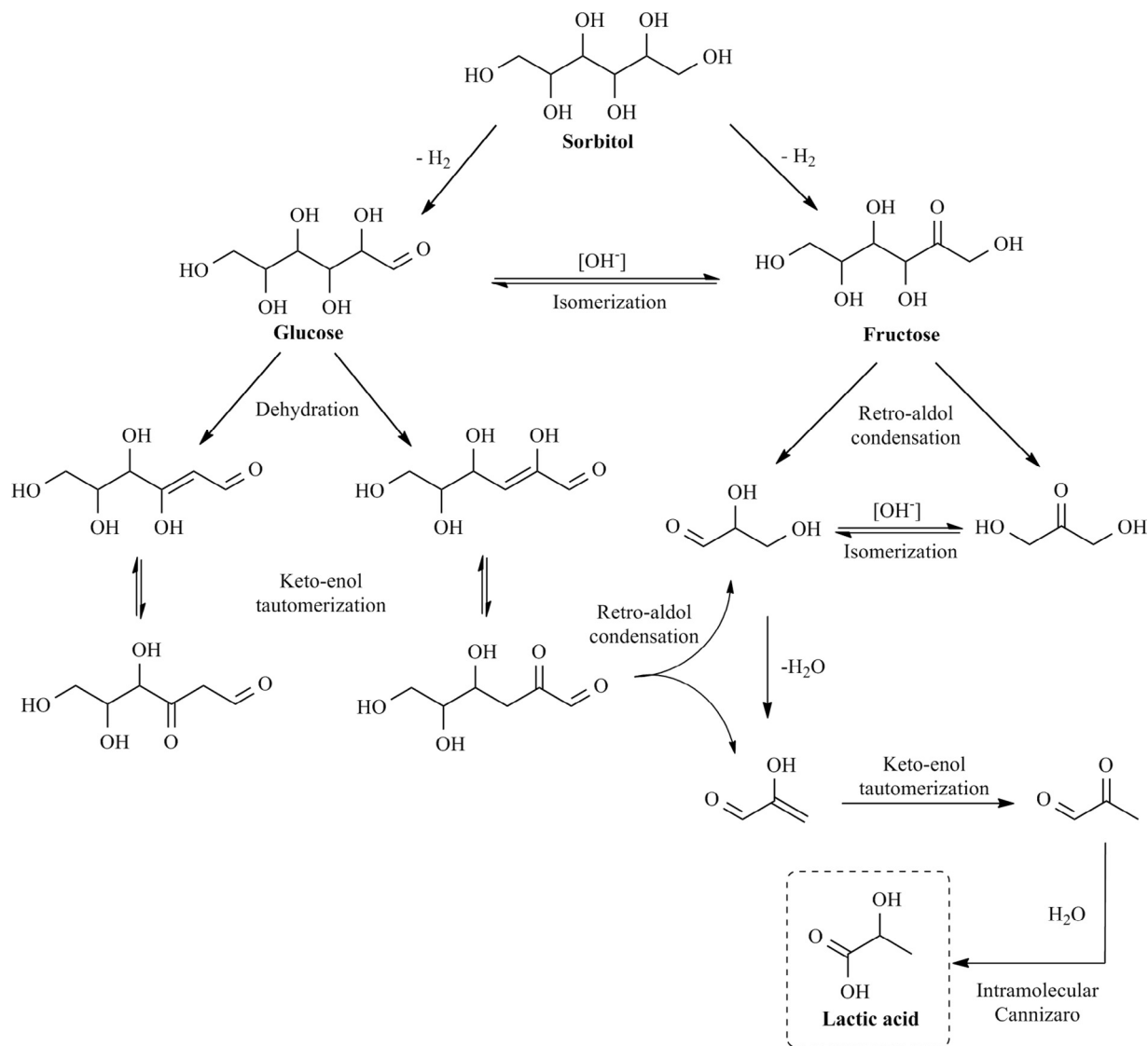


Fig. 24. Proposed reaction pathway from sorbitol to lactic acid through glucose and fructose. Adapted with permission from Ref. 460, Copyright © 2014 Royal Society of Chemistry.

via dehydration lead to totally different products, in which the 2-hydroxy enol is converted to a 1,2-di-ketone, followed by cleavage to yield two C₃ molecules that both are then converted to lactic acid, while the 3-hydroxy enol results in the formation of C₂ and C₄ products (Table 5, Entry 46) [463,473]. Thus, suppressing the formation of 3-hydroxy enol by adjusting acidity/basicity of reaction solution or solid support is helpful to increase the selectivity of lactic acid.

In the catalytic conversion of carbohydrates to organic acids, the synergistic effect of metal and acid–base sites seems to be a major factor that affects product selectivity. In some cases, sugars can be efficiently converted to the desired molecules, however, appropriate control of the functionalities of the catalytic materials still needs research for application in practical biorefineries.

4.1.2. Oxidation of HMF and furfural

4.1.2.1. 2,5-Furandicarboxylic acid (FDCA). Furanic compounds bearing oxygenated groups such as –CHO and –COOR (R: H, CH₃, C_nH_{2n+1}) derived from biomass derivatives are expected to replace fuels and chemicals presently being produced from fossil fuels. FDCA, generated from selective oxidation of HMF, is a monomer for

furan-containing polymers and materials that has special properties [474–479]. Several oxidants such as H₂O₂, 2,2,6,6-tetramethyl-piperidin-1-oxyl (TEMPO), and classical metal oxides containing chromium or manganese can be used although toxicity and waste treatment issues exist [480–482]. Thus, the use of dioxygen as oxidant with the only byproduct being water is a current research topic with the goal to convert HMF into FDCA via oxidation (Table 6). Under alkaline conditions, carbon-supported ruthenium is reported to be an active catalyst for HMF-to-FDCA conversion, but it is associated with low stability (Table 6, Entries 1–3) [483,484]. Ruthenium on different magnesium-based supports including magnesium oxide, spinel, and HT show superior catalytic performance for the selective oxidation of HMF to FDCA [485], as compared with other solid supports such as titanium-, aluminum-, cerium-, zirconium-, and lanthanum oxides, magnetite, and hydroxyapatite (Table 6, Entries 4–11). Catalysts with high basicity generally exhibit high efficiency for the HMF-to-FDCA oxidation in aqueous media without adding free base, and FDCA yields higher than 90% have been obtained (Table 6, Entries 4 and 6). In these reaction systems (Table 6, Entries 4–11), a homogeneous alkaline mixture is formed in the case of both HT and MgO supports by partial

Table 6

Catalytic oxidation of 5-hydroxymethylfurfural, carbohydrates and furfural derivatives with summary of reaction conditions, oxidant, maximum catalytic activity and catalyst reusability.

Entry	Substrate	Catalyst ^a	Reaction conditions			Oxidant	Main Product	Catalytic activity		Reusability		Ref.
			Solvent	Temp.	Time			Conv.	Yield	Cycles	Yield ^b	
1	HMF (4.8 wt%)	5 wt% Pt/Al ₂ O ₃	Basic H ₂ O	60 °C	160 min	0.02 MPa O ₂	FDCA	100%	95%	NM ^c	NM	[483]
2	HMF (1.3 wt%)	5 wt% Pd/Al ₂ O ₃	Basic H ₂ O	60 °C	160 min	0.02 MPa O ₂	FDCA	100%	50%	NM	NM	[484]
3	HMF (1.3 wt%)	5 wt% Ru/Al ₂ O ₃	Basic H ₂ O	60 °C	160 min	0.02 MPa O ₂	FDCA	100%	75%	NM	NM	[484]
4	HMF (0.6 wt%)	5 mol% Ru(OH) _x /MgO	H ₂ O	140 °C	6 h	0.25 MPa O ₂	FDCA	100%	92%	NM	NM	[485]
5	HMF (0.6 wt%)	5 mol% Ru(OH) _x /Spinel	H ₂ O	140 °C	6 h	0.25 MPa O ₂	FDCA	100%	40%	NM	NM	[485]
6	HMF (0.6 wt%)	5 mol% Ru(OH) _x /HT	H ₂ O	140 °C	6 h	0.25 MPa O ₂	FDCA	100%	90%	NM	NM	[485]
7	HMF (0.6 wt%)	5 mol% Ru(OH) _x /TiO ₂	H ₂ O	140 °C	6 h	0.25 MPa O ₂	FDCA	100%	21%	NM	NM	[485]
8	HMF (0.6 wt%)	5 mol% Ru(OH) _x /Al ₂ O ₃	H ₂ O	140 °C	6 h	0.25 MPa O ₂	FDCA	100%	23%	NM	NM	[485]
9	HMF (0.6 wt%)	5 mol% Ru(OH) _x /Fe ₃ O ₄	H ₂ O	140 °C	6 h	0.25 MPa O ₂	FDCA	100%	48%	NM	NM	[485]
10	HMF (0.6 wt%)	5 mol% Ru(OH) _x /ZrO ₂	H ₂ O	140 °C	6 h	0.25 MPa O ₂	FDCA	100%	37%	NM	NM	[485]
11	HMF (0.6 wt%)	5 mol% Ru(OH) _x /CeO ₂	H ₂ O	140 °C	6 h	0.25 MPa O ₂	FDCA	100%	38%	NM	NM	[485]
12	HMF (2.9 wt%)	2.5 wt% Ru(OH) _x /La ₂ O ₃	[EMIm][OAc]	100 °C	5 h	3.0 MPa O ₂	FDCA	99%	48%	NM	NM	[486]
13	HMF (1.3 wt%)	1 wt% Au/TiO ₂	Basic H ₂ O	30 °C	18 h	2.0 MPa O ₂	FDCA	100%	71%	NM	NM	[487]
14	HMF (1.9 wt%)	2 mol% Au/CeO ₂	Basic H ₂ O	65 °C	8 h	1.0 MPa O ₂	FDCA	100%	100%	NM	NM	[488]
15	HMF (1.9 wt%)	2 mol% Au/TiO ₂	Basic H ₂ O	65 °C	8 h	1.0 MPa O ₂	FDCA	100%	99%	NM	NM	[488]
16	HMF (1.9 wt%)	2 mol% Au/Fe ₂ O ₃	Basic H ₂ O	65 °C	8 h	1.0 MPa O ₂	FDCA	100%	15%	NM	NM	[488]
17	HMF (1.9 wt%)	2 mol% Au/C	Basic H ₂ O	65 °C	8 h	1.0 MPa O ₂	FDCA [HMFCA]	100%	44%	NM	NM	[488]
18	HMF (2.1 wt%)	2 mol% Au/HT	H ₂ O	90 °C	20 h	0.34 MPa O ₂	FDCA	100%	99%	NM	NM	[489]
19	HMF (2.1 wt%)	2 mol% Au/TiO ₂	H ₂ O	95 °C	7 h	1.0 MPa O ₂	FDCA	100%	99%	3	90%	[490]
20	HMF (1.3 wt%)	2.0 wt% AuCu/TiO ₂	Basic H ₂ O	95 °C	6 h	1.0 MPa O ₂	FDCA	100%	99%	5	>90%	[491]
21	HMF (1.3 wt%)	1.5 wt% AuCu/TiO ₂	Basic H ₂ O	60 °C	6 h	1.0 MPa O ₂	FDCA	–	31%	NM	NM	[491]
22	HMF (1.3 wt%)	1.5 wt% Au/TiO ₂	Basic H ₂ O	60 °C	6 h	1.0 MPa O ₂	FDCA	–	13%	3	2%	[491]
23	HMF (1.3 wt%)	0.36 wt% Cu/TiO ₂	Basic H ₂ O	60 °C	6 h	1.0 MPa O ₂	FDCA	–	0	NM	NM	[491]
24	HMF (0.45 wt%)	1.0 wt% AuPd/CNT	Basic H ₂ O	100 °C	12 h	0.5 MPa O ₂	FDCA [DFF]	100%	94%	NM	NM	[492]
25	HMF (0.45 wt%)	1.0 wt% Au/CNT	Basic H ₂ O	100 °C	12 h	0.5 MPa O ₂	FDCA [DFF]	78%	11%	NM	NM	[492]
26	HMF (0.45 wt%)	1.0 wt% Pd/CNT	Basic H ₂ O	100 °C	12 h	0.5 MPa O ₂	FDCA [DFF]	63%	7%	NM	NM	[492]
27	HMF (1.3 wt%)	1.5 wt% AuCu/CeO ₂	Basic H ₂ O	70 °C	6 h	1.0 MPa O ₂	FDCA [HMFCA]	100%	90%	NM	NM	[493]
28	HMF (1.3 wt%)	1.5 wt% Au/CeO ₂	Basic H ₂ O	70 °C	6 h	1.0 MPa O ₂	FDCA [HMFCA]	100%	55%	NM	NM	[493]
29	HMF (1.9 wt%)	3.0 wt% Pt/C	Basic H ₂ O	22 °C	6 h	0.69 MPa O ₂	FDCA [HMFCA]	100%	79%	NM	NM	[494]
30	HMF (1.9 wt%)	3.0 wt% Pd/C	Basic H ₂ O	22 °C	6 h	0.69 MPa O ₂	FDCA [HMFCA]	100%	71%	NM	NM	[494]
31	HMF (1.9 wt%)	0.8 wt% Au/C	Basic H ₂ O	22 °C	6 h	0.69 MPa O ₂	FDCA [HMFCA]	100%	7%	NM	NM	[494]
32	HMF (1.9 wt%)	1.6 wt% Au/TiO ₂	Basic H ₂ O	22 °C	6 h	0.69 MPa O ₂	FDCA [HMFCA]	100%	8%	NM	NM	[494]
33	HMF (3.0 wt%)	Co(OAc) ₂ /Zn(OAc) ₂ /Br [–]	H ₂ O	90 °C	4.5 h	Atmospheric O ₂	DFF	100%	96%	NM	NM	[495]
34	HMF (3.0 wt%)	Co(OAc) ₂ /Zn(OAc) ₂ /Br [–] + HTFA	H ₂ O	90 °C	3 h	Atmospheric O ₂	FDCA [FFCA]	90%	60%	NM	NM	[495]
35	HMF (3.0 wt%)	1.9 wt% Au/TiO ₂	H ₂ O	130 °C	3 h	Atmospheric O ₂	FFCA	62%	45%	NM	NM	[495]

(continued on next page)

Table 6 (continued)

Entry	Substrate	Catalyst ^a	Reaction conditions			Oxidant	Main Product	Catalytic activity		Reusability		Ref.
			Solvent	Temp.	Time			Conv.	Yield	Cycles	Yield ^b	
36	HMF (3.0 wt%)	1.9 wt% Au/TiO ₂ + HTFA	H ₂ O	130 °C	3 h	Atmospheric O ₂	FFCA	84%	79%	NM	NM	[495]
37	HMF (3.0 wt%)	1.9 wt% Au/CeO ₂	H ₂ O	130 °C	3 h	Atmospheric O ₂	FFCA	29%	19%	NM	NM	[495]
38	HMF (3.0 wt%)	1.9 wt% Au/CeO ₂ + HTFA	H ₂ O	130 °C	3 h	Atmospheric O ₂	FFCA	83%	71%	NM	NM	[495]
39	HMF (3.0 wt%)	5 wt% Pt/ZrO ₂	Acidic H ₂ O	100 °C	75 min	1.0 MPa air	FFCA	80%	56%	NM	NM	[496]
40	HMF (3.0 wt%)	5 wt% Pt/ZrO ₂	Acidic H ₂ O	140 °C	15 min	1.0 MPa O ₂	FDCA	100%	85%	NM	NM	[496]
41	HMF (3.0 wt%)	5 wt% Pt/SiO ₂	Basic H ₂ O	100 °C	15 min	1.0 MPa air	FDCA	100%	100%	NM	NM	[496]
42	HMF (3.0 wt%)	5 wt% Pt/SiO ₂	H ₂ O	100 °C	60 min	1.0 MPa air	DFF [FFCA]	90%	41%	NM	NM	[496]
43	Fructose (1.0 wt%)	5 wt% PtBi/C + Lewatit SPC 108	H ₂ O/MIBK	70 °C	70 h	1.0 MPa air	FDCA	–	25%	NM	NM	[497]
44	Fructose (1.7 wt%)	5 wt% Co(acac) ₃ /SiO ₂	H ₂ O/MIBK	160 °C	65 min	2.0 MPa air	FDCA	72%	71%	NM	NM	[498]
45	HMF (2.0 wt%)	2.1 wt% Fe ³⁺ -POP-1	H ₂ O	100 °C	10 h	1.0 MPa air	FDCA	100%	79%	NM	NM	[499]
46	HMF (1.4 wt%)	Merrifield resin-Co-Py	CH ₃ CN	100 °C	24 h	t-BuOOH	FDCA	96%	90%	6	60%	[500]
47	HMF (0.3 wt%)	1 mol% Pd/PVP	Basic H ₂ O	90 °C	7 h	0.1 MPa O ₂	FDCA	99%	93%	NM	NM	[501]
48	HMF (0.5 wt%)	3.5 wt% Pt/γ-Al ₂ O ₃	Basic H ₂ O	75 °C	12 h	0.1 MPa O ₂	FDCA	96%	96%	NM	NM	[502]
49	HMF (2.0 wt%)	7 mol% Li ₂ CoMn ₃ O ₈	Basic H ₂ O	150 °C	8 h	5.5 MPa O ₂	FDCA	100%	80%	NM	NM	[503]
50	HMF (1.3 wt%)	1 mol% Pt/ZrO ₂	Basic H ₂ O	100 °C	24 h	4.0 MPa O ₂	FDCA	97%	95%	NM	NM	[504]
51	HMF (1.3 wt%)	1 mol% Pt/TiO ₂	Basic H ₂ O	100 °C	12 h	4.0 MPa O ₂	FDCA	100%	96%	4	95%	[504]
52	HMF (0.6 wt%)	5.4 wt% Pd/C@Fe ₃ O ₄	Basic H ₂ O	80 °C	6 h	0.1 MPa O ₂	FDCA	98%	87%	5	84%	[505]
53	HMF (0.6 wt%)	2.5 wt% γ-Fe ₂ O ₃ @HAP–Pd	Basic H ₂ O	100 °C	6 h	0.1 MPa O ₂	FDCA	97%	93%	5	92%	[506]
54	Fructose (2.5 wt%)	Fe ₃ O ₄ @SiO ₂ –SO ₃ H/nano-Fe ₃ O ₄ –CoO _x	DMSO	100 °C	12 h	75 wt% t-BuOOH	FDCA	99%	60%	6	~60%	[507]
55	HMF (4.7 wt%)	0.05 wt% Co/Mn/Br/Zr	H ₂ O	75 °C	2 h	7.0 MPa air	DFF	100%	61%	NM	NM	[508]
56	HMF (4.7 wt%)	0.05 wt% Co/Mn/Br	H ₂ O	75 °C	2 h	7.0 MPa air	DFF	92%	65%	NM	NM	[508]
57	HMF (2.9 wt%)	10 mol% CuCl ₂ ·2H ₂ O	DMSO	130 °C	72 h	Atmospheric air	DFF	46%	46%	NM	NM	[509]
58	HMF (2.9 wt%)	10 mol% Cu/PVP	Toluene	130 °C	72 h	Atmospheric air	DFF	66%	48%	NM	NM	[509]
59	HMF (2.9 wt%)	3.3 mol% VO/PVP	Toluene	130 °C	24 h	0.1 MPa air	DFF	75%	62%	NM	NM	[509]
60	HMF (2.9 wt%)	3.3 mol% VO/PVP	TFT	130 °C	4 h	1 MPa air	DFF	77%	76%	2	64%	[509]
61	HMF (2.9 wt%)	3.3 mol% VO/PVP	Basic TFT	130 °C	24 h	1 MPa air	DFF	82%	81%	NM	NM	[509]
62	HMF (2.9 wt%)	3.3 mol% VO/SBA	Basic TFT	130 °C	24 h	1 MPa air	DFF	50%	49%	NM	NM	[509]
63	HMF (3.0 wt%)	1.3 wt% FeVOP	Dimethylformamide	100 °C	8 h	0.1 MPa O ₂	DFF	59%	51%	NM	NM	[510]
64	HMF (3.0 wt%)	2.6 wt% CrVOP	Dimethylformamide	100 °C	8 h	0.1 MPa O ₂	DFF	63%	43%	NM	NM	[510]
65	HMF (3.0 wt%)	2.6 wt% GaVOP	Dimethylformamide	100 °C	8 h	0.1 MPa O ₂	DFF	55%	32%	NM	NM	[510]
66	HMF (3.0 wt%)	2.6 wt% MgVOP	Dimethylformamide	100 °C	8 h	0.1 MPa O ₂	DFF	74%	58%	NM	NM	[510]
67	HMF (3.0 wt%)	2.6 wt% CuVOP	Dimethylformamide	100 °C	8 h	0.1 MPa O ₂	DFF	21%	18%	NM	NM	[510]
68	HMF (3.0 wt%)	2.6 wt% PdVOP	Dimethylformamide	100 °C	8 h	0.1 MPa O ₂	DFF	49%	29%	NM	NM	[510]
69	HMF (0.3 wt%)	5.1 wt% VO _x /TiO ₂	Toluene	90 °C	–	1.6 MPa air	DFF	~30%	21%	NM	NM	[511]
70	HMF (0.3 wt%)	8.0 wt% VO _x /ZrO ₂	Toluene	90 °C	--	1.6 MPa air	DFF	~30%	21%	NM	NM	[511]
71	HMF (0.3 wt%)	9.0 wt% VO _x /Al ₂ O ₃	Toluene	90 °C	–	1.6 MPa air	DFF	~30%	17%	NM	NM	[511]
72	HMF (0.3 wt%)	3.0 wt% VO _x /Nb ₂ O ₅	Toluene	90 °C	–	1.6 MPa air	DFF	~30%	22%	NM	NM	[511]
73	HMF (0.3 wt%)	5.5 wt% VO _x /MgO	Toluene	90 °C	–	1.6 MPa air	DFF	~30%	13%	NM	NM	[511]
74	HMF (1.3 wt%)	1.3 mol% Ru/C	Toluene	110 °C	–	2.0 MPa O ₂	DFF	~30%	29%	NM	NM	[512]
75	HMF (1.3 wt%)	1.3 mol% Ru/Mg ₂ AlO _x	Toluene	110 °C	–	2.0 MPa O ₂	DFF	~30%	28%	NM	NM	[512]
76	HMF (1.3 wt%)	1.3 mol% Ru/MgO	Toluene	110 °C	–	2.0 MPa O ₂	DFF	~30%	6%	NM	NM	[512]
77	HMF (1.3 wt%)	1.3 mol% Ru/Al ₂ O ₃	Toluene	110 °C	–	2.0 MPa O ₂	DFF	~30%	25%	NM	NM	[512]
78	HMF (1.3 wt%)	1.3 mol% Ru/ZSM-5	Toluene	110 °C	–	2.0 MPa O ₂	DFF	~30%	4%	NM	NM	[512]
79	HMF (1.3 wt%)	1.3 mol% Ru/TiO ₂	Toluene	110 °C	–	2.0 MPa O ₂	DFF	~30%	17%	NM	NM	[512]

(continued on next page)

Table 6 (continued)

Entry	Substrate	Catalyst ^a	Reaction conditions			Oxidant	Main Product	Catalytic activity		Reusability		Ref.
			Solvent	Temp.	Time			Conv.	Yield	Cycles	Yield ^b	
80	HMF (1.3 wt%)	1.3 mol% Ru/ZrO ₂	Toluene	110 °C	–	2.0 MPa O ₂	DFF	~30%	20%	NM	NM	[512]
81	HMF (1.3 wt%)	1.3 mol% Ru/CeO ₂	Toluene	110 °C	–	2.0 MPa O ₂	DFF	~30%	18%	NM	NM	[512]
82	HMF (1.3 wt%)	1.3 mol% Ru/C	Benzotrifluoride	110 °C	–	2.0 MPa O ₂	DFF	~30%	28%	NM	NM	[512]
83	HMF (1.3 wt%)	1.3 mol% Ru/C	1,4-Dioxane	110 °C	–	2.0 MPa O ₂	DFF	~30%	12%	NM	NM	[512]
84	HMF (1.3 wt%)	1.3 mol% Ru/C	H ₂ O	110 °C	–	2.0 MPa O ₂	DFF	~30%	25%	NM	NM	[512]
85	HMF (1.3 wt%)	1.3 mol% Ru/C	DMSO	110 °C	–	2.0 MPa O ₂	DFF	~30%	25%	NM	NM	[512]
86	HMF (1.3 wt%)	1.3 mol% Ru/C	Dimethylformamide	110 °C	–	2.0 MPa O ₂	DFF	~30%	14%	NM	NM	[512]
87	Glucose (8.0 wt%)	6 mol% CrCl ₃ ·6H ₂ O/NaBr	DMA	100 °C	6 h	21 mol% NaVO ₃ ·2H ₂ O	HMF	–	–	5	54%	[513]
				[110 °C]	[20 h]		[DFF]		[55%]			
88	Fructose (6.0 wt%)	Fe ₃ O ₄ –SBA–SO ₃ H + K–OMS-2 (1:1)	DMSO	100 °C	2 h + 6 h	Air + O ₂ flow	HMF	99%	81%	NM	NM	[514]
89	Glucose (6.0 wt%)	Fe ₃ O ₄ –SBA–SO ₃ H + K–OMS-2 (1:1)	DMSO	100 °C	2 h + 6 h	Air + O ₂ flow	HMF	99%	–	NM	NM	[514]
90	Inulin (6.0 wt%)	Fe ₃ O ₄ –SBA–SO ₃ H + K–OMS-2 (1:1)	DMSO	100 °C	2 h + 6 h	Air + O ₂ flow	HMF	99%	[<5%]			
91	Glucose (3.3 wt%)	HT + Amberlyst-15 + Ru/HT (1:1:1)	Dimethylformamide	120 °C	3 h + 6 h	N ₂ flow + O ₂ flow	HMF	98%	9%	NM	NM	[515]
92	HMF (1.0 wt%)	15 wt% Ag/OMS-2	2-Propanol	165 °C	6 h	1.5 MPa Air	DFF	100%	99%	NM	NM	[516]
93	HMF (1.3 wt%)	3 wt% Ru/C	Toluene	110 °C	–	2.0 MPa O ₂	DFF	30%	29%	5	25%	[517]
94	HMF (1.3 wt%)	3 wt% Ru/C	Toluene	110 °C	7 h	2.0 MPa O ₂	DFF	100%	29%	NM	NM	[517]
							[FFCA] (FDCA)		[52%] (8%)			
95	HMF (1.3 wt%)	3 wt% Ru/C + HT	Toluene	110 °C	6 h	2.0 MPa O ₂	DFF	100%	1%	NM	NM	[517]
							[FFCA] (FDCA)		[83%] (5%)			
96	HMF (1.3 wt%)	3 wt% Ru/C + HT	Toluene	110 °C	8 h	2.0 MPa O ₂	DFF	100%	0	NM	NM	[517]
							[FFCA] (FDCA)		[3%] (75%)			
97	HMF (25.2 wt%)	2 mol% VOSO ₄ + 2 mol% Cu(NO ₃) ₂	CH ₃ CN	80 °C	1.5 h	0.1 MPa O ₂	DFF	99%	98%	NM	NM	[518]
98	HMF (1.0 wt%)	0.93%V–0.26%Cu/sulfonated carbon	CH ₃ CN	140 °C	4 h	4.0 MPa Air	DFF	100%	98%	3	98%	[519]
99	HMF (1.8 wt%)	10 mol% RuCo(OH) ₂ CeO ₂	MIBK	120 °C	12 h	O ₂ flow	DFF [FDCA]	96%	83% [9%]	5	75%	[520]
100	Fructose (10 wt%)	50 wt% Cs ₃ HPMo ₁₁ VO ₄₀	DMSO	110 °C	2 h + 6 h	0.1 MPa N ₂ + 0.1 MPa O ₂	HMF [DFF]	99%	72% [60%]	4	53%	[521]
101	Fructose (4.5 wt%)	11.1 wt% Cs _{0.5} H _{2.5} PMo ₁₂	DMSO	160 °C	4 h	Atmospheric air	DFF	–	69%	5	52%	[522]
102	HMF (1.3 wt%)	39.7 wt% KMn ₈ O ₁₆ ·nH ₂ O	Dimethylformamide	110 °C	1 h	0.5 MPa O ₂	DMF	100%	97%	NM	NM	[523]
103	Fructose (10 wt%)	50 wt% g-C ₃ N ₄ (H ⁺)	DMSO	130 °C	2 h + 6 h	0.1 MPa N ₂ 0.1 MPa O ₂	HMF [DFF]	99%	80% 63%	NM	NM	[524]
104	HMF (1.0 wt%)	5 mol% V ₂ O ₅ /AC	MIBK	100 °C	4 h	0.2 MPa O ₂	DFF	95%	92%	2	62%	[525]
105	HMF (1.3 wt%)	80 wt% Polyaniline-VO(acac) ₂	4-Chlorotoluene	100 °C	12 h	0.1 MPa O ₂	DFF	99%	86%	6	75%	[526]
106	HMF (2.0 wt%)	10 wt% V ₂ O ₅ /Beta	Dimethylformamide	125 °C	180 min	1.0 MPa O ₂	DFF	84%	83%	NM	NM	[527]
107	HMF (1.3 wt%)	2 mol% Cu(NO ₃) ₂ /NHPI	CH ₃ CN	50 °C	7 h	0.1 MPa O ₂	DFF	–	71%	NM	NM	[528]
108	HMF (8.4 wt%)	20 mol% CuI + 7.5 mol% HBT	DMSO	130 °C	10 h	0.3 MPa O ₂	DFF	93%	92%	NM	NM	[529]

(continued on next page)

Table 6 (continued)

Entry	Substrate	Catalyst ^a	Reaction conditions			Oxidant	Main Product	Catalytic activity		Reusability		Ref.
			Solvent	Temp.	Time			Conv.	Yield	Cycles	Yield ^b	
109	HMF (1.3 wt%)	2.2 wt% Ru-PVP/CNT	Dimethylformamide	120 °C	12 h	2.0 MPa O ₂	DFF	100%	94%	NM	NM	[530]
110	HMF (0.8 wt%)	2.5 mol% Ru/CTF	MTBE	80 °C	1 h	2.0 MPa O ₂	DFF	86%	55%	NM	NM	[531]
111	HMF (5.6 wt%)	5 wt% Pd-V(3:2)@MIL-101	DMSO	140 °C	10 h	0.1 MPa O ₂	DFF [HMF]	100%	40%	NM	NM	[532]
112	HMF (6.3 wt%)	30 mol% HBr or 30 mol% NaBr	DMSO	150 °C	18 h	Atmospheric air	DFF	100%	85%	NM	NM	[533]
113	HMF (1.8 wt%)	133.3 wt% Mn ₃ O ₄ /Fe ₃ O ₄	Dimethylformamide	120 °C	4 h	O ₂ flow	DFF	100%	82%	NM	NM	[534]
114	HMF (6.3 wt%)	2 mol% MNST + TEMPO-SiO ₂ @Fe ₃ O ₄	Toluene + AcOH	50 °C	12 h	0.1 MPa O ₂	DFF	100%	99%	5	97%	[535]
115	HMF (1.4 wt%)	2 wt% Ru-HAP@γ-Fe ₂ O ₃	4-Chlorotoluene	90 °C	4 h	O ₂ flow	DFF	100%	89%	6	80%	[536]
116	HMF (1.4 wt%)	1.4 wt% Ru(III)-NH ₂ -SiO ₂ @Fe ₃ O ₄	Toluene	120 °C	16 h	Atmospheric air or O ₂ flow	DFF	100%	87%	6	81%	[537]
117	HMF (6.3 wt%)	5 mol% VO(acac) ₂	CH ₃ CN	90 °C	4 h	0.1 MPa O ₂	MA [DFF]	15%	<1% [7%]	NM	NM	[538]
118	HMF (6.3 wt%)	5 mol% VO(acac) ₂	CH ₃ CN	90 °C	4 h	1.0 MPa O ₂	MA [DFF]	100%	52% [14%]	NM	NM	[538]
119	HMF (9.2 wt%)	0.8 mol% H ₅ PV ₂ Mo ₁₀ O ₄₀ ·xH ₂ O	CH ₃ CN +AcOH	90 °C	8 h	1.0 MPa O ₂	MA [FA]	–	32% [32%]	NM	NM	[539]
120	Furfural (15 vol%)	H ₄ PMo ₁₂ O ₄₀ /Cu(NO ₃) ₂ (2:1)	H ₂ O	98 °C	14 h	2.0 MPa O ₂	MA	95%	50%	NM	NM	[540]
121	Furfural (11.5 wt%)	H ₅ PV ₂ Mo ₁₀ O ₄₀ /Cu(CF ₃ SO ₃) ₂ (1:1)	CH ₃ CN	110 °C	14 h	2.0 MPa O ₂	MA	99%	54%	NM	NM	[541]
122	Furfural (1.6 kPa)	8.9 wt% VO _x /Al ₂ O ₃	H ₂ O	320 °C	–	5.7 kPa O ₂	MA	100%	73%	NM	NM	[542]
123	Furfural (4.6 wt%)	4.6 wt% Titanium silicalite	H ₂ O	50 °C	24 h	12.3 wt% H ₂ O ₂	MA	100%	78%	NM	NM	[543]
124	Furfural (4.6 wt%)	4.6 wt% Titanium silicalite + Amberlyst 70	H ₂ O	50 °C	28 h (52 h)	7.2 wt% H ₂ O ₂	MA	100%	80% (92%) (7 h)	6	45%	[543]
125	Xylose (3.0 wt%)	Vanadyl pyrophosphate	H ₂ O	300 °C	–	10 vol% O ₂	MA [Acrylic acid] (Acrolein)	100%	25% [17%] (11%)	NM	NM	[544]
126	Xylose (3.0 wt%)	Iron molybdate	H ₂ O	300 °C	–	10 vol% O ₂	MA [Acrylic acid] (Acrolein)	100%	2% [3%] (2%)	NM	NM	[544]
127	Xylose (3.0 wt%)	Molybdenum trioxide-cobalt oxide	H ₂ O	300 °C	–	10 vol% O ₂	MA [Acrylic acid] (Acrolein)	100%	2% [3%] (7%)	NM	NM	[544]
128	HMF (4.0 wt%)	0.3 mol% Au/TiO ₂	MeOH + CH ₃ ONa	130 °C	3 h	0.4 MPa O ₂	FDMC	100%	98%	NM	NM	[545]
129	HMF (1.3 wt%)	2.1 wt% Au/CeO ₂	MeOH	130 °C	5 h	1.0 MPa O ₂	FDMC	99%	98%	5	96%	[545]
130	Furfural (1.3 wt%)	2.1 wt% Au/CeO ₂	MeOH	130 °C	5 h	1.0 MPa O ₂	MFA	99%	90%	NM	NM	[545]
131	Furfural (0.2 wt%)	1.2 wt% Au/ZrO ₂	MeOH	60 °C	90 min	0.6 MPa O ₂	MFA	25%	25%	NM	NM	[546]
132	Furfural (0.2 wt%)	1.2 wt% Au/ZrO ₂	MeOH	120 °C	90 min	0.1 MPa O ₂ or Air	MFA	100%	90%	NM	NM	[546]
133	HMF (0.2 wt%)	1.2 wt% Au/ZrO ₂	MeOH	130 °C	5 h	0.1 MPa O ₂	MFA	100%	30%	NM	NM	[546]
134	Furfural (0.2 wt%)	1.0 wt% Au/ZrO ₂	MeOH	120 °C	90 min	0.6 MPa O ₂	MFA	82%	74%	2	70%	[547]
135	Furfural (0.2 wt%)	2.2 wt% Au/CeO ₂	MeOH	120 °C	90 min	0.6 MPa O ₂	MFA	66%	46%	2	42%	[547]
136	Furfural (0.2 wt%)	1.2 wt% Au/TiO ₂	MeOH	120 °C	90 min	0.6 MPa O ₂	MFA	20%	18%	2	7%	[547]
137	HMF (0.2 wt%)	1.5 wt% Au/TiO ₂	MeOH	130 °C	5 h	0.3 MPa O ₂	FDMC	90%	5%	NM	NM	[548]
138	HMF (0.2 wt%)	1.5 wt% Au/ZrO ₂	MeOH	130 °C	5 h	0.3 MPa O ₂	FDMC	100%	23%	NM	NM	[548]
139	HMF (0.2 wt%)	1.5 wt% Au/ZrO ₂ -SO ₄	MeOH	130 °C	5 h	0.3 MPa O ₂	FDMC	100%	32%	NM	NM	[548]

(continued on next page)

Table 6 (continued)

Entry	Substrate	Catalyst ^a	Reaction conditions			Oxidant	Main Product	Catalytic activity		Reusability		Ref.
			Solvent	Temp.	Time			Conv.	Yield	Cycles	Yield ^b	
140	Levulinic acid (0.6 wt%)	5.0 wt% Ru-MNP	H ₂ O	150 °C	6 h	1.0 MPa O ₂	Succinic acid	54%	52%	4	53%	[549]
141	Furfural (3.2 wt%)	52.1 wt% Amberlyst-15	H ₂ O	80 °C	24 h	30 wt% H ₂ O ₂	Succinic acid	100%	74%	3	70%	[550]
142	Methyl levulinate (0.8 wt%)	10 mol% <i>p</i> -TsOH	MeOH	80 °C	6 h	200 mol% H ₂ O ₂	Methyl succinate [Methyl acetate] [22%]	56%	34%	NM	NM	[551]
143	Methyl levulinate (0.8 wt%)	10 mol% MeSO ₃ H	MeOH	80 °C	6 h	200 mol% H ₂ O ₂	Methyl succinate [Methyl acetate] [22%]	48%	26%	NM	NM	[551]
144	Methyl levulinate (0.8 wt%)	10 mol% H ₂ SO ₄	MeOH	80 °C	6 h	200 mol% H ₂ O ₂	Methyl succinate [Methyl acetate] [21%]	54%	33%	NM	NM	[551]
145	Methyl levulinate (0.8 wt%)	10 mol% TFOH	MeOH	80 °C	6 h	200 mol% H ₂ O ₂	Methyl succinate [Methyl acetate] [19%]	49%	30%	NM	NM	[551]
146	Methyl levulinate (0.8 wt%)	10 mol% Amberlyst-15	MeOH	80 °C	6 h	200 mol% H ₂ O ₂	Methyl succinate [Methyl acetate] [5%]	13%	8%	NM	NM	[551]
147	Methyl levulinate (0.8 wt%)	10 mol% Hf(OTf) ₄	MeOH	80 °C	6 h	200 mol% H ₂ O ₂	Methyl succinate [Methyl acetate] [14%]	36%	21%	NM	NM	[551]
148	Methyl levulinate (0.8 wt%)	10 mol% Hg(OTf) ₂	MeOH	80 °C	6 h	200 mol% H ₂ O ₂	Methyl succinate [Methyl acetate] [19%]	40%	19%	NM	NM	[551]
149	Methyl levulinate (0.8 wt%)	10 mol% Sc(OTf) ₃	MeOH	80 °C	6 h	200 mol% H ₂ O ₂	Methyl succinate [Methyl acetate] [13%]	38%	19%	NM	NM	[551]
150	Levulinic acid (1.7 wt%)	435 mol% KOH + [10 wt% Pd/C]	H ₂ O + [MeOH]	0 °C	6 h + [40 min]	30 wt% H ₂ O ₂ × 2 + [0.38 MPa H ₂]	3-(Hydroperoxy)propanoic acid + 3-hydroxypropanoic acid	100%	80%	NM	NM	[552]
151	Levulinic acid (20.0 wt%)	79 wt% HTFA	H ₂ O	90 °C	20 min	30 wt% H ₂ O ₂	Succinic acid	100%	60%	NM	NM	[553]

^a Metal loading of the catalyst or catalyst dosage relative to the substrate.^b Product yield in the last cycle.

c NM: not mentioned.

HMF: 5-hydroxymethylfurfural, FDCA: 2,5-furandicarboxylic acid, HT: hydrotalcite, [EMIm][OAc]: 1-ethyl-3-methylimidazolium acetate, HMFCA: 5-hydroxymethyl-2-furancarboxylic acid, DFF: 2,5-diformylfuran, CNT: carbon nanotube, FFCA: 5-formyl-2-furancarboxylic acid, HTFA: trifluoroacetic acid, Lewatit SPC 108: a microporous cationic ion exchanger in H⁺ form, MIBK: methyl isobutyl ketone, Co(acac)₃: cobalt acetylacetone, Fe³⁺-POP-1: Fe³⁺-porous organic polymer, Merrifield resin-Co-Py: Merrifield resin supported Co(II)-meso-tetra(4-pyridyl)-porphyrin, *t*-BuOOH: tert-butyl hydroperoxide, PVP: polyvinyl pyrrolidone, TFT: trifluorotoluene, K-OMS-2: H_{0.2}K_{0.8}Mn₂O₁₆·*n*H₂O is an octahedral molecular sieve, NHPI: *N*-hydroxyphthalimide, HBT: 1-hydroxybenzotriazole, PVP/CNT: poly(4-vinylpyridine)-functionalized carbon-nanotube, CTF: covalent triazine frameworks, MTBE: methyl *t*-butyl ether, AcOH: acetic acid, MNST: immobilized nitroxyl radical, TEMPO: 2,2,6,6-tetramethylpiperidine-*N*-oxide, HAP: hydroxyapatite, MA: maleic anhydride, FDMC: 2,5-dimethylfuroate, MFA: methyl furoate, MNP: magnetic nanoparticles, *p*-TsOH: *p*-toluenesulfonic acid, MeSO₃H: methane sulfonic acid, TFOH: triflic acid.

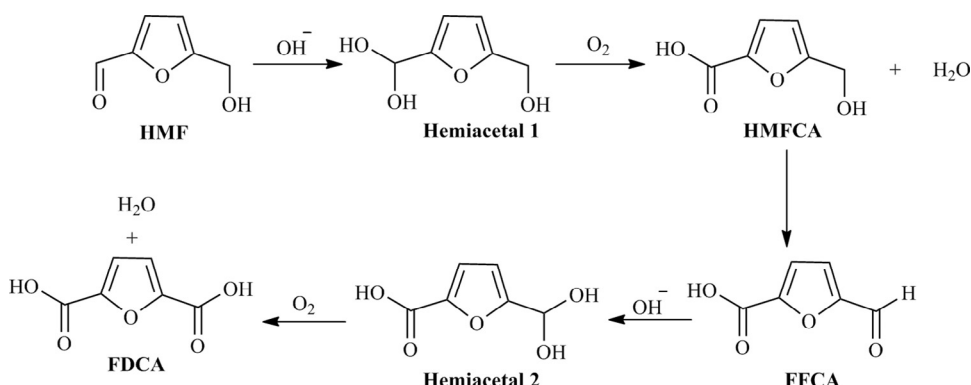


Fig. 25. Proposed reaction pathway for aqueous HMF (5-hydroxymethylfurfural) aerobic oxidation. HMFCa: 5-hydroxymethyl-2-furancarboxylic acid, FFCA: 5-formyl-2-furancarboxylic acid, FDCA: 2,5-furandicarboxylic acid. Adapted with permission from Ref. 488, Copyright © 2009 Wiley-VCH.

dissolution of Mg^{2+} ions under the reaction conditions, resulting in the generation of Mg-FDCA salts that are stabilized against further degradation. Among these salts, the spinel form remains stable and allows the oxidation reaction to proceed under base-free conditions [554]. By using ILs as the reaction solvent, Ståhlberg et al. [486] found that Ru(OH)_x on La_2O_3 support was suitable for oxidation in IL 1-ethyl-3-methylimidazolium acetate ($[\text{EMIM}][\text{OAc}]$), affording an FDCA yield of 48% (Table 6, Entry 12). In comparison with other ILs such as $[\text{EMIM}]\text{Cl}$, $[\text{BMIM}]\text{Cl}$, $[\text{BMIM}][\text{PF}_6]$, $[\text{BMIM}][\text{BF}_4]$, and $[\text{EMIM}][\text{HSO}_4]$, $[\text{EMIM}][\text{OAc}]$ appears to possess a higher solubility for oxygen, but rapidly degrades HMF [555], which renders it to be the best IL solvent among those studied for this catalytic process.

Besides ruthenium containing catalysts, gold particles supported on metal oxides are promising catalysts for oxidation reactions. In the presence of a base promoter (e.g., NaOH or KOH), the oxidation of aqueous HMF occurs with a commercial heterogeneous Au/TiO_2 catalyst, giving an FDCA yield of 71% (Table 6, Entry 13) [487]. The Cannizzaro reaction along with favorable reaction conditions for HMF degradation seems to be the reason why high the FDCA yields are obtained. Compared with Au/TiO_2 , $\text{Au}/\text{Fe}_2\text{O}_3$ and Au/C , Casanova et al. [488] found that Au/CeO_2 displays a relatively higher catalytic activity for the aerobic oxidation of HMF-to-FDCA in water than other Au/supports and gives and a maximum FDCA yield of 100% (Table 6, Entries 14–17). The nanoparticulate ceria support with gold nanoparticles is possibly responsible for the accelerated reaction rate, while the increased amount of Ce^{3+} from the reductive pretreatment of Au/CeO_2 catalyst probably enhances its catalytic reactivity. The reaction mechanism proposed (Fig. 25), and the alcohol oxidation of 5-hydroxymethyl-2-furancarboxylic acid (HMFCa) to FDCA was speculated to be the rate-limiting step. In the proposed reaction pathway (Fig. 25), HMFCa is initially formed from HMF via rapid oxidation of the intermediate Hemiacetal 1, while the oxidation of HMFCa to 5-formyl-2-furancarboxylic acid (FFCA) is slow, and then in situ generates the second hemiacetal intermediate (Hemicetal 2), which is rapidly converted into FDCA.

Desorption of the acid product from the gold surface with a base seems to be always required for the oxidation of HMF [556]. Then, neutralization of the produced salts of carboxylic acid products with a homogeneous base is necessary at the end of the reaction. In this regard, solid base catalysts appear to be promising candidates for the reaction. Gold supported on HT with moderate basicity facilitates the formation of FDCA that exceeds Au/TiO_2 , and 99% selectivity of FDCA at HMF conversion of 100% is obtained at 90 °C in 20 h (Table 6, Entry 18) [489]. Unfortunately, extensive leaching of magnesium from HT results in the formation of a homogeneous basic solution. By using the same catalyst Au/HT , Gupta et al. [490] detected that gold species do not leach out of the HT support as confirmed by ICP analysis, and the catalyst efficiently promotes HMF

oxidation to afford FDCA in an almost constant yield of >99%, 92% and 90% for the first, second and third runs, respectively (Table 6, Entry 19). To further enhance the reusability and stability of gold nanoparticles, Pasini et al. [491] show that a relatively stronger synergistic effect in terms of sample stability and resistance to poisoning is evident with the addition of copper to gold, compared with their monometallic analogs (Table 6, Entries 20–23). Moreover, bimetallic gold–copper nanoparticles supported on TiO_2 are more active for the oxidation of HMF to FDCA than Au/TiO_2 and Cu/TiO_2 , which might be the result of gold site isolation caused by alloying. The stabilization effect and catalytic performance of the alloy are strongly related to the amount of copper, and the highest level of reusability and the best catalytic activity are obtained with the bimetallic system of 1.5 wt% AuCu/TiO_2 at Au/Cu atomic ratios of 1 and 3, respectively [557]. Significant synergistic effects have been observed between two alloyed metals for the base-free oxidation of HMF to FDCA in AuPd/CNT (carbon nanotube; Table 6, Entries 24–26) [492] and AuCu/CeO_2 (Table 6, Entries 27 and 28) [493].

Both catalyst site basicity and type of oxidant are important to selectively and efficiently oxidize HMF to FDCA. The roles of added base and molecular oxygen in the formation of FDCA from HMF with Pt/C or Au/TiO_2 catalyst have been investigated through labeling experiments with $^{18}\text{O}_2$ and H_2^{18}O [558] (Fig. 26): (1) initial nucleophilic addition of a hydroxide ion to the carbonyl group with the subsequent proton transfer from water gives a geminal diol; (2) the carboxylic acid formed from dehydrogenation of the geminal diol intermediate is facilitated by the hydroxide ions adsorbed onto the metal surface; (3) the hydroxide ions further assist the activation of C–H bond of the alcohol side-chain to afford HMFCa (aldehyde intermediate); (4 and 5) the aldehyde side-chain of HMFCa is oxidized to produce FDCA, analogous to the oxidation of HMF to HMFCa in steps (1) and (2). Molecular oxygen is proposed to scavenge the electrons deposited into the metal particles so as to close the catalytic cycle, preferable to directly participating in oxidation or dehydrogenation steps. Under identical conditions, platinum particles show higher selectivity for FDCA during HMF oxidation than gold, which might be attributed to the platinum being able to activate the geminal hydrogen atoms of alcohol. Comparison of the rate and product distribution in the oxidation of HMF to FDCA over Pt/C , Pd/C , Au/C and Au/TiO_2 shows the reactivity of platinum, palladium and gold particles (Table 6, Entries 29–32) [494] for which the rate of HMF oxidation to the intermediate HFCA with gold catalyst is an order of magnitude higher than that with either platinum or palladium catalyst, while FDCA is directly formed by further oxidation of HFCA over platinum, palladium except gold particles. For Au/TiO_2 , the formation of FDCA from HFCA is realized under relatively higher O_2 partial pressures (ca. 2000 or 3000 kPa) and base concentrations (ca. 2.0 M) in which the base concentration has a

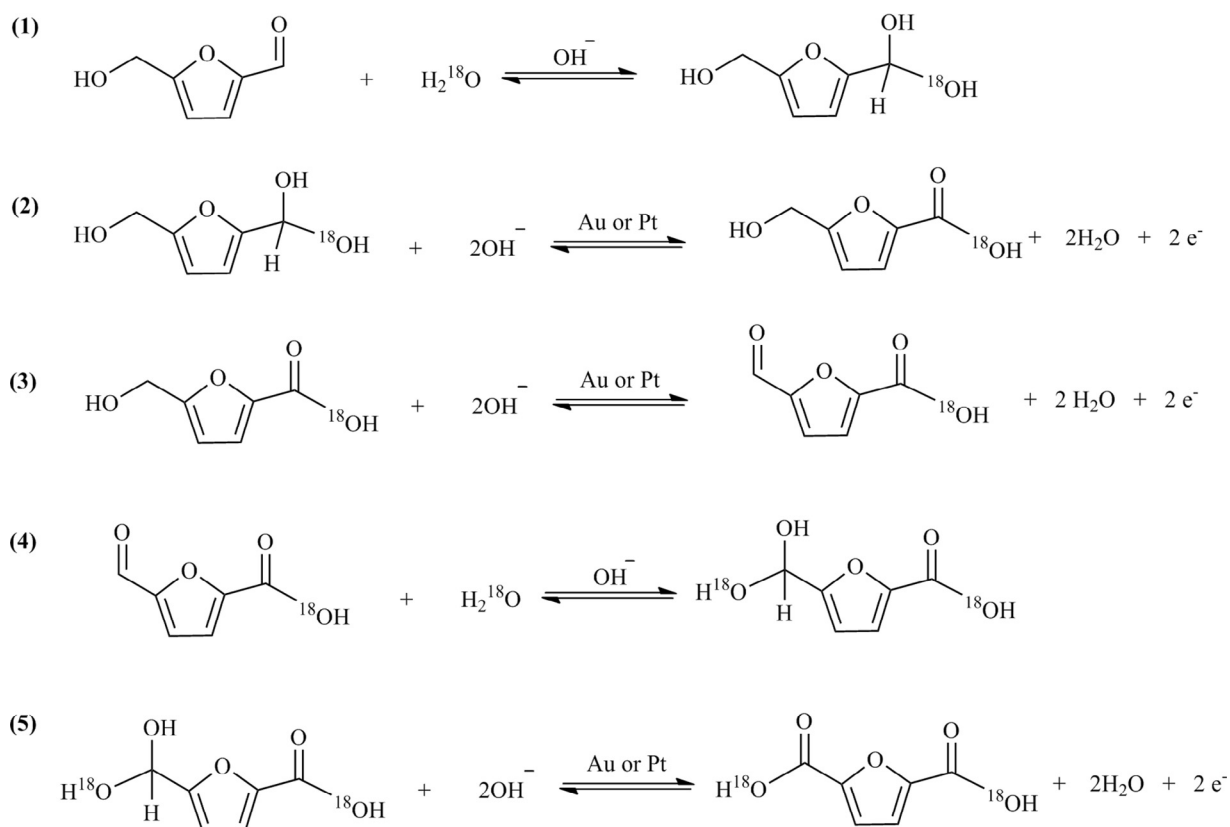
HMF oxidation mechanism:

Fig. 26. Overall reaction pathway for HMF (5-hydroxymethylfurfural) oxidation in aqueous solution (H_2^{18}O) in the presence of dioxygen ($^{18}\text{O}_2$), excess base (OH^-) and either platinum or gold catalyst. Adapted with permission from Ref. 558, Copyright © 2011 Royal Society of Chemistry.

stronger effect on the reaction than the O_2 partial pressure [494]. For example, the selectivity for FDCA over Au/TiO_2 increases from 3% to 28% when O_2 partial pressure is increased from 690 to 2000 kPa at 50% HMF conversion in 0.3 M NaOH solution, while 80% FDCA selectivity and 100% HMF conversion are achieved in the presence of 2 M NaOH under 2000 kPa O_2 partial pressure.

Saha et al. [495] aerobically oxidized HMF in acetic acid (HOAc) with $\text{Co}(\text{OAc})_2/\text{Zn}(\text{OAc})_2/\text{Br}^-$ homogeneous catalyst, but 2,5-diformylfuran (DFF) is the only oxidation product with high yield (ca. 96%) (Table 6, Entry 33). When 1 wt% trifluoroacetic acid (HTFA) is added together with HOAc as acid additive, HMF is directly oxidized to FDCA with a maximum yield of 60% and FFCA (29% yield) (Table 6, Entry 34). Supported catalysts Au/TiO_2 and Au/CeO_2 improve HMF conversions from 62% to 84% and 29% to 83%, respectively, with corresponding FFCA yields increasing from 45% to 79% and 17% to 71% in the absence and presence of 1 wt% HTFA (Table 6, Entries 35–38). Among these Au/support catalysts, Au/TiO_2 has a higher gold content and BET surface area than Au/CeO_2 , which probably contributes to its higher catalytic activity.

Lilga et al. [496] investigated the effect of basic, neutral, and acidic feeds on HMF oxidation. FDCA has low solubility in water (0.086 wt% at 25 °C), but has moderate solubility in carboxylic acid solvents (e.g., for aqueous 40 vol% acetic acid, FDCA solubility is 0.153 wt% at 25 °C). In acidic solutions, DFF is the preferred product with about 70% selectivity over Pt/ZrO_2 at 100 °C using air as oxidant (Table 6, Entry 39). By increasing the temperature from 100 to 140 °C and introducing O_2 instead of air, HMF conversion rises to 100% and FDCA selectivity increases to 85% (Table 6, Entry 40). With basic

solutions, high yields of FDCA, fast rates, and good product solubilities are attained (Table 6, Entry 41), while reactions in neutral solutions are slower and generally produce both DFF and FDCA (Table 6, Entry 42). The product distribution of HMF oxidation can be controlled to some extent by adjusting the acid–base properties of the reaction solution, which is possibly useful in practical processes.

Kröger et al. [497] converted fructose directly into FDCA in a two-phase system composed of water and MIBK, in which a microporous cationic ion exchanger in H^+ form (Lewatit SPC 108) catalyzes the dehydration of fructose to HMF in the aqueous phase and a subsequent oxidation reaction occurs in the MIBK phase with a MIBK-modified PtBi/C catalyst encapsulated in silicone beads. With this catalytic system, a moderate FDCA yield of 25% is obtained at 80 °C at the end of the in situ oxidation process (Table 6, Entry 43). A bi-functional acidic and redox catalyst prepared by encapsulation of cobalt acetylacetone into a sol-gel silica matrix is highly efficient for direct fructose-to-FDCA conversion (Table 6, Entry 44) [498]. Extraction purification [559] in a triphasic system consisting of tetraethylammonium bromide (TEAB) or water–MIBK–water [560] allows an integrated process for cascade dehydration and oxidation of fructose in a single pot, affording an overall FDCA yields of 83% and 78%, respectively, for those solvent systems.

A few other catalytic systems have been proposed for the selective oxidation of HMF to FDCA. A highly cross-linked and thermally stable Fe^{3+} -porous organic polymer (Fe^{3+} -POP-1) containing basic porphyrin subunits and iron metal center is an efficient heterogeneous catalyst for HMF oxidation, and a FDCA yield of 79% at HMF

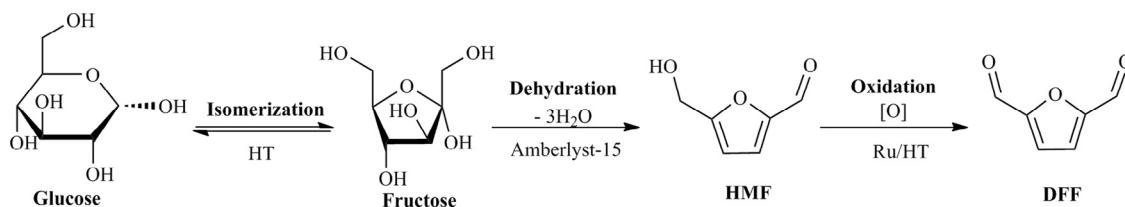


Fig. 27. One-pot synthesis of DFF (2,5-diformylfuran) from glucose via successive isomerization, dehydration, and selective oxidation. Adapted with permission from Ref. 515, Copyright © 2011 American Chemical Society.

conversion of 100% is obtained (Table 6, Entry 45) [499]. Merrifield resin supported Co(II)-meso-tetra(4-pyridyl)-porphyrin with tert-butyl hydroperoxide as oxidant converts 96% HMF to yield 90% FDCA (Table 6, Entry 46) [500]. Pd nanoparticles stabilized by PVP (poly-vinyl pyrrolidone; Table 6, Entry 47) [501], Pt/ γ -Al₂O₃ (Table 6, Entry 48) [502], Li₂CoMn₃O₈ (Table 6, Entry 49) [503], Pt/TiO₂ and Pt/ZrO₂ (Table 6, Entries 50 and 51) [504] afford FDCA in high yields from HMF. The properties of the supports affect both reactivity and stability of the metal nanoparticles in a direct way. In an external magnetic field, solid catalysts being paramagnetic and oxidizable, such as nano-Fe₃O₄–CoO_x, γ -Fe₂O₃@HAP–Pd and Pd/C@Fe₃O₄, are stable, magnetically separable, and active for HMF-to-FDCA oxidation (Table 6, Entries 52–54) [505–507].

4.1.2.2. 2,5-Diformylfuran (DFF). Synthesis of DFF from the oxidation of the primary hydroxyl group in HMF without affecting the more reactive α,β -unsaturated aldehyde group is a challenging route for fabricating macrocyclic ligands, pharmaceuticals, and functional materials [561–563]. One of the first representative studies on the aerobic oxidation of HMF to DFF used homogeneous metal/bromide catalysts (Co/Mn/Br and Co/Mn/Zr/Br) and was reported by Partenheimer and Grushin (Table 6, Entries 55 and 56) [508]. When copper and vanadium immobilized in poly(4-vinylpyridine) are crosslinked with 33% divinylbenzene (DVB) or supported on organofunctionalized SBA-15 mesoporous materials, relatively higher activity and better chemoselectivity were observed, as compared with the corresponding homogeneous catalysts (Table 6, Entries 57–62) [509]. Among these heterogeneous catalysts, vanadium-containing polymeric catalysts are more active than their copper analogs and afford DFF selectivities greater than 99% for 82% HMF conversions (Table 6, Entry 61). However, metal leaching occurs during the reaction. In contrast, SBA-15 mesoporous silica immobilized pyridine-VO(acac)₂ is able to avoid metal leaching, but its catalytic activity is far lower, with a maximum DFF selectivity of 98% at HMF conversion of 50% (Table 6, Entry 62). To further improve the reactivity of vanadium catalysts, partial substitution of VO³⁺ with different metal cations (Fe³⁺, Cr³⁺, Ga³⁺, Mg²⁺, Cu²⁺ and Pd²⁺) can be used (Table 6, Entries 63–68) [510], however, no significant improvement in the catalytic performance is observed. Different metal oxide supports including TiO₂, Al₂O₃, Nb₂O₅, ZrO₂, and MgO have been employed to immobilize VO_x catalysts at varying VO_x surface densities (Table 6, Entries 69–73) [511], and the support surfaces covered with acidity, polyvanadates and V₂O₅ clusters are demonstrated to favor the formation of DFF. V₂O₅ clusters appear to show superior activity to VO³⁺ species in the oxidation of HMF to DFF, and both catalytic systems are likely to be promoted by acidic supports.

The influence of supports, solvents, and metal oxidation states on the activity and DFF selectivity of ruthenium catalysts has been examined to understand structural requirements of immobilized metal catalysts [512]. Solid supports including activated carbon, typical solid bases Mg₂AlO_x and MgO, solid acids Al₂O₃ and ZSM-5, and amphoteric and redox oxides TiO₂, CeO₂, and ZrO₂ have been adopted to support Ru (Table 6, Entries 74–81). The weak acidity and basicity in the supports promote DFF formation, and in particular,

activated carbon supported Ru shows superior reactivity in the synthesis of DFF from HMF.

The effect of toluene, benzotrifluoride, 1,4-dioxane, H₂O, DMSO and N,N-dimethylformamide solvents on HMF-to-DFF conversion for of Ru/C catalyst has been studied (Table 6, Entries 82–86) [512]. Among the solvents, benzotrifluoride has comparable activity with toluene (79.4 h⁻¹ vs. 61.2 h⁻¹) for almost the same DFF selectivity (95 %). In 1,4-dioxane solvent, Ru/C catalyst has high activity (74.8 h⁻¹) but low DFF selectivity (40 %), while water has a higher activity (160.7 h⁻¹) with moderate DFF selectivity (84%). Solvents N,N-dimethylformamide and DMSO exhibit poor activities of 4.4 and 1.9 h⁻¹, respectively. The Ru⁰ species on Ru/C (61.2 h⁻¹) is more active for HMF oxidation than that on RuO_x/C (48.9 h⁻¹) and RuCl₃/C (29.3 h⁻¹) under identical conditions, and DFF selectivities of ~96% are achieved over Ru/C [512]. Ru/C characterized by XPS (X-ray photoelectron spectroscopy) shows the dominant presence of metallic Ru⁰ particles with no essential change (76.5% vs. 75.6% Ru⁰) before and after the oxidation of HMF, demonstrating the Ru/C catalyst is stable and recyclable under the reaction conditions.

It is desirable to replace a two-step process that produces DFF from carbohydrates through sequential dehydration and oxidation reactions with a one-step process [564]. Xiang et al. [513] developed a one-pot, one-step approach for direct conversion of glucose to DFF with a catalytic system consisting of CrCl₃·6H₂O/NaBr//NaVO₃·2H₂O. The two-step process gives higher DFF yields (55%; Table 6, Entry 87) than the one-step process (18%). Yang et al. [514] examined the direct synthesis of DFF from fructose by successively using a solid acid Fe₃O₄–SBA–SO₃H and an oxygenant K–OMS-2 (H_{0.2}K_{0.8}Mn₈O₁₆·nH₂O, octahedral molecular sieve) in a single pot. Both catalytic processes are complementary to each other, in which Fe₃O₄–SBA–SO₃H is able to dehydrate fructose to HMF with a yield of 81%, while K–OMS-2 promotes the successive oxidation of HMF to produce DFF with a 99% yield and 100% selectivity (Table 6, Entry 88). The catalytic system when used for the transformation of glucose and inulin to DFF gives low to moderate DFF yields (Table 6, Entries 89 and 90). When a combination of HT, Amberlyst-15, and Ru/HT catalysts via stepwise addition was used for the successive isomerization, dehydration, and selective oxidation in one pot (Fig. 27), an improved DFF yield of 25% is obtained from glucose (Table 6, Entry 91) [515].

Several approaches to simplify the catalytic system for synthesis of DFF deserve to be mentioned. Impregnation of silver in K–OMS-2 not only improves the activity by increasing the concentration of basic sites and decreasing acidic sites, but also lowers the required temperature of the reaction [516] (Table 6, Entry 92). Ruthenium supported on activated carbon (Ru/C) efficiently catalyzes the oxidation of HMF to DFF with high selectivity and the product distribution can be varied by adding water and HT, giving either FFCA or FDCA as the dominant product (Table 6, Entries 93–96) [517]. Promotion effects by Cu(NO₃)₂ on VOSO₄-catalyzed aerobic oxidation for transforming HMF to DFF in acetonitrile reveals that the activation of VOSO₄ occurs to generate active V⁵⁺ species that effectively inhibit the oxidative C–C bond cleavage of HMF and suppresses radical reactions of DFF that form humins (Table 6, Entry 97) [518].

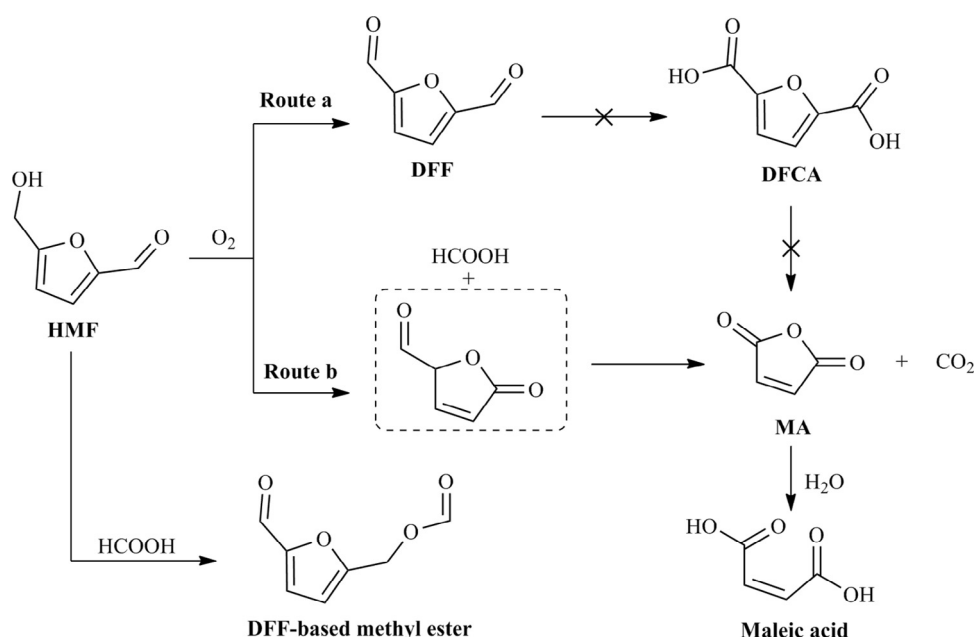


Fig. 28. Proposed reaction pathway for the oxidation of HMF (5-hydroxymethylfurfural) over $\text{VO}(\text{acac})_2$. Adapted with permission from Ref. 538, Copyright © 2011 Royal Society of Chemistry.

As vanadyl (VO^{2+}) and cupric (Cu^{2+}) are immobilized on sulfonated carbon, the resulting catalyst with 0.93% V and 0.26% Cu exhibits the best performance (Table 6, Entry 98) among catalysts in this group (Table 6, Entries 97 and 98) [519]. The trimetallic mixed oxide $\text{RuCo}(\text{OH})_2\text{CeO}_2$ (Table 6, Entry 99) [520], acidic cesium salt of molybdovanadophosphoric HPA $\text{Cs}_3\text{HPMo}_{11}\text{VO}_{40}$ (Table 6, Entry 100) [521], $\text{Cs}_{0.5}\text{H}_{2.5}\text{PMo}_{12}$ (Table 6, Entry 101) [522], manganese oxide catalysts (Table 6, Entry 102) [523], protonated graphitic carbon nitride $\text{g-C}_3\text{N}_4(\text{H}^+)$ (Table 6, Entry 103) [524], vanadium supported on activated carbon ($\text{V}_2\text{O}_5/\text{AC}$), polymers and zeolites ($\text{V}_2\text{O}_5/\text{zeolite}$; Table 6, Entries 104–106) [525–527], *N*-hydroxyphthalimide/ $\text{Cu}(\text{NO}_3)_2$ (Table 6, Entry 107) [528], 1-hydroxybenzotriazole/copper(I) iodate (Table 6, Entry 108) [529], ruthenium complex immobilized on poly(4-vinylpyridine)-functionalized carbon-nanotube (Table 6, Entry 109) [530], ruthenium clusters supported on covalent triazine frameworks (Table 6, Entry 110) [531], 5 wt% Pd-V(3:2)@MIL-101 (Table 6, Entry 111) [532], and even HBr/DMSO or NaBr/DMSO (Table 6, Entry 112) [533] are efficient for the synthesis of DFF from HMF or sugars. A series of magnetically recyclable catalysts including Mn_3O_4 (Table 6, Entry 113) [534], TEMPO (Table 6, Entry 114) [535], and ruthenium (Table 6, Entries 115 and 116) [536,537] supported on Fe_3O_4 nanoparticles are active for aerobic oxidation of HMF into DFF with many yields shown being more than 80%. As a common characteristic, redox sites as well as the promoting sub-units such as acidity/basicity, reaction media, catalyst structure and texture are involved in these catalytic systems, thus, synergistic actions may be present in the oxidative processes.

4.1.2.3. Maleic anhydride. Maleic anhydride (MA), which is produced via selective oxidation of petroleum-based feedstocks at high temperatures (e.g., 400 °C), is a versatile intermediate for 1,4-butanediol, fumaric acid, unsaturated polyester resins, and THF [565–567]. Du et al. [538] explored a potential route to prepare MA from biomass derivatives using $\text{VO}(\text{acac})_2$ in acetonitrile and found that HMF is mainly oxidized into DFF (Fig. 28, Route a) and the MA yield can be significantly enhanced by increasing oxygen partial pressure (Table 6, Entries 117 and 118). The C–C bond adjacent to the hydroxymethyl group is easily broken and apparently, the second

α -hydroxy ketone forms on the other side via resonance and is oxidized to MA as the dominant product (Fig. 28, Route b). Although DFF is stable against further oxidation into FDCA or MA, the HMF can react with HCOOH formed in Route b, giving the methyl ester. In acetonitrile/acetic acid solvent, control experiments with vanadium-substituted HPA $\text{H}_5\text{PV}_2\text{Mo}_{10}\text{O}_{40}\text{xH}_2\text{O}$ catalyst reveal that DFF, FFCA, FDCA and HMFCA do not appear in the pathway of MA formation (Table 6, Entry 119), despite some of these being identified in product analyses [539]. Thereby, the oxidation is verified to be initiated by the C–C bond cleavage between the furan and hydroxymethyl group of HMF.

Furfural can be used instead of HMF as the starting material to form MA via homogeneous or heterogeneous catalysis. For instance, Yin et al. [540,541] reported that copper(II) nitrate in combination with phosphomolybdic acid or $\text{H}_3\text{PMo}_{12}\text{O}_{40}\text{xH}_2\text{O}$ affords MA with around 50% yields from aerobic oxidation (Table 6, Entries 120 and 121). In the dominant oxidation pathway, the abstraction of hydrogen from the 5-position of furfural initiates the reaction and subsequently yields MA and 5-acetyl-2(5H)-furanone [568]. Alonso-Fagollndez et al. [542] used $\text{VO}_x/\text{Al}_2\text{O}_3$ solid catalyst for upgrading furfural by selective gas phase oxidation to obtain MA in 73% yield for 100% furfural conversion (Table 6, Entry 122). In the oxidative upgrading process, furfural is oxidized successively to furan and 2-furanone that is followed by rapid oxidative dehydration to give MA (Fig. 29). Relatively high MA yields are obtained from furfural using H_2O_2 as oxidant and titanium silicalite (TS-1) as catalyst (Table 6, Entries 123 and 124) [543]. Ghaznavi et al. [544] used a catalytic process at high temperatures to atomize a xylose-water solution into a capillary fluidized bed containing vanadyl pyrophosphate catalyst. Compared with molybdenum trioxide–cobalt oxide and iron molybdate, vanadyl pyrophosphate exhibits relatively higher activity (Table 6, Entries 125–127). The surface density of vanadium and molybdenum along with characteristics of the supports probably affect the electronic properties and catalytic properties of the supported metallic species.

4.1.3. Oxidation of biomass derivatives to other oxygenates

4.1.3.1. 2,5-Dimethylfuroate (FDMC) and methyl furoate (MFA). An analog to FDCA is 2,5-dimethylfuroate (FDMC), which can be

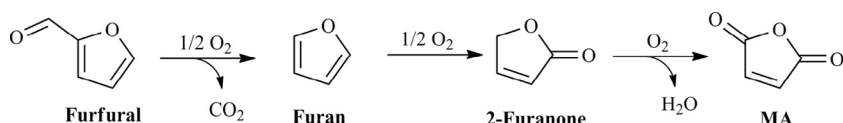


Fig. 29. Possible reaction pathway for the oxidation of furfural to MA (maleic anhydride) over $\text{VO}_x/\text{Al}_2\text{O}_3$.

synthesized from HMF dissolved in methanol via oxidation–esterification in the presence of Au/TiO_2 catalyst aided by CH_3ONa (Table 6, Entry 128) [545]. The possible reaction route involves initial oxidation of the aldehyde moiety of HMF to yield 5-hydroxymethyl methylfuroate (HMMF) in a high yield of ca. 90% under mild conditions (0.1 MPa O_2 , 22 °C and 1.5 h), and then formation of methyl 5-formyl-2-furoate (MFF) by oxidation of the hydroxymethyl group to the aldehyde, followed by the same oxidation–esterification process to afford FDMC with 98% yield at a high temperature of 130 °C and 0.4 MPa in 3 h (Fig. 30). Methyl furoate (MFA), which is used in flavors and fragrances, can be produced from furfural through the same catalytic process (Fig. 30).

Nanoparticulate CeO_2 is able to adsorb oxygen due to its large number oxygen vacancies. Moreover, the Lewis acid character of non-fully saturated cerium atoms is favorable for alcohol oxidation and stabilization of positive metal particles. Casanova et al. [569] employed Au/CeO_2 solely as catalyst without base additive for the synthesis of FDMC and MFA to obtain >99% selectivity for FDMC from HMF with >99% conversion, as well as 91% selectivity of MFA for furfural at a conversion of >99% (Table 6, Entries 129 and 130). Casanova et al. [569] proposed a reaction network (Fig. 31): both compounds **2** and **3** are derived from the same hemiacetal intermediate **1** though successively dominant oxidation and subordinate acetalization reaction to provide compound **4** in two separate pathways, and the resulting monoester acetal is further oxidized into the diester FDMC. When Au/ZrO_2 is employed as catalyst, oxidative esterification of furfural proceeds under mild conditions, giving almost complete selectivity to methyl-2-furoate, while oxygen partial pressures lower than 0.1 MPa do not significantly affect the catalytic performance for either system (Table 6, Entries 131–133) [546]. Catalytic activities for the oxidative esterification of furfural and HMF have the following trends: $\text{Au}/\text{ZrO}_2 > \text{Au}/\text{CeO}_2 \gg \text{Au}/\text{TiO}_2$, for which the surface area of the supports and surface sites (e.g., 2 wt% nominal sulfate content) separately affect conversions and the selectivities (Table 6, Entries 134–139) [547,548].

4.1.3.2. FDCA-, DFF- and PBF-based polymers. FDCA- and DFF-based polymers can be synthesized from HMF or furfural via multistep reactions [570]. Pan et al. [570] prepared poly(butylene 2,5-furandicarboxylate) (PBF) starting from furfural through a four-step synthetic sequence including nanoscale CuO catalyzed oxidation of furfural into furoate (93% yield); catalytic disproportionation of furoate to furan and FDCA (86% selectivity) with ZnCl_2 ; and polymerization of FDCA with 1,4-butanediol (1,4-BDO), which was pre-synthesized with 70% selectivity through hydrogenation and hydrolysis of furan over $\text{Re}-\text{Ru}/\text{C}$, to produce polyester PBF with total carbon utilization of furfural (Fig. 32). Several other related synthetic routes have been put forward based on FDCA. For example, the catalytic polytransesterification of FDCA with ethylene glycol (EG) and 1,4-butanediol (BG) affords furan-based copolymers using $\text{Ti}(\text{OC}_4\text{H}_9)_4$ as catalyst [571]. Polyethylene furandicarboxylate (PEF) formed via the polymerization of FDCA with EG is a promising candidate to replace fossil fuel-derived polyethylene terephthalate (PET) [572], especially since the synthesis of poly(2,5-furan dicarboxylate)s has been realized from diols [573].

Besides FDCA, DFF as a partially oxygenated compound with two aldehyde groups also shows great potential in production of bio-polymers. A series of porous furan-based organic frameworks (FOF) have been prepared by condensation of DFF with diamines through the formation of imine linkages without the presence of catalyst [574]. The condensation of monomer DFF with urea at 110 °C by melting a solid mixture can give a crystalline polymer resin in 90% yield [575].

4.1.3.3. Succinic acid and 3-hydroxypropanoic acid from levulinic acid. Levulinate derivatives are readily produced from lignocellulosic carbohydrates. Podolean et al. [549] found that Ru-based magnetic nanoparticles are efficient for the oxidation of LA to succinic acid (96% selectivity) (Table 6, Entry 140), in which strong Bronsted acid sites are responsible for catalyzing the oxidation of the carbon backbone of LA via a Baeyer–Villiger (BV) mechanism.

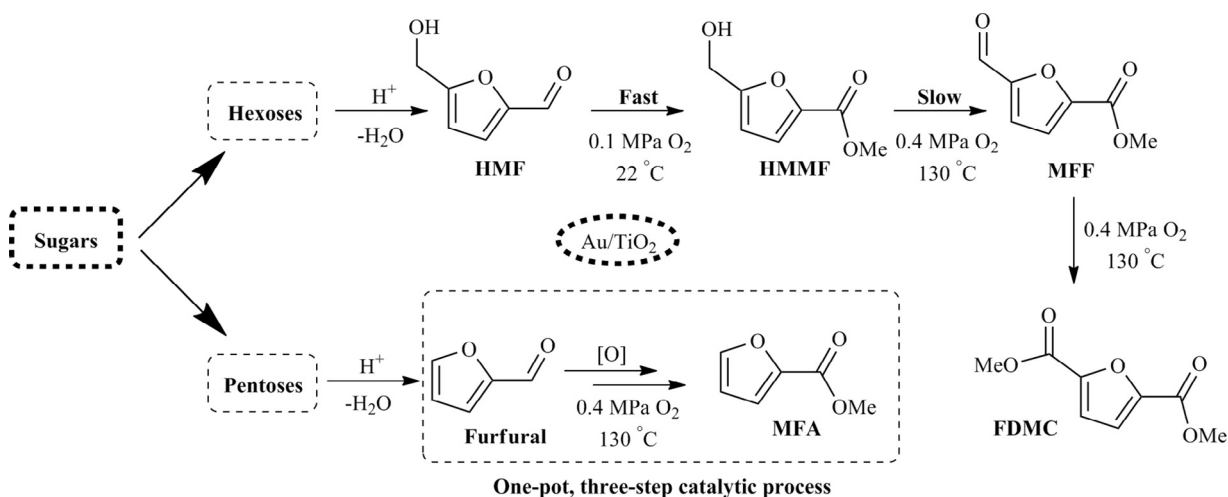


Fig. 30. Biomass sugar feedstock transformed into 2,5-dimethylfuroate (FDMC) and methyl furoate (MFA) via oxidation–esterification.

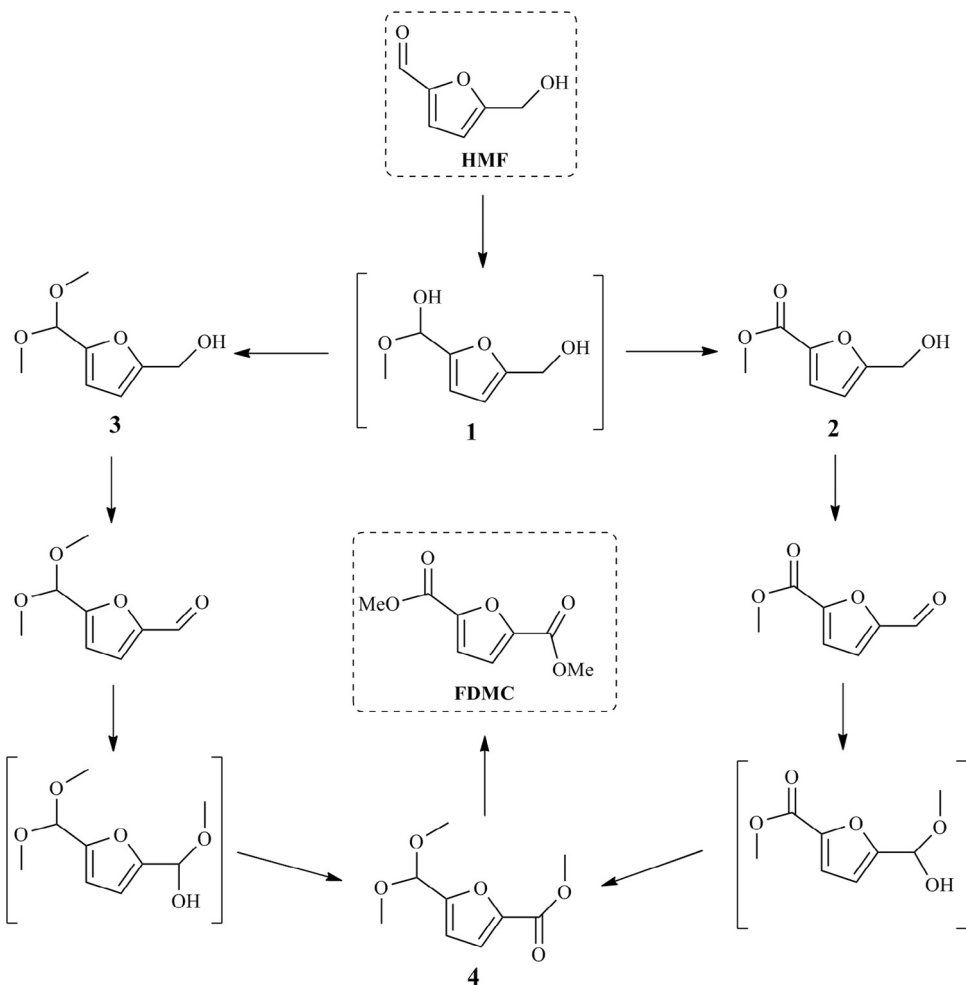


Fig. 31. Proposed oxidation–esterification pathway starting from 5-hydroxymethylfurfural (HMF). Adapted with permission from Ref. 569, Copyright © 2009 Elsevier.

Choudhary et al. [550] demonstrated that the use of a strong Bronsted acid Amberlyst-15 and 30% aqueous H_2O_2 catalyzes the oxidation of LA to SA (Table 6, Entry 141). By changing the solvent from water to methanol, Wang et al. [551] found that selectivities to methyl succinate and methyl acetate of around 60 and 40%, respectively, are obtained from methyl levulinate (ML) in aqueous H_2O_2

with strong Bronsted acids like $p\text{-TsOH}$, $MeSO_3H$, H_2SO_4 , $TfOH$, and Amberlyst-15 (Table 6, Entries 142–149). Lewis acidic triflate salts are active for the oxidation of ML, and the metal cation influences the reaction selectivity. The succinate/acetate ratio decreases from 1.6 to 0.3 as the solvent is switched from methanol to heptane, and the higher degree of branching in the carbon backbone caused by

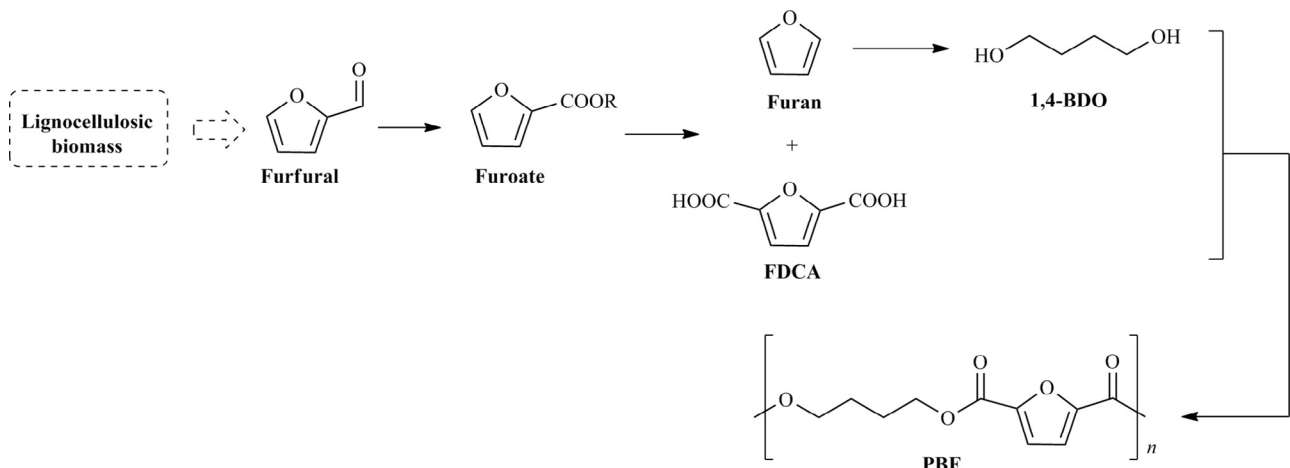


Fig. 32. Multiple conversion of furfural into FDCA (2,5-furandicarboxylic acid)-based polyester PBF [poly(butylene 2,5-furandicarboxylate)]. Adapted with permission from Ref. 570, Copyright © 2013 Wiley-VCH.

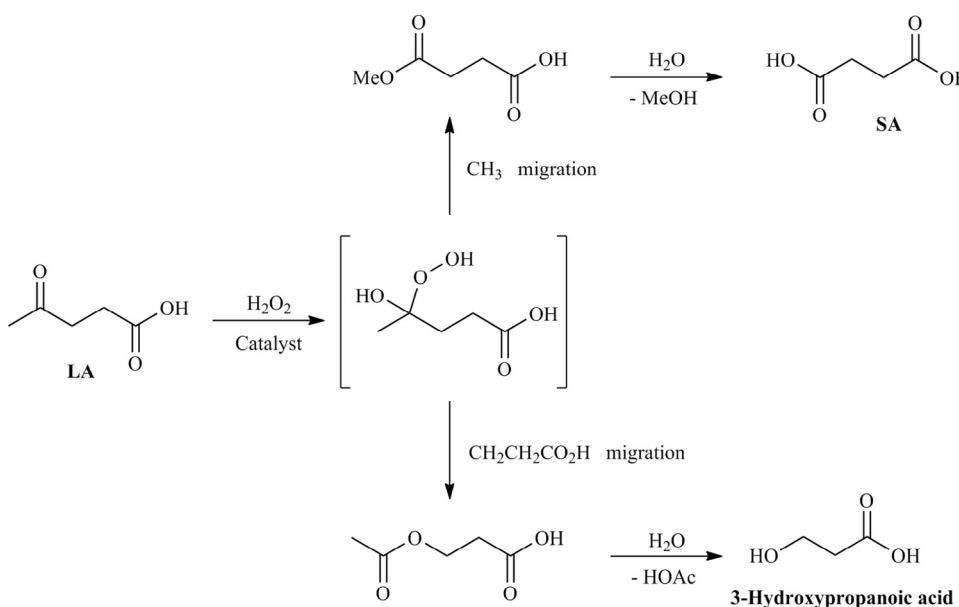


Fig. 33. Baeyer–Villiger oxidation of LA (levulinic acid) to SA (succinic acid) and 3-hydroxypropanoic acid. Adapted with permission from Ref. 552, Copyright © 2015 Wiley-VCH.

methanol is thought to result in a high molar ratio of methyl succinate and acetate (up to 1.6:1). Either $-CH_3$ or $-CH_2CH_2COOH$, migration in the oxidation of LA occurs such that the dominant product can be selectively fixed to SA or 3-hydroxypropanoic acid (Table 6, Entries 150 and 151) [552], as illustrated in Fig. 33. Under acidic conditions in 30% aqueous H_2O_2 , direct treatment of LA gives predominantly SA [553], while 3-hydroxypropanoic acid is obtained from LA via an intermediate 3-(hydroperoxy)propanoic acid under basic conditions proceeds through a two-step catalytic process involving partial oxidation with H_2O_2 at 0 °C to room temperature and subsequent hydrogenation reaction over Pd/C [552]. The proper adjustment of pH appears to be a key factor in controlling the product distribution, even though conditions of the catalytic system must be chosen to suppress the formation of byproducts.

4.1.3.4. α -Conidendrin (*Coni*) and α -conidendric acid (*ConiA*) from lignans. Lignans, which are a group of phenolic compounds possessing anti-carcinogenic and anti-oxidative properties, can be applied to cosmetic and pharmaceutical products [576]. Among these phenolic chemicals, oxomatairesinol (oxoMAT) can be synthesized from hydroxymatairesinol (HMR) via oxidation of its secondary alcohol group over supported palladium and gold catalysts [577–579]. Both isomers HMR 1 and HMR 2 can be oxidized to oxoMAT with the major contaminants of α -conidendrin (*Coni*) and α -conidendric acid (*ConiA*) over Au/Al₂O₃ catalysts in a basic solution at 70 °C and atmospheric pressure (Fig. 34) [580]. The maximum activity of supported gold catalysts corresponds to an Au particle diameter of 4 nm. In addition to the acid–base properties of solid supports and reaction media, the morphological structures of metal particles, such as degree of dispersion and particle size, affect the performance of the bifunctional materials.

Lignin, which is a complex aromatic polymer that is widely-dispersed in nature, has great potential for producing engineering plastics and thermoplastic elastomers, low-cost carbon fibers, fungible fuels, polymeric foams, and commodity chemicals [581]. Hydrothermal gasification, wet oxidation and hydrothermal liquefaction convert lignin to fuel gas, aromatic aldehydes and phenolic products, respectively [582–584], while integrated pretreatment with subsequent valorization is necessary for developing lignin-to-bioproduct processes [585–589]. One-pot catalytic oxidation of

biomass with bifunctional solid materials has the potential to simplify pretreatment, intermediate separation, and post-treatment steps required for producing chemical products. However, only a limited number of one-pot oxidation examples have been reported, indicating the infancy of this topic in the field. Nevertheless, increasing research into bifunctional solid catalytic systems is certain to allow clear examples to be developed in the near future.

4.2. Production of hydrogenates

Catalytic dehydration, esterification, etherification and acetalization over functional materials are used to convert sugars, glycerol, LA, furans and fatty acids into fuel additives, whereas biomass-derived liquid hydrocarbon fuels are obtained by combining oxygen removal processes such as hydrogenolysis, hydrogenation and decarbonylation with C–C coupling reactions including aldol condensation, hydroxyalkylation, oligomerization and ketonization to adjust the molecular weight of platform molecules [590,591]. In this section, an overview of catalytic processes that use deoxygenation of biomass derivatives is presented and bifunctional material-mediated reaction pathways are emphasized.

4.2.1. Hydrolysis–hydrogenation of bio-polymers to polyols

Hexitols, which are considered as important platform chemicals for the production of H_2 , liquid alkanes, and value-added chemicals such as sorbitan, isosorbide, glycerol and lactic acid, can be derived from polysaccharides [592–594]. Pretreatment/hydrolysis steps are generally required to overcome the recalcitrance of lignocelluloses, for which bifunctional catalytic systems have shown great promise in the successive hydrolysis–hydrogenation reactions to afford sorbitol and mannitol (Fig. 35) [595]. In an acidic solution ($pH = 2$), Ru nanoclusters promote quantitative production of sorbitol (100% yield) from cellobiose at 120 °C and 4 MPa H_2 partial pressure, while low yields of sorbitol are obtained under neutral or basic conditions ($pH = 7$ or 10; Table 7, Entries 1–3) [596]. The direct conversion of cellobiose into sorbitol under a hydrogen atmosphere has been achieved with acid-modified carbon nanotube (CNT)-supported ruthenium catalysts in neutral water (Table 7, Entry 4) [597]. The presence of H_2O in Ru/CNT renders the formation of oxygen-containing groups and uniform defects on the tube-walls,

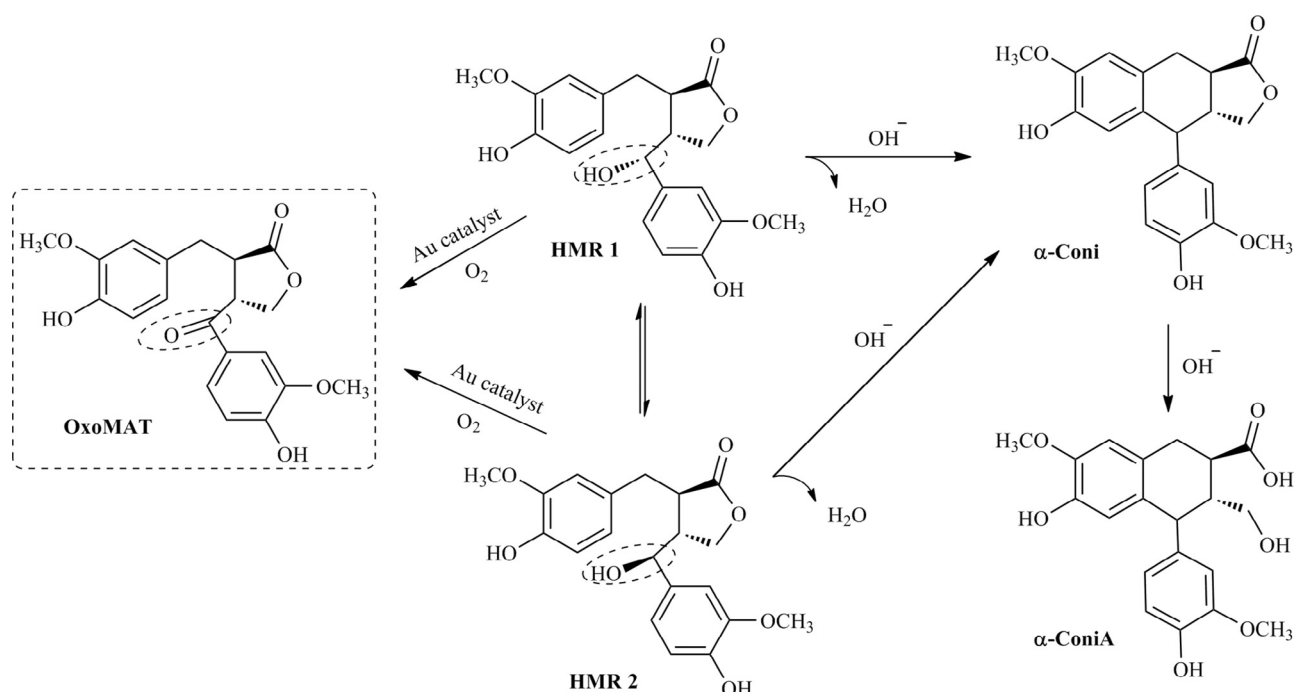


Fig. 34. Schematic of converting the lignan hydroxymatairesinol (NMR) to α -conidendrin (Coni) and α -conidendric acid (ConiA) over gold catalysts. oxoMAT: oxomatairesinol. Adapted with permission from Ref. 580, Copyright © 2015 Elsevier.

resulting in the highly stable and dispersed Ru nanoparticles, as well as higher yields of sugar alcohols (39%) and conversion of cellobiose (74%) than Ru/CNT without water (21% and 29%, respectively; Table 7, Entries 5–8) [598,599].

If the substrate is changed from cellobiose to cellulose, carbon-supported Ru clusters together with in-situ generated $[\text{H}^+]$ ions in hot water afford hexitols with a sorbitol/mannitol molar ratio of about 3.6/1 in a yield of 22% at 39% conversion under 6 MPa H_2 partial pressure at 245 °C in 5 min (Table 7, Entries 9 and 10) [600]. The catalytic performance of ZrP combined with commercial 5% Ru/C in hydrolytic hydrogenation of cellulose to sorbitol/mannitol has been evaluated, and maximum sorbitol/mannitol yields of 62% and 81% are obtained from microcrystalline and ball-milled cellulose, respectively (Table 7, Entry 11) [601]. Both the adsorbed hydrogen species concentrations and the acidic functional groups on the support surfaces affect the sorbitol formation [629,630]. A great number of ruthenium-based catalysts have been studied for this reaction. In particular, a sorbitol yield of 71% could be achieved from cellulose with Ru nanoparticles on carbon treated with sulfuric acid (Ru/AC– SO_3H) in a neutral aqueous solution (Table 7, Entry 12) [602]. Other bifunctional catalysts such as Keggin-type polyoxometalates loaded with ruthenium nanoparticles (Ru/Cs₂HPW₁₂O₄₀ and Ru/[Bmim]₃PW₁₂O₄₀; Table 7, Entries 13 and 14) [603,604], ruthenium supported on a Beta and Y zeolite (Ru/Beta and Ru/Y; Table 7, Entries 15–17) [605,606], mesoporous niobium phosphate (Ru/NbOPO₄; Table 7, Entry 18) [607] and arenesulfonic acid functionalized mesoporous silica (Ru/SBA–15– SO_3H ; Table 7, Entry 19) [608], and Bronsted acid-promoted ruthenium catalysts (e.g., Ru/C + MCM-41– SO_3H or ZrP; Table 7, Entries 20–22) [609,610], as well as PTA/metal-organic-framework-hybrid immobilized ruthenium catalyst (Ru–PTA/MIL-100(Cr); Table 7, Entry 23) [611] are efficient for the sequential hydrolysis and hydrogenation of cellulose into sorbitol in neutral water under a hydrogen atmosphere. When the molar ratio of acid sites to the number of Ru surface atoms (e.g., 8.84–12.90) [611] has sufficient density, hexitol yields reach a maximum from di- and polysaccharide (e.g., cellobiose and cellulose) substrates.

Apart from Ru nanoparticles, some other supported metal nanoparticles such as Pt and Ni efficiently convert cellobiose and cellulose into sugar alcohols. Comparable yields of sugar alcohols (~25%) are obtained over $\gamma\text{-Al}_2\text{O}_3$ supported Pt catalyst (Table 7, Entry 24) [612], while the acid sites for the hydrolysis of cellulose are generated in-situ from H_2 [631]. To enhance the affinity between cellulose and catalyst, a fibrous three-dimensional (3D) carbon material mimicking the shape of a sea urchin (*Echinometra mathae*) has been used to support Pt particles [613]. The resulting catalyst is very active for the hydrolysis of cellulose even though the support was not treated with $[\text{H}^+]$ species, affording hexitols in a total yield of ~80% (Table 7, Entry 25). Instead of hydrogen gas, the combined use of carbon monoxide (CO)/ H_2O as a hydrogen source with Pt–Mo₂C/C catalyst can promote the hydrolysis–hydrogenation of cellulose to produce polyols in a yield of 42% with 60% selectivity to hexitols (Table 7, Entry 26) [614]. In this catalytic process, the Pt–Mo₂C domains are responsible for the formation of active hydrogen species from the water–gas shift reaction rather than from the C–C bond cleavage reaction, while the Pt–C domains mainly catalyze the succedent hydrogenation/hydrogenolysis reaction. In contrast, Ni nanoparticles on aluminum hydroxide (Ni/AlOH) are more stable and active than pyrophoric Raney Ni in the two sequential reactions, giving sugar alcohols in a total yield of 89% at a cellobiose conversion of 90% (Table 7, Entries 27 and 28) [615]. The presence of aluminum hydroxide causes a high dispersion of Ni metal species, in particular, the NiNPs/AlOH catalyst is able to be reused at least five consecutive cycles with almost no loss of activity (conversion rate) with selectivity successively decreasing from 99 to 98% and >99 to 98% for sucrose hydrogenolysis. Notably, nickel-based bimetallics on activated carbon (AC) or mesoporous carbon (MC) exhibit improved catalytic performance and stability in comparison with isolated metals such as Ir and Ni (Table 7, Entries 29–38) [616], which might be the result from tunable electronic and chemical properties of the bimetallic catalysts that are superior to those of the single metal particles [632,633]. Ni-containing carbon nanofibers (Ni/CNFs) synthesized through catalytic vapor deposition (CVD) of CH_4

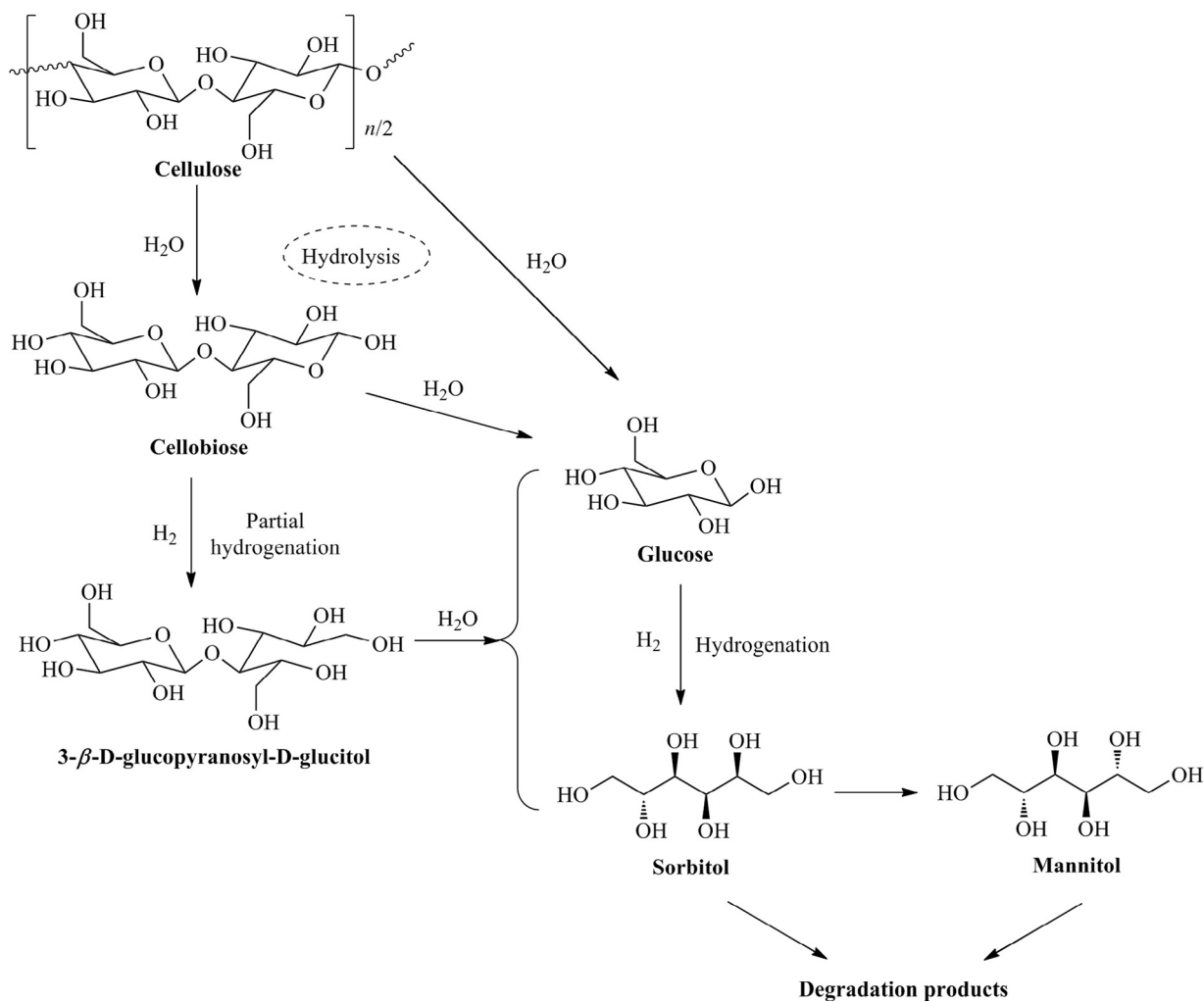


Fig. 35. Plausible reaction pathways for the conversion of cellulose to hexitols.

over Ni nanoclusters on γ -alumina afford a moderate yield of hexitols (35%) from the degradation of microcrystalline cellulose with 87% conversion (Table 7, Entry 39) [617]. Since Ni particles attach at the tip of the inert CNF (carbon nanofiber), the metal sites in the porous supports are fully accessible. Anchoring and dispersing Ni precursors onto CNFs can be realized by the oxidative activation of the CNFs with HNO_3 [634–636], and the acid strength/concentration of Ni/CNF-catalysts can be adjusted by tailoring the preparation methods [618]. Among various CNF-supported Ni particles, the Ni/CNFs with a catalyst loading of 7.5 wt % prepared by chemical vapor deposition of CH_4 on a Ni/ γ -Al₂O₃ catalyst, followed by oxidation in HNO_3 (twice for 1 h at 110 °C), incipient wetness impregnation, and reduction at 550 °C under a H_2 atmosphere are highly active for the hydrolytic hydrogenation of cellulose, affording a maximum hexitols yield of 76% with 69% sorbitol selectivity and 93% cellulose conversion (Table 7, Entries 40–43). Properly balanced Ni/CNF catalysts in terms of Ni dispersion, hydrogenation capacity, and the number of acidic surface–oxygen groups are likely to be responsible for the enhanced activity in hydrolytic hydrogenation of cellulose to hexitols.

The cleavage of C–C bonds of saccharides is efficiently promoted by tungsten-based catalysts, yielding EG rather than hexitols as the dominant product in the sequential hydrolysis and hydrogenolysis of cellulose (Fig. 36; Table 7, Entries 44–46) [619,620,637]. Tungsten carbide (WC_x) or tungsten phosphide (WP) without adding transition metal particles has the capability to produce EG directly from cellulose. In this catalytic process, [H⁺]

emerging from both hot H_2O and the surface tungsten oxides or phosphates act on cellulose hydrolysis, while WC_x or WP with the platinum-like electronic properties is responsible for the subsequent hydrogenation (Table 7, Entries 47–49) [621,622]. For the case of a 3D mesoporous carbon (MC) supported WC_x nanoparticles, the 3D interconnected mesoporous structure of MC support is able to facilitate the accessibility/dispersion of active component WC_x and the transportation of molecules, thereby enhancing hydrogenation activity [638] and gives an EG yield of 73% (Table 7, Entries 50–52) [623]. In contrast, tungsten and tungsten oxide species (e.g., WO₃, W, insoluble H₂WO₄, soluble H_xWO₃ and HPAs) are only active for C–C cleavage of cellulose, while an extra transition metal in the form of M–W species is responsible for the subsequent hydrogenation accessible to EG (Table 7, Entries 53–68) [624–627]. Xi et al. [628] reported that NbPO₄ as a support and catalyst can accelerate the cleavage of a C–C bond while supported Ru particles are responsible for the further hydrogenation, so as to convert cellulose into EG and EG monoether (EGME) in a total yield of 55% (Table 7, Entry 69). The dopant Ni rather than W, Sn and Cu is more effective for the production of EG + EGME with a 64% total yield, which is probably because Ni can restrain the further hydrogenolysis of the resulting products to byproducts such as CO and alkanes, while W, Sn, and Cu are all able to promote degradation of EG and EGME (Table 7, Entries 70–73). Therefore, appropriate combination of metal species with acid sites is necessary for enhancing and controlling the selectivity of polyols from carbohydrates involving multi-step

Table 7

Catalytic conversion of carbohydrates to polyols through cascade hydrolysis (Cat-1) and hydrogenation (Cat-2) with summary of reaction conditions, H-donor, maximum catalytic activity and catalyst reusability.

Entry	Substrate	Catalyst		Reaction condition ^b			H-donor	Main product	Catalytic activity		Reusability		Ref.
		Cat-1	Cat-2	Solvent	Temp.	Time			Conv	Yield	Cycles	Yield ^c	
1	Celllobiose (1.1 wt%)	HCl (pH = 2)	0.7 mol% ^a Ru/PVP	H ₂ O	120 °C	12 h	4.0 MPa H ₂	Sorbitol [Glucose]	100%	100% [0]	NM ^d	NM	[596]
2	Celllobiose (1.1 wt%)	– (pH = 7)	0.7 mol% Ru/PVP	H ₂ O	120 °C	12 h	4.0 MPa H ₂	Sorbitol [Glucose]	88%	23% [1%]	NM	NM	[596]
3	Celllobiose (1.1 wt%)	NaOH (pH = 10)	0.7 mol% Ru/PVP	H ₂ O	120 °C	12 h	4.0 MPa H ₂	Sorbitol [Glucose]	76%	18% [2%]	NM	NM	[596]
4	Celllobiose (0.9 wt%)	1.0 wt% Ru/CNT pretreated with 68 wt% HNO ₃		H ₂ O	185 °C	3 h	5.0 MPa H ₂	Sorbitol	100%	87%	NM	NM	[597]
5	Celllobiose (0.9 wt%)	1.5 wt% Ru/CNT pretreated with H ₂ O		H ₂ O	185 °C	3 h	5.0 MPa H ₂	Sorbitol	74%	39%	NM	NM	[598]
6	Celllobiose (0.9 wt%)	1.5 wt% Ru/CNT without H ₂ O pretreatment		H ₂ O	185 °C	3 h	5.0 MPa H ₂	Sorbitol	29%	21%	NM	NM	[598]
7	Celllobiose (0.9 wt%)	2.0 wt% Ru-in-CNT pretreated with 68 wt% HNO ₃		H ₂ O	185 °C	3 h	5.0 MPa H ₂	Sorbitol	60%	44%	NM	NM	[599]
8	Celllobiose (0.9 wt%)	2.0 wt% Ru-in-CNT pretreated with 23 wt% HNO ₃		H ₂ O	185 °C	3 h	5.0 MPa H ₂	Sorbitol	47%	35%	NM	NM	[599]
9	Cellulose (2.0 wt%)	In situ generated H ⁺	4 wt% Ru/C	H ₂ O	245 °C	5 min	6.0 MPa H ₂	Sorbitol [Mannitol]	39%	17% [5%]	NM	NM	[600]
10	Cellulose (2.0 wt%)	In situ generated H ⁺	4 wt% Ru/C	H ₂ O	245 °C	30 min	6.0 MPa H ₂	Sorbitol [Mannitol]	86%	30% [10%]	NM	NM	[600]
11	Cellulose (10.0 wt%)	10 wt% ZrP	5 wt% Ru/C	H ₂ O	215 °C	3 h	6.0 MPa H ₂	Sorbitol + mannitol	99%	62%	4	57%	[601]
12	Cellulose (10.0 wt%)	10 wt% Ru/AC-SO ₃ H		H ₂ O	140 °C	36 h	5.0 MPa H ₂	Sorbitol	96%	71%	5	59% (24 h)	[602]
13	Celllobiose (1.0 wt%)	1.0 wt% Ru/Cs ₂ HPW ₁₂ O ₄₀		H ₂ O	140 °C	6 h	2.0 MPa H ₂	Sorbitol	99%	93%	5	72%	[603]
14	Cellulose (5.0 wt%)	5.0 wt% Ru/[Bmim] ₃ PW ₁₂ O ₄₀		H ₂ O	160 °C	24 h	5.0 MPa H ₂	Sorbitol	64%	45%	NM	NM	[604]
15	Celllobiose (2.8 wt%)	3.0 wt% SnF ₄	3.0 wt% Ru/Beta	H ₂ O	180 °C	3 h	1.6 MPa H ₂	Sorbitol	99%	72%	NM	NM	[605]
16	Glucose (2.8 wt%)	3.0 wt% Ru/Beta		H ₂ O	180 °C	3 h	1.6 MPa H ₂	Sorbitol	100%	73%	NM	NM	[605]
17	Glucose (20 wt%)	1.0 wt% Ru/Y		H ₂ O	120 °C	3 h	5.5 MPa H ₂	Sorbitol	100%	99%	4	~90%	[606]
18	Cellulose (0.8 wt%)	5.0 wt% Ru/NbOPO ₄		H ₂ O	170 °C	24 h	4.0 MPa H ₂	Sorbitol	93%	60%	4	58%	[607]
19	Cellulose (2.0 wt%)	4.0 wt% Ru/SBA-15-SO ₃ H		H ₂ O	110 °C ^e	1 h	3.5 MPa H ₂	Sorbitol	39%	27%	NM	NM	[608]
20	Cellulose (2.0 wt%)	3.0 wt% Ru/C		H ₂ O	230 °C	40 min	6.0 MPa H ₂	Sorbitol [Mannitol] (EG)	61%	46% [7%] (5%)	NM	NM	[609]
21	Cellulose (2.0 wt%)	100 wt% MCM-41-SO ₃ H	3.0 wt% Ru/C	H ₂ O	230 °C	40 min	6.0 MPa H ₂	Sorbitol [Mannitol] (EG)	100%	7% [1%] (49%)	NM	NM	[609]
22	Cellulose (1.0 wt%)	180 wt% ZrP	5.0 wt% Ru/C	H ₂ O	215 °C	3.0 h	6.0 MPa H ₂	Sorbitol + mannitol	99%	64%	5	55%	[610]
23	Celllobiose (1.0 wt%)	3.2 wt% Ru-PTA/MIL-100(Cr)		H ₂ O	150 °C	10 h	2.0 MPa H ₂	Sorbitol [Mannitol]	100%	92% [5%]	2	9% [–]	[611]
24	Cellulose (0.8 wt%)	In situ generated H ⁺	2.5 wt% Pt/ γ -Al ₂ O ₃	H ₂ O	190 °C	24 h	5.0 MPa H ₂	Sorbitol [Mannitol]	100%	25% [6%]	3	20% [5%]	[612]
25	Cellulose (1.0 wt%)	5 wt% Pt-Echinometra mathae		H ₂ O	180 °C	24 h	5.0 MPa H ₂	Sorbitol [Mannitol]	96%	67% [12%]	3	56% [11%]	[613]
26	Cellulose (0.8 wt%)	5 wt% Pt-Mo ₂ C/C		H ₂ O	240 °C	30 min	4.5 MPa CO	Sorbitol [Mannitol]	–	22% [4%]	NM	NM	[614]
27	Sucrose (2.4 wt%)	4.0 wt% Raney Ni		H ₂ O	130 °C	24 h	2.0 MPa H ₂	Sorbitol [Mannitol]	94%	<1% [84%]	NM	NM	[615]
28	Sucrose (2.4 wt%)	3.5 wt% Ni/AI OH		H ₂ O	130 °C	24 h	2.0 MPa H ₂	Sorbitol [Mannitol]	99%	<1% [95%]	5	<1% [93%]	[615]
29	Cellulose (1.0 wt%)	1 wt% Ir/AC		H ₂ O	245 °C	30 min	6.0 MPa H ₂	Sorbitol [Mannitol]	66%	2% [1%]	NM	NM	[616]
30	Cellulose (1.0 wt%)	5 wt% Ni/AC		H ₂ O	245 °C	30 min	6.0 MPa H ₂	Sorbitol [Mannitol]	59%	6% [2%]	NM	NM	[616]
31	Cellulose (1.0 wt%)	1 wt% Ir-5 wt% Ni/AC		H ₂ O	245 °C	30 min	6.0 MPa H ₂	Sorbitol [Mannitol]	79%	8% [5%]	NM	NM	[616]
32	Cellulose (1.0 wt%)	1 wt% Ir/MC		H ₂ O	245 °C	30 min	6.0 MPa H ₂	Sorbitol [Mannitol]	90%	4% [1%]	NM	NM	[616]

(continued on next page)

Table 7 (continued)

Entry	Substrate	Catalyst		Reaction condition ^b			H-donor	Main product	Catalytic activity		Reusability		Ref.
		Cat-1	Cat-2	Solvent	Temp.	Time			Conv	Yield	Cycles	Yield ^c	
33	Cellulose (1.0 wt%)	5 wt% Ni/MC		H ₂ O	245 °C	30 min	6.0 MPa H ₂	Sorbitol [Mannitol]	86%	8% [3%]	NM	NM	[616]
34	Cellulose (1.0 wt%)	1 wt% Ir–5 wt% Ni/MC		H ₂ O	245 °C	30 min	6.0 MPa H ₂	Sorbitol [Mannitol]	100%	48% [10%]	5	45% [5%]	[616]
35	Cellulose (1.0 wt%)	1 wt% Pt–5 wt% Ni/MC		H ₂ O	245 °C	30 min	6.0 MPa H ₂	Sorbitol [Mannitol]	100%	40% [8%]	NM	NM	[616]
36	Cellulose (1.0 wt%)	1 wt% Pd–5 wt% Ni/MC		H ₂ O	245 °C	30 min	6.0 MPa H ₂	Sorbitol [Mannitol]	100%	48% [6%]	NM	NM	[616]
37	Cellulose (1.0 wt%)	1 wt% Ru–5 wt% Ni/MC		H ₂ O	245 °C	30 min	6.0 MPa H ₂	Sorbitol [Mannitol]	100%	42% [13%]	NM	NM	[616]
38	Cellulose (1.0 wt%)	1 wt% Rh–5 wt% Ni/MC		H ₂ O	245 °C	30 min	6.0 MPa H ₂	Sorbitol [Mannitol]	100%	52% [8%]	NM	NM	[616]
39	Cellulose (2.0 wt%)	3.0 wt% Ni/CNFs		H ₂ O	210 °C	24 h	6.0 MPa H ₂	Sorbitol [Mannitol]	87%	30% [5%]	NM	NM	[617]
40	Cellulose (2.0 wt%)	2.6 wt% Ni/CNFs		H ₂ O	190 °C	24 h	6.0 MPa H ₂	Sorbitol [Mannitol]	91%	40% [9%]	NM	NM	[618]
41	Cellulose (2.0 wt%)	5.2 wt% Ni/CNFs		H ₂ O	190 °C	24 h	6.0 MPa H ₂	Sorbitol [Mannitol]	93%	58% [11%]	NM	NM	[618]
42	Cellulose (2.0 wt%)	7.5 wt% Ni/CNFs		H ₂ O	190 °C	24 h	6.0 MPa H ₂	Sorbitol [Mannitol]	93%	64% [12%]	NM	NM	[618]
43	Cellulose (2.0 wt%)	7.5 wt% Ni/CNFs		H ₂ O	190 °C	24 h	6.0 MPa H ₂	Sorbitol [Mannitol]	93%	53% [11%]	NM	NM	[618]
44	Cellulose (1.0 wt%)	2.0 wt% Ni–W ₂ C/AC		H ₂ O	245 °C	30 min	6.0 MPa H ₂	EG [PG]	100%	61% [8%]	NM	NM	[619]
45	Corn stalk (1.0 wt%)	2.0 wt% Ni–W ₂ C/AC		H ₂ O	245 °C	2 h	6.0 MPa H ₂	EG [PG]	96%	18% [14%]	NM	NM	[620]
46	Xylose (1.0 wt%)	2.0 wt% Ni–W ₂ C/AC		H ₂ O	245 °C	2 h	6.0 MPa H ₂	EG [PG]	100%	11% [17%]	NM	NM	[620]
47	Cellulose (1.0 wt%)	2.0 wt% Ni–WP/AC		H ₂ O	245 °C	30 min	6.0 MPa H ₂	EG [PG]	100%	46% [6%]	NM	NM	[621]
48	Cellulose (1.0 wt%)	10.0 wt% Ni/AC		H ₂ O	245 °C	30 min	6.0 MPa H ₂	EG [PG]	74%	10% [5%]	NM	NM	[621]
49	Cellulose (1.0 wt%)	30.0 wt% W ₂ C/AC		H ₂ O	245 °C	30 min	6.0 MPa H ₂	EG [PG]	98%	27% [6%]	3	23% [3%]	[622]
50	Cellulose (1.0 wt%)	30 wt% WC _x /MC		H ₂ O	245 °C	30 min	6.0 MPa H ₂	EG [PG]	100%	73% [5%]	3	57% [8%]	[623]
51	Cellulose (1.0 wt%)	2 wt% Ni–WC _x /MC		H ₂ O	245 °C	30 min	6.0 MPa H ₂	EG [PG]	98%	27% [6%]	3	23% [3%]	[623]
52	Cellulose (1.0 wt%)	2 wt% Ni–WC _x /AC		H ₂ O	245 °C	30 min	6.0 MPa H ₂	EG [PG]	100%	62% [3%]	NM	NM	[623]
53	Cellulose (1.0 wt%)	10.0 wt% H ₂ WO ₄	1.2 wt% Ru/AC	H ₂ O	245 °C	30 min	6.0 MPa H ₂	EG [PG]	100%	54% [6%]	20	50% [–]	[624]
54	Cellulose (1.0 wt%)	10.0 wt% H ₂ WO ₄	10.0 wt% Raney Ni	H ₂ O	245 °C	30 min	6.0 MPa H ₂	EG [PG]	100%	65% [3%]	21	50% [5%]	[625]
55	Cellulose (1.0 wt%)	10.0 wt% WO ₃	10.0 wt% Raney Ni	H ₂ O	245 °C	30 min	6.0 MPa H ₂	EG [PG]	100%	53% [2%]	NM	NM	[625]
56	Cellulose (1.0 wt%)	10.0 wt% H ₃ PW ₁₂ O ₄₀	10.0 wt% Raney Ni	H ₂ O	245 °C	30 min	6.0 MPa H ₂	EG [PG]	100%	49% [5%]	NM	NM	[625]
57	Cellulose (1.0 wt%)	10.0 wt% H ₃ SiW ₁₂ O ₄₀	10.0 wt% Raney Ni	H ₂ O	245 °C	30 min	6.0 MPa H ₂	EG [PG]	100%	35% [5%]	NM	NM	[625]
58	Glucose (0.3 wt%)	–	3.0 wt% Ru/C	H ₂ O	205 °C	10 min	6.0 MPa H ₂	EG [PG] (Sorbitol)	100%	9% [6%]	NM	NM	[626]

(continued on next page)

Table 7 (continued)

Entry	Substrate	Catalyst		Reaction condition ^b			H-donor	Main product	Catalytic activity		Reusability		Ref.
		Cat-1	Cat-2	Solvent	Temp.	Time			Conv	Yield	Cycles	Yield ^c	
59	Glucose (0.3 wt%)	1000 wt% WO ₃	3.0 wt% Ru/C	H ₂ O	205 °C	10 min	6.0 MPa H ₂	EG [PG] (Sorbitol)	100%	59% [14%] (9%)	NM	NM	[626]
60	Cellulose (1.0 wt%)	5 wt% Pd–W/AC		H ₂ O	245 °C	30 min	6.0 MPa H ₂	EG [PG]	100%	60% [4%]	NM	NM	[627]
61	Cellulose (1.0 wt%)	5 wt% Pt–W/AC		H ₂ O	245 °C	30 min	6.0 MPa H ₂	EG [PG]	97%	57% [3%]	NM	NM	[627]
62	Cellulose (1.0 wt%)	5 wt% Ru–W/AC		H ₂ O	245 °C	30 min	6.0 MPa H ₂	EG [PG]	100%	62% [3%]	NM	NM	[627]
63	Cellulose (1.0 wt%)	5 wt% Ir–W/AC		H ₂ O	245 °C	30 min	6.0 MPa H ₂	EG [PG]	100%	51% [3%]	NM	NM	[627]
64	Cellulose (1.0 wt%)	30 wt% W/AC		H ₂ O	245 °C	30 min	6.0 MPa H ₂	EG [PG]	100%	2% [0]	NM	NM	[627]
65	Cellulose (1.0 wt%)	5 wt% Pd/AC		H ₂ O	245 °C	30 min	6.0 MPa H ₂	EG [PG]	67%	8% [0]	NM	NM	[627]
66	Cellulose (1.0 wt%)	5 wt% Pt/AC		H ₂ O	245 °C	30 min	6.0 MPa H ₂	EG [PG]	64%	12% [3%]	NM	NM	[627]
67	Cellulose (1.0 wt%)	5 wt% Ru/AC		H ₂ O	245 °C	30 min	6.0 MPa H ₂	EG [PG]	74%	2% [0]	NM	NM	[627]
68	Cellulose (1.0 wt%)	5 wt% Ir/AC		H ₂ O	245 °C	30 min	6.0 MPa H ₂	EG [PG]	64%	10% [7%]	NM	NM	[627]
69	Cellulose (3.8 wt%)	3 wt% Ru/NbOPO ₄		MeOH	220 °C	20 h	3.0 MPa H ₂	EG [PG] (EGMG)	96%	26% [3%] (29%)	NM	NM	[628]
70	Cellulose (3.8 wt%)	3 wt% Ru–0.9 wt% W/NbOPO ₄		MeOH	220 °C	20 h	3.0 MPa H ₂	EG [PG] (EGMG)	93%	20% [3%] (23%)	NM	NM	[628]
71	Cellulose (3.8 wt%)	3 wt% Ru–0.9 wt% Sn/NbOPO ₄		MeOH	220 °C	20 h	3.0 MPa H ₂	EG [PG] (EGMG)	90%	13% [2%] (25%)	NM	NM	[628]
72	Cellulose (3.8 wt%)	3 wt% Ru–0.9 wt% Ni/NbOPO ₄		MeOH	220 °C	20 h	3.0 MPa H ₂	EG [PG] (EGMG)	90%	20% [2%] (40%)	NM	NM	[628]
73	Cellulose (3.8 wt%)	3 wt% Ru–0.9 wt% Cu/NbOPO ₄		MeOH	220 °C	20 h	3.0 MPa H ₂	EG [PG] (EGMG)	89%	11% [1%] (25%)	NM	NM	[628]

^a Metal loading in the catalyst or solid acid dosage.^b Reaction conditions used for hydrodeoxygenation.^c Product yield in the last cycle.^d NM: not mentioned.^e Irradiation at 300 W.

PVP: poly(*N*-vinyl-2-pyrrolidone), CNT: carbon nanotube, EG: ethylene glycol, PG: 1,2-propylene glycol, Ru-PTA/MIL-100(Cr): phosphotungstic acid (PTA)/metal-organic-framework-hybrid-supported ruthenium catalyst, AC: activated carbon, MC: mesoporous carbon, CNFs: carbon nanofibers (treated with HNO₃), EGME: EG monoether.

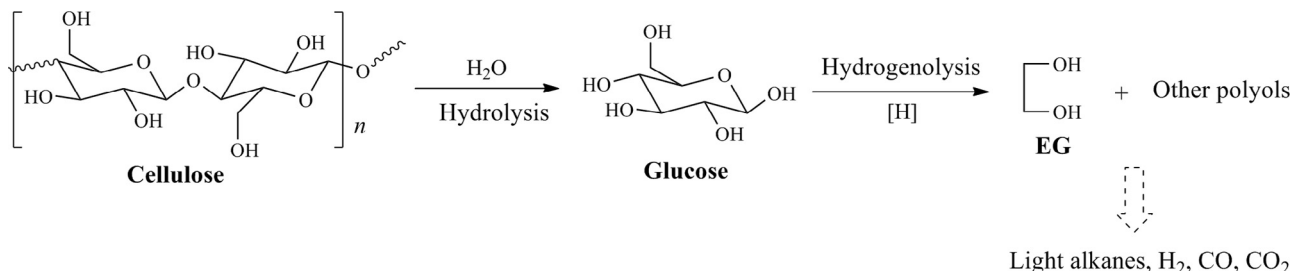


Fig. 36. Schematic of catalytic conversion of cellulose to ethylene glycol (EG).

reactions such as hydrolysis, hydrogenation/hydrogenolysis, and C–C bond cleavage.

4.2.2. Hydrodeoxygenation of biomass derivatives with HMF as an intermediate

Variation of reaction conditions and catalysts allows DMF, 2,5-bis(hydroxymethyl) tetrahydrofuran (BHMTF), 2,5-bis(hydroxymethyl)furan (BHMF), DMTHF, and ring-opened products like 5-hydroxy-2,5-hexanedione (HHD) to be selectively obtained from HMF hydrogenation, as shown in Fig. 37. HMF, which has a moderate boiling point (92–94 °C) and high energy density (31.5 MJ·L⁻¹) is of high interest [639–641]. Using different sugars as substrates, a series of catalytic systems efficient for the transformation of biomass derivatives into DMF with HMF or 5-chloromethylfurfural (CMF) as an intermediate have been elucidated [642,643].

4.2.2.1. 2,5-Dimethylfuran (DMF). A two-step process involving the dehydration of fructose to HMF catalyzed by HCl in H_2O /2-butanol (a biphasic system) and the succedent liquid phase hydrogenolysis to DMF over Cu–Ru/C catalyst has been shown to give high catalytic efficiency (up to 71% DMF yield; Table 8, Entry 1) [644]. Combination of fructose-to-HMF dehydration over a solid acid Amberlyst-15 catalyst and subsequent hydrogenolysis to DMF over Ru–Sn/ZnO catalyst efficiently produces DMF with an overall yield of 92% with no leaching of the active sites as assessed with ICP-AES analyses (Table 8, Entry 2) [645]. Starting from glucose, Chidambaram and Bell [646] reported that HPAs such as 12-molybdo-phosphoric acid (12-MPA) were extremely active for dehydration of glucose in a mixed solution consisting of [EMIM][Cl] and acetonitrile, producing approximately 100% yield of HMF after 3 h at 120 °C (Table 8, Entry 3), while carbon-supported metals such as Pd/C catalyst in a second step could convert 44–47% HMF to DMF

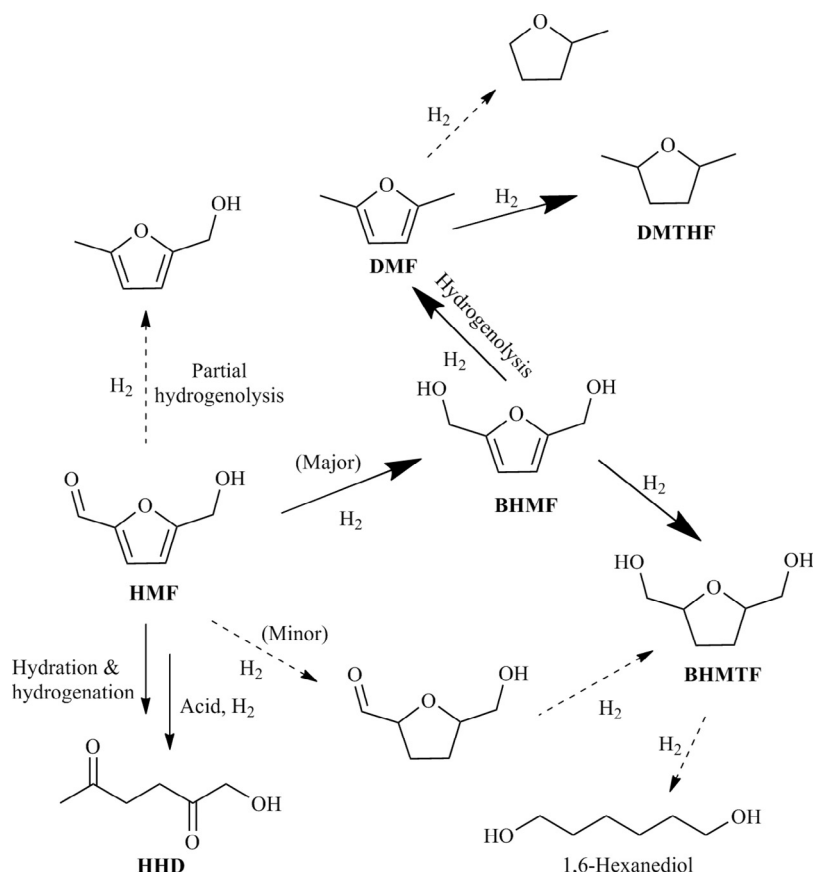


Fig. 37. Major products in the hydrogenation/hydrogenolysis of HMF (5-hydroxymethylfurfural). DMF: 2,5-dimethylfuran, DMTHF: 2,5-dimethyltetrahydrofuran, BHMF: 2,5-bis(hydroxymethyl)furan, HHD: 5-hydroxy-2,5-hexanedione.

Table 8Hydrodeoxygenation of 5-hydroxymethylfurfural (Cat-2) derived from C₆ sugars (Cat-1) to furanic compounds with summary of reaction conditions, H-donor, maximum catalytic activity and catalyst reusability.

Entry	Substrate	Catalyst		Reaction condition ^b			H-donor	Main product	Catalytic activity		Reusability		Ref.
		Cat-1	Cat-2	Solvent	Temp.	Time			Conv.	Yield	Cycles	Yield ^c	
1	Fructose (30 wt%)	HCl	10 wt% Cu—Ru/C	1-BuOH	220 °C	10 h	0.68 MPa H ₂	DMF	100%	71%	NM ^d	NM	[644]
2	Fructose (17.6 wt%)	Amberlyst-15	5 wt% Ru—Sn/ZnO	1-BuOH	240 °C	0.5 h ^{1e}	0.1 MPa H ₂	DMF	100%	92%	5	~90%	[645]
3	Glucose (9 wt%)	12-MPA	0.2 wt% Pd/C	EMIMCl + MeCN	120 °C	3 h	6.2 MPa H ₂	DMF	100%	~100%	NM	NM	[646]
4	Xylose/Glucose (20/50 wt%)	Sn-Mont + NbOPO ₄	3.5 wt% Ru/Co ₃ O ₄	H ₂ O + THF	170 °C	24 h	1.0 MPa H ₂	MF	99%	91%	NM	NM	[647]
5	HMF (5.3 wt%)	—	28.5 wt% PtCo/Ac	1-BuOH	180 °C	2 h	1.0 MPa H ₂	DMF	100%	98%	3	72%	[648]
6	HMF (4.3 wt%)	—	53.7% Cu/ZnO	1,4-Dioxane	220 °C	5 h	1.5 MPa H ₂	DMF	100%	92%	5	10%	[649]
7	HMF (2.5 wt%)	—	10 wt% Ni/Co ₃ O ₄	THF	180 °C	24 h	1.0 MPa H ₂	DMF	99%	76%	6	~80%	[650]
8	HMF (0.63 wt%)	—	10 wt% PdAu/C + HCl	THF	60 °C	6 h	H ₂ balloon	DMF	99%	96%	NM	NM	[651]
9	HMF (1.0 wt%)	—	3.2 wt% Ru/Co ₃ O ₄	THF	130 °C	24 h	0.7 MPa H ₂	DMF	99%	93%	6	~89%	[652]
10	HMF (0.5 wt%)	—	2 wt% Ru/NaY	THF	220 °C	1 h	1.5 MPa H ₂	DMF	100%	78%	6	~78%	[653]
11	HMF (3.3 wt%)	—	0.2 wt% Pd/C—ZnCl ₂	THF	150 °C	8 h	0.8 MPa H ₂	DMF	99%	85%	5	~66%	[654]
12	HMF (0.5 wt%)	—	0.56 wt% Ru/HT	2-PrOH	220 °C	4 h	1.0 MPa H ₂	DMF	100%	58%	6	~55%	[641]
13	HMF (2.1 wt%)	—	0.4 wt% Pt/rGO	1-BuOH	120 °C	2 h	3.0 MPa H ₂	DMF	100%	73%	5	NM	[655]
14	HMF (1.1 wt%)	—	7 wt% Ni—W ₂ C/AC	THF	180 °C	3 h	4.0 MPa H ₂	DMF	100%	96%	4	~85%	[656]
15	Fructose (36 wt%)	H ₂ SO ₄	H ₂ SO ₄ + 5 wt% Pd/C	THF	70 °C	15 h	FA	DMF	100%	51%	NM	NM	[657]
16	Fructose (36 wt%)	FA	H ₂ SO ₄ + 5 wt% Ru/C	THF	75 °C	45 min ^f	FA	DMF	100%	32%	NM	NM	[658]
17	Cellulose (10 wt%)	DMA/LiCl + IL + FA	H ₂ SO ₄ + 5 wt% Ru/C	THF	75 °C	45 min ^f	FA	DMF	100%	16%	NM	NM	[658]
18	Agar (10 wt%)	DMA/LiCl + IL + FA	H ₂ SO ₄ + Ru/C	THF	75 °C	45 min ^f	FA	DMF	100%	27%	NM	NM	[658]
19	HMF (6.3 wt%)	—	10 wt% NiPd/SiO ₂	H ₂ O	40 °C	2 h	8.0 MPa H ₂	BHMTF	99%	96%	NM	NM	[659]
20	HMF (6.3 wt%)	—	10 wt% Ni/SiO ₂	H ₂ O	40 °C	2 h	8.0 MPa H ₂	BHMTF	~5%	0	NM	NM	[659]
21	HMF (6.3 wt%)	—	10 wt% Pd/SiO ₂	H ₂ O	40 °C	2 h	8.0 MPa H ₂	BHMTF	~57%	~5%	NM	NM	[659]
22	HMF (5 wt%)	—	1 wt% Ru/CeO _x	1-BuOH/H ₂ O	130 °C	12 h	2.7 MPa H ₂	BHMTF	100%	91%	NM	NM	[660]
23	HMF (5.0 wt%)	—	1 wt% Ru/MgZrO _x	1-BuOH/H ₂ O	130 °C	12 h	2.7 MPa H ₂	BHMTF	100%	88%	NM	NM	[660]
24	HMF (5 wt%)	—	1 wt% Ru/C	1-BuOH/H ₂ O	130 °C	12 h	2.7 MPa H ₂	BHMTF	100%	56%	NM	NM	[660]
25	HMF (5 wt%)	—	1 wt% Pd/C	1-BuOH/H ₂ O	130 °C	12 h	2.7 MPa H ₂	BHMTF	100%	25%	NM	NM	[660]
26	HMF (5.0 wt%)	—	1 wt% Pt/C	1-BuOH/H ₂ O	130 °C	12 h	2.7 MPa H ₂	BHMTF	83%	11%	NM	NM	[660]
27	Fructose (36 wt%)	[BMIM]Cl	5 wt% Pd/C	H ₂ O	50 °C	3 h	6.0 MPa H ₂	BHMTF	99%	63%	NM	NM	[661]
28	Fructose (36.0 wt%)	[BMIM]Cl	5 wt% Ru/C	H ₂ O	50 °C	3 h	6.0 MPa H ₂	BHMTF	99%	27%	NM	NM	[661]
29	Fructose (36.0 wt%)	[BMIM]Cl	5 wt% Ir/C	H ₂ O	50 °C	3 h	6.0 MPa H ₂	BHMTF	93%	[39%]	NM	NM	[661]
30	Fructose (36 wt%)	[BMIM]Cl	5 wt% Pt/C	H ₂ O	50 °C	3 h	6.0 MPa H ₂	BHMTF	89%	5%	NM	NM	[661]
31	Fructose (36 wt%)	[BMIM]Cl	5 wt% Ni/C	H ₂ O	50 °C	3 h	6.0 MPa H ₂	BHMTF	66%	5%	NM	NM	[661]
32	Fructose (36 wt%)	[BMIM]Cl	5 wt% Ir/TiO ₂	H ₂ O	50 °C	3 h	6.0 MPa H ₂	BHMTF	99%	[35%]	NM	NM	[661]
33	Fructose (4.2 wt%)	Amberlyst-15	Ru/SiO ₂ —TM	Cyclohexane/H ₂ O	130 °C	4 h	4.0 MPa H ₂	BHMTF	~60%	65%	5	20%	[662]
34	HMF (1.3 wt%)	—	1 wt% Au/CeO ₂	H ₂ O	140 °C	4 h	3.8 MPa H ₂	BHMF	—	7%	NM	NM	[663]
35	HMF (1.3 wt%)	—	1 wt% Au/La ₂ O ₃	H ₂ O	140 °C	4 h	3.8 MPa H ₂	BHMF	—	15%	NM	NM	[663]
36	HMF (1.3 wt%)	—	1 wt% Au/Al ₂ O ₃	H ₂ O	140 °C	4 h	3.8 MPa H ₂	BHMF	100%	66%	NM	NM	[663]

(continued on next page)

Table 8 (continued)

Entry	Substrate	Catalyst		Reaction condition ^b			H-donor	Main product	Catalytic activity		Reusability		Ref.
		Cat-1	Cat-2	Solvent	Temp.	Time			Conv.	Yield	Cycles	Yield ^c	
37	HMF (1.3 wt%)	–	1 wt% Au/ZrO ₂	H ₂ O	140 °C	4 h	3.8 MPa H ₂	BHMF	32%	0	NM	NM	[663]
38	HMF (1.3 wt%)	–	1 wt% Au/TiO ₂	H ₂ O	140 °C	4 h	3.8 MPa H ₂	BHMF	85%	0	NM	NM	[663]
39	HMF (1.3 wt%)	–	1 wt% Au/Ta ₂ O ₅	H ₂ O	140 °C	4 h	3.8 MPa H ₂	BHMF	40%	6%	NM	NM	[663]
40	HMF (1.3 wt%)	–	1 wt% Au/TiO ₂ –SiO ₂	H ₂ O	140 °C	4 h	3.8 MPa H ₂	BHMF	23%	0	NM	NM	[663]
41	HMF (1.3 wt%)	–	1 wt% SO ₄ –ZrO ₂	H ₂ O	140 °C	4 h	3.8 MPa H ₂	BHMF	17%	0	NM	NM	[663]
42	HMF (1.3 wt%)	–	1 wt% Au/Al ₂ O ₃	H ₂ O	120 °C	2 h	6.5 MPa H ₂	BHMF	100%	96%	NM	NM	[663]
43	HMF (25 wt%)	–	1 wt% Pt/MCM-41	–	35 °C	2 h	0.8 MPa H ₂	BHMF	40%	6%	NM	NM	[664]
44	HMF (25 wt%)	–	1 wt% Pt/MCM-41	H ₂ O	35 °C	2 h	0.8 MPa H ₂	BHMF	100%	99%	6	98%	[664]
45	Fructose (6 wt%)	HI	1 wt% RhCl ₃ ·xH ₂ O	H ₂ O	140 °C	2.5 h	2.1 MPa H ₂	DMTHF	100%	81%	7	86%	[665]
46	Glucose (6 wt%)	HI	1 wt% RhCl ₃ ·xH ₂ O	H ₂ O	140 °C	16 h	2.1 MPa H ₂	DMTHF	100%	70%	NM	NM	[665]
47	Inulin (6 wt%)	HI	1 wt% RhCl ₃ ·xH ₂ O	H ₂ O	140 °C	16 h	2.1 MPa H ₂	DMTHF	96%	73%	NM	NM	[665]
48	Sucrose (6 wt%)	HI	1 wt% RhCl ₃ ·xH ₂ O	H ₂ O	140 °C	16 h	2.1 MPa H ₂	DMTHF	96%	82%	NM	NM	[665]
49	Cellulose (6 wt%)	HI	1 wt% RhCl ₃ ·xH ₂ O	H ₂ O/chlorobenzene	140 °C	16 h	2.1 MPa H ₂	DMTHF	90%	54%	NM	NM	[665]
50	Glucose (10 wt%)	–	2 wt% Cu/Al-SBA	H ₂ O	175 °C	30 min ^f	FA	MFFA [DMF]	99%	29%	NM	NM	[666]
51	Glucose (10 wt%)	–	2 wt% Cu/AlZn–SBA	H ₂ O	175 °C	30 min ^f	FA	MFFA [DMF]	99%	24%	NM	NM	[666]
52	HMF (2.5 wt%)	–	5 wt% Pd/C	Dioxane	120 °C	20 h	Decarbonylation	FfA	95%	90%	NM	NM	[667]
53	HMF (2.5 wt%)	–	5 wt% Pd/C	Dioxane	120 °C	15 h	0.2 MPa H ₂ + FA	DMF	95%	85%	NM	NM	[667]
54	HMF (2.5 wt%)	–	5 wt% Pd/C	Dioxane	120 °C	15 h	0.2 MPa H ₂ + AA	DMF	95%	42%	NM	NM	[667]
55	HMF (2.5 wt%)	–	5 wt% Pd/C	Dioxane	120 °C	15 h	0.2 MPa H ₂	DMTHF [DMF]	95%	43%	NM	NM	[667]
56	Fructose (4.5 wt%)	Amberlyst-15	13 wt% Pd/C	DMSO	80 °C	15 h	1 MPa H ₂	HHD	95%	50%	NM	NM	[668]
57	Fructose (4.5 wt%)	Amberlyst-15	13 wt% Pd/C	DMSO	80 °C	36 h	3.5 MPa H ₂	HHD	95%	27%	NM	NM	[668]
58	HHD (25 wt%)	Amberlite®IR-120H	1 wt% Pd/C	H ₂ O	90 °C	2 h	2 MPa H ₂	DMTHF	99%	99%	5	98%	[669]
59	Fructose (10 wt%)	–	3.8 wt% sulfide Pt/C	EtOH	175 °C	2 h	10.3 MPa H ₂	DMTHF	100%	50%	NM	NM	[670]
60	Fructose (10 wt%)	–	3.8 wt% sulfide Pt/C	H ₂ O	175 °C	2 h	10.3 MPa H ₂	DMTHF	100%	9%	NM	NM	[670]

^a Metal loading in the catalyst.^b Reaction conditions used for hydrodeoxygenation.^c Product yield in the last cycle.^d NM: not mentioned.^e Weight hourly space velocity.^f Irradiation at 300 W.

DMF: 2,5-dimethylfuran, 12-MPA: 12-molybdophosphoric acid, EMIMCl: 1-ethyl-3-methylimidazolium chloride, MeCN: acetonitrile, THF: tetrahydrofuran, Y: Y type zeolites, HT: hydrotalcite, rGO: reduced graphene oxide, AC: active carbon, FA: formic acid, IL: [DMA]⁺[CH₃SO₃]⁻ (DMA: N,N-dimethylacetamide), DMF: 2,5-dimethylfuran, BHMTF: 2,5-bis(hydroxymethyl)tetrahydrofuran, [BMIM]Cl: 1-butyl-3-methylimidazolium chloride, BHMF: 2,5-bis(hydroxymethyl)furan, DMTHF: 2,5-dimethyltetrahydrofuran, AA: acetic acid, MFFA: 5-methylfurfuryl alcohol, FfA: furfuryl alcohol, DMSO: dimethylsulfoxide, HHD: 5-hydroxy-2,5-hexanedione.

in 1 h. The high selectivity of HMF catalyzed by HPAs is attributed to the stabilization of reaction intermediates including 1,2-enediol, isomerized 2,3-enediol, and the in-situ formed furylhydroxymethyl ketone, while the presence of acetonitrile as a cosolvent inhibits the formation of humins in both dehydration and subsequent hydrogenation processes. With a THF/H₂O–NaCl biphasic system in combination with a dehydration process over Sn-Mont or NbOPO₄ catalyst and a succedent hydrogenolysis over Ru/Co₃O₄ catalyst, DMF and MF could be produced in high yields (>90%) from glucose/xylose mixed substrates (Table 8, Entry 4) [647]. The in-situ separation of the upper organic phase containing furfural and HMF is an important step for obtaining enhanced yields of hydrogenated products.

A DMF yield of 98% from HMF (100% conversion within 10 min) over PtCo bimetallic nanoparticles (3.6 ± 0.7 nm diameter) in 2 h can be obtained without involving the catalytic step of sugar dehydration (Table 8, Entry 5) [648]. The small particle sizes and the stable homogeneous alloying in the hollow carbon spheres probably contribute to the high activity of the catalyst and the remarkable DMF yield (Table 8, Entry 5). Well-dispersed metal sites, well-controlled surface sites of solid supports, and optimized reaction conditions can also provide enhanced catalytic reaction systems (Table 8, Entries 6–14) [641,649–656].

Instead of using H₂ as H-donor, Thananathanthanachon and Rauchfuss [657] demonstrated that formic acid acts as an acid catalyst for fructose-to-HMF dehydration and as a hydrogen source over a Pd/C catalyst for HMF deoxygenation to produce DMF, resulting in a total reaction efficiency of about 51% after diethyl ether extraction (Table 8, Entry 15). The one-pot conversion of lignocellulosic and algal biomass with a multicomponent catalytic system comprising [DMA]⁺[CH₃SO₃⁻], Ru/C and formic acid affords DMF in a maximum yield of 32% (Table 8, Entries 16–18) [658]. For a possible reaction route, 5-(formyloxymethyl)furfural was shown by ¹H and ¹³C NMR spectra to be a key intermediate.

4.2.2.2. 2,5-bis(Hydroxymethyl)tetrahydrofuran (BHMTF). In the manufacture of plastics, 1,6-hexanediol is used on a large scale and it is derived from petroleum sources [671]. It is possible to produce 1,6-hexanediol beginning from a biomass derivative BHMTF (Fig. 37). However, that method requires high temperatures and high hydrogen pressures and large amounts of noble metal catalysts to obtain BHMTF in high yields [672,673]. A series of Ni–Pd bimetallic particles supported on silica with various Ni/Pd molar ratios suitable for the reaction have been prepared using a co-impregnation technique [659]. The best catalytic performance in the total hydrogenation of HMF to BHMTF (up to 96% yield) is for supported catalyst (NiPd/SiO₂) with a Ni/Pd ratio of 7 that is more selective than Pd/SiO₂ and more active than commercial Raney Ni (Table 8, Entries 19–21). Ruthenium supported on materials such as ceria, magnesia-zirconia and γ-alumina with high isoelectric points exhibits higher BHMTF yields of 88–91% than platinum and palladium catalysts at the same catalyst weight percent of 1 wt% (Table 8, Entries 22–26) [660]. The superior overall selectivity to BHMTF is dependent not only on the high rates of hydrogenation (Ru > Pd) other than C–C scission reactions promoted by Pt, but also on the suitable solution acidity (pH = ~5) provided by solid supports or reaction media. Starting from carbohydrates, Cai et al. [661] performed the direct production of furan-based diols with yields of 34–89% via one-pot tandem reactions so that the controllable production of BHMF or BHMTF is realized by selecting the suitable support and metal species in a two-step process (Table 8, Entries 27–32). After checking various supported 5 wt% metal particles including Pd/C, Ru/C, Ir/C, Ir/TiO₂, Pt/C and Ni/C, the catalyst Ir/TiO₂ affords >99% HMF conversion with BHMF in 95% selectivity from fructose, in which both Ir particles and the reductive support TiO₂ favor C:O hydrogenation. Under identical conditions, Pd/C provides BHMTF with 84%

selectivity at >99% conversion, which might be related to the relatively higher specific rate of Pd in HMF hydrogenation (Pd ≈ Ru > Ir > Pt > Ni). Instead of multi-step catalytic steps in a single pot, a combination of acid (Amberlyst-15) and hydrophobic Ru/SiO₂-TM in a water/cyclohexane biphasic system can be used to achieve one-step hydrogenation of fructose to produce BHMTF in a maximum selectivity of 65% (Table 8, Entry 33), although the selectivity toward BHMTF seems to be strongly dependent on the acid catalyst used [662]. The selectivity of BHMTF increases in the order of HY-zeolite (15%) < SO₄²⁻/ZrO₂ (~40%) < Nb₂O₅–P (~58%) < Amberlyst-15 (65%) < H₂SO₄ (75%), which is proportional to the Bronsted acidity. It appears that the strong acid sites are prone to accelerate the dehydration of fructose to HMF, thus facilitating the subsequent hydrogenation process to yield BHMTF without rehydration to LA.

4.2.2.3. 2,5-bis(Hydroxymethyl)furan (BHMF). BHMF, which is obtained from the catalytic hydrogenation of the aldehyde in HMF, is used in polymers, resin additives, and intermediates for drugs and crown ethers [674,675]. Metal oxides supported gold with 1 wt% Au loading prepared by deposition impregnation are active in the hydrogenation of HMF to BHMF [663]. Among the catalysts (Table 8, Entries 34–41), relatively high activity and selectivity toward BHMF over Au/Al₂O₃ is obtained. For comparison, Au/La₂O₃ and Au/CeO₂ are also selective in the production of BHMF but low reactivity is observed (Table 8, Entries 35 and 36). Whereas, almost no BHMF is produced from HMF catalyzed by those metal particles supported on acidic metal oxides including TiO₂, ZrO₂, Ta₂O₅, TiO₂–SiO₂ (TS) and sulfated zirconia (SZ) (Table 8, Entries 37–41). Under optimized reaction conditions, HMF is rapidly converted into BHMF with Au/Al₂O₃ catalyst with a yield of >96% (Table 8, Entry 42). The catalyst prepared under H₂ at 200 °C had the smallest gold particles with sub-nanometer diameter of 0.88 ± 0.30 nm, indicating the formation of a magic number Au₁₃ cluster. In neutral aqueous medium, Pt/MCM-41 catalyst is able to hydrogenate HMF into BHMF with complete conversion and selectivity of 99% (Table 8, Entry 43) [664]. Particularly, the amount of water plays a significant role in the conversion and selectivity of the reaction. It is speculated that hydrogen bonding occurs between water molecules and the hydroxyl groups on the support surface, which can help the water molecules surrounding the catalyst surface to disperse the catalyst. Thus, better catalytic activity (100% HMF conversion and ~100% BHMF selectivity) can be achieved in an aqueous medium by using a specific amount of water (Table 8, Entry 44). However, too much water results in decreased conversion (71%) and selectivity (<90%), which is possibly due to the reduced collisions between the reactant and catalyst caused by substrate dilution.

4.2.2.4. 2,5-Dimethyltetrahydrofuran (DMTHF). DMTHF, which has low miscibility with water, a moderate boiling point (90 °C) and high energy density (31 MJ·L⁻¹), is a promising transportation fuel candidate. In a single step procedure, a coupled catalyst RhCl₃/HI is able to promote the formation of DMTHF from poly- and monosaccharides including corn stover, cellulose, inulin, sucrose, glucose and fructose, and a maximum DMTHF yield of 86% can be obtained (Table 8, Entries 45–49) [665]. It was found that HI functions as both a dehydrating agent in the initial sugar-to-HMF conversion and a reducing agent for the subsequent transformation of HMF to 5-methylfurfural (MFF) [676]. The regeneration of HI from I₂ formed in the reduction step is realized by rhodium-catalyzed hydrogenation, and moreover, the metal catalyst also acts on the hydrogenation of C:O and C:C bonds (Fig. 38). Before full hydrogenation of HMF to DMF, the key intermediate 5-methylfurfuryl alcohol (MFFA) is formed with a high selectivity of 60% in a short time (2–30 min) over Cu-based catalysts (Table 8, Entries 50 and 51), and it is rapidly converted to DMF after prolonged reaction time [666].

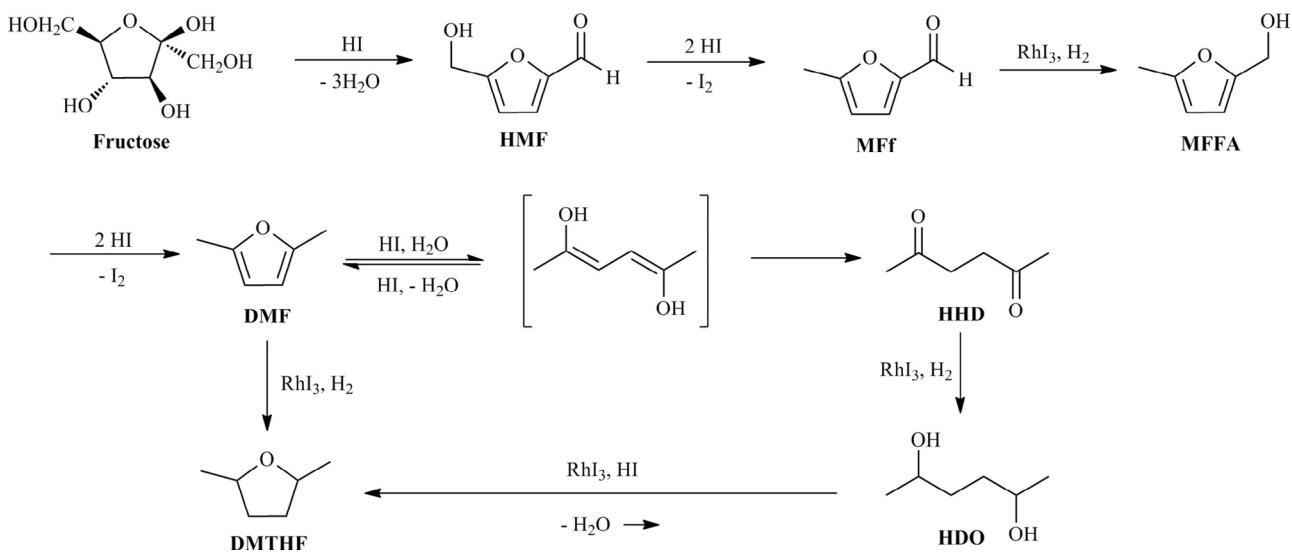


Fig. 38. Proposed mechanism for the conversion of fructose to DMTHF (2,5-dimethyltetrahydrofuran). HMF: 5-hydroxymethylfurfuralhydroxymethylfurfural, MFf: 5-methylfurfural, MFFA: 5-methylfurfuryl alcohol, DMF: 2,5-dimethylfuran, HHD: 5-hydroxy-2,5-hexanedione, DHH: 2,5-dihydroxyhexane. Adapted with permission from Ref. 676, Copyright © 2012 Wiley VCH.

From above discussion, it is clear that the reactivity of HMF in the presence of metal-containing catalysts is diverse. Mitra et al. [667] stated especially for HMF that the product distribution/selectivity is affected by the additives. As shown in Fig. 39, Pd/C catalyst is capable of selectively mediating three broad reactions of HMF covering decarbonylation, hydrogenation, and hydrogenolysis. Without adding any additives but at high reaction temperature (≥ 120 °C) in suitable solvents like dioxane, HMF can be decarbonylated to FFA in high yields reaching 90% in air (Table 8, Entry 52). The decarbonylation of HMF is suppressed in the presence of formic acid, while DMF is formed as the exclusive product (85% yield) in dioxane (Table 8, Entry 53). Similar to formic acid (FA), acetic acid (AA) also displays favorable effects on the production of DMF (42% yield) from HMF (Table 8, Entry 54). In the absence of formic acid, DMF undergoes further hydrogenation to DMTHF, indicating that the acid inhibits the hydrogenation of the furan-ring (Table 8, Entry 55).

In another case, the combined use of Pd/C and Amberlyst-15 allows the one-pot transformation of fructose and inulin into 5-hydroxy-2,5-hexanedione (HHD) with a maximum yield of 77% and 100% carbon balance in a solution of THF and 0.3 wt% DMSO at 80 °C and 1.0–3.5 MPa H₂ partial pressure after 15–36 h (Table 8, Entry 56) [668], implying that a synergistic effect exists for the acid and hydrogenating sites in the reaction system [677]. An increase of the amount of Amberlyst-15 from 11 to 35 wt% along with the addition of 0.3 wt% of DMSO into THF leads to the complete

conversion of fructose and inulin to the dominant product HMF and minor HHD, while further increasing the pressure of hydrogen from 1.0 to 2.0 MPa allows an increase in the yield of HHD by consuming HMF in a concomitant route (Table 8, Entry 57). The combined use of Pd/C and Amberlyst-15 in a single reactor for the efficient and direct transformation of fructose and inulin into HHD illustrates the cooperativity of these two catalytic systems. Zhou et al. [669] demonstrated that 1 wt% Pt/C and a solid acid Amberlite®IR-120H have a cooperative effect on conversion of HHD to DMTHF with yields up to 99% being obtained (Table 8, Entry 58) through a key intermediate 2,5-dihydroxyhexane (DHH; Table 8, Entries 59 and 60) [670] as illustrated in Fig. 38. The dual catalyst system exhibits constant activity and DMTHF selectivity for five recovery and reuse cycles. Single bifunctionalized solid materials are likely to improve catalytic efficiency [678,679], wherein metal particles and Lewis acid sites can synergistically catalyze the course of hydrogenations.

4.2.3. Hydrodeoxygenation of biomass derivatives with furfural as an intermediate

Furfural, which is the major dehydration product of pentoses, is capable of providing hydrogenated products through reduction (Fig. 40) [680,681]. As shown in Route a, hydrogenation of the C:O group in HMF gives FfA, and the furan ring can be further hydrogenated to yield tetrahydrofurfuryl alcohol (THFA). Rather than reducing the unsaturated bond, the hydrogenolysis of C–O bond of FfA to MF and 2-methyltetrahydrofuran (MTHF) can take place

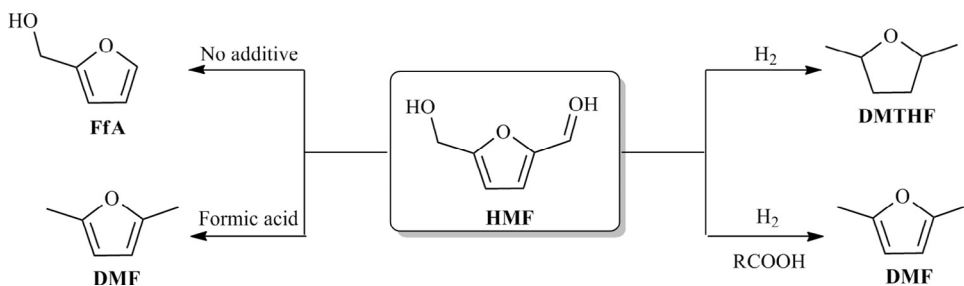


Fig. 39. Reaction pathways of HMF (5-hydroxymethylfurfural) catalyzed by Pd/C with and without additives. FfA: furfuryl alcohol, DMF: 2,5-dimethylfuran, DMTHF: 2,5-dimethyltetrahydrofuran.

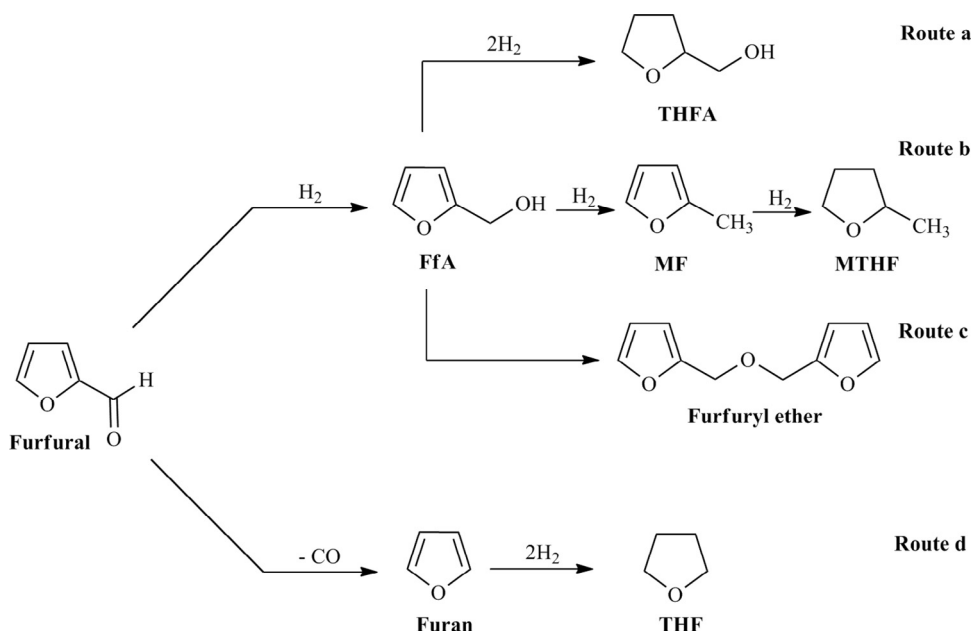


Fig. 40. Catalytic pathways for the hydrogenation of furfural. THFA: tetrahydrofurfuryl alcohol, FfA: furfuryl alcohol, MTHF: 2-methyltetrahydrafuran, MF: 2-methylfuran, THF: tetrahydrofuran. Adapted with permission from Ref. 680, Copyright © 2012 Elsevier.

(Fig. 40, Route b). Moreover, furfuryl ether formed via a condensation process (Fig. 40, Route c), as well as THF from the cascade decarbonylation at high temperature [682] and succedent hydrogenation of furfural with furan as the intermediate (Fig. 40, Route d) can also be realized.

4.2.3.1. Furfuryl alcohol (FfA). FfA is a promising feedstock for the production of resins, rubbers, polymers and valuable chemicals like THFA and EL, and can also be used as a non-reactive diluent and solvent [683–689]. Industrial methods to produce FfA from furfural are typically mediated by Cu–Cr based catalysts under H₂ pressure via gas phase and liquid phase reactions [690,691]. However, these catalytic processes have high toxicity and only moderate efficiency, therefore, the pre-requisite but challenging task is to design active catalytic systems that avoid the negative effects of this reaction system. Avoiding Cr additives, copper-containing catalysts such as Cu–Fe, Pd–Cu/SiO₂, Cu–MgO, CuNi–MgAlO and Cu/C could also give rise to high activity in terms of furfural conversion (up to 98%) and FfA selectivity (up to 98%; Table 9, Entries 1–3) [692–694,718–720]. Likewise, Co- and Ni-based amorphous catalysts are highly selective for furfural-to-FfA conversion (around 99%; Table 9, Entries 4–7) [695–698,721]. Unfortunately, the stability of these heterogeneous catalysts is rarely reported [722,723]. The re-usability of Pt/C catalyst has been explored in the liquid-phase hydrogenation of furfural to FfA and no adverse effect is detected for azeotropic mixtures of water and 2-propanol (Table 9, Entry 8) [699]. Nevertheless, when the support is changed from carbon to oxides, undesirable reactions such as hydrogenolysis of the C–O bond, decarbonylation, furan ring hydrogenation and opening occurs that causes a decrease in the selectivity of FfA from 99% to 94% with Pt/TiO₂–SiO₂ or to 34% with Pt/SiO₂ (Table 9, Entries 9 and 10) [700]. After modification by SnBu₄, the selectivity of Pt-based monometallic catalyst reaches 98%, and an almost constant FfA selectivity of 96% is observed over the bimetallic catalyst PtSn_{0.3} during the three cycles of reaction (Table 9, Entry 11) [701]. The nature of the catalyst support directly affects the stability and selectivity of metal particles, and the use of carbon as the solid support seems to be the good candidate for selective production of FfA. Bimetallic catalysts are likely to enhance both stability and selectivity for the partial

hydrogenation reaction, which deserves to be further studied for producing biomass-derived products with high selectivity.

Some other supported catalysts have been developed for the synthesis of FfA from furfural. In comparison to NiB and NiMoB catalyst, amorphous NiMoB/Al₂O₃ alloy catalysts prepared from reduction of γ-Al₂O₃ supported NiCl₂·6H₂O and (NH₄)₆Mo₇O₂₄·4H₂O by NaBH₄ could convert 99% furfural into FfA with a high yield of 91% in methanol (Table 9, Entries 12–14) [702]. The CuCa/SiO₂ catalyst prepared by sol–gel technique is found to have a relatively higher dispersion of copper than that fabricated by impregnation [703]. Correspondingly, the former catalyst (CuCa/SiO₂-SG) affords a higher and more constant activity (99% selectivity and 100% conversion) than CuCa/SiO₂-IM in the synthesis of FfA from furfural (Table 9, Entries 15 and 16), which might be attributed to the presence of calcium acting as a structural promoter that improves catalyst stability as well as selectivity.

The distribution of products is a strong function of the employed metal catalyst (Fig. 41) [704]. Over Cu/SiO₂ catalyst, FfA in high selectivity with only a small amount of MF is obtained, while furan from furfural decarbonylation occurs with Pd/SiO₂, and THF would be generated by further hydrogenation (Table 9, Entries 17 and 18). Ring opening products (ROP) such as butanal, butanol and butane would be formed in significant amounts if Ni/SiO₂ catalyst is used (Table 9, Entry 19) [704]. In agreement with these results, a DFT study illustrated that thermodynamics favors the production of furan and CO, while the formation of MF requiring lower activation energy occurs through the dehydration of FfA or a dehydrogenation pathway involving a methoxy intermediate [724]. Apart from metal types, the nature of supports affects catalytic performance. In this regards, Mironenko et al. [705] demonstrated that 1.5 wt% Pd/CB (carbon black) affords a high FfA selectivity of 99% from furfural (Table 9, Entries 20 and 21). In contrast, 1.5 wt% Pd/CNT (carbon nanotubes) are not active for FfA production under mild conditions, while the reduction of both C:O group and furan ring to THFA occur at 90 °C (Table 9, Entries 22 and 23). Selectivity toward FfA directly from xylose in a one-step process over a dual catalyst system composed of Pt/SiO₂ and sulfated ZrO₂ strongly depends on the solvent that can inhibit the product polymerization [706]. With the help of H₂O/2-propanol in a ratio of 1:3 (v/v), a selectivity as

Table 9

Hydrodeoxygenation of furfural (Cat-2) derived from C₅ sugars (Cat-1) for producing furfuryl alcohol (FfA) with summary of reaction conditions, H-donor, maximum catalytic activity and catalyst reusability.

Entry	Substrate	Catalyst		Reaction condition ^b			H-donor	Main product	Catalytic activity		Reusability		Ref.
		Cat-1	Cat-2	Solvent	Temp.	Time			Conv.	Yield	Cycles	Yield ^c	
1	Furfural (42 wt%)	–	33 wt% CuFe ₂ O ₄	Octane	160 °C	5 h	9 MPa H ₂	FfA	91%	90%	5	~80%	[692]
2	Furfural (–)	–	16 wt% Cu/MgO	–	180 °C	0.05 h ^{-1d}	0.1 MPa H ₂	FfA	98%	96%	NM ^e	NM	[693]
3	Furfural (33 wt%)	–	12.5 wt% CuNi/MgAlO	Ethanol	200 °C	2 h	1 MPa H ₂	FfA	93%	83%	NM	NM	[694]
4	Furfural (10 wt%)	–	65 wt% Co–Mo–B	Ethanol	100 °C	3 h	1 MPa H ₂	FfA	100%	100%	NM	NM	[695]
5	Furfural (25 wt%)	–	34 wt% Ni–Fe–B	Ethanol	100 °C	4 h	1 MPa H ₂	FfA	100%	100%	NM	NM	[696]
6	Furfural (25 wt%)	–	75 wt% Ni–Fe–B	Ethanol	80 °C	3 h	1 MPa H ₂	FfA	100%	97%	NM	NM	[697]
7	Furfural (25 wt%)	–	76 wt% Co–B	Ethanol	80 °C	1.4 h ^{-1d}	1 MPa H ₂	FfA	100%	100%	NM	NM	[698]
8	Furfural (1.6 wt%)	–	5 wt% Pt/C	2-PrOH/H ₂ O	150 °C	1.5 h	2.1 MPa H ₂	FfA	58%	57%	NM	NM	[699]
9	Furfural (–)	–	5 wt% Pt/TiO ₂ –SiO ₂	–	150 °C	2 h ^{-1d}	0.1 MPa H ₂	FfA	68%	64%	NM	NM	[700]
10	Furfural (–)	–	5 wt% Pt/SiO ₂	–	150 °C	2 h ^{-1d}	0.1 MPa H ₂	FfA	68%	23%	NM	NM	[700]
11	Furfural (4 wt%)	–	70 wt% PtSn _{0.3}	2-PrOH	100 °C	8 h	0.1 MPa H ₂	FfA	100%	96%	3	77%	[701]
12	Furfural (20 wt%)	–	5 wt% NiMoB/Al ₂ O ₃	MeOH	80 °C	3 h	5 MPa H ₂	FfA	99%	91%	NM	NM	[702]
13	Furfural (20 wt%)	–	5 wt% NiB	MeOH	80 °C	3 h	5 MPa H ₂	FfA	17%	15%	NM	NM	[702]
14	Furfural (20 wt%)	–	5 wt% NiMoB	MeOH	80 °C	3 h	5 MPa H ₂	FfA	87%	85%	NM	NM	[702]
15	Furfural (–)	–	20 wt% CuCa/SiO ₂ –SG	–	130 °C	0.33 h ^{-1d}	0.1 MPa H ₂	FfA	100%	99%	80 h	99%	[703]
16	Furfural (–)	–	20 wt% CuCa/SiO ₂ –SG	–	130 °C	0.33 h ^{-1d}	0.1 MPa H ₂	FfA	100%	94%	15–25 h	66%	[703]
17	Furfural (–)	–	10 wt% Cu/SiO ₂	–	230 °C	0.5 h ^{-1d}	0.1 MPa H ₂	FfA	69%	68%	NM	NM	[704]
18	Furfural (–)	–	1 wt% Pd/SiO ₂	–	230 °C	0.5 h ^{-1d}	0.1 MPa H ₂	[MF] FfA [Furan] (THF)	69%	10% [41%] (14%)	NM	NM	[704]
19	Furfural (–)	–	5 wt% Ni/SiO ₂	–	230 °C	0.5 h ^{-1d}	0.1 MPa H ₂	FfA [Furan] (ROP)	72%	18% [31%] (18%)	NM	NM	[704]
20	Furfural (8.6 wt%)	–	1.5 wt% Pd/CB	H ₂ O	50 °C	0.5 h	0.5 MPa H ₂	FfA	29%	29%	NM	NM	[705]
21	Furfural (8.6 wt%)	–	1.5 wt% Pd/CB	H ₂ O	90 °C	2 h	2 MPa H ₂	FfA	76%	62%	NM	NM	[705]
22	Furfural (8.6 wt%)	–	1.5 wt% Pd/CNT	H ₂ O	50 °C	0.5 h	0.5 MPa H ₂	FfA	0	0	NM	NM	[705]
23	Furfural (8.6 wt%)	–	1.5 wt% Pd/CNT	H ₂ O	90 °C	2 h	2 MPa H ₂	FfA	95%	49%	NM	NM	[705]
24	Xylose (–)	ZrO ₂ –SO ₄	1 wt% Pt/SiO ₂	2-PrOH/H ₂ O	130 °C	6 h	3 MPa H ₂	FfA	65%	33%	3	16%	[706]
25	Furfural (–)	–	10 wt% Ni/SiO ₂	NM	140 °C	1 h	0.1 MPa H ₂	THFA	100%	94%	NM	NM	[707]
26	Furfural (3.5 wt%)	–	60 wt% NiSn/TiO ₂	2-PrOH	110 °C	75 min	3 MPa H ₂	FfA	99%	99%	5	43%	[708]
27	Furfural (3.5 wt%)	–	RANEY Ni/AiOH	2-PrOH	130 °C	75 min	3 MPa H ₂	THFA	99%	99%	NM	NM	[708]
28	Xylose (3.3 wt%)	Amberlyst-15	5 wt% Ru/C	H ₂ O	165 °C	50 min	2.5 MPa H ₂	THFA	78%	1%	NM	NM	[709]
29	Xylose (3.3 wt%)	Amberlyst-15	5 wt% Ru/C	BuOH/H ₂ O	165 °C	450 min	2.5 MPa H ₂	[Xylitol] THFA [Xylitol]	41%	6% [23%]	NM	NM	[709]
30	Xylose (3.3 wt%)	Amberlyst-15	5 wt% Ru/C	MTHF/H ₂ O	165 °C	350 min	2.5 MPa H ₂	THFA [Xylitol]	72%	15% [13%]	NM	NM	[709]
31	Xylose (3.3 wt%)	Amberlyst-15	5 wt% Ru/C	Cyclohexane/H ₂ O	165 °C	350 min	2.5 MPa H ₂	THFA [Xylitol]	67%	19% [7%]	NM	NM	[709]
32	Furfural (–)	–	59 wt% Cu–Zn	–	250 °C	0.3 h ^{-1d}	0.1 MPa H ₂	MF [Furan]	100%	87% [< 1%]	NM	NM	[710]
33	Furfural (–)	–	43 wt% Cu–Cr	–	250 °C	0.3 h ^{-1d}	0.1 MPa H ₂	MF [Furan]	100%	36% [25%]	NM	NM	[710]
34	FfA (–)	–	59 wt% Cu–Zn	–	220 °C	0.3 h ^{-1d}	0.1 MPa H ₂	MF [Furan]	98%	92% [< 1%]	NM	NM	[710]
35	FfA (–)	–	43 wt% Cu–Cr	–	220 °C	0.3 h ^{-1d}	0.1 MPa H ₂	MF [Furan]	97%	60% [23%]	NM	NM	[710]

(continued on next page)

Table 9 (continued)

Entry	Substrate	Catalyst		Reaction condition ^b			H-donor	Main product	Catalytic activity		Reusability		Ref.
		Cat-1	Cat-2	Solvent	Temp.	Time			Conv.	Yield	Cycles	Yield ^c	
36	Furfural (-)	-	5 wt% Ni/SiO ₂	-	250 °C	0.025 h ^{-1d}	0.1 MPa H ₂	FfA [Furan] (MF)	51%	7% [23%] (1%)	NM	NM	[711]
37	Furfural (-)	-	5 wt% NiFe/SiO ₂	-	250 °C	0.025 h ^{-1d}	0.1 MPa H ₂	FfA [Furan] (MF)	28%	5% [4%] (5%)	NM	NM	[711]
38	Furfural (-)	-	5 wt% NiFe/SiO ₂	-	250 °C	0.1 h ^{-1d}	0.1 MPa H ₂	FfA [Furan] (MF)	96%	10% [12%] (39%)	NM	NM	[711]
39	Furfural (-)	-	Mo ₂ C	-	150 °C	0.2 h ^{-1d}	0.1 MPa H ₂	MF [Furan]	12%	6–7% [1%]	NM	NM	[712]
40	Xylose (12 wt%)	H-mordenite	30 wt% Cu–Fe	Toluene/H ₂ O	260 °C/ 252 °C	3 min/48 h ^{-1d}	5.5 MPa N ₂ / 0.1 MPa H ₂	Furfural/MF	98%/99%	98%/98%	20 h	98%	[713]
41	Furfural (1 wt%)	-	2.2 wt% Ru/C	2-BuOH	180 °C	10 h	2-BuOH	MF	100%	76%	NM	NM	[714]
42	Furfural (1 wt%)	-	2.2 wt% Ru/C	2-BuOH	180 °C	5 h	2-BuOH	MF	85%	62%	NM	NM	[714]
43	Furfural (1 wt%)	-	2.2 wt% Ru/C	2-PeOH	180 °C	5 h	2-PeOH	MF	92%	68%	NM	NM	[714]
44	Furfural (1 wt%)	-	2.2 wt% Ru/C	2-PrOH	180 °C	5 h	2-PrOH	MF	89%	43%	NM	NM	[714]
45	Furfural (1 wt%)	-	2.2 wt% Ru/C	1-BuOH	180 °C	5 h	1-BuOH	MF	68%	32%	NM	NM	[714]
46	Furfural (1 wt%)	-	2.2 wt% Ru/C	1-PrOH	180 °C	5 h	1-PrOH	MF	76%	32%	NM	NM	[714]
47	Furfural (1 wt%)	-	2.2 wt% Ru/C	EtOH	180 °C	5 h	1-PrOH	MF	72%	20%	NM	NM	[714]
48	Furfural (1 wt%)	-	2.2 wt% Ru/C	2-MBuOH	180 °C	5 h	2-MBuOH	MF	16%	<1%	NM	NM	[714]
49	Furfural (1 wt%)	-	2.2 wt% Ru/C	t-BuOH	180 °C	5 h	t-BuOH	MF	12%	0	NM	NM	[714]
50	MF (-)	-	Pt nanoparticles	-	40 °C	-	0.01 MPa H ₂	1-Pentanol [2-Pentanol] (MTHF)	-	98% [1%] (<1%) f	NM	NM	[715]
51	MF (-)	-	Pt nanoparticles	-	95 °C	-	0.01 MPa H ₂	1-Pentanol [2-Pentanol] (MTHF)	-	45% [45%] f (9%) f	NM	NM	[715]
52	Furfural (5 wt%)	-	3 wt% Pd/C	2-PrOH	220 °C	5 h	3.5 MPa H ₂	THF [THFA] (MTHF)	100%	20% [32%] (18%)	NM	NM	[716]
53	Furfural (5 wt%)	-	3 wt% Pd/CaCO ₃	2-PrOH	220 °C	5 h	3.5 MPa H ₂	THF [THFA] (MTHF)	92%	0 [45%] (15%)	NM	NM	[716]
54	LA (4.8 wt%)	-	2 wt% PtMo/H β	H ₂ O	130 °C	24 h	5 MPa H ₂	MTHF	99%	86%	3	85%	[717]

^a Metal loading in the catalyst.^b Reaction conditions used for hydrodeoxygenation.^c Product yield in the last cycle.^d Weight hourly space velocity.^e NM: not mentioned.^f Product selectivity.

THF: tetrahydrofuran, FfA: furfuryl alcohol, MF: 2-methylfuran, ROP: ring opening products, CB: carbon black, CNT: carbon nanotubes, THFA: tetrahydrofurfuryl alcohol, 2-BuOH: 2-butanol, 2-PeOH: 2-pentanol, 2-PrOH: 2-propanol, 1-BuOH: 1-butanol, 1-PrOH: 1-propanol, EtOH: ethanol, 2-MBuOH: 2-methyl-2-butanol, t-BuOH: tert-butanol, MTHF: 2-methyltetrahydrofuran, LA: levulinic acid.

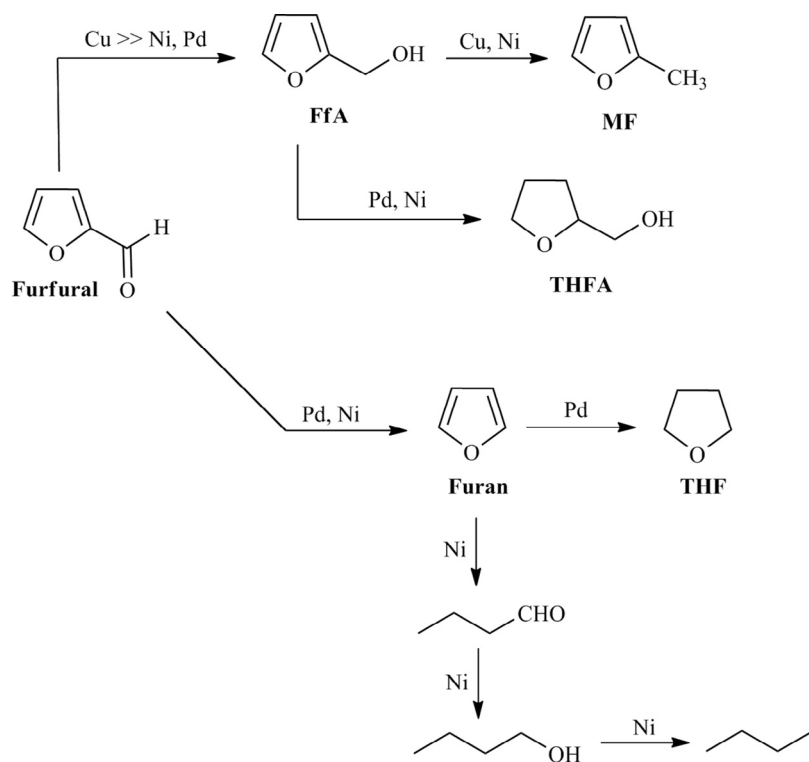


Fig. 41. Plausible reaction routes in furfural hydrogenation with copper, palladium and nickel catalysts. THFA: tetrahydrofurfuryl alcohol, FfA: furfuryl alcohol, MF: 2-methylfuran, THF: tetrahydrofuran. Adapted with permission from Ref. 704, Copyright © 2011 Springer.

high as 51% toward FfA can be achieved directly from xylose (65% conversion) in a single pot (Table 9, Entry 24). For the hydrogenation step, alcoholic solvents show outstanding effects on kinetics due to their good hydrogen solubility. With respect to carbohydrate dehydration, the use of biphasic media is superior for producing furfural, which is realized by transferring the formed furanic compound into the organic phase, thus avoiding its degradation and condensation in the acidic aqueous solution.

4.2.3.2. Tetrahydrofurfuryl alcohol (THFA). THFA, which is extensively used in industry as a chemical intermediate, is manufactured from the hydrogenation of FfA and furfural in the presence of nickel palladium, rhodium and platinum catalysts [725–727]. The gas-phase direct hydrogenation of furfural to THFA is preferable to liquid-phase reactions in terms of productivity and the prevention of leaching [728]. Over Ni/SiO₂ catalysts with <4 nm nickel particle sizes were prepared from the reduction of supported nickel nitrate, the gas-phase total hydrogenation of furfural proceeds giving THFA at yields of 94% (Table 9, Entry 25) [707]. Moreover, both bulk and supported Sn–Ni-based alloy catalysts are active for converting furfural to THFA (up to 99% selectivity), and relatively high temperatures (ca. 130 versus 110 °C) are necessary for efficient hydrogenation of C:O rather than C:C (Table 9, Entries 26 and 27) [708]. With the assistance of a biphasic system, Ordomsky et al. [709] combined the processes of xylose dehydration with Amberlyst-15 and consecutive furfural hydrogenation over a hydrophobic Ru/C catalyst into a single reactor. For increasing the hydrophobicity of solvents in the order: 1-butanol < MTHF < cyclohexane, the hydrogenation of xylose to xylitol is suppressed, thus facilitating the formation of THFA (up to 50% selectivity) directly from xylose via the intermediate furfural (Table 9, Entries 28–31).

4.2.3.3. 2-Methylfuran (MF). Analogous to DMF, 2-methylfuran is a model biomass-derived liquid fuel that can be used for the

synthesis of crysanthenate pesticides, perfume and medical intermediates [729–731]. Using furfural or FfA as the substrate, both commercial Cu–Zn and self-made Cu–Cr bimetallic catalysts exhibit nearly complete conversion for MF production (up to 96% yield) at 200–300 °C with the activity of Zn-promoted catalyst being superior to Cr-mediated ones (Table 9, Entries 32–35) [710]. The high yield of MF over Zn-promoted catalyst results from a synergistic effect of the metal and the weak acid sites [732]. The influence of mono- and bimetallic catalysts (i.e., Ni/SiO₂ and NiFe/SiO₂) on the product distribution in the conversion of furfural has been examined (Table 9, Entries 36–38) [711], where it is found that monometallic catalyst facilitated the formation of FfA and furan through separate hydrogenation and decarbonylation, while the yield of MF greatly increases through suppressing the formation of furan probably caused by Fe species in bimetallic catalyst (Fig. 42). In this catalytic process, the C:O hydrogenation occurs at low temperatures (ca. 140 °C) via either an alkoxide or a hydroxylalkyl intermediate [733], while the C–O hydrogenolysis requires relatively high temperatures.

Under ambient pressure at 150 °C, molybdenum carbide (Mo₂C) catalysts are robust for the cleavage of the C:O bond of furfural in vapor phase HDO without concurrent scission of the side C–C bond, yielding MF with a selectivity of ~50–60% for less than 1% furan selectivity (Table 9, Entry 39) [712]. The metal-like sites on Mo₂C catalysts prove to be involved in the HDO of furfural via the invariance of MF site time yield normalized by the catalytic sites. A sequential reaction process of xylose-to-MF carried out with a continuous two-liquid-phase (aqueous-toluene) plug-flow reactor, in which xylose was dehydrated to furfural (98% yield) in water over H-mordenite at 260 °C and 5.5 MPa N₂ and furfural extracted from the aqueous phase into the toluene was further hydrogenated to give MF (98% yield) at 252 °C and 0.1 MPa H₂ (gas flow: 48 h⁻¹) over a Cu–Fe catalyst (Table 9, Entry 40) [713]. Besides H₂, alcohol hydrogen donor was found to be efficient for MF production (up to 76% yield) from the catalytic transfer hydrogenation of furfural over

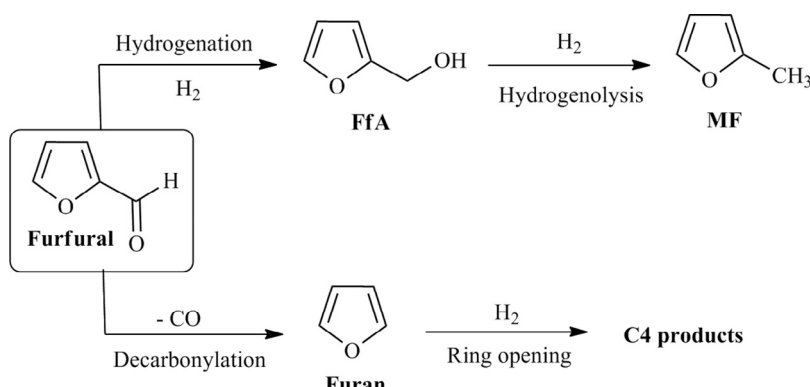


Fig. 42. Reaction pathways for furfural conversion over Ni-based catalysts. FfA: furfuryl alcohol, MF: 2-methylfuran. Adapted with permission from Ref. 711, Copyright © 2011 Elsevier.

a calcined Ru/C catalyst in liquid phase at 110–200 °C [714]. The yield of MF is influenced by the alcohol dehydrogenation activity as well as solvent polarity, and increased following the order: 2-methyl-2-butanol < tert-butanol < ethanol < 1-propanol ≈ 1-butanol < 2-propanol < 2-butanol ≈ 2-pentanol (Table 9, Entries 41–49).

4.2.3.4. 2-Methyltetrahydrofuran (MTHF). The chemical, MTHF, which can be used as a pharmaceutical solvent and an oxygenated gasoline additive in P-series fuel [734–738] can be synthesized from selective hydrogenation of MF over cubic platinum nanoparticles of 7 nm average size (Fig. 43), where the distribution of products varies with reaction temperature (40–120 °C) [715]. At 40 °C, the main product is 1-pentanol (~98% selectivity) formed via a ring-opening process; while the dominant ring-opening product changes to 2-pentanol with an increase of temperature to 95 °C (Table 9, Entries 50 and 51). Unfortunately, the relative concentration of the hydrogenated ring product MTHF remains low, regardless of how temperature is varied. To solve the mass transfer limitations caused by low solubility of hydrogen gas in the solvent, Liu et al. [739] introduced a packed-bed microreactor with Pd/C catalyst offering a safe and alternative approach to high-pressure hydrogenation of MF into MTHF. In another case, the decarbonylation of furfural to furan over the same Pd/C catalyst was demonstrated to be a prerequisite for THF formation (Table 9, Entries 52 and 53) [716]. In the presence of a metal-acid bifunctional catalyst 2 wt% PtMo/H β , Mizugaki et al. [717] demonstrated that levulinic acid (LA) could be successively hydrogenated to 1,4-pentanediol and dehydrated to form MTHF in a yield of 86% (Table 9, Entry 54). A synergistic effect between Pt nanoparticles and MoO $_x$ species promotes the hydrogenation of LA to 1,4-pentanediol, while H β possesses a dual function

as an effective support for high dispersion of Pt nanoparticles and MoO $_x$, as well as acid catalyst promoting the cyclodehydration of 1,4-pentanediol to MTHF.

4.2.4. (Hydrolysis)-hydrogenation-cyclization of biomass derivatives to γ -valerolactone (GVL)

The chemical, GVL, is useful as a solvent [740–742], intermediate [743–745], perfume and food additive [746], and in particular, is a potential fuel additive [747,748]. One possible pathway to synthesize GVL from biomass-derived LA involves an unstable intermediate γ -hydroxyvaleric acid produced via hydrogenation, followed by elimination of a water molecule in the intramolecular esterification to give GVL through ring closure (Fig. 44) [749,750]. In another pathway, angelica lactone (α and β isomer) formed from LA dehydration is hydrogenated to produce GVL [751,752]. To achieve high performance in the synthesis of GVL from different feedstocks, much attention has been paid to develop environmentally benign and cost efficient processes with heterogeneous catalysis. Compared with in-situ hydrogen sources, the catalytic transfer hydrogenation (CTH) of levulinates via Meerwein-Ponndorf-Verley (MPV) reduction with alcohols is thought to be a favorable method for GVL production. Handling liquid alcohols used in the CTH route is not only more convenient than molecular H $_2$ but also allows high selectivity of the hydrogenation of alkyl levulinates to GVL without over-hydrogenating GVL to byproducts. Furthermore, the CTH route to GVL can be carried out over inexpensive base metal catalysts with Zr, Ni and Sn as the active sites, which is attractive for the production of GVL on a commercial scale.

4.2.4.1. Direct catalytic hydrogenation. In general, LA and esters can be produced from C₆ sugars via an anaerobic oxidation process

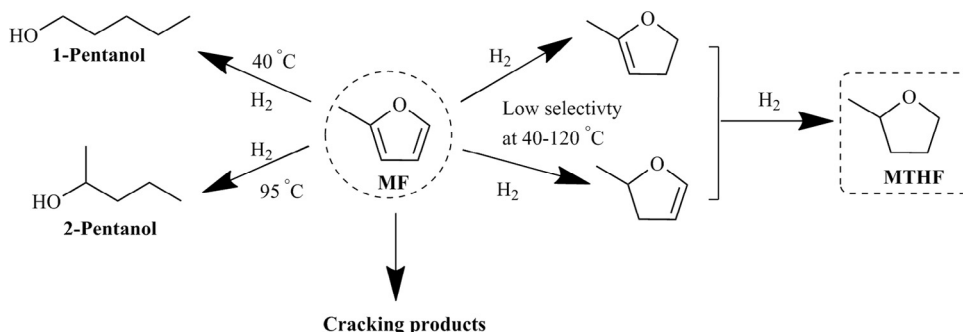


Fig. 43. Related products formed in 2-methylfuran (MF) hydrogenation over platinum nanoparticles. MTHF: 2-methyltetrahydrafuran. Adapted with permission from Ref. 715, Copyright © 2011 American Chemical Society.

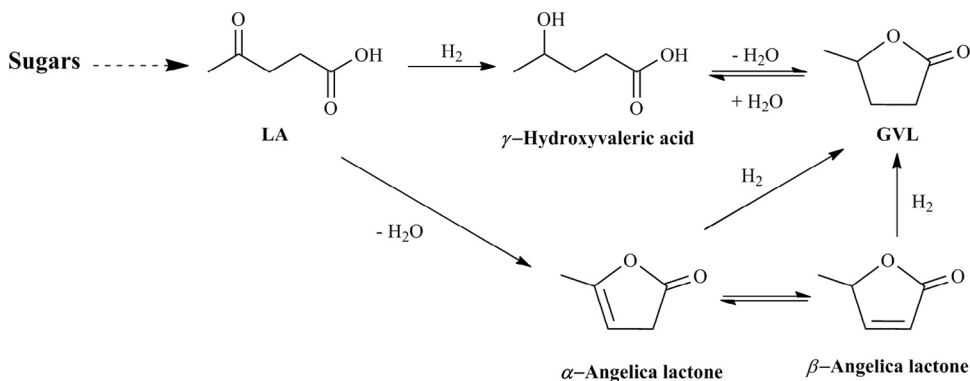


Fig. 44. Reaction pathways to produce GVL (γ -valerolactone) from LA (levulinic acid).

[753–757]. If furfural synthesized from C₅ carbohydrates is in-situ hydrogenated into FfA, then high yields of LA are obtained in a single pot as well via subsequent rehydration [758,759]. Zeolites, which are acid catalysts active for hydrolysis [760], are efficient for the synthesis of LA from xylose under hot-compressed water [761]. In a one-pot process, a maximum LA yield of 30% is achieved over 0.25 M NaOH-treated HY zeolite at 170 °C and 1.5 MPa N₂ partial pressure in 3 h, and the in-situ generated formic acid is thought to be the hydrogen source in the key step of furfural-to-FfA hydrogenation. Starting from biomass derived LA, a number of studies focus on using metal particles and oxides as catalysts to produce GVL under molecular hydrogen, formic acid, and alcohols. When different solvents like water and alcohols are employed, reaction pathways from LA to GVL are dissimilar (Fig. 45) [762]. In water medium, the first step is direct hydrogenation of the keto group in LA to give 4-hydroxyvaleric acid, followed by dehydration to yield cyclic GVL, while GVL in the presence of methanol is formed through sequential esterification of the carboxyl group to methyl levulinate (ML), hydrogenation to methyl 4-hydroxypentanoate, and intramolecular transesterification to eliminate methanol.

Ruthenium-based catalysts often exhibit high activity in the process of LA-to-GVL conversion, and due attention has been paid to seek mild reaction conditions [763]. In a continuous down-flow fixed-bed reactor system, 5% Ru/C in comparison to Pt/C and Pd/C is found to be more active (100% conversion) and product selective toward GVL (up to 100% selectivity) in dioxane from the vapor phase hydrogenation of LA (Table 10, Entries 1–3) [764], and comparable GVL selectivity (99%) and LA conversion (92%) are obtained in methanol over the same catalyst Ru/C at a lower temperature of 130 °C (Table 10, Entry 4) [765]. When an acidic support (e.g., hydroxyapatite and DOWEX 50WX2-100) is used, reaction temperatures tend to decrease for the one-pot conversion of LA to GVL.

(Table 10, Entries 5–8) [766,767]. The complete LA conversion is obtained at 130 °C in an alcohol solvent (e.g., ethanol) over ruthenium supported with different solid acid supports such as TiO₂, SiO₂ and Al₂O₃ (Table 10, Entries 9–12) [768]. Cross-linked sulfonated polyethersulfone supported Ru nanoparticle catalysts highly hydrogenate LA (88% conversion) into GVL (100% selectivity) at 70 °C (Table 10, Entries 13–17) [769]. The combined use of a ruthenium catalyst (Ru/C) with an acid such as Amberlyst-70 or Amberlyst-15, niobium phosphate, and oxides increases the reaction rate in both esterification and hydrogenation steps, and a high GVL yields of 99% with an activity of 558 h⁻¹ are realized from LA over a co-catalyst consisting of Ru/C and Amberlyst-70 (Table 10, Entries 18 and 19) [770]. Many other types of metal particles have been studied for this catalytic process, namely iridium nanoparticles and complexes (Table 10, Entries 20–22) [771–773], palladium based mono and bimetallic catalysts (Table 10, Entries 23–25) [774–776], Raney and supported Ni catalysts (Table 10, Entries 26–28) [777–779], and noble-metal-free catalysts such as copper (Table 10, Entries 29–31) [780–782], ferrous (Table 10, Entry 32) [783] and cobalt (Table 10, Entry 33) [784] nanoparticles, which are efficient to synthesize GVL from LA under a H₂ atmosphere. Nevertheless, relative high hydrogen pressures and reaction temperatures are always required.

Instead of using LA as the starting material, the direct synthesis of GVL from C₅- and C₆-sugar sources is possible without isolating the intermediate LA from the reaction mixture, which may reduce the number of processing steps (Fig. 46). Using molecular hydrogen as hydrogen donor, an acid catalyst (e.g., trifluoroacetic acid) in combination with a hydrogenation catalyst Ru/C could produce GVL in yields of 29–62% from glucose, fructose, sucrose and cellulose via a two-step process conducted (Table 10, Entries 34–37) [785]. It is clear that a strong acid is required to produce LA from C₆-sugars in the first step, and then integration with the hydrogenation

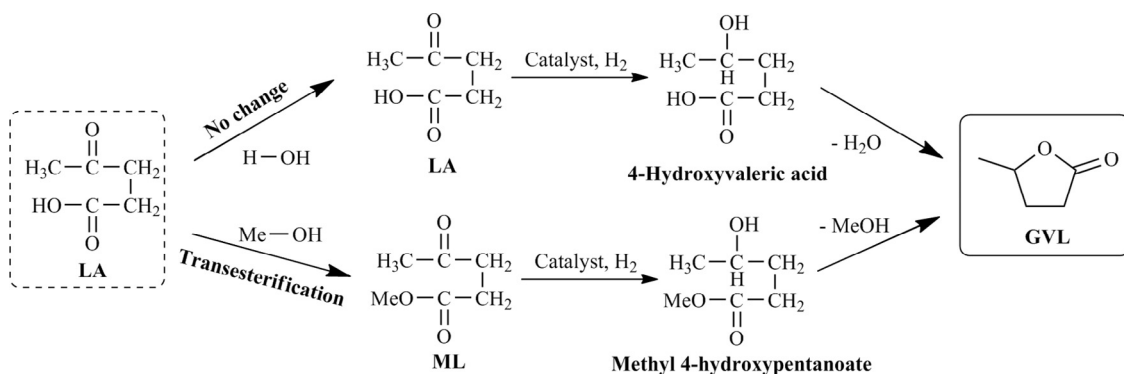


Fig. 45. Catalytic hydrogenation of levulinic acid (LA) in water or methyl levulinate (ML) in methanol to form γ -valerolactone (GVL).

Table 10

Catalytic conversion of carbohydrates or levulinic acid/levulinates derived from carbohydrates for producing γ -valerolactone with summary of reaction conditions, H-donor, maximum catalytic activity and catalyst reusability.

Entry	Substrate	Catalyst ^a	Reaction condition ^b			H-donor	Main product	Catalytic activity		Reusability		Ref.
			Solvent	Temp.	Time			Conv.	Yield	Cycles	Yield ^c	
1	LA (10.0 wt%)	5 wt% Ru/C	1, 4-Dioxane	265 °C	0.512 h ^{-1d}	0.1 MPa H ₂	GVL [Anjelica lactone]	100%	99% [1%]	7 d	97%	[764]
2	LA (10.0 wt%)	5 wt% Pd/C	1, 4-Dioxane	265 °C	0.512 h ^{-1d}	0.1 MPa H ₂	GVL [Anjelica lactone]	100%	90% [10%]	NM ^e	NM	[764]
3	LA (10.0 wt%)	5 wt% Pt/C	1, 4-Dioxane	265 °C	0.512 h ^{-1d}	0.1 MPa H ₂	GVL [Anjelica lactone]	100%	30% [69%]	NM	NM	[764]
4	LA (5.0 wt%)	5 wt% Ru/C	MeOH	130 °C	160 min	1.2 MPa H ₂	GVL	92%	91%	4	20%	[765]
5	LA (5.0 wt%)	5 wt% Ru/hydroxyapatite	H ₂ O	70 °C	4 h	0.5 MPa H ₂	GVL	99%	99%	5	89%	[766]
6	LA (5.0 wt%)	5 wt% Pd/hydroxyapatite	H ₂ O	70 °C	4 h	0.5 MPa H ₂	GVL	26%	23%	NM	NM	[766]
7	LA (5.0 wt%)	5 wt% Pt/hydroxyapatite	H ₂ O	70 °C	4 h	0.5 MPa H ₂	GVL	42%	37%	NM	NM	[766]
8	LA (0.3 wt%)	0.87 wt% Ru/DOWEX 50WX2-100	H ₂ O	70 °C	0.15 min ^{-1d}	0.5 MPa H ₂	GVL	100%	99%	33 h	90%	[767]
9	LA (5.0 wt%)	5 wt% Ru/C	EtOH	130 °C	160 min	1.2 MPa H ₂	GVL	76%	61%	NM	NM	[768]
10	LA (5.0 wt%)	5 wt% Ru/TiO ₂	EtOH	130 °C	160 min	1.2 MPa H ₂	GVL	67%	62%	NM	NM	[768]
11	LA (5.0 wt%)	5 wt% Ru/Al ₂ O ₃	EtOH	130 °C	160 min	1.2 MPa H ₂	GVL	38%	32%	NM	NM	[768]
12	LA (5.0 wt%)	5 wt% Ru/SiO ₂	EtOH	130 °C	160 min	1.2 MPa H ₂	GVL	83%	77%	NM	NM	[768]
13	LA (5.0 wt%)	2 wt% Ru/SPES	H ₂ O	70 °C	2 h	3.0 MPa H ₂	GVL	88%	88%	5	90%	[769]
14	LA (5.0 wt%)	2 wt% Ru/SiO ₂	H ₂ O	70 °C	2 h	3.0 MPa H ₂	GVL	22%	21%	NM	NM	[769]
15	LA (5.0 wt%)	2 wt% Ru/C	H ₂ O	70 °C	2 h	3.0 MPa H ₂	GVL	55%	53%	NM	NM	[769]
16	LA (5.0 wt%)	2 wt% Ru/SiO ₂ + 2 wt% Amberlyst-15	H ₂ O	70 °C	2 h	3.0 MPa H ₂	GVL	40%	39%	NM	NM	[769]
17	LA (5.0 wt%)	2 wt% Ru/C + 2 wt% Amberlyst-15	H ₂ O	70 °C	2 h	3.0 MPa H ₂	GVL	68%	67%	NM	NM	[769]
18	LA (5.0 wt%)	5 wt% Ru/C + 12 wt% Amberlyst-15	H ₂ O	70 °C	518.3 h ^{-1d} (3 h)	3.0 MPa H ₂	GVL	91%	90%	NM	NM	[770]
19	LA (5.0 wt%)	5 wt% Ru/C + 12 wt% Amberlyst-70	H ₂ O	70 °C	569.6 h ^{-1d} (3 h)	3.0 MPa H ₂	GVL	100%	100%	5	95%	[770]
20	LA (5.0 wt%)	4.5 wt% Ir/CNT	H ₂ O	50 °C	1 h	2.0 MPa H ₂	GVL	96%	95%	NM	NM	[771]
21	LA (15.0 wt%)	0.01 mol% iridium complex	Acidic H ₂ O	120 °C	4 h	1.01 MPa H ₂	GVL	100%	98%	5	94%	[772]
22	LA (10.0 wt%)	0.05 mol% [Ir(CO) ₂ Cl] ₂	EtOH + 47wt% KOH	100 °C	15 h	5.0 MPa H ₂	GVL	100%	96%	NM	NM	[773]
23	LA (2.5 wt%)	2 wt% Pd-2 wt% Au/HMS	H ₂ O	160 °C	1 h	15.0 MPa H ₂	GVL	100%	99%	3	65%	[774]
24	LA (37.7 wt%)	5 wt% Pd/CNT	H ₂ O	200 °C	6 h	6.0 MPa H ₂	GVL	58%	56%	NM	NM	[775]
25	LA (50.0 wt%)	5 wt% Pd/SiO ₂	H ₂ O	180 °C	6 h	9.0 MPa H ₂	GVL	97%	97%	4	~90%	[776]
26	LA (6.9 wt%)	10 wt% Ni–7 wt% MoO _x /C	H ₂ O	140 °C	5 h	0.8 MPa H ₂	GVL	100%	97%	NM	NM	[777]
27	LA (1 mL/h)	30 wt% Ni/SiO ₂	H ₂ O	250 °C	0.8506 h ^{-1d}	0.1 MPa H ₂	GVL	99%	87%	25 h	85%	[778]
28	LA (2.5 wt%)	40 wt% Raney Ni	2-PrOH	100 °C	4 h	1.5 MPa H ₂	GVL	100%	100%	5	55%	[779]
29	LA (10.0 wt%)	5 wt% Cu/ γ -Al ₂ O ₃	H ₂ O	265 °C	0.169 h ^{-1d}	H ₂ stream	GVL	98%	85%	25 h	70%	[780]
30	LA (16.9 wt%)	10 wt% Cu–Cr	H ₂ O	200 °C	10 h	7.0 MPa H ₂	GVL	100%	91%	NM	NM	[781]
31	LA (10.0 wt%)	5 wt% Cu/ZrO ₂	H ₂ O	265 °C	0.169 h ^{-1d}	H ₂ stream	GVL	81%	67%	28 h	60%	[782]
32	LA (10.0 wt%)	4 wt% Fe/C nanoparticles	H ₂ O	170 °C	3 h	0.5 MPa H ₂	GVL	100%	99%	6	95%	[783]
33	LA (5.0 wt%)	5 wt% Co ₂ O ₃	H ₂ O	130 °C	13 h	3.0 MPa H ₂	GVL	100%	98%	10	50%	[784]
										(3 h)		
34	Fructose (16.5 wt%)	11.4 wt% TFA + 5 wt% Ru/C	H ₂ O	180 °C	8 h	6.0 MPa H ₂	GVL	–	62%	NM	NM	[785]
35	Glucose (16.5 wt%)	11.4 wt% TFA + 5 wt% Ru/C	H ₂ O	180 °C	8 h	6.0 MPa H ₂	GVL	–	38%	NM	NM	[785]
36	Sucrose (16.5 wt%)	11.4 wt% TFA + 5 wt% Ru/C	H ₂ O	180 °C	8 h	6.0 MPa H ₂	GVL	–	52%	NM	NM	[785]
37	Cellulose (16.5 wt%)	11.4 wt% TFA + 5 wt% Ru/C	H ₂ O	180 °C	8 h	6.0 MPa H ₂	GVL	–	29%	NM	NM	[785]
38	Cellulose (5.0 wt%)	80 wt% Al-NbOPO ₄ + 5 wt% Ru/C	H ₂ O	180 °C	24 h + 12 h	5.0 MPa H ₂	GVL	–	53%	NM	NM	[786]
39	Cellulose (36 mM)	0.5 M H ₂ SO ₄ + Raney Ni	MTHF	220 °C/125 °C	8 h/0.5 mL min ^{-1d}	H ₂ stream	LA/GVL	100%	50%/50%	NM	NM	[787]

(continued on next page)

Table 10 (continued)

Entry	Substrate	Catalyst ^a	Reaction condition ^b			H-donor	Main product	Catalytic activity		Reusability		Ref.
			Solvent	Temp.	Time			Conv.	Yield	Cycles	Yield ^c	
40	Giant reed (7.0 wt%)	0.4 M HCl/5 wt% Ru/C + NbOPO ₄	H ₂ O	200 °C/70 °C	1 h/5 h	3.0 MPa H ₂	LA/GVL	100%	61%/17%	3	15%	[788]
41	FFA (5 wt%)	60 wt% [BMLm-SH][HSO ₄]/5 wt% Ru/C	MeOH	130 °C	2 h/5 h	3.4 MPa H ₂	LA/GVL	99%	94%/89%	4	75%	[789]
42	LA (1 wt%)	200 wt% ZrO ₂	2-BuOH	150 °C	16 h	2-BuOH	GVL	100%	92%	NM	NM	[790]
43	LA (1 wt%)	200 wt% MgO/ZrO ₂	2-BuOH	150 °C	16 h	2-BuOH	GVL	100%	54%	NM	NM	[790]
44	LA (1 wt%)	200 wt% γ-Al ₂ O ₃	2-BuOH	150 °C	16 h	2-BuOH	GVL	80%	56%	NM	NM	[790]
45	LA (1 wt%)	200 wt% CeZrO _x	2-BuOH	150 °C	16 h	2-BuOH	GVL	43%	11%	NM	NM	[790]
46	EL (5 wt%)	50 wt% Zr(OH) ₂ ·xH ₂ O	2-PrOH	200 °C	1 h	2-PrOH	GVL	94%	88%	10	50%	[791]
47	EL (5 wt%)	50 wt% ZrO ₂	EtOH	250 °C	3 h	EtOH	GVL	96%	82%	4	43%	[792]
48	EL (2.4 wt%)	138.9 wt% Zr-HBA	2-PrOH	150 °C	4 h	2-PrOH	GVL	100%	94%	5	92%	[793]
49	EL (2.4 wt%)	173.9 wt% Zr-Beta	2-Pentanol	150 °C	4 h	2-Pentanol	GVL	100%	96%	87 h	99%	[794]
50	LA (7.0 wt%)	5 wt% Raney Ni	2-PrOH	25 °C/120 °C	9 h/1 h	2-PrOH	GVL	100%	99%/94%	NM	NM	[795,796]
51	LA (6.0 wt%)	5 wt% Pd/C + 2 equiv. KOH	EtOH	–	50 s ^f	EtOH	GVL	–	86%	5	82%	[797]
52	LA (47.9 wt%)	0.1 mol% Ru-P/SiO ₂ + 1 equiv. NaOH	H ₂ O	150 °C	12 h	1 equiv. formic acid	GVL	100%	96%	NM	NM	[798]
53	LA (47.9 wt%)	0.1 mol% Ru-P/SiO ₂	H ₂ O	150 °C	1 h	1 equiv. formic acid	GVL	447 h ⁻¹ (TOF)	–	NM	NM	[798]
54	LA (47.9 wt%)	0.1 mol% Ru-S/SiO ₂	H ₂ O	150 °C	1 h	1 equiv. formic acid	GVL	173 h ⁻¹ (TOF)	–	NM	NM	[798]
55	LA (47.9 wt%)	0.1 mol% Ru-N/SiO ₂	H ₂ O	150 °C	1 h	1 equiv. formic acid	GVL	112 h ⁻¹ (TOF)	–	NM	NM	[798]
56	LA (71.9 wt%)	0.04 mol% Shvo catalyst	Formic acid	100 °C	8 h	1.5 equiv. formic acid	GVL	100%	100%	NM	NM	[799]
57	LA (20.0 wt%)	0.3 wt% [Ru ₃ (CO) ₁₂] + 18.3 mol% Et ₃ N	H ₂ O	130 °C	24 h	2 equiv. formic acid	GVL	100%	100%	3	99%	[800]
58	LA (5.0 wt%)	0.1 mol% Au/ZrO ₂	H ₂ O	150 °C	6 h	1 equiv. formic acid	GVL	100%	99%	NM	NM	[801]
59	BL (10.0 mol%)	0.1 mol% Au/ZrO ₂	H ₂ O	170 °C	6 h	1 equiv. formic acid	GVL	98%	95%	NM	NM	[802]
60	LA (5.0 wt%)	0.1 mol% Cu/ZrO ₂	H ₂ O	200 °C	5 h	1 equiv. formic acid	GVL	100%	100%	NM	NM	[803]

^a Metal loading in the catalyst or the catalyst dosage relative to the substrate.^b Reaction conditions used for hydrodeoxygenation.^c Product yield in the last cycle.^d Weight hourly space velocity.^e NM: not mentioned.^f Microwave irradiation.

LA: levulinic acid, MeOH: methanol, GVL: γ-valerolactone, DOWEX 50WX2-100: a SO₃H-functionalized gel-type resin, EtOH: ethanol, SPES: cross-linked sulfonated polyethersulfone, CNT: carbon nanotubes, HMS: mesoporous silica, TFA: trifluoroacetic acid, MTHF: 2-methyltetrahydrofuran, FFA: furfuryl alcohol, EL: ethyl levulinate, Zr-HBA is prepared by the coprecipitation of 4-hydroxybenzoic acid dipotassium salt and ZrOCl₂, TOF: turnover frequency, BL: butyl levulinate, Et₃N: triethylamine.

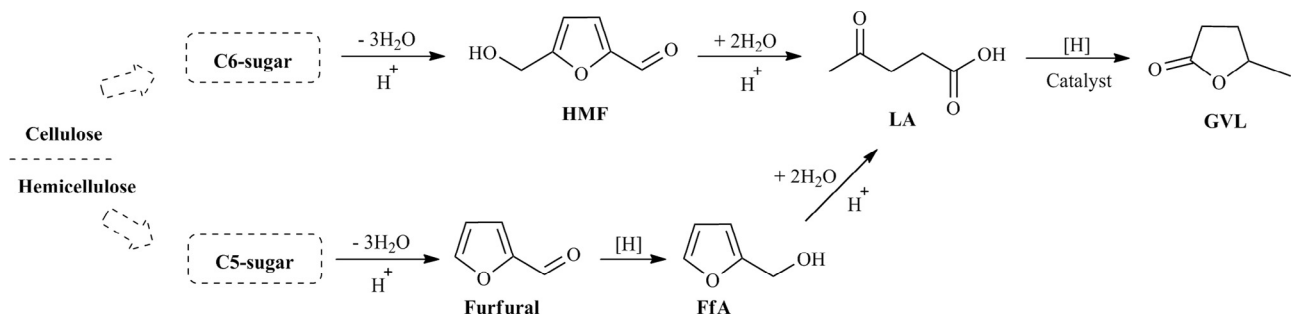


Fig. 46. Production of γ -valerolactone (GVL) from C5- and C6-sugars involving levulinic acid (LA), furfuryl alcohol (FfA), 5-hydroxymethylfurfural (HMF), and furfural as intermediates.

step over a metal catalyst yields GVL (Table 10, Entries 38 and 39) [786,787,804,805]. Employing GVL as a co-solvent, transformation of C6-sugars, in particular, cellulose in a biphasic reaction system consisting of GVL and aqueous solution could eliminate the need to purify GVL from the extraction solvent [806–808]. By adopting a bifunctional catalytic system based on Ru/C and niobium oxide or niobium phosphate, straight production of GVL from water slurries of giant reed was realized, producing a moderate GVL yield of 17% with an almost complete conversion of intermediate LA (Table 10, Entry 40) [788]. The acid component favors initial activation of the carbonyl group toward hydrogenation and subsequent esterification reaction to produce GVL. In the case of C5-sugar derivatives, a combination of an acidic IL [BMIM-SH][HSO₄] and 5% Ru/C catalyst is efficient for the sequential alcoholysis and hydrogenation of FfA to GVL via the corresponding levulinic esters in methanol, ethanol, *n*-butanol and isopropyl alcohol solvents (Table 10, Entry 41) [789], while an extra hydrogenation step to produce FfA is necessary when furfural used as substrate [809]. Since LA is the shared intermediate for the production of GVL from both C5- and C6-sugars, the integrated conversion of hemicellulose and cellulose to GVL has also been proposed [810]. This process allows for the simultaneous conversion of hemicellulose and cellulose to small molecules in a single reactor, thus eliminating pre-treatment steps that would be required to fractionate biomass. The integrated process has great potential for directly converting sugar components into a common product LA with improved selectivity so that it also offers the possibility of producing downstream chemicals like GVL.

4.2.4.2. Catalytic transfer hydrogenation (CTH). As an attractive alternative to the hydrogenation of LA to GVL using molecular H₂ over metal catalyst, CTH with the hydrogen source being a secondary alcohol through the MPV reaction has been proposed as in Fig. 47

[790]. Among the catalytic systems, zirconia-based catalysts are frequently studied. Chia et al. [790] found that metal oxides such as ZrO₂, MgO/ZrO₂, γ -Al₂O₃, and CeZrO_x could efficiently catalyze the transfer hydrogenation of LA and esters with 2-butanol as solvent and hydrogen donor, giving GVL in a maximum yield of 92% (Table 10, Entries 42–45). Basic sites in a cooperative manner with acid sites of ZrO₂-based catalysts are proposed to be active for the MPV reaction, leading to concerted direct CTH through a six-membered cyclic transition state. Similarly, ZrO(OH)₂ \cdot xH₂O is active for the conversion of EL (94% conversion) to GVL with a selectivity of 95% when 2-propanol is used as hydrogen donor (Table 10, Entry 46) [791]. The selectivities to GVL and by-products are not affected noticeably by reaction temperature, duration and catalyst loading. Although hydrogen transfer from ethanol to EL is likely to be suppressed when temperatures exceed 240 °C, a high GVL yield of 82% with 96% EL conversion is obtained in supercritical ethanol at 250 °C after 3 h over an amorphous ZrO₂ catalyst calcined at 300 °C with a high specific surface area and a large number of acid–base sites (Table 10, Entry 47) [792]. After recycling of ZrO₂ for 4 times, EL conversion and the GVL yield gradually decline to 55 and 43%, respectively. The deposition of humins, probably generated by an aldol condensation among EL, GVL and aldehyde, onto the surface of ZrO₂ are speculated to cause the partial deactivation of ZrO₂. A porous Zr-containing catalyst as well as zirconium–Beta zeolite also prove to be robust for the transformation of EL and LA to GVL via MPV reduction (Table 10, Entries 48 and 49) [793,794], and the isolated Lewis acid and base sites contribute to the high catalytic activity [811]. The stability of zirconium enhanced by organic or inorganic framework renders the catalysts to be reusable without noticeable decreases in the conversion, yield and selectivity after several consecutive cycles. Furthermore, some other metals like Raney Ni (Table 10, Entry 50) [795,796] and Pd/C (Table 10, Entry 51) [797] are stable and effective for the hydrogenation of LA and EL to GVL

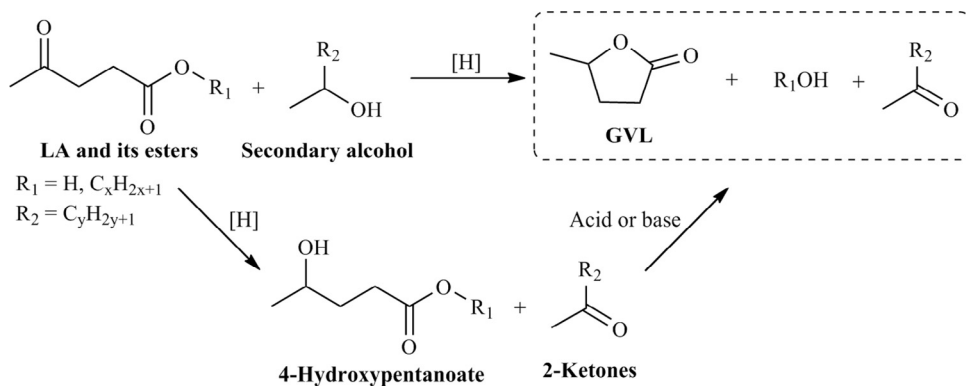


Fig. 47. Catalytic transfer hydrogenation (CTH) of levulinic acid (LA) and its esters to γ -valerolactone (GVL) in a secondary alcohol.

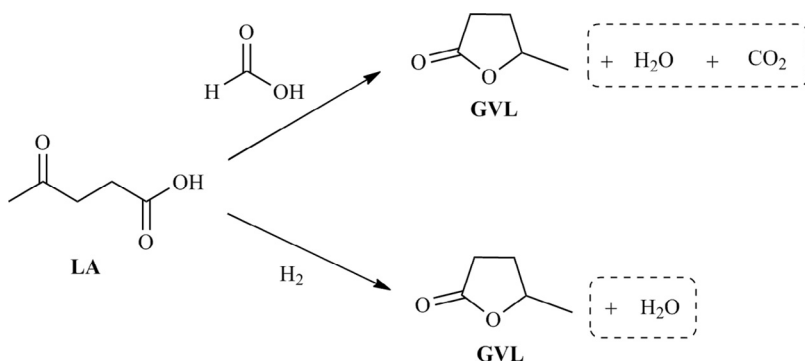


Fig. 48. Catalytic hydrogenation of LA (levulinic acid) to GVL (γ -valerolactone) using formic acid or H₂ as hydrogen source.

in a secondary alcohol solvent such as 2-sec-butyl-phenol and isopropanol. The hydride shift is confirmed to be the rate-limiting step, and increasing polarity of the hydrogen donor leads to a decrease in the reaction rates. Importantly, a first-order dependence on alkyl levulinate and secondary alcohol supports a dual-binding mechanism, where the ketone and alcohol interact with a single metal site to form a six-membered transition state [811]. A synergistic effect between base and acid sites has been demonstrated to be responsible for the enhanced activity in levulinates-to-GVL conversion [812–814], wherein basic sites (e.g., O²⁻) assisted with Lewis acidic sites (e.g., Zr⁴⁺) can activate the dissociation of the hydroxyl groups in alcohols for MPV reaction to produce an unstable intermediate 4-hydroxypentanoate, followed by intramolecular esterification or transesterification to yield GVL promoted by acid or base sites.

Using formic acid as the hydrogen source, Deng et al. [798] state that the transformation of LA to GVL is achieved over a heterogeneous ruthenium based catalyst including Ru–P/SiO₂, Ru–N/SiO₂ and Ru–S/SiO₂ in basic water with equimolar formic acid (Fig. 48; Table 10, Entries 52–55). The immobilized Ru²⁺ is speculated to act as a bifunctional catalyst to decompose formic acid and hydrogenate LA in a single step, producing a high GVL yield of 96%. The only side products, water and carbon dioxide, are easily removed and separated from the product GVL under reduced pressure (Table 10, Entries 56 and 57) [799,800]. Similarly, Du et al. [801] developed a hydrogen-independent reductive process for the conversion of LA and esters to GVL over supported gold catalysts, especially Au/ZrO₂ (Table 10, Entries 58 and 59) [802]. Hydrophobic alcohols like butanol are able to be used for the intermediate production of levulinate and formate esters and can be recovered by extraction protocol after elimination from the esters caused by the subsequent formation of GVL. Afterwards, the same group describe an earth-abundant, inexpensive, and robust copper-based metal oxide catalyst Cu/ZrO₂ for the direct conversion of an aqueous mixture of LA and formic acid (1:1, n/n), giving GVL in high yields (up to 100%) (Table 10, Entry 60) [803]. The use of formic acid produced during acid hydrolysis of biomass provides in-situ generation of H₂ gas in the system for the subsequent hydrogenation process. As compared to platinum or palladium catalyst in the hydrogenation of ketones, ruthenium generally exhibits relatively lower activity in gas phase, but is efficient under aqueous/liquid phase conditions [815–817]. The presence of an H-bonded water molecule has been verified to dramatically reduce the energetic span of the reaction pathway and to enhance catalytic activity [818]. Among various hydrogen sources used for GVL production, molecular hydrogen, formic acid and secondary alcohols are always demonstrated to exhibit high catalytic performance. However, high pressure is involved in the storage/usage of hydrogen, which is expensive and unsafe. For using formic acid as the H-donor, only limited number of catalysts bearing acid-resistant property can selectively decompose formic acid into

H₂ rather than CO and H₂O. The use of inexpensive and abundant alcohols as hydrogen donor and solvent over cheap acid-base bi-functional solid catalysts appears to be promising for GVL production through MPV reduction. In this regard, the development of functionalized catalysts active for CTH process is of high demand.

4.2.4.3. Upgrading of GVL. GVL is a platform molecule that has many potential applications in the production of chemicals and fuels (Fig. 49) [819]. Through hydrogenation, 1,4-pentanediol can be formed, which may readily undergo dehydration to give MTHF. Subsequently, the in-situ generated pentanoic acid can be converted to 5-nonenone with ketonization, followed by subsequent deoxygenation and oligomerization to produce nonane and C18–C27 alkanes, respectively. The decarboxylation of ring-opening product pentenoic acid leads to the formation of butene, which is able to be dimerized to C8 alkanes. By means of transesterification, alkyl pentenoate is yielded from GVL, which can be transformed into caprolactone, caprolactam, and adipic acid by hydroformylation, hydrocyanation, and hydroxycarbonylation, respectively. Moreover, a precursor of acrylic polymers, α -methylene- γ -valerolactone, can be created from GVL by reacting with formaldehyde [820]. All of these reaction pathways demonstrate that GVL is a versatile platform for the production of chemicals and biofuels.

Besides the complete catalytic hydrogenation of MF and furfural to produce MTHF [821,822], GVL has recently emerged as a promising sustainable substrate as well [823]. A simple, yet versatile heterogeneous catalyst system comprised of highly dispersed copper in a zirconia matrix (Cu/ZrO₂–OG) prepared by an oxalate-gel-coprecipitation method is efficient to selectively catalyze the hydrogenolysis of GVL in ethanol [824]. Both products 1,4-pentanediol and MTHF can be selectively produced by controlling the calcination temperature for Cu/ZrO₂–OG catalyst. A high MTHF yield of 91% with a remarkable conversion of GVL (up to 98%) is realized at 240 °C and 6 MPa H₂ partial pressure within 6 h, when the calcination temperature is set at 300 or 400 °C. Under identical reaction conditions but increasing the calcination temperature to above 600 °C, 1,4-pentanediol is observed to be the major product (76% selectivity) with a very poor selectivity to MTHF (11%) for GVL conversion of 96%. The H₂ pressure and copper loading are also found to affect the distribution of the products [825]. At a fixed temperature of 265 °C with 5 wt% Cu/SiO₂ catalyst in the hydrogenation of LA with a complete conversion, the selectivity toward GVL increases from 94 to ~100% with an increase in H₂ partial pressure from 0.1 to 1.0 MPa, while a further increase in pressure gives rise to the formation of 1,4-pentanediol at the expense of GVL. An increase in copper loading leads to further hydrogenation of GVL to MTHF with a high yield of 64% at copper loading up to 80 wt%. Notably, the addition and the formation of water in the catalytic process of LA hydrogenation over Ru/C catalyst inhibit the

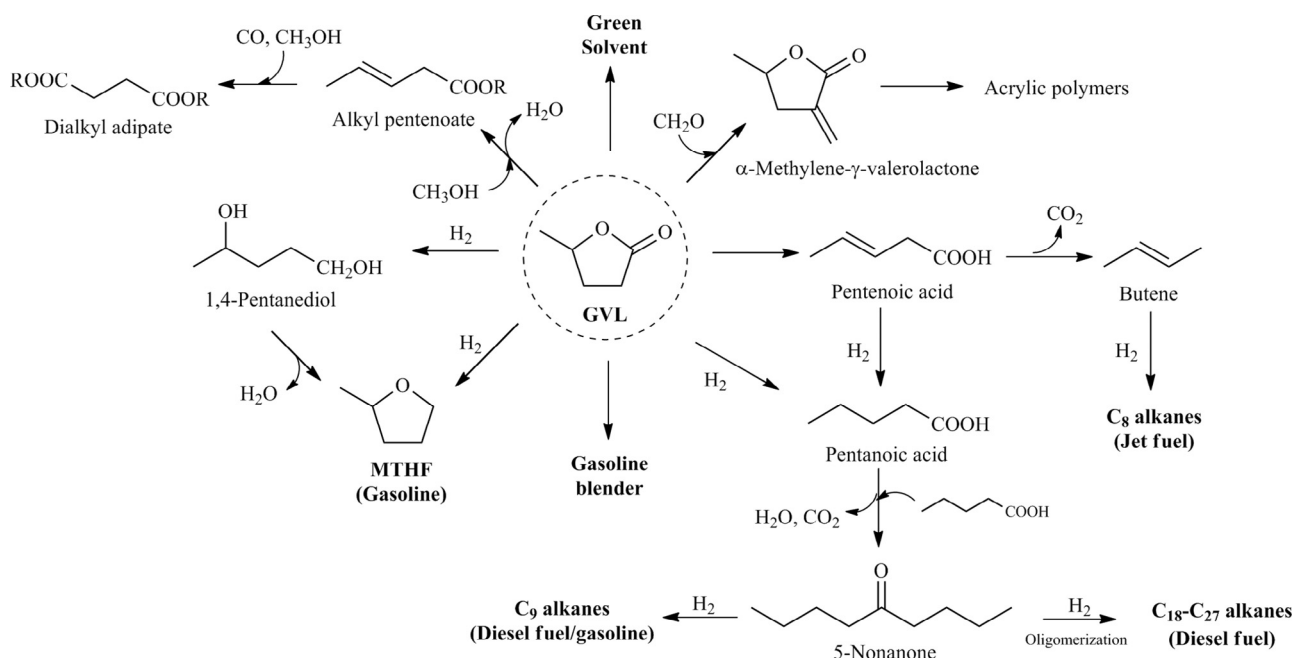


Fig. 49. Pathways for upgrading of γ -valerolactone (GVL) to biofuels and valuable chemicals. MTHF: 2-methyltetrahydrofuran. Adapted with permission from Ref. 819, Copyright © 2010 American Chemical Society.

dehydration step and shift the dominant reaction toward the generation of 2-pentanol (Fig. 50). In line with this, the desired product MTHF in a yield of 61% is obtained from LA via a two-step reaction involving an intermediate removal of water [826].

In an aqueous solution at temperatures above 350 °C and water partial pressure of 100 kPa, GVL reactant over a solid acid catalyst undergoes ring-opening to produce 3- and 4-pentenoic acids, and succent isomerization to form 2-pentenoic acid, followed by irreversible decarboxylation to yield 1-butene and carbon dioxide in an equimolar amount [827]. However, the isomerization of 1-butene to trans- and cis-2-butene essentially proceeds to equilibrium, and only 23% of 1-butene in C4 stream is retained [828]. Unexpectedly, almost pure 1-butene of C4 stream (>99%) is achieved with a Lewis acid catalyst like γ -Al₂O₃ for the decarboxylation of GVL in water at 275 °C [829]. On the contrary, the decarboxylation of GVL under anhydrous conditions is correlated strongly with the Bronsted rather than Lewis acidity of the catalyst [830]. With an integrated biorefining strategy [831], GVL can be produced simultaneously from the cellulose and hemicellulose fractions using GVL as solvent, which is converted to butene and then into butene oligomers in the presence of a number of acids and metal catalysts (Fig. 51) [832].

In the presence of acid sites, the ring-opening reaction of GVL to pentenoic acid takes place easily, whereas further hydrogenation rather than decarboxylation of the unsaturated carboxylic acid

produces pentanoic or valeric acid and its esters [833–835]. The counterpart alkyl (mono/di) valerate esters are regarded as platform chemicals for cellulosic transportation fuels [836], which can be manufactured from lignocellulosic materials through the sequential hydrolysis to LA, hydrogenation of the organic acid to GVL, ring-opening and hydrogenation to valeric acid, and esterification with alcohols (Fig. 52) [837]. In line with this, a cooperative mechanism of Pt and Bronsted acid sites of HMFI zeolite has been proposed for the case of LA conversion to valeric biofuels, in which the formation of alkyl valerate is driven by Pt-catalyzed hydrogenation of LA to GVL, which undergoes proton-assisted ring-opening by the acidic zeolite, followed by Pt-catalyzed hydrogenation and acid-mediated esterification [838]. In particular, one-pot conversion directly from LA is realized over 1 wt% Ru/H-ZSM5 catalyst, and a moderate yield of valeric acid and its esters (46%) is obtained at 200 °C and 4 MPa H₂ partial pressure [839]. The GVL ring-opening step appears to be the rate-determining step on the pathway to valeric acid, and the increase in acid sites on the support improves the selectivity to ethyl valerate and valeric acid [840]. As an interesting alternative to noble metals, a bifunctional catalyst consisting of copper supported on an amorphous material with weak acidity (e.g., ZrO₂–SiO₂) converts 90% GVL directly into pentyl valerate with a selectivity up to 83% at 250 °C and 1 MPa H₂ partial pressure after 20 h [841]. Without using an acidic support such as

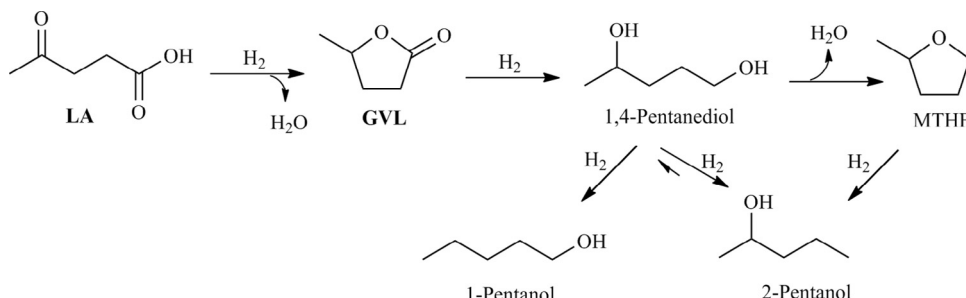


Fig. 50. Schematic of MTHF (2-methyltetrahydrofuran) and 2-pentanol formation in LA-to-GVL (levulinic acid-to- γ -valerolactone) conversion.

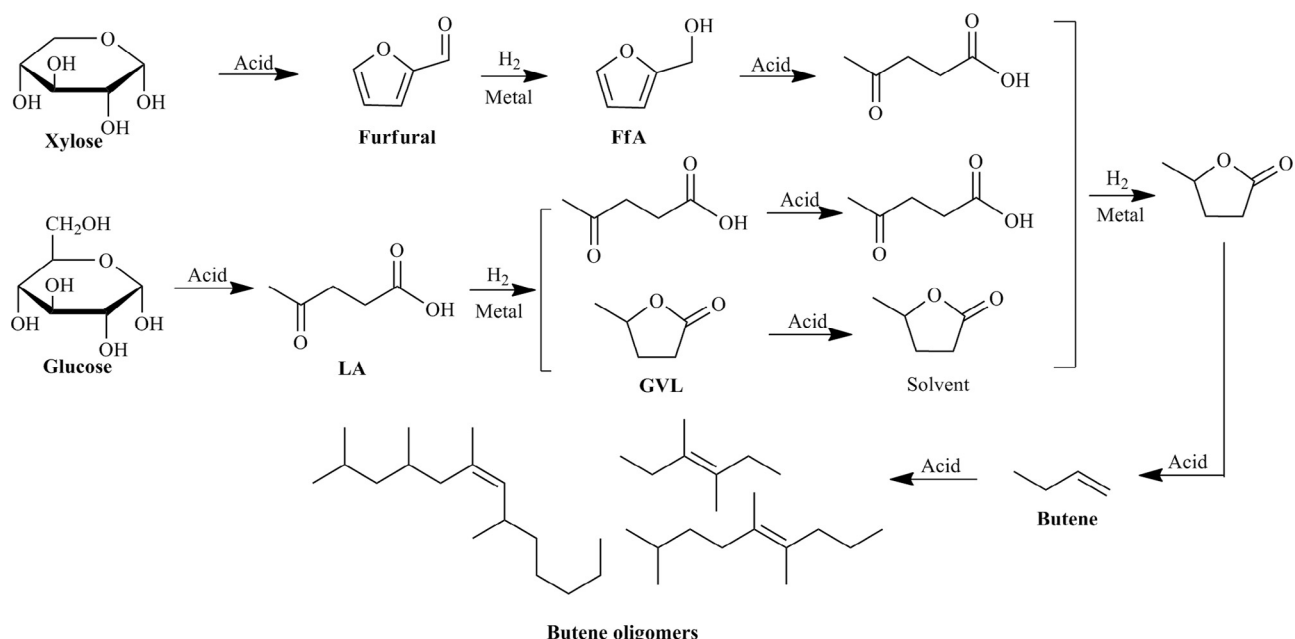


Fig. 51. Schematic of butene oligomers produced from simultaneous conversion of hemicellulose and cellulose over acid–metal catalysts via LA (levulinic acid) and GVL (γ -valerolactone). FfA: furfuryl alcohol. Adapted with permission from Ref. 832, Copyright © 2013 Royal Society of Chemistry.

Cu/ZrO₂–SiO₂, the Cu/SiO₂ catalyst exhibits comparable activity (91% conversion) and improved selectivity of 92% in the one-pot transformation of GVL into pentyl valerate [842]. It is speculated that the small copper particles display catalytically relevant Lewis acidity which is increased with reduction of CuO phase to the metallic state [842]. The subsequent conversion of valeric acid via ketonization leads to the formation of 5-nonenone over niobia and/or a ceria-zirconia catalyst, and a diesel fuel *n*-nonane is produced from this C₉ ketone through successive hydrogenation and dehydration to a mixture of linear C₉ alkenes, followed by a second time hydrogenation [843]. By another way, the oligomerization of C₉ alkenes can occur at 160 °C over an acid catalyst such as Amberlyst-70 to produce

C₁₈ alkenes, which is a precursor for jet fuel upon hydrogenation [844]. Using different substrates (e.g., LA and cellulose) as starting materials, the appropriate combination of acids with metals through integrated biorefinery processes also produces corresponding hydrocarbon fuels via the key intermediate C₉ ketone [845,846]. The production of bio-based polymers can be achieved from further upgrading of GVL to di-functional monomers, followed by copolymerization [847–852]. GVL, which has been identified as an important precursor, is being extensively used for the production of chemicals and fuels on the lab scale and it is likely to find attractive applications in industrial manufacture in the near future.

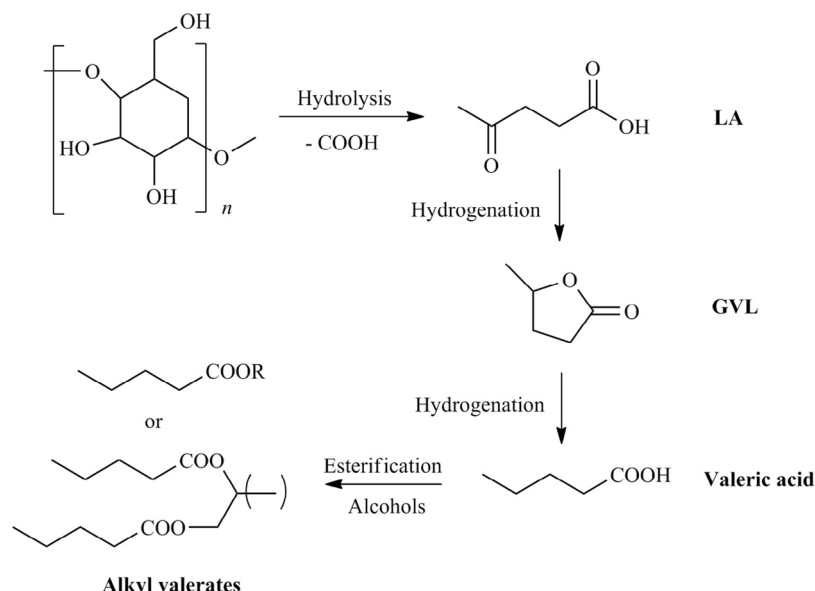


Fig. 52. Routes to the valeric biofuels from lignocellulosic materials involving levulinic acid (LA) and γ -valerolactone (GVL). Adapted with permission from Ref. 837, Copyright © 2010 Wiley-VCH.

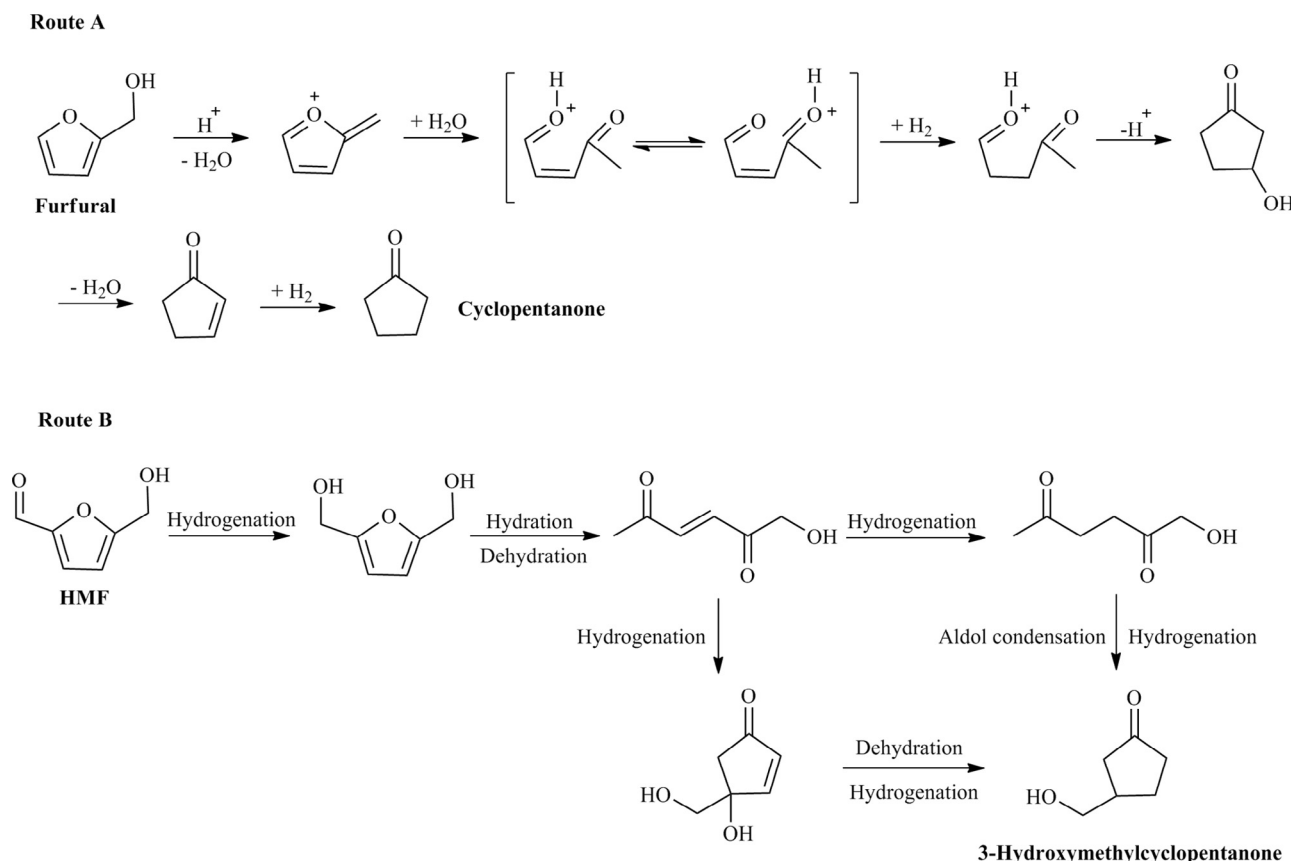


Fig. 53. Possible reaction pathways for the formation of cyclopentanol and 3-hydroxymethylcyclopentanone from furfural and HMF (5-hydroxymethylfurfural), respectively. Adapted with permission from Ref. 868, Copyright © 2014 Elsevier.

4.2.5. Hydrogenation/hydrodeoxygenation of biomass derivatives to other hydrogenated products

Bifunctional materials have been used to prepare a number of other products via hydrogenation-involved processes. For example, acid–metal binary catalysts mediated selective hydrogenation of MA to succinic anhydride or propionic acid [853–855], reduction of LA to diols, alkenes or alkanes [856–858], reductive amination of LA to pyrrolidones [859], hydrogenolysis of diethyl succinate to THF [860], and selective H₂ synthesis from carbohydrates [861,862] have great potential for producing hydrogenated products derived from biomass.

4.2.5.1. Cyclopentanone and 3-hydroxymethylcyclopentanone. Cyclopentanone, which is a versatile intermediate for the synthesis of rubbers, fungicides, pharmaceuticals, flavors, fragrances, and C₁₅–C₁₇ diesel or jet fuels [863–865], is generally prepared from petroleum-based products via the vapor-phase cyclization of 1,6-hexanediol [866] or the liquid phase oxidation of cyclopentene [867]. However, selective rearrangement of FfA to cyclopentanone can be realized with the promotion of hydrogen ions created by self-dissociation of water (Fig. 53, Route A) [868]. Namely, cyclopentanone as the exclusive product forms in a high yield of 95% over metal catalysts with a low metal concentration of 0.25–1.0 wt% at 0.8–2.5 MPa H₂ partial pressure. In contrast, relatively higher hydrogen partial pressures and catalyst concentrations favor the formation of THFA. When furfural is selected as the substrate, an additional hydrogenation step is required for the production of hydrogenated intermediate FfA. In an organic solvent like *n*-butanol, *n*-decanol and THF, the main products of the reaction are the hydrogenated derivatives of furfural such as FfA, THFA, MF, and MTHF, while furfural dissolved in

water is mainly converted into cyclopentanone at yields of up to 77% over 5wt% Pt/C catalyst at 160 °C and 8 MPa H₂ partial pressure along with a small amount of cyclopentanol (5% yield) [869] generated from further hydrogenation of cyclopentanone [870]. The attack of a H₂O molecule on the 5-position of FfA contributes to the opening and closure of the furan ring, and to the high selectivity of cyclopentanone that is closely related to the presence of 2-cyclopentenone [871]. The stabilization of the carbocation of FfA produced in an excess of hydrogen by the favorable scission of the C–O bond in the alkoxide or hydroxyalkyl intermediates seems to influence the selectivity of subsequent reactions [872]. Furthermore, the rate balance between the formation of FfA polymers on the catalyst surface and their decomposition also results in the high selectivity of FfA rearrangement to cyclopentanone [873]. Similarly, the ring rearrangement of HMF to a cyclopentanone derivative, 3-hydroxymethylcyclopentanone, can be achieved through the hydrogenation with metal nanoparticles and the Lewis acid catalysis of metal oxide supports (Fig. 53, Route B) [874], and a highest 3-hydroxymethylcyclopentanone yield of 86% is obtained over Au/Nb₂O₅ catalyst at 140 °C and 8 MPa H₂ partial pressure within 12 h. By taking advantage of the selective hydrogenation on metal particles and the Lewis acid catalysis of solid supports, HMF can be selectively converted into 3-hydroxymethylcyclopentanone. For furfural, the balance between the rates of formation of furfuryl alcohol polymers on the catalyst surface and their decomposition is likely to be responsible for the high selectivity of furfural rearrangement to cyclopentanone.

4.2.5.2. Diols. In the liquid-phase hydrogenation of FfA, THFA is generally the dominant product [875], while harsh reaction conditions

tend to drive the hydrogenolysis of the furan ring to synthesize diols such as 1,2-pentanediol, 1,5-pentanediol, and 1,4-pentanediol. In the case of 1,2-pentanediol, low pressure and high temperature favor its generation, in which water is found to significantly enhance the reaction rate [876]. Moreover, the cooperative catalysis of metal nanoparticles and a basic support like HT drastically increases the selectivity for 1,2-pentanediol [877]. However, a one-pot two-step process with controlled temperatures is beneficial for the synthesis of 1,5-pentanediol from furfural over bimetallic catalysts such as Pd–Ir–ReO_x/SiO₂, Rh–Ir–ReO_x/SiO₂ and Pt/Co₂AlO₄, in which the lower-temperature reaction step is very crucial for the total hydrogenation of furfural into THFA intermediate and the hydrogenolysis occurs during the high temperature step [878–880]. An integrated conversion of furfural to 1,4-butanediol with a yield of 85% has been realized over a multifunctional Pt/TiO₂–ZrO₂ catalyst with H₂O₂ in HCOOH/H₂O/MeOH at 120 °C and 3.5 MPa H₂ partial pressure after 6 h. The conversion involves two sequential reaction steps consisting of selectively oxidizing furfural to furanones and hydrogenation of the mixture of furanones to 1,4-butanediol [881]. Likewise, the production of 1,3-propanediol and 1,6-hexanediol has been realized from the hydrogenolysis of glycerol and HMF over metal particles with an acidic support, respectively [882,883]. In comparison with Bronsted and Lewis acidic supports like ZrP, HY zeolite, Nb₂O₅, HZSM-5, SiO₂–Al₂O₃, Al₂O₃ and SO₄/ZrO₂, the specific Bronsted acidity on ZrP support can effectively accelerate the cleavage of C–O bond in a furan ring, while the presence of a transition metal is responsible for FA dissociation, hence supplying in-situ the required hydrogen for hydrogenation.

4.2.5.3. Upgrading of bio-oil. Bio-oil produced from biomass through flash pyrolysis and hydrothermal liquefaction can be upgraded to engine fuels via HDO and zeolite cracking [884–886]. In the process of syngas conversion to hydrocarbons, Fischer–Tropsch (FT) synthesis is considered as a crucial step, while the biggest challenge is the control of selectivity [887,888]. In this regard, the combination of acidic zeolites with an active FT catalyst considerably increases the product selectivity toward liquid hydrocarbons [889]. As a model reaction for bio-oil upgrading, a one-step hydrogenation–esterification of furfural with acetic acid over a bifunctional catalyst 5 wt% Pd/Al₂(SiO₃)₃ or Pd/Al–SBA-15 proceeds under mild conditions to give FFA and ester in a selectivity of 66% [890,891]. Synergistic effect of metal sites and acid sites for the one-step hydrogenation–esterification over composite bifunctional catalyst of 5% Pd/Al₂(SiO₃)₃ is more efficient than the corresponding physically mixed monofunctional catalysts. In a similar manner, Hf-, Zr- or Sn-Beta zeolites effectively catalyze the coupled transfer hydrogenation and etherification of HMF with primary and secondary alcohols into renewable fuel additives 2,5-bis(alkoxymethyl)furans without using an external hydrogen source or precious metals [378,892]. Among these zeolites, Hf- and Zr-Beta appear to be more active in the MPV reduction whereas Sn-Beta exhibits the highest stability and selectivity toward etherification.

4.2.5.4. Alkanes. Renewable routes have been developed to produce liquid alkanes from biomass derivatives. The aqueous phase catalytic hydrogenation/dehydration of furfural produces pentane over bifunctional nickel-based catalysts [893]. On the nickel active sites of these catalysts, some hydrogenated intermediates such as FfA, THFA, 1,5-pentanediol, and tetrahydro-2-furancarboxaldehyde derived from furfural, followed by migration to acid sites of the bi-functional catalyst and undergo dehydration to form alkenes, and in the subsequent hydrogenation step saturate the C:C bonds of pentene to give pentane. The product distributions are greatly affected by the type of metals with respect to the interaction strength of the furan ring with the metal surface and the type of surface intermediates stabilized by each metal [894]. Specifically, high

selectivity to FfA is obtained over Cu/SiO₂, but with only small amounts of 2-methyl furan formed at high reaction temperatures (ca. 290 °C). In strong contrast, furan is mainly produced from the conversion of furfural by decarbonylation over Pd/SiO₂, which is capable of further reacting with hydrogen to give THF. For Ni/SiO₂ catalyst, ring opening products such as butanal, butanol and butane are observed in significant amounts [894]. Besides pentane, lighter alkanes including C₁, C₂, C₃, and C₄ were also detected, which might depend on the relative rates of C–C bond cleavage, dehydration and hydrogenation reactions [895]. Notably, C₆ alkane in minor percentages is observed in the products and was probably formed through FT reactions [896]. Likewise, an aqueous-phase HDO of sorbitol to the gasoline-range products including C₅–C₆ alkanes, C₂–C₆ alcohols, THFs, tetrahydropyrans, and small amounts of C₂–C₆ aldehydes, ketones and organic acids could be realized in a continuous flow reactor [897]. It was found that the gasoline-range yields on Pt/Zr–P and Pt–ReO_x/C were 67% and 44%, respectively. With respect to the distribution of products, Pt–ReO_x/C had a higher CO₂ selectivity than Pt/Zr–P, suggesting the Pt–ReO_x/C showed a higher rate of decarbonylation than Pt/Zr–P, while Pt/Zr–P had a higher rate of C–O bond cleavage than Pt–ReO_x/C, leading to a higher C₆ product selectivity (36% vs. 12%). With sorbitol as intermediate [898], a metal–acid binary catalyst system composed of {Ir–ReO_x/SiO₂ + HZSM-5} is effective in the one-pot conversion of cellulose in H₂O/n-dodecane, giving n-hexane yields of 83% and 78% from ball-milled cellulose and microcrystalline cellulose, respectively [899]. The yield of n-hexane remains above 70% even when ball-milled cellulose at a water weight ratio of 1:1 is used. The hydrolysis of cellulose to glucose via water-soluble oligosaccharides catalyzed by protons produced from HZSM-5 or hot water is considered to be the rate-determining step. In a more fast reaction rate, glucose can be hydrogenated to sorbitol over Ir–ReO_x/SiO₂, followed by hydrogenolysis over Ir–ReO_x/SiO₂ and HZSM-5 to produce the end product, n-hexane.

The use of extractive solvents like alkylphenol to separate GVL from sulfuric acid following the LA hydrogenation step is an essential step for butene oligomerization [900]. The conversion of GVL to aromatic hydrocarbons takes place over a zeolite catalyst at 500 °C, and gives a carbon yield of 57% of aromatics from GVL with HZSM-5 (Si/Al: 25) catalyst [901]. To increase the length of carbon chains, coupling and condensation reactions are involved [902,903]. Liu et al. [904,905] developed an integrated catalytic process for the conversion and upgrading of biomass feedstocks like fructose into 5,5'-dihydroxymethyl furin (DHMF), through self-coupling of HMF via organocatalysis with a N-heterocyclic carbene, and subsequently into n-C₁₂H₂₆ alkane over a bifunctional catalyst system consisting of {Pd/C + acetic acid + La(OTf)₃} via metal–acid tandem catalysis. In particular, the third step HDO of DHMF is carried out with metal (Pd/C)-acid (La(OTf)₃) catalyst in acetic acid to afford 78% alkanes with a 64% selectivity to n-C₁₂H₂₆ at 250 °C and 2.1 MPa H₂ partial pressure for 16 h. In combination with dehydration, aldol-condensation/hydrogenation, and dehydration/hydrogenation processing, Chheda and Dumesic [906] demonstrated the possibility of converting carbohydrate feedstocks to produce liquid alkanes (Fig. 54). Initially, the catalytic hydrolysis reaction involves breaking C–O–C linkages to form simpler carbohydrate molecules at high temperatures in the presence of acids. The resulting soluble carbohydrates could subsequently undergo acid-mediated dehydration to produce furanic compounds (e.g., HMF and furfural) through loss of three water molecules at moderate temperatures of 100–200 °C. The subsequent aldol-condensation involving the C–C coupling between two compounds containing carbonyl groups is capable of forming larger organic molecules, which is generally carried out over base catalysts at low temperatures in polar solvents like water and water–methanol. Finally, the hydrogenation step could saturate the C:C and C:O bonds of the aldol-adducts over a

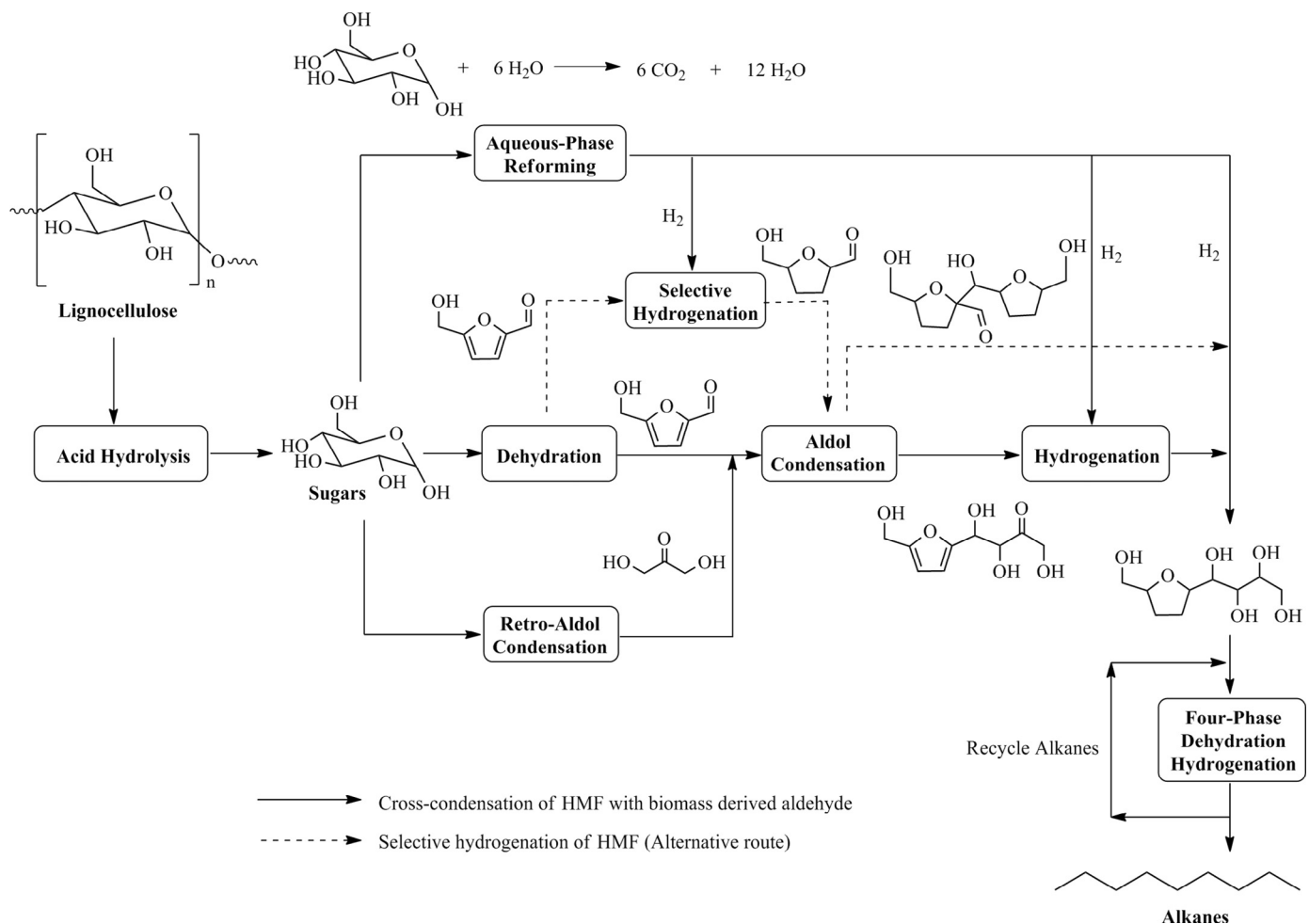


Fig. 54. Schematic diagram for production of liquid alkanes from sugars in biorefinery. Adapted with permission from Ref. 906, Copyright © 2007 Elsevier.

metal catalyst, thus forming large water-soluble organic compounds, followed by repeated dehydration and hydrogenation reactions catalyzed by bifunctional materials containing acid and metal sites to produce liquid alkanes in a four-phase reactor system. Dedsuksophon et al. [907] reported that 15–20% maximum yields of C₅–C₁₅ could be detected from tapioca flour and corncobs through three sequential steps involving WO₃–ZrO₂ catalyzed hydrolysis/dehydration at 300 °C for 5 min, aldol-condensation of HMF or furfural with acetone at 80 °C within 30 h, and hydrogenation over supported Pd particles at 120 °C after 6 h in a single pot. Notably, the yields of hydrocarbon compounds increase with an increase in reaction temperatures from 80 to 120 °C, but decrease at higher reaction temperatures of 150 and 180 °C, which is possibly due to further conversion or cracking of water-soluble organic compounds.

4.2.5.5. Cycloalkanes. Lignin-derived components are commonly used as model chemicals for HDO to investigate possible reaction pathways and susceptibilities dominated by several typical oxygen functionalities including hydroxyl groups bound to aromatic and aliphatic carbons and methoxy groups in phenolic compounds [908]. A large number of studies on hydrogenation/hydrogenolysis of simple aromatic compounds have been carried out, so as to facilitate the valorization of lignin. For instance, the direct hydrogenation of phenol to cyclohexanone is always hindered by over-reduction to cyclohexanol, while the introduction of Lewis acid sites can sequentially enhance the hydrogenation of phenol to cyclohexanone over palladium nanoparticles and inhibit further hydrogenation of

the ketone [909]. Deutscher et al. [910] found that the dehydration of cyclohexanol derivatives was the rate limiting step in producing cyclohexane derivatives in the deoxygenation of phenols over a copper chromite catalyst via hydrogenation, dehydration and hydrogenation. Likewise, the combination of noble metals (Ru, Rh and Pt) supported on Al₂O₃ (or C) with solid acid zeolites tested for HDO activity of the oligomeric technical lignins predominantly contain 8–O–4' inter-unit linkages, to give 35–60% conversions of lignin with 65–70% product selectivity for aromatic hydrocarbons such as toluene at 250 °C and 4–5 MPa for 8–12 h [911]. Specifically, high yields of toluene (up to 100%) are obtained from the HDO of dibenzyl ether at 250 °C and 10 MPa H₂ partial pressure for 2 h when a supported FeS₂ catalyst is used [912]. The chemical transformation of FeS₂ into Fe_(1-x)S has been demonstrated to be responsible for the high activity and selectivity gained in the conversion of dibenzyl ether into toluene.

The one-pot dehydroxylation of phenols to arenes like benzene can be realized by catalytic tandem reactions with 2-propanol as an H-donor and concurrent use of Raney Ni and H-Beta-35 (Fig. 55) [913]. The production of low boiling point arenes instead of high boiling phenols from lignin can greatly facilitate the valorization of lignin products by conventional refinery processes. Through a cleavage of C–O bonds in phenolics followed by an integrated metal- and acid-catalyzed hydrogenation and dehydration, cycloalkanes-containing transportation biofuels (>90% selectivities) are synthesized from the full HDO of lignin-derived phenolic monomers and dimers over a bifunctional catalyst of Ru supported in HZSM-5 at 200 °C

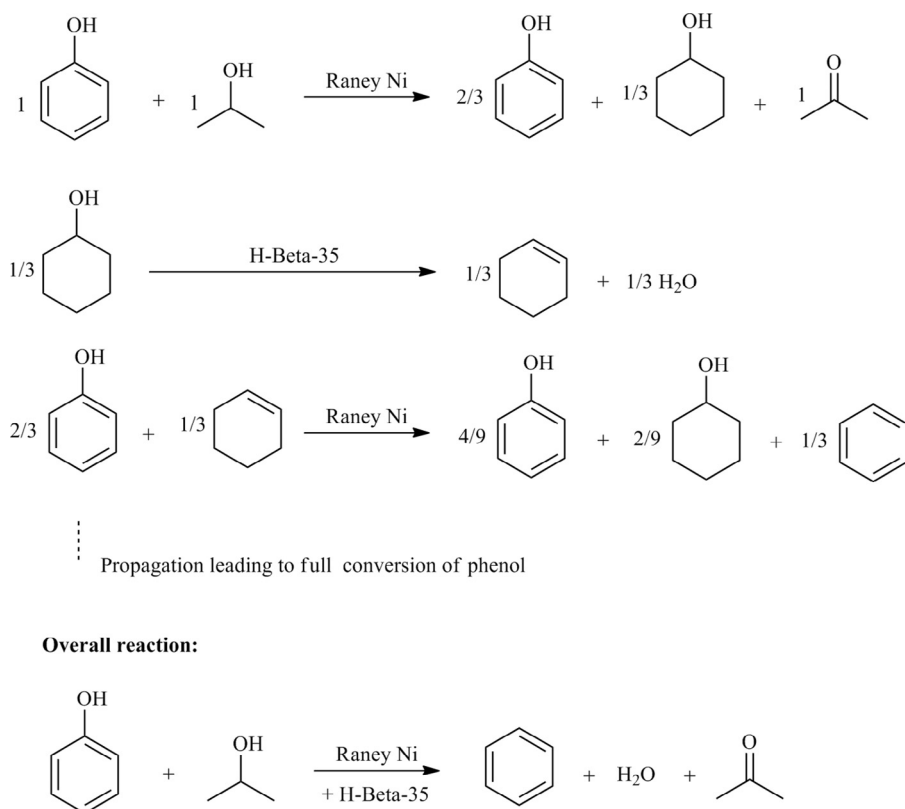


Fig. 55. Proposed main reaction pathway and overall reaction for the dehydroxylation of phenols to arenes by catalytic tandem reactions with concurrent use of Raney Ni and H-Beta-35 catalysts. Adapted with permission from Ref. 913, Copyright © 2013 Wiley-VCH.

and 5 MPa H₂ partial pressure after 4 h [914]. However, issues on the recycling of catalysts for complex catalytic systems at relatively high temperatures (200–250 °C) are not commonly studied and it is likely that the structure of these heterogeneous catalysts becomes deactivated with time due to the formation of chars or humins and adsorption on the catalytic surfaces.

5. Other bifunctional materials and catalytic routes

Catalytic transformation of biomass into chemicals products via chemical routes has been reviewed and analyzed [915], and updated in follow-up studies [916–918]. Fuel cells coupled with biomass-derived fuel processors are able to provide renewable energy and chemicals in a CO₂-neutral manner [919]. Electrocatalytic oxidation of glucose has been extensively studied, since this reaction has applications in glucose-air fuel cells as well as in medical and food industries as glucose sensors [920–924].

5.1. Metals (Au, Ag, Cd, Ru, Pt, Pd, Cu, Ni) dispersed into nano-sized particles

Gold dispersed into nano-sized scale particles or alloyed with other metals normally has high stability and enhanced activity in electrocatalytic glucose oxidation [925–930], in which gluconic acid can be the final product [931]. Noble metals like Ag, Cd, Ru, Pt, and Pd have been developed for this catalytic process [932–935], while more attention has been paid to non-precious metal (e.g., Cu and Ni) catalysts [936–939]. Carbohydrates including mannose, galactose, fructose, arabinose and xylose can be detected through electrocatalytic oxidation [940–942], and some interesting sugar transformations such as simultaneous production of xylitol and xylonic acid from xylose, isomerization of lactose into lactulose,

hydrogenation of glucose to sorbitol or 2-deoxysorbitol, and oxidation of sorbitol to fructose and sorbose can be realized via electrocatalytic processes [943–946]. In parallel, electro-oxidative cleavage of lignin is likely to be achieved through disruption of biphenyl linkages (a), diphenylether linkages (b), dibenzylether linkages (c), β-O-4 linkages (d), β-5 linkages (e), β-β linkages (f) and β-1 couplings (g) (Fig. 56) [947], and further upgrading of the lignin monomers is possibly through electrocatalytic hydrogenolysis/hydrogenation [948]. The coupling of sequential electrocatalytic processes generally involving degradation of biopolymers to small molecules and subsequent hydrogenation/oxidation appears to be one of efficient ways for the direct transformation of biomass resources into biofuels and value-added chemicals.

In comparing the upgrading of biomass-derived platform molecules with heterogeneous catalysts, electrochemical catalysis offers relatively high selectivity of products and increased reaction rates. In electrochemical catalysis, the electrode potential and the Faradaic current are two additional external control parameters that allow tuning of the thermodynamic driving force and activation energy [949]. Over supported metal nanoparticles (e.g., Au and Pd), the electrocatalytic oxidation of HMF in alkaline media was able to selectively produce FDCA at high selectivity giving trace amounts of DFF [950], while the corresponding hydrogenation reactions give BHMF, BHMTF or even DMF in neutral or acidic solutions [951–953]. For furfural, attention has been paid to electrocatalytic reduction to synthesize the dominant product FFA in different reaction media [954–957], and THFA, MF and MTHF are found to form in a continuous electrocatalytic membrane reactor [958]. When substrate is selected as LA, the electrocatalytic hydrogenation in parallel with the heterogeneous bifunctional catalysts-mediated chemical process produced GVL or valeric acid in high yields [959–962]. Likewise, a series of organic acids or aldehydes can probably be produced from

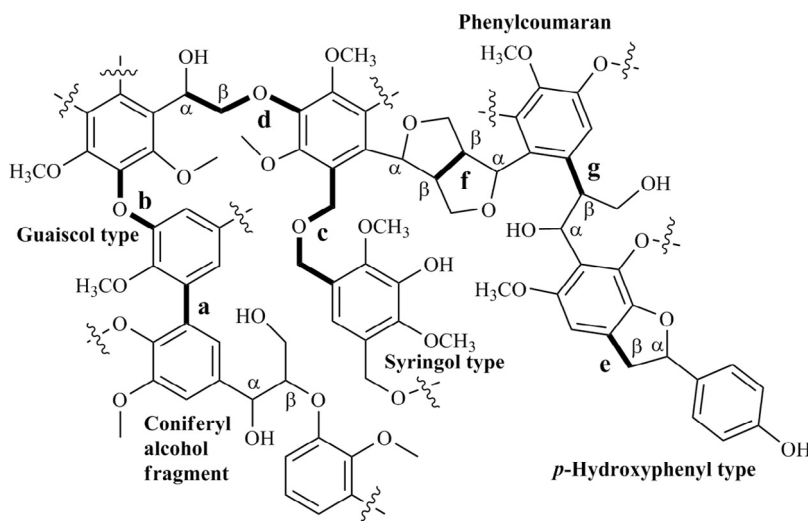


Fig. 56. Schematic of the lignin structure with (a) biphenyl linkages, (b) diphenylether linkages, (c) dibenzylether linkages, (d) β -O-4 linkages, (e) β -5 linkages, (f) β - β linkages, and (g) β -1 couplings. Adapted with permission from Ref. 947, Copyright © 2012 Royal Society of Chemistry.

electrocatalytic oxidation of biomass derived alcohols such as ethanol, ethylene glycol, and glycerol [963–968].

5.2. Cascade reactions with enzymes and electrocatalytic methods

Combining an enzyme, oxalate oxidase, with an organic oxidation catalyst, 4-amino-TEMPO can allow the complete electrochemical oxidation of the biofuel glycerol to CO_2 (Fig. 57) [969]. In this hybrid cascade process, TEMPO-NH₂ catalyzes the oxidation of glycerol to mesoxalic acid, while a combination of oxalate oxidase and TEMPO-NH₂ transforms mesoxalic acid to glyoxalic acid, oxalic acid, and finally CO_2 . Importantly, CO_2 possibly captured from the ambient air [970] might be able to be directly employed in biomass processing [971] or hydrogenated to form a range of carbon-rich fuels like CO, oxalate, formic acid, and methanol via electrochemical catalysis [972–974]. The production of hydrogen can also be realized from water electrolysis or reforming of renewable chemicals such as glucose and ethanol [975–977]. Many types of biomass-derived fuels (e.g., ethanol, biodiesel and biogas) as well as bio-based chemicals (e.g., HMF, glycerol and LA) can be used as the feedstock for a fuel processor that

can be coupled with fuel cell to provide renewable energy in the future.

The combination of biocatalysis with inorganic catalysis is a method for one-pot conversion of biomass-related feedstocks [978]. Vennestrøm et al. [979] provide examples on combined enzyme and chemical catalysts for the production of commodity chemicals from renewable feedstocks. In the case of oxidase enzymes-mediated reactions, oxygen was reduced to hydrogen peroxide. Pyranose oxidase, which is an oxidase enzyme, catalyzes the oxidation of aldopyranoses to form 2-keto sugars and H_2O_2 [980], and a combined chemical hydrogenation as a second step is capable of producing fructose from glucosone (2-keto sugar) [981]. In fact, isomerase is able to separately realize the glucose-to-fructose conversion [982,983]. An integrated enzyme cascade-chemocatalytic transformation of cellulose oligomers into HMF (up to 46% yield) has been achieved in aqueous (enzyme) and organic (chemical) media with enzyme and acid functionalized mesoporous silica nanoparticles (MSNs), respectively (Fig. 58) [984]. The catalytic process generally involves thermophilic glucose isomerase enzyme for glucose isomerization to fructose and an acid catalyst for fructose dehydration to HMF

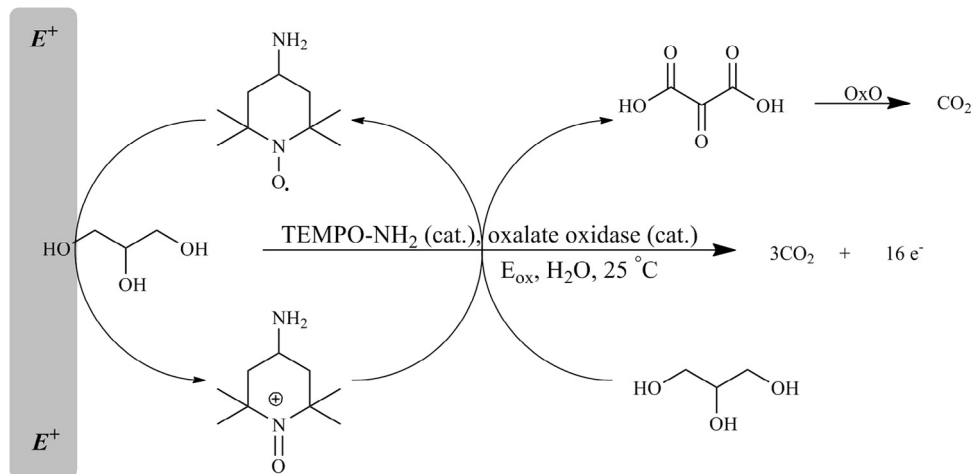


Fig. 57. Possible electrocatalytic cascade oxidation of glycerol by TEMPO (2,2,6,6-tetramethyl-piperidin-1-oxyl)-NH₂ and oxalate oxidase (OxO). Adapted with permission from Ref. 969, Copyright © 2014, American Chemical Society.

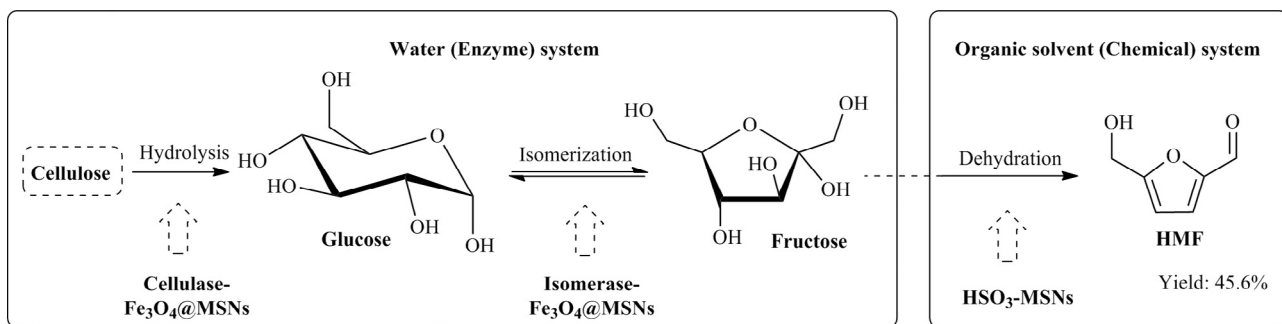


Fig. 58. An integrated enzyme cascade-chemocatalytic conversion of cellulose into HMF (5-hydroxymethylfurfural) in a biphasic system with enzyme and acid functionalized MSNs (mesoporous silica nanoparticles). Adapted with permission from Ref. 984, Copyright © 2014 Wiley-VCH.

[985,986]. After further introduction of an HMF/furfural oxidoreductase into the catalytic systems, FDCA and furoic acid are formed from hexoses and pentoses, respectively [987–989]. HMF and furfural can be successively hydrogenated into BHMF and FfA through anaerobic biotransformation by using the aldehyde (–CHO) as an electron acceptor [990,991]. Biotransformation appears to enhance overall metabolic capacity of other anaerobic bacteria (e.g., sulfate-reducing bacteria and acetogenic bacteria) in anaerobic digestion processes, demonstrating that synergistic effects exist among different enzymes. The introduction of chemo-catalytic methods can play a valuable role in both upstream and downstream processing of biomass by improving efficiency and selectivity of target products.

Chemo-enzymatic routes have been developed to produce other biomass-derived chemicals. For instance, GVL can be produced from LA with an integrated bioprocessing system involving the production of intermediate 4-hydroxyvaleric acid from LA with an intracellular enzyme *P. putida*, and subsequent lactonization that occurs extracytosolically in acidic medium (Fig. 59) [992]. In a 2 L bioreactor, the production of 4-hydroxyvalerate and GVL from levulinic acid have been examined, and titers of 27.1 g L⁻¹ and 8.2 g L⁻¹ are achieved for the two respective compounds. Immobilized lipase B from *Candida antarctica* not only afforded a high yield of GVL (90%) from LA via EL as intermediate promoted by Amberlyst-15, but also exhibits a remarkable enantiomeric excess of the desired (S)-GVL (>99% ee) [993]. In the overall process, catalyst recycle is possible especially in the case of Amberlyst-15 and *C. Antarctica*. Moreover, organic solvents used in the extraction or reaction can be reused after distillation, leading to an overall decrease in waste production. Starting from the same substrate LA, 2-butanone is obtained

by acetoacetate decarboxylase from *Clostridium acetobutylicum* [994]. In this catalytic system, mediators such as methyl viologen and 2,2'-azino-bis(3-ethylbenzothiazoline-6-sulfonic acid) are capable of accepting the overcrowded electrons around carboxylate group of LA and of assisting spontaneous electron flow from β- to γ-carbon. Through corresponding chemo-enzymatic catalysis, biorefinery products like methyl ethyl ketone, methane, polyhydroxylalkanoates, xylogluco-oligosaccharides, and starch can be produced from non-edible biomass [995–1000]. The combination of chemical and enzymatic catalysis can be used to integrate cascade reactions in a single pot, thus avoiding the separation of intermediates from the reaction mixtures and maintaining the separate advantages of the two different catalytic systems for efficient biomass transformations.

Photocatalysis shows good potential for transformation of lignocellulosic biomass to valuable products [1001]. The rapid elucidation of reaction routes mediated by functional catalytic materials can widen the scope of biomass transformations.

6. Auxiliary processes to boost catalytic efficiency

In multi-catalytic processes involving biomass conversion, catalyst selectivity, on some level, is a function of the ratio and distribution of active sites for both heterogeneous and homogeneous reactions. For the case of Lewis–Bronsted acid-mediated hydrolysis and dehydration processes, presence of Lewis acid sites responsible for sugar isomerization is necessary to accelerate the thermokinetic performance. However, catalysts with excess of Lewis acid sites often lead to a decrease in product selectivity that is associated with the formation of humins [1002,1003]. Therefore,

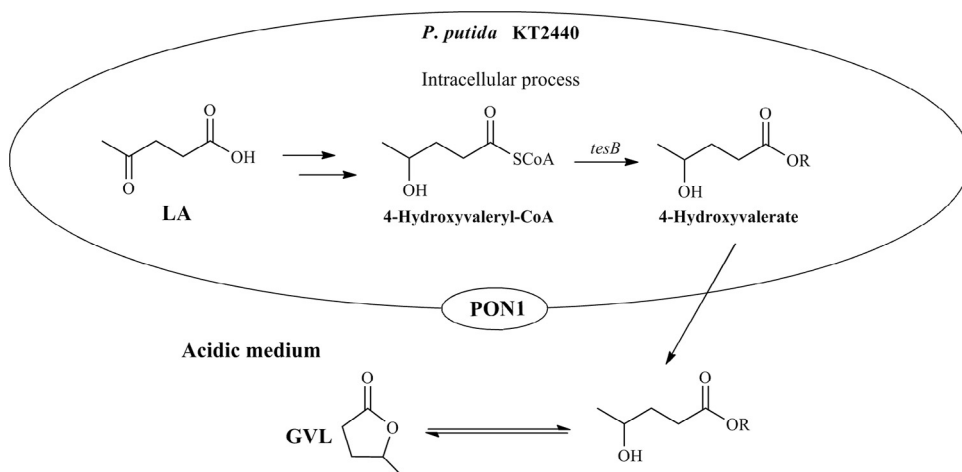


Fig. 59. Integrated bioprocessing system for the production of GVL (γ-valerolactone) from LA (levulinic acid). PON1: paraoxonase I.

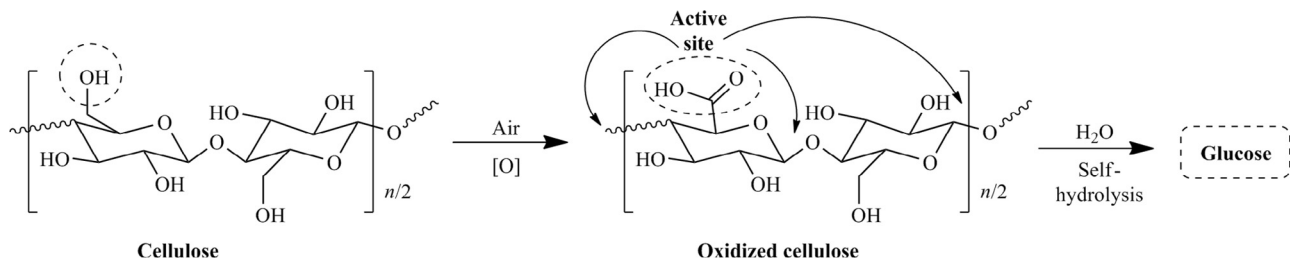


Fig. 60. *In-situ* catalytic hydrolysis of air-preoxidized-cellulose to glucose. Adapted with permission from Ref. 1032, Copyright © 2014 Royal Society of Chemistry.

suitable adjustment of active site distribution is one of the key issues in realizing high product selectivity. Several other factors like reaction media, diffusion limitations, and hydrophobic/hydrophilic environment of the solid catalysts are also important in determining the performance of catalytic systems [1004]. In these past few years, much attention has been paid to developing integrated catalytic processes for direct conversion of waste biomass, algae, and energy crops into desired compounds like food, proteins, sugars, polymers, platform chemicals, and liquid fuels. Nevertheless, solid-solid interactions between biomass and solid catalysts are necessary for the lignocellulose substrates to degrade. As such, coupling pretreatment processes with suitable auxiliaries like heating modes may boost biomass valorization.

6.1. Biomass pretreatment

Biomass pretreatment can breakdown or weaken the tight linkages among cell-wall components of lignocellulosic biomass, thus enhancing its degradation in subsequent upgrading stages [1005,1006]. Typical physical pretreatment methods are milling, chipping, grinding and thermal treatment that decrease particle size and crystallinity of biomass, but consume much energy [1007]. Biological pretreatment can enhance delignification and enzymatic digestibility of lignocellulosic substrates, while it is time-consuming and expensive [1008–1010]. For the case of chemical pretreatment, acid-catalyzed processes are capable of increasing the porosity of substrates through breakage of covalent bonds, hydrogen bonds, and van der Waals forces in biomass [1011,1012], while alkali can destroy linkages between lignin and carbohydrates by saponification of intermolecular ester bonds [1013]. However, these two processes are usually accompanied with equipment corrosion, formation of side products, and issues in the recovery and recycle of acids and bases.

6.1.1. Molten salt hydrates and dual metal salts

Molten salt hydrates including $ZnCl_2$, $CaCl_2$, and $LiCl$ are able to convert cellulose and hemicellulose into monosaccharides at mild conditions in water, wherein the strong interaction between the ionic species and hydroxyls promotes cleavage of the hydrogen-bonding network [1014]. Traditional solvents like cadoxen/water, DMSO/tetrabutylammonium fluoride, $NaOH$ /urea, and $LiCl/DMA$ can be used either for biomass pretreatment or directly for cellulose dissolution [1015–1018], but these solvents have several drawbacks such as volatility or generation of toxic gases and the need for multi-step and prolonged process operations. Due to their low vapor pressure and high solvation capacity, ILs have attracted much attention for the homogeneous processing of lignocelluloses [1019–1023]. Some challenges such as high solvent cost, limited toxicological data, and regeneration requirements of ILs still remain to be addressed before they can be widely used in biomass valorization processes [1024–1027].

Chemical pretreatment of biomass has been widely studied. In particular, some chemical agents like peroxides and high pressure

oxygen, which can dissolve lignin and loosen the remaining hemicellulose from insoluble crystalline cellulose, have gained increasing interest [1028–1030]. For example, sugarcane bagasse pretreated in combination of dual metal salts such as $MnSO_4 \cdot H_2O$ and ZnO with H_2O_2 allows cellulose recovery and delignification, thus enhancing the downstream ethanol production [1031].

6.1.2. Preoxidation–hydrolysis

Two-step preoxidation–hydrolysis strategy can transform cellulose into glucose (Fig. 60), in which the hydroxymethyl group is first oxidized to a carboxyl group by preoxidation treatment using air as an oxidant, and reduction of the polymerization degree of cellulose as well as the subsequent cellulose-to-glucose hydrolysis is realized with the *in-situ* generated acid sites [1032]. The combination of chemical or biological pretreatment with irradiation including microwave, ultrasound, gamma-ray, and electron beam can provide more efficient results than a single pretreatment method that only possesses limited specific functioning mode and intrinsic disadvantages. In this case, alkali pretreatment integrated with ultrasound or microwave is able to enhance the removal of lignin from lignocelluloses [1033–1035]. Similarly, ultrasound-promoted IL pretreatment [1036] and acid catalyzed steam treatment [1037] can increase the digestibility of lignocellulosic biomass. Other related techniques for treating a broad range of biomass feedstocks for the production of biofuels are provided in a review [1038].

6.2. Reaction media

Lignocellulosic biomass is mainly nonmelting solid material before decomposition and charring occur in thermocatalytic processes. As such, it is necessary to use a suitable reaction medium for controlled depolymerization of lignocelluloses, as well as for subsequent upgrading of solvent-soluble components and stabilization of products. Water is potentially a green and cheap solvent for the conversion of biomass to specific products although most biopolymers have low solubility in water [1039–1041]. However, water at high temperatures (ca. 250 °C) or at supercritical conditions (>375 °C, >22.1 MPa) can enhance the degradation of biopolymers despite selectivity is typically low [1042–1045]. For the dissolution, fractionation and valorization of lignocellulosic biomass components, ILs are considered to be promising candidates [1046–1049]. Particularly, metal chlorides in chloride-based ILs are robust catalytic systems for efficient conversion of cellulose, hemicelluloses, and lignin [1050]. In the case of transformation of sugars to furanic compounds in ILs, the presence of Cl^- ions can promote the formation of the 1,2-enediol from the acyclic form of sugars, resulting in a significant improvement of catalytic activity [1051,1052], while metal cations play role in sugar isomerizations to facilitate the succedent dehydration [1053]. Adding a certain amount of water into ILs-mediated reaction media seems to raise the hydrolysis efficiency of biopolymers, thus increasing the yields of furan-type compounds, but too much water promotes rehydration of products [1054–1056]. Likewise, the addition of DMSO lowers the high viscosity of ILs to facilitate the mass transfer between the catalyst and substrate without affecting solubility

of biopolymers [1057–1059], and also enhances the stability of mono-saccharides [1060] and products such as HMF and EMF [1061,1062]. However, other high boiling organic solvents such as DMA and *N,N*-dimethylformamide are not so selective for the desired products, and metal chlorides are required for DMA [1063–1065]. An NMR study showed that DMSO is likely to act as a catalyst besides a solvent for fructose-to-HMF dehydration at 150 °C via an intermediate (4*R,5R*)-4-hydroxy-5-hydroxymethyl-4,5-dihydrofuran-2-carbaldehyde [1066]. The functional IL 1-hydroxyethyl-3-methylimidazolium tetrafluoroborate used as a catalyst, rather than as solvent can directly promote glucose dehydration in DMSO, giving HMF in yields as high as 67% at 180 °C within 1 h [1067]. In contrast, SO₃H-functionalized ILs in water or ethanol will lead to the formation of LA or EL from sugars via HMF or EMF rehydration, respectively [1068–1070]. As an effective way to improve LA yields, metal salts like NaCl and KCl can interrupt the hydrogen bonding network of cellulose at high temperatures and pressures, thus facilitating hydrolysis, dehydration, and rehydration processes [1071]. Moreover, the subsequent esterification of LA with long chain alcohols can facilitate the separation of product for reuse of ILs [1072].

In the context, ILs and DMSO are two important reaction media to control or increase the selectivity of products especially furanic compounds. Nevertheless, ILs are still expensive and have limited applications in scale-up processes for biomass, while DMSO which has a high boiling point of 189 °C requires much energy in its separation from the products. As such, organic solvents with a moderate volatility seem to be promising alternatives [1073,1074]. In a monophasic THF–water system, increased reaction performance, for either furans or for LA is observed [1075–1078]. Notably, the increase of electrical conductivity of water to THF can be achieved with the dissolution of a small amount of ionic material like NaCl, rendering the formation of a biphasic system that will promote the in-situ separation of products like HMF and furfural from aqueous mixture [1079–1081]. Other organic solvents such as toluene, MIBK, acetonitrile, alcohols, and their mixtures have also been widely utilized as extractive phases [1082–1087]. Among them, the use of water-miscible solvents as organic phase is expected to dissolve HMF better than common non-water-miscible solvents. Biomass-derived solvents like MTHF, alkylphenols and GVL have been proposed as sustainable co-solvents or extraction solvents [1088–1090]. In particular, GVL with water used as the reaction medium can mediate the formation of monosaccharides, furfural, HMF, and even GVL directly from corresponding biomass derivatives [1091–1094]. It is interesting to note that solvent or catalyst may act as a reagent to directly influence product distributions. Considering LA upgrading in dimethylcarbonate as an example, K₂CO₃ can catalyze the formation of methyl levulinate through methylation, as well as the subsequent dimethylketal to produce dimethyl succinate at 200 °C after 4 h [1095]. In this catalytic process, dimethylcarbonate is not only a solvent but also a reagent under a basic condition. Either HCl or HBr as an acid catalyst may react with the desired product HMF to yield a more stable compound 5-chloromethylfurfural (CMF) or 5-bromomethylfurfural (BMF) [1096,1097].

6.3. Control of functional materials

Apart from selecting suitable biomass pretreatment and reaction media, design of an optimal catalytic system including the type of reactor and heating, as well as catalyst itself is needed to achieve the efficient and selective transformation of biomass into desired products [1098–1100]. From the preceding sections, it can be seen that much emphasis has been placed on the preparation and application of the multifunctional catalysts containing acid/base sites and/or metal particles for biomass processing. After modification with selected functional groups [1101–1103], the resulting multifunctional catalytic materials have many possibilities for efficiently converting biomass through:

- (1) combination of several types of active sites within a unique solid catalyst that are incompatible in a homogeneous phase;
- (2) combination of complex transformations in a single pot process;
- (3) implementation of cascade reactions and multistep conversions; and
- (4) elimination of intermediate separation and purification steps.

There are a number of common characteristics of the catalytic materials such as porosity and surface polarity important in catalyst design that discussed in the next sections.

6.3.1. Porosity

Porosity of solid materials directly affects surface area. Porous materials that have high surface areas with highly accessible active sites are crucial for substrate sorption and high activity. In general, most of the catalytic sites of porous materials are located inside the pore system, and the reaction selectivity can be controlled because of the size limitation between pores and reagents, products or transition-states [1104]. It seems that the best choice for catalytic processes of large molecules is mesoporous and macroporous materials [1105]. Unlike micropores which hinder the contact of substrate and active sites, if pores are too large to offer the steric restrictions, it will reduce the transition-state selectivity. Careful selection of functionalized materials and tailoring of the pore sizes are necessary to overcome the mass transfer limitations in the processing of polymeric species. Ordered porous materials such as metal oxides and carbonaceous materials with narrow pore size distribution show enhanced selectivity in some cases for sugar and lignin chemistry [1106,1107]. Metal oxides are not resistant to aqueous reaction media, while they are stable on carbon supports with exclusive micropores that appear to be unsuitable for conversion of polymeric biomolecules. Biomass-derived mesoporous carbons with well-defined pore architecture are preferable for applications in the catalytic conversion of biomass [1108,1109]. Modified zeolites and metal-organic frameworks (MOFs) with well-tailored pore sizes and active sites are promising candidates [1110–1113].

6.3.2. Surface polarity

Catalytic transformation of biomass via multiple steps may sequentially involve hydrophilic and hydrophobic molecules. Therefore, the proper adjustment of the adsorption and desorption processes between active sites and reagents is necessary to optimize the overall catalytic performance [1114]. Normally, the surface polarity of solid materials is affected by their own surface groups such as hydroxyl, carbonyl, carboxyl, alkyl, ether, and ionic species. In most cases, functional materials with hydrophilic surfaces can facilitate the access of the substrates bearing many hydroxyl groups and the desorption of the hydrophobic products, thus simultaneously optimizing catalytic activity and selectivity. Notably, water as a convenient dispersant for lignocellulosic materials [1115] can be generated in situ by dehydration and hydrogenolysis, while it is likely to cause poisoning of active sites [1116]. From the discussion above, solid functional catalysts with high water tolerance, adjusted surface polarity, and tailored porosity can enhance efficiency in transformations to a large degree. Paramagnetic and nano-sized materials have also been suggested as methods in catalyst design, however these materials are still in their infancy stage, regarding their uniformity, recyclability and accessibility [1117–1119].

6.4. Heating modes including microwave and ultrasound

In past decades, valorization of biomass using conventional heating modes, especially pyrolysis, has been extensively investigated. A wide range of feedstocks ranging from organic residues to biopolymers have been studied and simple scale-up for pyrolysis

is possible, while high energy consumption ($T > 600$ °C) and low quality products containing the formation of polycyclic aromatic hydrocarbons and CO₂ are issues that require urgent attention [1120]. In this respect, microwave irradiation can offer appropriate process control by its instantaneous heating mode with rapid and convenient start-up and shutdown, thus facilitating the adjustment of reaction parameters such as time, temperature and power for biomass processing [1121,1122]. In microwave processes, both thermal and non-thermal effects are often involved in processing of biomass. In the overall heating process, the rapid rise in temperature resulting from microwave irradiation causes the vaporization of intramolecular water contained in biomass, hence increasing the intra-particle pressure to loosen the structure of bio-polymers by expansion [1123]. The destructive effect of ultrasound causes generation of rapidly expanding and contracting water bubbles within the lignocellulosic units, leading to the compression and extension of the particles [1124]. Both microwave and ultrasound are promising auxiliaries for increasing the contact area between solid bifunctional catalysts and lignocellulosic substrates and still need to be studied for many reaction systems [1125,1126].

Apart from biomass pretreatment using microwave or ultrasound irradiation, the combination of hydrothermal conditions with microwave irradiation involving moderate temperatures of 100–200 °C has been demonstrated to be applicable to the transformation of many kinds of lignocellulosic biomass into molecules with a high degree of functionality [1127]. Xie et al. [1128] found that Ni/Al₂O₃ was effective for tar removal and for the fast microwave-assisted gasification of corn stover at 900 °C, in which syngas in a yield above 80% was produced. Little change in the structure of Ni/Al₂O₃ catalyst was detected with XRD (X-ray diffraction) even after being reused for three times, indicating the good stability of the nickel based catalyst to resist the deactivation caused by coking or sintering. With the assistance of char as microwave absorber, rapid heat-up to high temperatures within seconds can be achieved in the pyrolysis of oil palm biomass (shell and fibers) [1128]. In particular, the yields and rapid heating of microwave pyrolysis products such as bio-oils, chars, and gases are closely dependent on the ratio of biomass substrate to microwave absorber [1129]. Furthermore, biomass in large particle sizes is able to be used directly in microwave heating, hence saving the cost of grinding and moisture removal.

In the presence of activated carbon under the reaction conditions of temperature and retention time varied with a fixed microwave power input of 700 W, bio-oils with high concentrations of phenol (39%) and phenolics (67%) are obtained in the catalytic microwave pyrolysis of lignocellulosic biomass, while a high concentration of esters (42%) is obtained in a formic acid/ethanol reaction medium using Zn powder as catalyst [1130]. It is apparent that fossil fuel substitutes are likely to be generated from biomass pyrolysis assisted and enhanced with microwave irradiation [1131]. In parallel, the microwave-assisted conversion of carbohydrates to make a wide range of sugar-derivative scaffolds has been proposed [1132].

In comparison to conventional oil bath heating mode (100 °C, 10 h), microwave irradiation at a power of 400 W was able to significantly reduce the reaction time (8 min) with increased yields of reducing sugars (7% vs. 48%) in the hydrolysis of cellulose over a solid acid like HY(5) [1133]. To some extent, this microwave-assisted catalytic system is capable of simplifying the downstream processing. Related studies on the efficient and rapid production of LA and furans (e.g., HMF and furfural) from simple sugars and even lignocellulosic biomass with microwave well confirm the promotion effect of such the microwave heating mode [1134–1137]. Both microwave and ultrasound show enhanced activity on the direct transesterification of the as-harvested algae biomass [1138], which was illustrated to be realized by accelerating the disruption of the

microalgae cells to promote oil release [1139]. With respect to the production of biodiesel from as-prepared oils with the assistance of base, acid and/or enzyme functionalized catalysts, ultrasound can promote the mass transfer of immiscible reactants, thus shortening reaction time [1140,1141]. Nevertheless, ultrasound is less efficient for transesterification than magnetic stirring at a low methanol/oil ratio of <7/1 and temperature of 65 °C, but could tolerate excess methanol (>7/1) through vaporizing some of methanol caused by the effect of ultrasonic cavitation [1142]. Enzymatic hydrolysis of lignocelluloses for bioethanol production can be intensified with ultrasound [1143,1144], with biodiesel and bioethanol being favorably produced from different fractions of biomass.

7. Conclusions and future outlook

Bifunctional catalytic materials have been demonstrated to have outstanding potential in producing chemicals and biofuels efficiently and with high selectivity through multi-step conversions of biomass in one-pot processes. The role of basicity or Lewis acidity is mainly in sugar isomerization, as well as in upgrading of platform molecules through condensation and Diels–Aldol reactions. Simultaneous addition or presence of strong Bronsted acid sites accelerates the process of dehydration and oxygen removal. By introducing noble metals or transition metals into acid-initiated reactions, the oxygen removal capacity can be further enhanced through hydrolytic hydrogenation or hydrogenolysis, notably, decarboxylation reactions may occur at relatively high temperatures. On the contrary, some types of oxygenates can be produced from bio-based small molecules over base–metal dual-functional catalysts, or directly from biomass derivatives promoted by acid–metal dual active sites. However, incompatibility issues associated with competing reactions are often obstacles to increasing product selectivity. For example, the catalytic production of hydrogenated furanic compounds from mono-saccharides is likely to be realized through cascade dehydration–hydrogenation. In fact, hexitols such as sorbitol and mannitol are generally formed as dominant products through direct hydrogenation of sugars rather than HMF or furfural in-situ generated by water-removing processes. In this regards, several points affecting biomass valorization may be taken into consideration for the establishment of well-defined catalytic systems, associated with bifunctionality and relevant auxiliaries:

- (1) According to specific reactions, the rate of Bronsted/Lewis acid sites should be well adjusted so as to suppress the formation of humins or byproducts. Besides optimizing catalyst composition, the coverage of undesirable catalytic sites with other chemical species in a bond-binding mode could be applied as a technique in catalyst design.
- (2) The coexistence of acid and base sites can be realized by concurrently immobilizing them into a solid material. However, the acid/base strength and content are limited with this approach, owing to the possible neutralization caused by [H⁺] liberation or leaching. In this case, the choice of appropriate solvents is important to inhibit this phenomenon. Discrete distribution of base and acid sites into different fractions (e.g., core/shell) of a solid catalyst may be another way to address this issue.
- (3) The incompatibility of cascade reactions catalyzed by acid–metal bifunctional materials can be undoubtedly overcome by controlling the pressure of H₂/O₂, hydrophilicity and hydrophobicity of catalysts, size/dispersion of metals, acid type/strength, and reaction time/temperature. Therefore, the reaction parameters must be considered with the most important ones being applicable for selective transformation of biomass via multiple catalytic processes.

- (4) In general, base–metal dual-functional catalysts are highly active for oxidation reactions, but rarely employed for multi-catalytic processes. In view of their basicity, the coupling of biomass pretreatment with succedent hydrogenation should find many new applications.
- (5) Apart from organocatalysis, the valorization of biomass derivatives through chemoenzymatic and electrochemical catalysis has been developed in recent years. Within all of these catalytic systems, biomass pretreatment is a vital step to achieve high digestibility, productivity and practicality. It can be expected that there will be an increase in use of chemoenzymatic and electrochemical catalysis methods to understand catalyst functionality as well as to develop unique transformation systems for biomass valorization.
- (6) As to the general characteristics of catalysts, functionality in aqueous systems, recoverability and dispersibility can be enhanced by innovative material composites, such as the introduction of paramagnetic cores and nano-sizing of the materials. Improvements in catalyst uniformity, stability and recyclability are essential for bifunctional catalytic systems to realize industrial practicality.
- (7) Although bifunctional catalysts still require experimental trials for their effective development, computational methods (e.g., DFT and ab initio methods) can provide some guidance into the inclusion of catalytic sites and insight into preferred configurations or site arrangements.

In conclusion, bifunctional catalytic materials have many advantages over monofunctional catalysts in efficiency and in simplicity of operation. Bifunctional catalytic materials will play a vital role in the development of efficient biorefinery production systems although their large-scale application will depend on catalyst stability, product selectivity, and possibly the use of creative auxiliaries such as reactor design and heating modes. Many opportunities exist for developing bifunctional catalytic materials on both fundamental and applied levels. The numerous studies presented in this review serve as the foundation for realizing practical multi-catalytic processes with bifunctional catalytic materials.

Acknowledgments

This work was financially supported by Nanjing Agricultural University, the Chinese Academy of Sciences [135 program (XTBG-T02) and equipment R&D grant (YZ201260)], Natural Science Foundation of China (21576059), and Yunnan Provincial Government (Hundreds of High-Level Overseas Talents).

References

- [1] Kamm B, Gruber PR, Kamm M. Biorefineries-industrial processes and products: status quo and future directions. 1st ed. Weinheim: Wiley-VCH; 2006.
- [2] Dusselier M, Mascle M, Sels BF. Top chemical opportunities from carbohydrate biomass: a chemist's view of the biorefinery. *Top Curr Chem* 2014;353:1–40.
- [3] Yung MM, Jablonski WS, Magrini-Bair KA. Review of catalytic conditioning of biomass-derived syngas. *Energ Fuel* 2009;23:1874–87.
- [4] Fang Z. Noncatalytic fast hydrolysis of wood. *Bioresour Technol* 2011;102:3587–90.
- [5] Cheng YT, Jae J, Shi J, Fan W, Huber GW. Production of renewable aromatic compounds by catalytic fast pyrolysis of lignocellulosic biomass with bifunctional Ga/ZSM-5 catalysts. *Angew Chem Int Ed* 2012;51:1387–90.
- [6] Baliban RC, Elia JA, Floudas CA. Biomass to liquid transportation fuels (BTL) systems: process synthesis and global optimization framework. *Energ Environ Sci* 2013;6:267–87.
- [7] Zhang Q, Chang J, Wang T, Xu Y. Review of biomass pyrolysis oil properties and upgrading research. *Energy Conv Manage* 2007;48:87–92.
- [8] Jin F, Enomoto H. Rapid and highly selective conversion of biomass into value-added products in hydrothermal conditions: chemistry of acid/base-catalysed and oxidation reactions. *Energy Environ Sci* 2011;4:382–97.
- [9] Li H, Bhadury PS, Riisager A, Yang S. One-pot transformation of polysaccharides via multi-catalytic processes. *Catal Sci Technol* 2014;4:4138–68.
- [10] Guo N, Caratzoulas S, Doren DJ, Sandler SI, Vlachos DG. A perspective on the modeling of biomass processing. *Energy Environ Sci* 2012;5:6703–16.
- [11] Notestein JM, Katz A. Enhancing heterogeneous catalysis through cooperative hybrid organic–inorganic interfaces. *Chem Eur J* 2006;12:3954–65.
- [12] Margelefsky EL, Zeidan RK, Davis ME. Cooperative catalysis by silica-supported organic functional groups. *Chem Soc Rev* 2008;37:1118–26.
- [13] Diaz U, Brunelab D, Corma A. Catalysis using multifunctional organosiliceous hybrid materials. *Chem Soc Rev* 2013;42:4083–97.
- [14] Clement MJ, Corma A, Iborra S, Sabater MJ. Heterogeneous catalysis for tandem reactions. *ACS Catal* 2014;4:870–91.
- [15] Mehdi H, Fábos V, Tuba R, Bodor A, Mika LT, Horváth IT. Integration of homogeneous and heterogeneous catalytic processes for a multi-step conversion of biomass: from sucrose to levulinic acid, γ -valerolactone, 1,4-pentanediol, 2-methyl-tetrahydrofuran, and alkanes. *Top Catal* 2008;48:49–54.
- [16] Cai CM, Zhang T, Kumar R, Wyman CE. Integrated furfural production as a renewable fuel and chemical platform from lignocellulosic biomass. *J Chem Technol Biotechnol* 2014;89:2–10.
- [17] Shibasaki M, Kanai M, Matsunaga S, Kumagai N. Recent progress in asymmetric bifunctional catalysis using multimetallic systems. *Acc Chem Res* 2009;42:1117–27.
- [18] Allen AE, MacMillan DWC. Synergistic catalysis: a powerful synthetic strategy for new reaction development. *Chem Sci* 2012;3:633–58.
- [19] Wasilke JC, Obrey SJ, Baker RT, Bazan GC. Concurrent tandem catalysis. *Chem Rev* 2005;105:1001–20.
- [20] Lee JM, Na Y, Han H, Chang S. Cooperative multi-catalyst systems for one-pot organic transformations. *Chem Soc Rev* 2004;33:302–12.
- [21] Sheldon RA. Atom efficiency and catalysis in organic synthesis. *Pure Appl Chem* 2000;72:1233–46.
- [22] Manzer LE. Recent developments in the conversion of biomass to renewable fuels and chemicals. *Top Catal* 2010;53:1193–6.
- [23] Luo L, van der Voet E, Hupperts G. Biorefining of lignocellulosic feedstock – Technical, economic and environmental considerations. *Bioresour Technol* 2010;101:5023–32.
- [24] Deng W, Zhang Q, Wang Y. Polyoxometalates as efficient catalysts for transformations of cellulose into platform chemicals. *Dalton Trans* 2012;41:9817–31.
- [25] Agbor VB, Ciciek N, Sparling R, Berlin A, Levin DB. Biomass pretreatment: fundamentals toward application. *Biotechnol Adv* 2011;29:675–85.
- [26] Clement MJ, Corma A, Iborra S. Converting carbohydrates to bulk chemicals and fine chemicals over heterogeneous catalysts. *Green Chem* 2011;13:520–40.
- [27] Li H, Zhang Q, Yang S. Catalytic cascade dehydration-etherification of fructose into 5-ethoxymethylfurfural with SO_3H -functionalized polymers. *Int J Chem Eng* 2014;2014:1–7.
- [28] Nakagawa Y, Tamura M, Tomishige K. Catalytic reduction of biomass-derived furanic compounds with hydrogen. *ACS Catal* 2013;3:2655–68.
- [29] Siankevich S, Savoglidis G, Fei Z, Laurenczy G, Alexander DTL, Yan N, et al. A novel platinum nanocatalyst for the oxidation of 5-hydroxymethylfurfural into 2,5-furandicarboxylic acid under mild conditions. *J Catal* 2014;315:67–74.
- [30] Liguori F, Moreno-Marrodán C, Barbaro P. Environmentally friendly synthesis of γ -valerolactone by direct catalytic conversion of renewable sources. *ACS Catal* 2015;5:1882–94.
- [31] James OO, Maity S, Usman LA, Ajanaku KO, Ajani OO, Siyanbola TO, et al. Towards the conversion of carbohydrate biomass feedstocks to biofuels via hydroxymethylfurfural. *Energy Environ Sci* 2010;3:1833–50.
- [32] Huang X, Korányi TI, Boot MD, Hensen EJM. Catalytic depolymerization of lignin in supercritical ethanol. *ChemSusChem* 2014;7:2276–88.
- [33] Bahadar A, Khan MB. Progress in energy from microalgae: a review. *Renew Sust Energy Rev* 2013;27:128–48.
- [34] Lee SB, Jeong GT. Catalytic conversion of chitosan to 5-hydroxymethylfurfural under low temperature hydrothermal process. *Appl Biochem Biotechnol* 2015;176:1151–61.
- [35] Borges ME, Diaz L. Recent developments on heterogeneous catalysts for biodiesel production by oil esterification and transesterification reactions: a review. *Renew Sust Energy Rev* 2012;16:2839–49.
- [36] Tan HW, Abdul Aziz AR, Aroua MK. Glycerol production and its applications as a raw material: a review. *Renew Sust Energy Rev* 2013;27:1118–27.
- [37] Alonso DM, Bond JQ, Dumesic JA. Catalytic conversion of biomass to biofuels. *Green Chem* 2010;12:1493–513.
- [38] Chatterjee C, Pong F, Sen A. Chemical conversion pathways for carbohydrates. *Green Chem* 2015;17:40–71.
- [39] Kobayashi H, Fukuoka A. Synthesis and utilisation of sugar compounds derived from lignocellulosic biomass. *Green Chem* 2013;15:1740–63.
- [40] Montingelli ME, Tedesco S, Olabi AG. Biogas production from algal biomass: a review. *Renew Sust Energy Rev* 2015;43:961–72.
- [41] Stöcker M. Biofuels and biomass-to-liquid fuels in the biorefinery: catalytic conversion of lignocellulosic biomass using porous materials. *Angew Chem Int Ed* 2008;47:9200–11.
- [42] Xavier NM, Lucas SD, Rauter AP. Zeolites as efficient catalysts for key transformations in carbohydrate chemistry. *J Mol Catal A Chem* 2009;305:84–9.

- [43] Tekin K, Karagöz S, Bektaş S. A review of hydrothermal biomass processing. *Renew Sust Energy Rev* 2014;40:673–87.
- [44] Moraes ARC, Lopes AMDC, Bogel-Lukasik R. Carbon dioxide in biomass processing: contributions to the green biorefinery concept. *Chem Rev* 2015;115:3–27.
- [45] Spivey JJ, Egbebi A. Heterogeneous catalytic synthesis of ethanol from biomass-derived syngas. *Chem Soc Rev* 2007;36:1514–28.
- [46] Lin YC, Huber GW. The critical role of heterogeneous catalysis in lignocellulosic biomass conversion. *Energy Environ Sci* 2009;2:68–80.
- [47] Sani YM, Dual WMAW, Aziz ARA. Activity of solid acid catalysts for biodiesel production: a critical review. *Appl Catal A Gen* 2014;470:140–61.
- [48] Dutta S, De S, Saha B. Advances in biomass transformation to 5-hydroxymethylfurfural and mechanistic aspects. *Biomass Bioenergy* 2013;55:355–69.
- [49] Pham TN, Sooknoi T, Crossley SP, Resasco DE. Ketonization of carboxylic acids: mechanisms, catalysts, and implications for biomass conversion. *ACS Catal* 2013;3:2456–73.
- [50] Williams PJB, Laurens LML. Microalgae as biodiesel & biomass feedstocks: review & analysis of the biochemistry, energetics & economics. *Energy Environ Sci* 2010;3:554–90.
- [51] Abbasi T, Abbasi SA. Biomass energy and the environmental impacts associated with its production and utilization. *Renew Sust Energy Rev* 2010;14:919–37.
- [52] Delidovich I, Leonhard K, Palkovits R. Cellulose and hemicellulose valorisation: an integrated challenge of catalysis and reaction engineering. *Energy Environ Sci* 2014;7:2803–30.
- [53] Shimizu K, Satsuma A. Toward a rational control of solid acid catalysis for green synthesis and biomass conversion. *Energy Environ Sci* 2011;4:3140–53.
- [54] Hu L, Zhao G, Hao W, Tang X, Sun Y, Lin L, et al. Catalytic conversion of biomass-derived carbohydrates into fuels and chemicals via furanic aldehydes. *RSC Adv* 2012;2:11184–206.
- [55] Simmie JM, Würmel J. Harmonising production, properties and environmental consequences of liquid transport fuels from biomass—2,5-Dimethylfuran as a case study. *ChemSusChem* 2013;6:36–41.
- [56] Li H, Zhang Q, Bhadury PS, Yang S. Furan-type compounds from carbohydrates via heterogeneous catalysis. *Curr Org Chem* 2014;18:547–97.
- [57] Rosatella AA, Simeonov SP, Frade RFM, Carlos AMA. 5-Hydroxymethylfurfural (HMF) as a building block platform: biological properties, synthesis and synthetic applications. *Green Chem* 2011;13:754–93.
- [58] Gandini A. Furans as offspring of sugars and polysaccharides and progenitors of a family of remarkable polymers: a review of recent progress. *Polym Chem* 2010;1:245–51.
- [59] Qian XH. Mechanisms and energetics for Bronsted acid-catalyzed glucose condensation, dehydration and isomerization reactions. *Top Catal* 2012;55:218–26.
- [60] Qian XH. Mechanisms and energetics for acid catalyzed Beta-D-glucose conversion to 5-hydroxymethylfurfural. *J Phys Chem A* 2011;115:11740–8.
- [61] Qian XH, Nimlos MR, Davis M, Johnson DK, Himmel ME. Ab initio molecular dynamics simulations of Beta-D-glucose and Beta-D-xylene degradation mechanisms in acidic aqueous solution. *Carbohydr Res* 2005;340:2319–27.
- [62] Guan J, Cao Q, Guo X, Mu X. The mechanism of glucose conversion to 5-hydroxymethylfurfural catalyzed by metal chlorides in ionic liquid: a theoretical study. *Comp Theor Chem* 2011;963:453–62.
- [63] Pidko EA, Degirmenci V, Hensen EJM. On the mechanism of Lewis acid catalyzed glucose transformations in ionic liquids. *ChemCatChem* 2012;4:1263–71.
- [64] Bao Q, Qiao K, Tomida D, Yokoyama C. Preparation of 5-hydroxymethylfurfural by dehydration of fructose in the presence of acidic ionic liquid. *Catal Commun* 2008;9:1383–8.
- [65] van Dam HE, Kieboom APG, van Bekkum H. The conversion of fructose and glucose in acidic media: formation of hydroxymethylfurfural. *Starch/Stärke* 1986;38:95–101.
- [66] Bao Q, Qiao K, Tomida D, Yokoyama C. 1-Methylimidazolium chlorosulfate ([HMIm]SO₃Cl): a novel ionic liquid with dual Bronsted–Lewis acidity. *Chem Lett* 2010;39:728–9.
- [67] Wrigstedt P, Keskküla J, Leskelä M, Repo T. The role of salts and Bronsted acids in Lewis acid-catalyzed aqueous-phase glucose dehydration to 5-hydroxymethylfurfural. *ChemCatChem* 2015;7:501–7.
- [68] Choudhary V, Mushrif SH, Ho C, Anderko A, Nikolakis V, Marinkovic NS, et al. Insights into the interplay of Lewis and Bronsted acid catalysts in glucose and fructose conversion to 5-(hydroxymethyl)furfural and levulinic acid in aqueous media. *J Am Chem Soc* 2013;135:3997–4006.
- [69] van Putten RJ, van der Waal JC, de Jong E, Rasrendra CB, Heeres HJ, de Vries JG. Hydroxymethylfurfural, a versatile platform chemical made from renewable resources. *Chem Rev* 2013;113:1499–597.
- [70] Zakrzewska ME, Bogel-Lukasik E, Bogel-Lukasik R. Ionic liquid mediated formation of 5-hydroxymethylfurfural: a promising biomass derived building block. *Chem Rev* 2011;111:397–417.
- [71] Li H, Chang F, Zhang Y, Hu D, Jin L, Song B, et al. Recent progress towards transition metal-catalyzed direct conversion of cellulose to 5-hydroxymethylfurfural. *Curr Catal* 2012;1:221–32.
- [72] Zhao HB, Holliday JE, Brown H, Zhang ZC. Metal chlorides in ionic liquid solvents convert sugars to 5-hydroxymethylfurfural. *Science* 2007;316:1597–600.
- [73] Su Y, Brown HM, Huang X, Zhou X, Amonette JE, Zhang ZC. Single-step conversion of cellulose to 5-hydroxymethylfurfural (HMF), a versatile platform chemical. *Appl Catal A Gen* 2009;361:117–22.
- [74] Binder JB, Raines RT. Simple chemical transformation of lignocellulosic biomass into furans for fuels and chemicals. *J Am Chem Soc* 2009;131:1979–85.
- [75] Yi YB, Lee JW, Choi YH, Park SM, Chung CH. Simple process for production of hydroxymethylfurfural from raw biomasses of girasol and potato tubers. *Biomass Bioenergy* 2012;39:484–8.
- [76] Hu L, Sun Y, Lin L, Liu S. Catalytic conversion of glucose into 5-hydroxymethylfurfural using double catalysts in ionic liquid. *J Taiwan Inst Chem Eng* 2012;43:718–23.
- [77] Yang Y, Hu C, Abu-Omar MM. The effect of hydrochloric acid on the conversion of glucose to 5-hydroxymethylfurfural in AlCl₃–H₂O/THF biphasic medium. *J Mol Catal A Chem* 2013;376:98–102.
- [78] Pagán-Torres YJ, Wang T, Gallo JMR, Shanks BH, Dumesic JA. Production of 5-hydroxymethylfurfural from glucose using a combination of Lewis and Bronsted acid catalysts in water in a biphasic reactor with an alkylphenol solvent. *ACS Catal* 2012;2:930–4.
- [79] Tao F, Song H, Yang J, Chou L. Catalytic hydrolysis of cellulose into furans in MnCl₂-ionic liquid system. *Carbohydr Polym* 2011;85:363–8.
- [80] Zhang ZH, Wang Q, Xie HB, Liu WJ, Zhao ZB. Catalytic conversion of carbohydrates into 5-hydroxymethylfurfural by germanium(IV) chloride in ionic liquids. *ChemSusChem* 2011;4:131–8.
- [81] Tao FR, Song HL, Chou LJ. Hydrolysis of cellulose by using catalytic amounts of FeCl₂ in ionic liquids. *ChemSusChem* 2010;3:1298–303.
- [82] Tao FT, Song HL, Chou LJ. Catalytic conversion of cellulose to chemicals in ionic liquid. *Carbohydr Res* 2011;346:58–63.
- [83] Zhou L, Liang R, Ma Z, Wu T, Wu Y. Conversion of cellulose to HMF in ionic liquid catalyzed by bifunctional ionic liquids. *Bioresour Technol* 2013;129:450–5.
- [84] Li H, Zhang Q, Liu X, Chang F, Hu D, Zhang Y, et al. InCl₃-ionic liquid catalytic system for efficient and selective conversion of cellulose into 5-hydroxymethylfurfural. *RSC Adv* 2013;3:3648–54.
- [85] Wu L, Song J, Zhang B, Zhou B, Zhou H, Fan H, et al. Very efficient conversion of glucose to 5-hydroxymethylfurfural in DBU-based ionic liquids with benzenesulfonate anion. *Green Chem* 2014;16:3935–41.
- [86] Hu Z, Liu B, Zhang Z, Chen L. Conversion of carbohydrates into 5-hydroxymethylfurfural catalyzed by acidic ionic liquids in dimethyl sulfoxide. *Ind Crops Prod* 2013;50:264–9.
- [87] Liu DJ, Chen EYX. Polymeric ionic liquid (PIL)-supported recyclable catalysts for biomass conversion into HMF. *Biomass Bioenergy* 2013;48:181–90.
- [88] Li H, Zhang Q, Liu X, Chang F, Zhang Y, Xue W, et al. Immobilizing Cr³⁺ with SO₃H-functionalized solid polymeric ionic liquids as efficient and reusable catalysts for selective transformation of carbohydrates into 5-hydroxymethylfurfural. *Bioresour Technol* 2013;144:21–7.
- [89] Degirmenci V, Pidko EA, Magusin PCMM, Hensen EJM. Towards a selective heterogeneous catalyst for glucose dehydration to 5-hydroxymethylfurfural in water: CrCl₂ catalysis in a thin immobilized ionic liquid layer. *ChemCatChem* 2011;3:969–72.
- [90] Crisci AJ, Tucker MH, Dumesic JA, Scott SL. Bifunctional solid catalysts for the selective conversion of fructose to 5-hydroxymethylfurfural. *Top Catal* 2010;53:1185–92.
- [91] Liu H, Wang H, Li Y, Yang W, Song C, Li H, et al. Glucose dehydration to 5-hydroxymethylfurfural in ionic liquid over Cr³⁺-modified ion exchange resin. *RSC Adv* 2015;5:9290–7.
- [92] Lee YY, Wu KCW. Conversion and kinetics study of fructose-to-5-hydroxymethylfurfural (HMF) using sulfonic and ionic liquid groups bi-functionalized mesoporous silica nanoparticles as recyclable solid catalysts in DMSO systems. *Phys Chem Chem Phys* 2012;14:13914–17.
- [93] Zhang Z, Zhao ZK. Production of 5-hydroxymethylfurfural from glucose catalyzed by hydroxyapatite supported chromium chloride. *Bioresour Technol* 2011;102:3970–2.
- [94] Wang J, Ren J, Liu X, Xi J, Xia Q, Zu Y, et al. Direct conversion of carbohydrates to 5-hydroxymethylfurfural using Sn-Mont catalyst. *Green Chem* 2012;14:2506–12.
- [95] Zhang Y, Pan J, Gan M, Ou H, Yan Y, Shi W, et al. Acid-chromic chloride functionalized natural clay particles for enhanced conversion of one-pot cellulose to 5-hydroxymethylfurfural in ionic liquids. *RSC Adv* 2014;4:11664–72.
- [96] Charoenlimkun A, Champreda V, Shotipruk A, Laosiripojana N. Reactions of C₅ and C₆-sugars, cellulose, and lignocellulose under hot compressed water (HCW) in the presence of heterogeneous acid catalysts. *Fuel* 2010;89:2873–80.
- [97] Joo JB, Vu A, Zhang Q, Dahl M, Gu M, Zaera F, et al. A sulfated ZrO₂ hollow nanostructure as an acid catalyst in the dehydration of fructose to 5-hydroxymethylfurfural. *ChemSusChem* 2013;6:2001–8.
- [98] Dutta A, Patra AK, Dutta S, Saha B, Bhaumik A. Hierarchically porous titanium phosphate nanoparticles: an efficient solid acid catalyst for microwave assisted conversion of biomass and carbohydrates into 5-hydroxymethylfurfural. *J Mater Chem* 2012;22:14094–100.
- [99] Kourieh R, Rakic V, Bennici S, Auroux A. Relation between surface acidity and reactivity in fructose conversion into 5-HMF using tungstated zirconia catalysts. *Catal Commun* 2013;30:5–13.

- [100] Li H, Zhang Q, Liu J, Liu X, Chang F, Liu Y, et al. Selective transformation of carbohydrates into HMF promoted by carboxylic acids modified ZrMo mixed oxides. *Biomass Conv Bioref* 2014;4:59–66.
- [101] De S, Dutta S, Patra AK, Bhawik A, Saha B. Self-assembly of mesoporous TiO₂ nanospheres via aspartic acid templating pathway and its catalytic application for 5-hydroxymethyl-furfural synthesis. *J Mater Chem* 2011;21:17505–10.
- [102] Dutta S, De S, Patra AK, Sasidharan M, Bhawik A, Saha B. Microwave assisted rapid conversion of carbohydrates into 5-hydroxymethylfurfural catalyzed by mesoporous TiO₂ nanoparticles. *Appl Catal A Gen* 2011;409:10:133–9.
- [103] Kuo IJ, Suzuki N, Yamauchi Y, Wu KCW. Cellulose-to-HMF conversion using crystalline mesoporous titania and zirconia nanocatalysts in ionic liquid systems. *RSC Adv* 2013;3:2028–34.
- [104] Atanda L, Mukundan S, Shrotri A, Ma Q, Beltramini J. Catalytic conversion of glucose to 5-hydroxymethyl-furfural with a phosphated TiO₂ catalyst. *ChemCatChem* 2015;7:781–90.
- [105] Armaroli T, Busca G, Carlini C, Giuttari M, Galletti AMR, Sbrana G. Acid sites characterization of niobium phosphate catalysts and their activity in fructose dehydration to 5-hydroxymethyl-2-furaldehyde. *J Mol Catal A Chem* 2000;151:233–43.
- [106] Zhang Y, Wang J, Ren J, Liu X, Li X, Xia Y, et al. Mesoporous niobium phosphate: an excellent solid acid for the dehydration of fructose to 5-hydroxymethylfurfural in water. *Catal Sci Technol* 2012;2:2485–91.
- [107] Nakajima K, Baba Y, Noma R, Kitano M, Kondo JN, Hayashi S, et al. Nb₂O₅/nH₂O as a heterogeneous catalyst with water-tolerant Lewis acid sites. *J Am Chem Soc* 2011;133:4224–7.
- [108] Yang F, Liu Q, Bai X, Du Y. Conversion of biomass into 5-hydroxymethylfurfural using solid acid catalyst. *Bioresour Technol* 2011;102:3424–9.
- [109] Jiménez-Morales I, Moreno-Recio M, Santamaría-González J, Maireles-Torres P, Jiménez-López A. Mesoporous tantalum oxide as catalyst for dehydration of glucose to 5-hydroxymethylfurfural. *Appl Catal B: Environ* 2014;154:5:190–6.
- [110] Yang F, Liu Q, Yue M, Bai X, Du Y. Tantalum compounds as heterogeneous catalysts for saccharide dehydration to 5-hydroxymethylfurfural. *Chem Commun* 2011;47:4469–71.
- [111] Jiménez-Morales I, Teckchandani-Ortiz A, Santamaría-González J, Maireles-Torres P, Jiménez-López A. Selective dehydration of glucose to 5-hydroxymethylfurfural on acidic mesoporous tantalum phosphate. *Appl Catal B: Environ* 2014;144:22–8.
- [112] Yamaguchi K, Sakurada T, Ogasawara Y, Mizuno N. Tin-tungsten mixed oxide as efficient heterogeneous catalyst for conversion of saccharides to furan derivatives. *Chem Lett* 2011;40:542–3.
- [113] Behera GC, Parida KM. One-pot synthesis of 5-hydroxymethylfurfural: a significant biomass conversion over tin-promoted vanadium phosphate (Sn-VPO) catalyst. *Catal Sci Technol* 2013;3:3278–85.
- [114] Daorattanachai P, Khemthong P, Viriya-empikul N, Laosiripojana N, Faungnawakij K. Conversion of fructose, glucose, and cellulose to 5-hydroxymethylfurfural by alkaline earth phosphate catalysts in hot compressed water. *Carbohydr Res* 2012;363:58–61.
- [115] Jiménez-Morales I, Santamaría-González J, Jiménez-López A, Maireles-Torres P. Glucose dehydration to 5-hydroxymethylfurfural on zirconium containing mesoporous MCM-41 silica catalysts. *Fuel* 2014;118:265–71.
- [116] Jiménez-Morales I, Moreno-Recio M, Santamaría-González J, Maireles-Torres P, Jiménez-López A. Production of 5-hydroxymethylfurfural from glucose using aluminium doped MCM-41 silica as acid catalyst. *Appl Catal B: Environ* 2015;164:70–6.
- [117] Fan C, Guan H, Zhang H, Wang J, Wang S, Wang X. Conversion of fructose and glucose into 5-hydroxymethylfurfural catalyzed by a solid heteropolyacid salt. *Biomass Bioenergy* 2011;35:2659–65.
- [118] JadHAV AH, Kim H, Hwang IT. An efficient and heterogeneous recyclable silicotungstic acid with modified acid sites as a catalyst for conversion of fructose and sucrose into 5-hydroxymethylfurfural in superheated water. *Bioresour Technol* 2013;132:342–50.
- [119] Zhao Q, Wang L, Zhao S, Wang X, Wang S. High selective production of 5-hydroxymethylfurfural from fructose by a solid heteropolyacid catalyst. *Fuel* 2011;90:2289–93.
- [120] Zhao S, Cheng M, Li J, Tian J, Wang X. One pot production of 5-hydroxymethylfurfural with high yield from cellulose by a Bronsted-Lewis-surfactant-combined heteropolyacid catalyst. *Chem Commun* 2011;47:2176–8.
- [121] Zheng H, Sun Z, Yi X, Wang S, Li J, Wang X, et al. A water-tolerant C₁₆H₃PW₁₁CrO₃₉ catalyst for the efficient conversion of monosaccharides into 5-hydroxymethylfurfural in a micellar system. *RSC Adv* 2013;3:23051–6.
- [122] Otomo R, Yokoi T, Kondo JN, Tatsumi T. Dealuminated Beta zeolite as effective bifunctional catalyst for direct transformation of glucose to 5-hydroxymethylfurfural. *Appl Catal A Gen* 2014;470:318–26.
- [123] Hu L, Wu Z, Xu J, Sun Y, Lin L, Liu S. Zeolite-promoted transformation of glucose into 5-hydroxymethylfurfural in ionic liquid. *Chem Eng J* 2014;244:137–44.
- [124] Nandiwalé KY, Galande ND, Thakur P, Sawant SD, Zambre VP, Bokade VV. One-pot synthesis of 5-hydroxymethylfurfural by cellulose hydrolysis over highly active bimodal micro/mesoporous HZSM5 catalyst. *ACS Sust Chem Eng* 2014;2:1928–32.
- [125] Nikolla E, Román-Leshkov Y, Moliner M, Davis ME. "One-pot" synthesis of 5-(hydroxymethyl)furfural from carbohydrates using tin-Beta zeolite. *ACS Catal* 2011;1:408–10.
- [126] Gallo JMR, Alonso DM, Mellmer MA, Dumesic JA. Production and upgrading of 5-hydroxymethylfurfural using heterogeneous catalysts and biomass-derived solvents. *Green Chem* 2013;15:85–90.
- [127] Crisci AJ, Tucker MH, Lee MY, Jang SG, Dumesic JA, Scott SL. Acid-functionalized SBA-15-type silica catalysts for carbohydrate dehydration. *ACS Catal* 2011;1:719–28.
- [128] Li Y, Liu H, Song CH, Gu XM, Li HM, Zhu WS, et al. The dehydration of fructose to 5-hydroxymethylfurfural efficiently catalyzed by acidic ion-exchange resin in ionic liquid. *Bioresour Technol* 2013;133:347–53.
- [129] Gao H, Peng Y, Pan J, Zeng J, Song C, Zhang Y, et al. Synthesis and evaluation of macroporous polymerized solid acid derived from pickering HIPEs for catalyzing cellulose into 5-hydroxymethylfurfural in an ionic liquid. *RSC Adv* 2014;4:43029–38.
- [130] Zhang Y, Pan J, Yan Y, Shi W, Yu L. Synthesis and evaluation of stable polymeric solid acid based on halloysite nanotubes for conversion of one-pot cellulose to 5-hydroxymethylfurfural. *RSC Adv* 2014;4:23797–806.
- [131] Wang J, Xu W, Ren J, Liu X, Lu G, Wang Y. Efficient catalytic conversion of fructose into hydroxymethylfurfural by a novel carbon-based solid acid. *Green Chem* 2011;13:2678–81.
- [132] Hu L, Zhao G, Tang X, Wu Z, Xu J, Lin L, et al. Catalytic conversion of carbohydrates into 5-hydroxymethylfurfural over cellulose-derived carbonaceous catalyst in ionic liquid. *Bioresour Technol* 2013;148:501–7.
- [133] Kuo CH, Poyraz AS, Jin L, Meng Y, Pahalagedara L, Chen SY, et al. Heterogeneous acidic TiO₂ nanoparticles for efficient conversion of biomass derived carbohydrates. *Green Chem* 2014;16:785–91.
- [134] Ordovsky VV, van der Schaaf J, Schouten JC, Nijhuis TA. Glucose dehydration to 5-hydroxymethylfurfural in a biphasic system over solid acid foams. *ChemSusChem* 2013;6:1697–707.
- [135] Chambon F, Rataboul F, Pinel C, Cabiac A, Guillou E, Essayem N. Cellulose hydrothermal conversion promoted by heterogeneous Bronsted and Lewis acids: remarkable efficiency of solid Lewis acids to produce lactic acid. *Appl Catal B: Environ* 2011;105:171–81.
- [136] Kourieh R, Bennici S, Marzo M, Gervasini A, Auroux A. Investigation of the WO₃/ZrO₂ surface acidic properties for the aqueous hydrolysis of cellobiose. *Catal Commun* 2012;19:119–26.
- [137] Carlini C, Giuttari M, Galletti AMR, Sbrana G, Armaroli T, Busca G. Selective saccharides dehydration to 5-hydroxymethyl-2-furaldehyde by heterogeneous niobium catalysts. *Appl Catal A Gen* 1999;183:295–302.
- [138] Carniti P, Gervasini A, Biella S, Auroux A. Niobic acid and niobium phosphate as highly acidic viable catalysts in aqueous medium: fructose dehydration reaction. *Catal Today* 2006;118:373–8.
- [139] Antal JM, Mok WSL. Mechanism of formation of 5-(hydroxymethyl)-2-furaldehyde from D-fructose and sucrose. *Carbohydr Res* 1990;199:91–109.
- [140] Ordovsky VV, Sushkevich VL, Schouten JC, van der Schaaf J, Nijhuis TA. Glucose dehydration to 5-hydroxymethylfurfural over phosphate catalysts. *J Catal* 2013;300:37–46.
- [141] Ogasawara Y, Uchida S, Yamaguchi K, Mizuno N. A tin-tungsten mixed oxide as an efficient heterogeneous catalyst for C–C bond-forming reactions. *Chem Eur J* 2009;15:4343–9.
- [142] Jin X, Oishi T, Yamaguchi K, Mizuno N. Heterogeneously catalyzed efficient hydration of alkynes to ketones by tin-tungsten mixed oxides. *Chem Eur J* 2011;17:1261–7.
- [143] Ranoux A, Djanashvili K, Arends IWCE, Hanefeld U. B-TUD-1: a versatile mesoporous catalyst. *RSC Adv* 2013;3:21524–34.
- [144] Baba T, Watanabe H, Ono Y. Generation of acidic sites in metal salts of heteropolyacids. *J Phys Chem* 1983;87:2406–11.
- [145] Shimizu K, Uozumi R, Satsuma A. Enhanced production of hydroxymethylfurfural from fructose with solid acid catalysts by simple water removal methods. *Catal Commun* 2009;10:1849–53.
- [146] Qu Y, Huang C, Zhang J, Chen B. Efficient dehydration of fructose to 5-hydroxymethylfurfural catalyzed by a recyclable sulfonated organic heteropolyacid salt. *Bioresour Technol* 2012;106:170–2.
- [147] Zhang Y, Degirmenci V, Li C, Hensen EJM. Phosphotungstic acid encapsulated in metal-organic framework as catalysts for carbohydrate dehydration to 5-hydroxymethylfurfural. *ChemSusChem* 2011;4:59–64.
- [148] Lanzafame P, Temi DM, Perathoner S, Spadaro AN, Centi G. Direct conversion of cellulose to glucose and valuable intermediates in mild reaction conditions over solid acid catalysts. *Catal Today* 2012;179:178–84.
- [149] Taarning E, Osmundsen CM, Yang X, Voss B, Andersen SI, Christensen CH. Zeolite-catalyzed biomass conversion to fuels and chemicals. *Energy Environ Sci* 2011;4:793–804.
- [150] Tan MX, Zhao L, Zhang Y. Production of 5-hydroxymethyl furfural from cellulose in CrCl₃/Zeolite/BMIMCl system. *Biomass Bioenergy* 2011;35:1367–70.
- [151] JadHAV H, Taarning E, Pedersen CM, Bols M. Conversion of D-glucose into 5-hydroxymethylfurfural (HMF) using zeolite in [Bmim]Cl or tetrabutylammonium chloride (TBAC)/CrCl₃. *Tetrahedron Lett* 2012;53:983–5.
- [152] Roman-Leshkov Y, Moliner M, Labinger JA, Davis ME. Mechanism of glucose isomerization using a solid Lewis acid catalyst in water. *Angew Chem Int Ed* 2010;49:8954–7.
- [153] Roy S, Bakhtutsky K, Mahmoud E, Lobo RF, Gorte RJ. Probing Lewis acid sites in Sn-Beta zeolite. *ACS Catal* 2013;3:573–80.

- [154] Bermejo-Deval R, Orazov M, Gounder R, Hwang SJ, Davis ME. Active sites in Sn-Beta for glucose isomerization to fructose and epimerization to mannose. *ACS Catal* 2014;4:2288–97.
- [155] Lange JP, van der Heide E, van Buijtenen J, Price R. Furfural – A promising platform for lignocellulosic biofuels. *ChemSusChem* 2012;5:150–66.
- [156] Aycock DF. Solvent applications of 2-methyltetrahydrofuran in organometallic and biphasic reactions. *Org Process Res Dev* 2007;11:156–9.
- [157] Gurbuz El, Wettstein SG, Dumesic JA. Conversion of hemicellulose to furfural and levulinic acid using biphasic reactors with alkylphenol solvents. *ChemSusChem* 2012;5:383–7.
- [158] Choudhary V, Pinar AB, Sandler SI, Vlachos DG, Lobo RF. Xylose isomerization to xylulose and its dehydration to furfural in aqueous media. *ACS Catal* 2011;1:1724–8.
- [159] Antal MJ Jr, Leesomboon T, Mok WS, Richards GN. Mechanism of formation of 2-furaldehyde from D-xylose. *Carbohydr Res* 1991;217:71–85.
- [160] De Jong W, Marcotullio G. Overview of biorefineries based on co-production of furfural, existing concepts and novel developments. *Int J Chem React Eng* 2010;8:1–27.
- [161] Choudhary V, Caratzoulas S, Vlachos DG. Insights into the isomerization of xylose to xylulose and lyxose by a Lewis acid catalyst. *Carbohydr Res* 2013;368:89–95.
- [162] Choudhary V, Sandler SI, Vlachos DG. Conversion of xylose to furfural using Lewis and Bronsted acid catalysts in aqueous media. *ACS Catal* 2012;2:2022–8.
- [163] Zhang J, Zhuang J, Lin L, Liu S, Zhang Z. Conversion of D-xylose into furfural with mesoporous molecular sieve MCM-41 as catalyst and butanol as the extraction phase. *Biomass Bioenergy* 2012;39:73–7.
- [164] Dias AS, Lima S, Brandão P, Pillinger M, Rocha J, Valente AA. Liquid-phase dehydration of D-xylose over microporous and mesoporous niobium silicates. *Catal Lett* 2006;108:179–86.
- [165] García-Sancho C, Sádaba I, Moreno-Tost R, Mérida-Robles J, Santamaría-González J, López-Granados M, et al. Dehydration of xylose to furfural over MCM-41-supported niobium-oxide catalysts. *ChemSusChem* 2013;6:635–42.
- [166] García-Sancho C, Agirrezabal-Telleria I, Güemez MB, Maireles-Torres P. Dehydration of D-xylose to furfural using different supported niobia catalysts. *Appl Catal B: Environ* 2014;152:3–10.
- [167] Antunes MM, Lima S, Fernandes A, Pillinger M, Ribeiro MF, Valente AA. Aqueous-phase dehydration of xylose to furfural in the presence of MCM-22 and ITQ-2 solid acid catalysts. *Appl Catal A Gen* 2012;417:8:243–52.
- [168] Lima S, Antunes MM, Fernandes A, Pillinger M, Ribeiro MF, Valente AA. Catalytic cyclodehydration of xylose to furfural in the presence of zeolite H-Beta and a micro/mesoporous Beta/TUD-1 composite material. *Appl Catal A Gen* 2010;388:141–8.
- [169] Lima S, Pillinger M, Valente AA. Dehydration of D-xylose into furfural catalysed by solid acids derived from the layered zeolite Nu-6(1). *Catal Commun* 2008;9:2144–8.
- [170] Gürbüz El, Gallo JMR, Alonso DM, Wettstein SG, Lim WY, Dumesic JA. Conversion of hemicellulose into furfural using solid acid catalysts in γ-valerolactone. *Angew Chem Int Ed* 2013;52:1270–4.
- [171] Lima S, Fernandes A, Antunes MM, Pillinger M, Ribeiro F, Valente AA. Dehydration of xylose into furfural in the presence of crystalline microporous silicoaluminophosphates. *Catal Lett* 2010;135:41–7.
- [172] Bhaumik P, Dhepe PL. Efficient, stable, and reusable silicoaluminophosphate for the one-pot production of furfural from hemicelluloses. *ACS Catal* 2013;3:2299–303.
- [173] Dias AS, Lima S, Carriazo D, Rives V, Pillinger M, Valente AA. Exfoliated titanate, niobate and titanoniobate nanosheets as solid acid catalysts for the liquid-phase dehydration of D-xylose into furfural. *J Catal* 2006;244:230–7.
- [174] Chareonlimkun A, Champreda V, Shotipruk A, Laosiripojana N. Catalytic conversion of sugarcane bagasse, rice husk and corncob in the presence of TiO₂, ZrO₂ and mixed-oxide TiO₂–ZrO₂ under hot compressed water (HCW) condition. *Bioresour Technol* 2010;101:4179–86.
- [175] Dias AS, Lima S, Pillinger M, Valente AA. Modified versions of sulfated zirconia as catalysts for the conversion of xylose to furfural. *Catal Lett* 2007;114:151–60.
- [176] Li H, Deng A, Ren J, Liu C, Lu Q, Zhong L, et al. Catalytic hydrothermal pretreatment of corncob into xylose and furfural via solid acid catalyst. *Bioresour Technol* 2014;158:313–20.
- [177] Antunes MM, Lima S, Fernandes A, Candeias J, Pillinger M, Rocha SM, et al. Catalytic dehydration of D-xylose to 2-furfuraldehyde in the presence of Zr-(W,Al) mixed oxides. Tracing by-products using two-dimensional gas chromatography-time-of-flight mass spectrometry. *Catal Today* 2012;195:127–35.
- [178] Sádaba I, Lima S, Valente AA, Granados ML. Catalytic dehydration of xylose to furfural: vanadyl pyrophosphate as source of active soluble species. *Carbohydr Res* 2011;346:2785–91.
- [179] Shi X, Wu Y, Li P, Yi H, Yang M, Wang G. Catalytic conversion of xylose to furfural over the solid acid SO₄²⁻/ZrO₂–Al₂O₃/SBA-15 catalysts. *Carbohydr Res* 2011;346:480–7.
- [180] Agirrezabal-Telleria I, Hemmann F, Jäger C, Arias PL, Kemnitz E. Functionalized partially hydroxylated MgF₂ as catalysts for the dehydration of D-xylose to furfural. *J Catal* 2013;305:81–91.
- [181] Weingarten R, Tompsett GA, Conner WC Jr, Huber GW. Design of solid acid catalysts for aqueous-phase dehydration of carbohydrates: the role of Lewis and Bronsted acid sites. *J Catal* 2011;279:174–82.
- [182] Zhang L, Yu H, Wang P. Solid acids as catalysts for the conversion of D-xylose, xylan and lignocellulosics into furfural in ionic liquid. *Bioresour Technol* 2013;136:513–21.
- [183] Bamufleh HS, Alhamed YA, Daous MA. Furfural from midribs of date-palm trees by sulfuric acid hydrolysis. *Ind Crops Prod* 2013;42:421–8.
- [184] Agirrezabal-Telleria I, Larreategui A, Requies J, Güemez MB, Arias PL. Furfural production from xylose using sulfonic ion-exchange resins (Amberlyst) and simultaneous stripping with nitrogen. *Bioresour Technol* 2011;102:7478–85.
- [185] Dias AS, Pillinger M, Valente AA. Dehydration of xylose into furfural over micro-mesoporous sulfonic acid catalysts. *J Catal* 2005;229:414–23.
- [186] Lam E, Chong JH, Majid E, Liu Y, Hrapovic S, Leung ACW, et al. Carbocatalytic dehydration of xylose to furfural in water. *Carbon* 2012;50:1033–43.
- [187] Hua D, Li PP, Wu Y, Chen Y, Yang M, Dang J, et al. Preparation of solid acid catalyst packing AAO/SBA-15-SO₃H and application for dehydration of xylose to furfural. *J Ind Eng Chem* 2013;19:1395–9.
- [188] Agirrezabal-Telleria I, Requies J, Güemez MB, Arias PL. Dehydration of D-xylose to furfural using selective and hydrothermally stable arennesulfonic SBA-15 catalysts. *Appl Catal B: Environ* 2014;145:34–42.
- [189] Agirrezabal-Telleria I, García-Sancho C, Maireles-Torres P, Arias PL. Dehydration of xylose to furfural using a Lewis or Brønsted acid catalyst and N₂ stripping. *Chin J Catal* 2013;34:1402–6.
- [190] Liu QY, Yang F, Liu ZH, Li G. Preparation of SnO₂–Co₃O₄/C biochar catalyst as a Lewis acid for corncob hydrolysis into furfural in water medium. *J Ind Eng Chem* 2015;26:46–54.
- [191] Jehng JM, Wachs IE. The molecular structures and reactivity of supported niobium oxide catalysts. *Catal Today* 1990;8:37–55.
- [192] Sahu R, Dhepe PL. A one-pot method for the selective conversion of hemicellulose from crop waste into C5 sugars and furfural by using solid acid catalysts. *ChemSusChem* 2012;5:751–61.
- [193] Gallo JMR, Alonso DM, Mellmer MA, Yeap JH, Wong HC, Dumesic JA. Production of furfural from lignocellulosic biomass using Beta zeolite and biomass-derived solvent. *Top Catal* 2013;56:1775–81.
- [194] Lima S, Antunes MM, Fernandes A, Pillinger M, Ribeiro MF, Valente AA. Acid-catalysed conversion of saccharides into furanic aldehydes in the presence of three-dimensional mesoporous Al-TUD-1. *Molecules* 2010;15:3863–77.
- [195] Zanardi S, Alberti A, Cruciani G, Corma A, Fornés V, Brunelli M. Crystal structure determination of zeolite Nu-6(2) and its layered precursor Nu-6(1). *Angew Chem Int Ed* 2004;43:4933–7.
- [196] Liu Y, Zhang W, Pinnavaia TJ. Steam-stable aluminosilicate mesostructures assembled from zeolite type Y seeds. *J Am Chem Soc* 2000;122:8791–2.
- [197] Dhepe PL, Saha R. A solid-acid-based process for the conversion of hemicelluloses. *Green Chem* 2010;12:2153–6.
- [198] Saha B, Mosier NS, Abu-Omar MM. Catalytic dehydration of lignocellulosic derived xylose to furfural. *Adv Plant Biol* 2014;4:267–76.
- [199] Dias AS, Lima S, Pillinger M, Valente AA. Acidic cesium salts of 12-tungstophosphoric acid as catalysts for the dehydration of xylose into furfural. *Carbohydr Res* 2006;341:2946–53.
- [200] Werpy T, Petersen G. Top value added chemicals from biomass: vol. I – results of screening for potential candidates from sugars and synthesis gas. Golden, CO: National Renewable Energy Lab; 2004.
- [201] Fernandes DR, Rocha AS, Mai EF, Mota CJA, Teixeira da Silva V. Levulinic acid esterification with ethanol to ethyl levulinic production over solid acid catalysts. *Appl Catal A Gen* 2012;425:426–199–204.
- [202] Kuwahara Y, Kaburagi W, Nemoto K, Fujitani T. Esterification of levulinic acid with ethanol over sulfated Si-doped ZrO₂ solid acid catalyst: study of the structure–activity relationships. *Appl Catal A Gen* 2014;476:186–96.
- [203] Hayes DJ. An examination of biorefining processes, catalysis and challenges. *Catal Today* 2009;145:138–51.
- [204] Lee A, Chaibakhsh N, Rahman MBA, Basri M, Tejo BA. Optimized enzymatic synthesis of levulinic ester in solvent-free system. *Ind Crops Prod* 2010;32:246–51.
- [205] Joshi H, Moser BR, Toler J, Smith WF, Walker T. Ethyl levulinic: a potential bio-based diluent for biodiesel which improves cold flow properties. *Biomass Bioenergy* 2011;35:3262–6.
- [206] Windom BC, Lovestead TM, Mascal M, Nikitin EB, Bruno TJ. Advanced distillation curve analysis on ethyl levulinic as a diesel fuel oxygenate and a hybrid biodiesel fuel. *Energy Fuels* 2011;25:1878–90.
- [207] Olson ES, Kjeldsen MR, Schlag AJ, Sharma RK. Chemicals and materials from renewable resources. *ACS Symp Ser* 2001;784:51–63.
- [208] Amarasekara AS, Wiresdu B. Acidic ionic liquid catalyzed one-pot conversion of cellulose to ethyl levulinic and levulinic acid in ethanol-water solvent system. *Bioenerg Res* 2014;7:1237–43.
- [209] Sun Z, Cheng M, Li H, Shi T, Yuan M, Wang X, et al. One-pot depolymerization of cellulose into glucose and levulinic acid by heteropolyacid ionic liquid catalysis. *RSC Adv* 2012;2:9058–65.
- [210] Zuo Y, Zhang Y, Fu Y. Catalytic conversion of cellulose into levulinic acid by a sulfonated chloromethyl polystyrene solid acid catalyst. *ChemCatChem* 2014;6:753–7.
- [211] Saravananurugan S, Riisager A. Solid acid catalysed formation of ethyl levulinic and ethyl glucopyranoside from mono- and disaccharides. *Catal Commun* 2012;17:71–5.
- [212] Yang F, Fu J, Mo J, Lu X. Synergy of Lewis and Bronsted acids on catalytic hydrothermal decomposition of hexose to levulinic acid. *Energy Fuels* 2013;27:6973–8.

- [213] Saravanamurugan S, Riisager A. Zeolite catalyzed transformation of carbohydrates to alkyl levulinates. *ChemCatChem* 2013;5:1754–7.
- [214] Ya'aini N, Amin NAS, Endud S. Characterization and performance of hybrid catalysts for levulinic acid production from glucose. *Micropor Mesopor Mat* 2013;171:14–23.
- [215] Ramli NAS, ANAS. Fe/HY zeolite as an effective catalyst for levulinic acid production from glucose: characterization and catalytic performance. *Appl Catal B: Environ* 2015;163:487–98.
- [216] Ramli NAS, Amin NAS. Catalytic hydrolysis of cellulose and oil palm biomass in ionic liquid to reducing sugar for levulinic acid production. *Fuel Process Technol* 2014;128:490–8.
- [217] Neves P, Lima S, Pillinger M, Rocha SM, Rocha J, Valente AA. Conversion of furfuryl alcohol to ethyl levulinate using porous aluminosilicate acid catalysts. *Catal Today* 2013;218:9–76–84.
- [218] Suacharoen S, Tungasmita DN. Hydrothermolysis of carbohydrates to levulinic acid using metal supported on porous aluminosilicate. *J Chem Technol Biotechnol* 2013;88:1538–44.
- [219] Yang H, Wang L, Jia L, Qiu C, Pang Q, Pan X. Selective decomposition of cellulose into glucose and levulinic acid over Fe-resin catalyst in NaCl solution under hydrothermal conditions. *Ind Eng Chem Res* 2014;53:6562–8.
- [220] Upare PP, Yoon JW, Kim MY, Kang HY, Hwang DW, Hwang YK, et al. Chemical conversion of biomass-derived hexose sugars to levulinic acid over sulfonic acid-functionalized graphene oxide catalysts. *Green Chem* 2013;15:2935–43.
- [221] Peng L, Lin L, Zhang J, Shi J, Liu S. Solid acid catalyzed glucose conversion to ethyl levulinate. *Appl Catal A Gen* 2011;397:259–65.
- [222] Peng L, Lin L, Li H, Yang Q. Conversion of carbohydrates biomass into levulinate esters using heterogeneous catalysts. *Appl Energy* 2011;88:4590–6.
- [223] Morales G, Osatianstiani A, Hernández B, Iglesias J, Melero JA, Paniagua M, et al. Conformal sulfated zirconia monolayer catalysts for the one-pot synthesis of ethyl levulinate from glucose. *Chem Commun* 2014;50:11742–5.
- [224] Chen H, Yu B, Jin S. Production of levulinic acid from steam exploded rice straw via solid superacid, $S_2O_8^{2-}/ZrO_2-SiO_2-Sm_2O_3$. *Bioresour Technol* 2011;102:3568–70.
- [225] Joshi SS, Zodge AD, Pandare KV, Kulkarni BD. Efficient conversion of cellulose to levulinic acid by hydrothermal treatment using zirconium dioxide as a recyclable solid acid catalyst. *Ind Eng Chem Res* 2014;53:18796–805.
- [226] Li K, Bai L, Amaniampong PN, Jia X, Lee JM, Yang Y. One-pot transformation of cellobiose to formic acid and levulinic acid over ionic-liquid-based polyoxometalate hybrids. *ChemSusChem* 2014;7:2670–7.
- [227] Lin H, Strull J, Liu Y, Karmiol Z, Plank K, Miller G, et al. High yield production of levulinic acid by catalytic partial oxidation of cellulose in aqueous media. *Energy Environ Sci* 2012;5:9773–7.
- [228] Peng L, Lin L, Li H. Extremely low sulfuric acid catalyst system for synthesis of methyl levulinate from glucose. *Ind Crops Prod* 2012;40:136–44.
- [229] Ya'aini N, Amin NAS, Asmadi M. Optimization of levulinic acid from lignocellulosic biomass using a new hybrid catalyst. *Bioresour Technol* 2012;116:58–65.
- [230] Kruger JS, Choudhary V, Nikolakis V, Vlachos DG. Elucidating the roles of zeolite HBEA in aqueous-phase fructose dehydration and hmf rehydration. *ACS Catal* 2013;3:1279–91.
- [231] Hegner J, Pereira KC, DeBoef B, Lucht BL. Conversion of cellulose to glucose and levulinic acid via solid-supported acid catalysis. *Tetrahedron Lett* 2010;51:2356–8.
- [232] Saravanamurugan S, Paniagua M, Melero JA, Riisager A. Efficient isomerization of glucose to fructose over zeolites in consecutive reactions in alcohol and aqueous media. *J Am Chem Soc* 2013;135:5246–9.
- [233] Pergo C, Bosetti A. Biomass to fuels: the role of zeolite and mesoporous materials. *Micropor Mesopor Mat* 2011;144:28–39.
- [234] Moliner M, Roman-Leshkov Y, Davis ME. Tin-containing zeolites are highly active catalysts for the isomerization of glucose in water. *Proc Natl Acad Sci USA* 2010;107:6164–8.
- [235] Gunther WR, Wang Y, Ji Y, Michaelis VK, Hunt ST, Griffin RG, et al. Sn-Beta zeolites with borate salts catalyze the epimerization of carbohydrates via an intramolecular carbon shift. *Nat Commun* 2012;3:1109–16.
- [236] Chang CC, Wang Z, Dornath P, Cho HJ, Fan W. Rapid synthesis of Sn-Beta for the isomerization of cellulosic sugars. *RSC Adv* 2012;2:10475–7.
- [237] Dapsens PY, Mondelli C, Pérez-Ramírez J. Design of Lewis-acid centres in zeolitic matrices for the conversion of renewable. *Chem Soc Rev* 2015;44:7025–43.
- [238] Taarning E, Saravanamurugan S, Holm MS, Xiong JM, West RM, Christensen CH. Zeolite-catalyzed isomerization of triose sugars. *ChemSusChem* 2009;2:625–7.
- [239] Wang K, Xing Z, Ma Y, Wang Q. One-step preparation of N-tosylimines using zeolite catalysts. *Catal Lett* 2008;123:129–34.
- [240] Peng L, Lin L, Zhang J, Zhuang J, Zhang B, Gong Y. Catalytic conversion of cellulose to levulinic acid by metal chlorides. *Molecules* 2010;15:5258–72.
- [241] Lourvanij K, Rorrer GL. Reactions of aqueous glucose solutions over solid-acid Y-zeolite catalyst at 110–160 °C. *Ind Eng Chem Res* 1993;32:11–19.
- [242] Cao X, Peng X, Sun S, Zhong L, Chen W, Wang S, et al. Hydrothermal conversion of xylose, glucose, and cellulose under the catalysis of transition metal sulfates. *Carbohydr Polym* 2015;118:44–51.
- [243] Anand R, Maheswari R, Hanefeld U. Catalytic properties of the novel mesoporous aluminosilicate ALTUD-1. *J Catal* 2006;242:82–91.
- [244] Telalović S, Ramanathan A, Mul G, Hanefeld U. TUD-1: synthesis and application of a versatile catalyst, carrier, material. *J Mater Chem* 2010;20:642–58.
- [245] Zhang Z-X, Bai P, Xu B, Yan ZF. Synthesis of mesoporous alumina TUD-1 with high thermostability. *J Porous Mat* 2006;13:245–50.
- [246] Waller P, Shan Z, Marchese L, Tartaglione G, Zhou W, Jansen JC, et al. Zeolite nanocrystals inside mesoporous TUD-1: a high-performance catalytic composite. *Chem Eur J* 2004;10:4970–6.
- [247] Maheshwari S, Jordan E, Kumar S, Bates FS, Penn RL, Shantz DF, et al. Layer structure preservation during swelling, pillaring, and exfoliation of a zeolite precursor. *J Am Chem Soc* 2008;130:1507–16.
- [248] Corma A, Fornés V, Pergher SB, Bougas JG, Maesen TLM. Delaminated zeolite precursors as selective acidic catalysts. *Nature* 1998;396:353–6.
- [249] Hamoudi S, Kaliaguine S. Sulfonic acid-functionalized periodic mesoporous organosilica. *Micropor Mesopor Mat* 2003;59:195–204.
- [250] Weingarten R, Kim YT, Tompsett GA, Fernández A, Han KS, Hagaman EW, et al. Conversion of glucose into levulinic acid with solid metal(IV) phosphate catalysts. *J Catal* 2013;304:123–34.
- [251] Chen B, Li F, Huang Z, Lu T, Yuan Y, Yuan G. Integrated catalytic process to directly convert furfural to levulinic ester with high selectivity. *ChemSusChem* 2014;7:202–9.
- [252] Yang G, Pidko EA, Hensen EJM. Mechanism of Bronsted acid-catalyzed conversion of carbohydrates. *J Catal* 2012;295:122–32.
- [253] Pileidis FD, Titirici MM. Levulinic acid biorefineries: new challenges for efficient utilization of biomass. *ChemSusChem* 2016;9:562–82.
- [254] Carlson TR, Jae J, Lin YC, Tompsett GA, Huber GW. Catalytic fast pyrolysis of glucose with HZSM-5: the combined homogeneous and heterogeneous reactions. *J Catal* 2010;270:110–24.
- [255] Vispute TP, Zhang H, Sanna A, Xiao R, Huber GW. Renewable chemical commodity feedstocks from integrated catalytic processing of pyrolysis oils. *Science* 2010;330:1222–7.
- [256] Carlson TR, Jae J, Huber GW. Mechanistic insights from isotopic studies of glucose conversion to aromatics over ZSM-5. *ChemCatChem* 2009;1:107–10.
- [257] Carlson TR, Vispute TP, Huber GW. Green gasoline by catalytic fast pyrolysis of solid biomass derived compounds. *ChemSusChem* 2008;1:397–400.
- [258] Carlson TR, Tompsett GA, Conner WC, Huber GW. Aromatic production from catalytic fast pyrolysis of biomass-derived feedstocks. *Top Catal* 2009;52:241–52.
- [259] Mukarakate C, Watson MJ, ten Dam J, Baucherel X, Budhi S, Yung MM, et al. Upgrading biomass pyrolysis vapors over β -zeolites: role of silica-to-alumina ratio. *Green Chem* 2014;16:4891–905.
- [260] Adjaye JD, Bakhshi NN. Production of hydrocarbons by catalytic upgrading of a fast pyrolysis bio-oil. Part II: comparative catalyst performance and reaction pathways. *Fuel Process Technol* 1995;45:185–202.
- [261] Adjaye D, Bakhshi NN. Production of hydrocarbons by catalytic upgrading of a fast pyrolysis bio-oil. Part I: conversion over various catalysts. *Fuel Process Technol* 1995;45:161–83.
- [262] Biscardi JA, Meitzner GD, Iglesia E. Structure and density of active Zn species in Zn/H-ZSM5 propane aromatization catalysts. *J Catal* 1998;179:192–202.
- [263] Biscardi JA, Iglesia E. Reaction pathways and rate-determining steps in reactions of alkanes on H-ZSM5 and Zn/H-ZSM5 catalysts. *J Catal* 1998;182:117–28.
- [264] Fanchiang WL, Lin YC. Catalytic fast pyrolysis of furfural over H-ZSM-5 and Zn/H-ZSM-5 catalysts. *Appl Catal A Gen* 2012;419–20:102–10.
- [265] Cheng YT, Jae J, Shi J, Fan W, Huber GW. Production of renewable aromatic compounds by catalytic fast pyrolysis of lignocellulosic biomass with bifunctional Ga/ZSM-5 catalysts. *Angew Chem* 2012;124:1416–19.
- [266] Jae J, Tompsett GA, Foster AJ, Hammond KD, Auerbach SM, Lobo RF, et al. Investigation into the shape selectivity of zeolite catalysts for biomass conversion. *J Catal* 2011;279:257–68.
- [267] Li J, Li X, Zhou G, Wang W, Wang C, Komarneki S, et al. Catalytic fast pyrolysis of biomass with mesoporous ZSM-5 zeolites prepared by desilication with NaOH solutions. *Appl Catal A Gen* 2011;470:115–22.
- [268] Shao S, Zhang H, Heng L, Luo M, Xiao R, Shen D. Catalytic conversion of biomass derivatives over acid dealuminated ZSM-5. *Ind Eng Chem Res* 2014;53:15871–8.
- [269] Foster AJ, Jae J, Cheng YT, Huber GW, Lobo RF. Optimizing the aromatic yield and distribution from catalytic fast pyrolysis of biomass over ZSM-5. *Appl Catal A Gen* 2012;423–4:154–61.
- [270] Mayes HB, Nolte MW, Beckham GT, Shanks BH, Broadbelt LJ. The alpha–beta(a) of glucose pyrolysis: computational and experimental investigations of 5-hydroxymethylfurfural and levoglucosan formation reveal implications for cellulose pyrolysis. *ACS Sust Chem Eng* 2014;2:1461–73.
- [271] Torri C, Lesci IG, Fabbri D. Analytical study on the pyrolytic behaviour of cellulose in the presence of MCM-41 mesoporous materials. *J Anal Appl Pyrolysis* 2009;85:192–6.
- [272] Leng S, Wang X, Cai Q, Ma F, Liu Y, Wang J. Selective production of chemicals from biomass pyrolysis over metal chlorides supported on zeolite. *Bioresour Technol* 2013;149:341–5.
- [273] Zhang H, Liu X, Lu M, Hu X, Lu L, Tian X, et al. Role of Bronsted acid in selective production of furfural in biomass pyrolysis. *Bioresour Technol* 2014;169:800–3.
- [274] Gayubo AG, Aguayo AT, Atutxa A, Valle B, Bilbao J. Undesired components in the transformation of biomass pyrolysis oil into hydrocarbons on an HZSM-5 zeolite catalyst. *J Chem Technol Biotechnol* 2005;80:1244–51.
- [275] Cheng YT, Huber GW. Chemistry of furan conversion into aromatics and olefins over HZSM-5: a model biomass conversion reaction. *ACS Catal* 2011;1:611–28.

- [276] Shiramizu M, Toste FD. On the Diels–Alder approach to solely biomass-derived polyethylene terephthalate (PET): conversion of 2,5-dimethylfuran and acrolein into *p*-xylene. *Chem Eur J* 2011;17:12452–7.
- [277] Vaitheswaran S, Green SK, Dauenhauer P, Auerbach SM. On the way to biofuels from furan: discriminating Diels–Alder and ring-opening mechanisms. *ACS Catal* 2013;3:2012–19.
- [278] Williams CL, Chang CC, Do P, Nikbin N, Caratzoulas S, Vlachos DG, et al. Cycloaddition of biomass-derived furans for catalytic production of renewable *p*-xylene. *ACS Catal* 2012;2:935–9.
- [279] Nikbin N, Do PT, Caratzoulas S, Lobo RF, Dauenhauer PJ, Vlachos DG. A DFT study of the acid-catalyzed conversion of 2,5-dimethylfuran and ethylene to *p*-xylene. *J Catal* 2013;297:35–43.
- [280] Wang D, Osmundsen CM, Taarning E, Dumesic JA. Selective production of aromatics from alkylfurans over solid acid catalysts. *ChemCatChem* 2013;5:2044–50.
- [281] Nikbin N, Feng S, Caratzoulas S, Vlachos DG. *p*-Xylene formation by dehydrogenative aromatization of a Diels–Alder product in Lewis and Bronsted acidic zeolites. *J Phys Chem C* 2014;118:24415–24.
- [282] Chang C-C, Green SK, Williams CL, Dauenhauer PJ, Fan W. Ultra-selective cycloaddition of dimethylfuran for renewable *p*-xylene with H-BEA. *Green Chem* 2014;16:585–8.
- [283] Pacheco JJ, Davis ME. Synthesis of terephthalic acid via Diels–Alder reactions with ethylene and oxidized variants of 5-hydroxymethylfurfural. *Proc Natl Acad Sci USA* 2014;111:8363–7.
- [284] Norton JA. The Diels–Alder diene synthesis. *Chem Rev* 1942;31:319–523.
- [285] Karger MH, Mazur Y. Mixed sulfonic-carboxylic anhydrides. II. Reactions with aliphatic ethers and amines. *J Org Chem* 1971;36:532–40.
- [286] Mahmoud E, Watson DA, Lobo RF. Renewable production of phthalic anhydride from biomass-derived furan and maleic anhydride. *Green Chem* 2014;16:167–75.
- [287] Viil I, Bredihhin A, Mæorg U, Vares L. Preparation of potential biofuel 5-ethoxymethylfurfural and other 5-alkoxymethylfurals in the presence of oil shale ash. *RSC Adv* 2014;4:5689–93.
- [288] Lanza F, Temi DM, Perathoner S, Centi G, Macario A, Aloise A, et al. Etherification of 5-hydroxymethyl-2-furfural (HMF) with ethanol to biodiesel components using mesoporous solid acidic catalysts. *Catal Today* 2011;175:435–41.
- [289] Kraus GA, Guney T. A direct synthesis of 5-alkoxymethylfurfural ethers from fructose via sulfonic acid-functionalized ionic liquids. *Green Chem* 2012;14:1593–6.
- [290] Bing L, Zhang Z, Deng K. Efficient one-pot synthesis of 5-(ethoxymethyl)furfural from fructose catalyzed by a novel solid catalyst. *Ind Eng Chem Res* 2012;51:15331–6.
- [291] Balakrishnan M, Sacia ER, Bell AT. Etherification and reductive etherification of 5-(hydroxymethyl)furfural: 5-(alkoxymethyl)furfurals and 2,5-bis(alkoxymethyl)furan as potential bio-diesel candidates. *Green Chem* 2012;14:1626–34.
- [292] Yang Y, Abu-Omar MM, Hu C. Heteropolyacid catalyzed conversion of fructose, sucrose, and inulin to 5-ethoxymethylfurfural, a liquid biofuel candidate. *Appl Energy* 2012;99:80–4.
- [293] Alam MI, De S, Dutta S, Saha B. Solid-acid and ionic-liquid catalyzed one-pot transformation of biorenewable substrates into a platform chemical and a promising biofuel. *RSC Adv* 2012;2:6890–6.
- [294] Ren Y, Liu B, Zhang Z, Lin J. Silver-exchanged heteropolyacid catalyst ($\text{Ag}_1\text{H}_2\text{PW}$): an efficient heterogeneous catalyst for the synthesis of 5-ethoxymethylfurfural from 5-hydroxymethylfurfural and fructose. *J Ind Eng Chem* 2015;21:1127–31.
- [295] Jia X, Ma J, Che P, Lu F, Miao H, Gao J, et al. Direct conversion of fructose-based carbohydrates to 5-ethoxymethylfurfural catalyzed by $\text{AlCl}_3\text{-H}_2\text{O/BF}_3\text{-}(\text{Et})_2\text{O}$ in ethanol. *J Energy Chem* 2013;22:93–7.
- [296] Lew CM, Rajabbeigi N, Tsapatsis M. One-pot synthesis of 5-(ethoxymethyl)furfural from glucose using Sn-BEA and amberlyst catalysts. *Ind Eng Chem Res* 2012;51:5364–6.
- [297] Liu B, Zhang Z, Huang K. Cellulose sulfuric acid as a bio-supported and recyclable solid acid catalyst for the synthesis of 5-hydroxymethylfurfural and 5-ethoxymethylfurfural from fructose. *Cellulose* 2013;20:2081–9.
- [298] Wang S, Zhang Z, Liu B, Li J. Silica coated magnetic Fe_3O_4 nanoparticles supported phosphotungstic acid: a novel environmentally friendly catalyst for the synthesis of 5-ethoxymethylfurfural from 5-hydroxymethylfurfural and fructose. *Catal Sci Technol* 2013;3:2104–12.
- [299] Wang H, Deng T, Wang Y, Cui X, Qi Y, Mu X, et al. Graphene oxide as a facile acid catalyst for the one-pot conversion of carbohydrates into 5-ethoxymethylfurfural. *Green Chem* 2013;15:2379–83.
- [300] Román-Leshkov Y, Davis ME. Activation of carbonyl-containing molecules with solid Lewis acids in aqueous media. *ACS Catal* 2011;1:1566–80.
- [301] Holm MS, Saravanamurugan S, Taarning E. Conversion of sugars to lactic acid derivatives using heterogeneous zeotype catalysts. *Science* 2010;328:602–5.
- [302] Holm MS, Pagán-Torres YJ, Saravanamurugan S, Riisager A, Dumesic JA, Taarning E. Sn-Beta catalysed conversion of hemicellulosic sugars. *Green Chem* 2012;14:702–6.
- [303] Shimizu K, Furukawa H, Kobayashi N, Itaya Y, Satsuma A. Effects of Bronsted and Lewis acidities on activity and selectivity of heteropolyacid-based catalysts for hydrolysis of cellobiose and cellulose. *Green Chem* 2009;11:1627–32.
- [304] de Clippel F, Dusselier M, Van Rompaey R, Vanelderen P, Dijkmans J, Makshina E, et al. Fast and selective sugar conversion to alkyl lactate and lactic acid with bifunctional carbon–silica catalysts. *J Am Chem Soc* 2012;134:10089–101.
- [305] Hayashi Y, Sasaki Y. Tin-catalyzed conversion of trioses to alkyl lactates in alcohol solution. *Chem Commun* 2005;2716–18.
- [306] West RM, Holm MS, Saravanamurugan S, Xiong J, Beversdorf Z, Taarning E, et al. Zeolite H-USY for the production of lactic acid and methyl lactate from C₃-sugars. *J Catal* 2010;269:122–30.
- [307] Wang JC, Masui Y, Onaka M. Conversion of triose sugars with alcohols to alkyl lactates catalyzed by Bronsted acid tin ion exchanged montmorillonite. *Appl Catal B: Environ* 2011;107:135–9.
- [308] Rasrendra CB, Fachri BA, Gusti I, Makertiharta BN, Adisasmto S, Heeres HJ. Catalytic conversion of dihydroxyacetone to lactic acid using metal salts in water. *ChemSusChem* 2011;4:768–77.
- [309] Assary RS, Curtiss LA. Theoretical study of 1,2-hydride shift associated with the isomerization of glyceraldehyde to dihydroxy acetone by Lewis acid active site models. *J Phys Chem A* 2011;115:8754–60.
- [310] Pescarmona PP, Janssen KPF, Delaet C, Stroobants C, Houchoofd K, Philippaerts A, et al. Zeolite-catalysed conversion of C₃ sugars to alkyl lactates. *Green Chem* 2010;12:1083–9.
- [311] Li L, Stroobants C, Lin K, Jacobs PA, Sels BF, Pescarmona PP. Selective conversion of trioses to lactates over Lewis acid heterogeneous catalysts. *Green Chem* 2011;13:1175–81.
- [312] Liu J, Li H, Liu YC, Lu YM, He J, Liu XF, et al. Catalytic conversion of glucose to 5-hydroxymethylfurfural over nano-sized mesoporous $\text{Al}_2\text{O}_3\text{-B}_2\text{O}_3$ solid acids. *Catal Commun* 2015;62:19–23.
- [313] Li H, Ren J, Zhong L, Sun R, Liang L. Production of furfural from xylose, water-insoluble hemicelluloses and water-soluble fraction of corn cob via a tin-loaded montmorillonite solid acid catalyst. *Bioresour Technol* 2015;176:242–8.
- [314] Schwiderski M, Kruse A, Grandl R, Dockendorf D. Comparison of the influence of a Lewis acid AlCl_3 and a Bronsted acid HCl on the organosolv pulping of beech wood. *Green Chem* 2014;16:1569–78.
- [315] Rai N, Caratzoulas S, Vlachos DG. Role of silanol group in Sn-Beta zeolite for glucose isomerization and epimerization reactions. *ACS Catal* 2013;3:2294–8.
- [316] Li G, Pidko EA, Hensen EJM. Synergy between Lewis acid sites and hydroxyl groups for the isomerization of glucose to fructose over Sn-containing zeolites: a theoretical perspective. *Catal Sci Technol* 2014;4:2241–50.
- [317] Zhang S, Jin F, Hu J, Huo Z. Improvement of lactic acid production from cellulose with the addition of $\text{Zn}/\text{Ni}/\text{C}$ under alkaline hydrothermal conditions. *Bioresour Technol* 2011;102:1998–2003.
- [318] Dijkmans J, Dusselier M, Gabriëls D, Houthooft K, Magusin PCMM, Huang S, et al. Cooperative catalysis for multistep biomass conversion with Sn/Al Beta zeolite. *ACS Catal* 2015;5:928–40.
- [319] Takagaki A, Jung JC, Hayashi S. Solid Lewis acidity of boehmite $\gamma\text{-Al(OH)}$ and its catalytic activity for transformation of sugars in water. *RSC Adv* 2014;4:43785–91.
- [320] Jiménez-Morales I, Santamaría-González J, Maireles-Torres P, Jiménez-López A. Mesoporous tantalum phosphate as acidic catalyst for the methanolysis of sunflower oil. *Appl Catal B: Environ* 2012;123–4:316–23.
- [321] Lee AF, Bennett JA, Manayil JC, Wilson K. Heterogeneous catalysis for sustainable biodiesel production via esterification and transesterification. *Chem Soc Rev* 2014;43:7887–916.
- [322] Di Serio M, Tesser R, Dimicoli M, Cammarota F, Nastasi M, Santacesaria E. Synthesis of biodiesel via homogeneous Lewis acid catalyst. *J Mol Catal A Chem* 2005;239:111–15.
- [323] Kulkarni MG, Gopinath R, Meher LC, Dalai AK. Solid acid catalyzed biodiesel production by simultaneous esterification and transesterification. *Green Chem* 2006;8:1056–62.
- [324] Shi W, Zhao J, Yuan X, Wang S, Wang X, Huo M. Effects of Bronsted and Lewis acidities on catalytic activity of heteropolyacids in transesterification and esterification reactions. *Chem Eng Technol* 2012;35:347–52.
- [325] Zhang L, Cui Y, Zhang C, Wang L, Wan H, Guan G. Biodiesel production by esterification of oleic acid over Bronsted acidic ionic liquid supported onto Fe-incorporated SBA-15. *Ind Eng Chem Res* 2012;51:16590–6.
- [326] Soriano NU, Venditti R, Argyropoulos DS. Biodiesel synthesis via homogeneous Lewis acid-catalyzed transesterification. *Fuel* 2009;88:560–5.
- [327] Werpy T, Petersen G. Top value added chemicals from biomass, vol. 1. US Department of Energy (USDOE); 2004.
- [328] Talebian-Kiakalaieh A, Amin NAS, Hezaveh H. Glycerol for renewable acrolein production by catalytic dehydration. *Renew Sust Energy Rev* 2014;40:28–59.
- [329] Alhanash A, Kozhevnikova EF, Kozhevnikov IV. Gas-phase dehydration of glycerol to acrolein catalysed by caesium heteropoly salt. *Appl Catal A Gen* 2010;378:11–18.
- [330] Gan H, Zhao X, Song B, Guo L, Zhang R, Chen C, et al. Gas phase dehydration of glycerol to acrolein catalyzed by zirconium phosphate. *Chin J Catal* 2014;35:1148–56.
- [331] Katryniok B, Paul S, Capron M, Dumeignil F. Towards the sustainable production of acrolein by glycerol dehydration. *ChemSusChem* 2009;2:719–30.
- [332] Foo GS, Wei D, Sholl DS, Sievers C. Role of Lewis and Bronsted acid sites in the dehydration of glycerol over niobia. *ACS Catal* 2014;4:3180–92.
- [333] Wang Z, Wang L, Jiang Y, Hunger M, Huang J. Cooperativity of Bronsted and Lewis acid sites on zeolite for glycerol dehydration. *ACS Catal* 2014;4:1144–7.
- [334] Collins CD, Willey N, editor. *Phytoremediation: methods and reviews*, vol. 23. Totowa: Humana Press Inc.; 2007. p. 99–108.

- [335] Xing R, Subrahmanyam AV, Olcay H, Qi W, van Walsum GP, Pendse H, et al. Production of jet and diesel fuel range alkanes from waste hemicellulose-derived aqueous solutions. *Green Chem* 2010;12:1933–46.
- [336] Harvey BG, Quintana RL. Synthesis of renewable jet and diesel fuels from 2-ethyl-1-hexene. *Energy Environ Sci* 2010;3:352–7.
- [337] West RM, Liu ZY, Peter M, Gartner CA, Dumesic JA. Carbon–carbon bond formation for biomass-derived furfural and ketones by aldol condensation in a biphasic system. *J Mol Catal A Chem* 2008;296:18–27.
- [338] Huber GW, Chheda JN, Barrett CJ, Dumesic JA. Production of liquid alkanes by aqueous-phase processing of biomass-derived carbohydrates. *Science* 2005;308:1446–50.
- [339] Subrahmanyam AV, Thayumanavan S, Huber GW. C–C bond formation reactions for biomass-derived molecules. *ChemSusChem* 2010;3:1158–61.
- [340] Sádaba I, Ojeda M, Mariscal R, Fierro JLG, Granados ML. Catalytic and structural properties of co-precipitated Mg–Zr mixed oxides for furfural valorization via aqueous aldol condensation with acetone. *Appl Catal B: Environ* 2011;101:638–48.
- [341] Xu WJ, Liu XH, Ren JW, Liu HH, Ma YC, Wang YQ, et al. Synthesis of nanosized mesoporous Co–Al spinel and its application as solid base catalyst. *Micropor Mesopor Mater* 2011;142:251–7.
- [342] Shen WQ, Tompsett GA, Hammond KD, Xing R, Dogan F, Grey CP, et al. Liquid phase aldol condensation reactions with MgO–ZrO₂ and shape-selective nitrogen-substituted NaY. *Appl Catal A Gen* 2011;392:57–68.
- [343] West RM, Liu ZY, Peter M, Dumesic JA. Liquid alkanes with targeted molecular weights from biomass-derived carbohydrates. *ChemSusChem* 2008;1:417–24.
- [344] Kikhtyanin O, Kelbichová V, Vitvarová D, Kubů M, Kubička D. Aldol condensation of furfural and acetone on zeolites. *Catal Today* 2014;227:154–62.
- [345] Kikhtyanin O, Chlubná P, Jindrová T, Kubička D. Peculiar behavior of MWW materials in aldol condensation of furfural and acetone. *Dalton Trans* 2014;43:10628–41.
- [346] Kikhtyanin O, Kubička D, Čejka J. Toward understanding of the role of Lewis acidity in aldol condensation of acetone and furfural using MOF and zeolite catalysts. *Catal Today* 2015;243:158–62.
- [347] Corma A, de la Torre O, Renz M. High-quality diesel from hexose- and pentose-derived biomass platform molecules. *ChemSusChem* 2011;4:1574–7.
- [348] Corma A, de la Torre O, Renz M, Villanueva N. Production of high-quality diesel from biomass waste products. *Angew Chem* 2011;123:2423–6.
- [349] Corma A, de la Torre O, Renz M. Production of high quality diesel from cellulose and hemicellulose by the Sylvan process: catalysts and process variables. *Energy Environ Sci* 2012;5:6328–44.
- [350] Li G, Li N, Yang J, Wang A, Wang X, Cong Y, et al. Synthesis of renewable diesel with the 2-methylfuran, butanal and acetone derived from lignocellulose. *Bioresour Technol* 2013;134:66–72.
- [351] Li G, Li N, Li S, Wang A, Cong Y, Wang X, et al. Synthesis of renewable diesel with hydroxyacetone and 2-methyl-furan. *Chem Commun* 2013;49:5727–9.
- [352] Bond JQ, Upadhye AA, Olcay H, Tompsett GA, Jae J, Xing R, et al. Production of renewable jet fuel range alkanes and commodity chemicals from integrated catalytic processing of biomass. *Energy Environ Sci* 2014;7:1500–23.
- [353] Li G, Li N, Wang Z, Li C, Wang A, Wang X, et al. Synthesis of high-quality diesel with furfural and 2-methylfuran from hemicellulose. *ChemSusChem* 2012;5:1958–66.
- [354] Gelman F, Blum J, Avnir D. Acids and bases in one pot while avoiding their mutual destruction. *Angew Chem* 2001;113:3759–61.
- [355] Li H, Wu H, Zhang Q, Liu J, Liu X, Liu Y, et al. Solid acid-base bifunctional catalysts in organic transformations. *Curr Catal* 2013;2:2173–212.
- [356] Watanabe M, Aizawa Y, Iida T, Aida TM, Levy C, Sue K, et al. Glucose reactions with acid and base catalysts in hot compressed water at 473K. *Carbohydr Res* 2005;340:1925–30.
- [357] Daorattanachai P, Namuangruk S, Viriya-empikul N, Laosiripojana N, Faungnawakij K. 5-Hydroxymethylfurfural production from sugars and cellulose in acid-and-base-catalyzed conditions under hot compressed water. *J Ind Eng Chem* 2012;18:1893–901.
- [358] Watanabe M, Aizawa Y, Iida T, Nishimura R, Inomata H. Catalytic glucose and fructose conversions with TiO₂ and ZrO₂ in water at 473K: relationship between reactivity and acid–base property determined by TPD measurement. *Appl Catal A Gen* 2005;295:150–6.
- [359] Qi X, Watanabe M, Aida TM, Smith RL Jr. Catalytical conversion of fructose and glucose into 5-hydroxymethylfurfural in hot compressed water by microwave heating. *Catal Commun* 2008;9:2244–9.
- [360] Yang L, Liu Y, Ruan R. Hydrolysis of glucose to 5-hydroxymethylfurfural. *Adv Mater Res* 2011;335–6:1448–53.
- [361] Qi X, Watanabe M, Aida TM, Smith RL Jr. Sulfated zirconia as a solid acid catalyst for the dehydration of fructose to 5-hydroxymethylfurfural. *Catal Commun* 2009;10:1771–5.
- [362] Yan H, Yang Y, Tong D, Hu C, Abu-Omar MM. Catalytic conversion of glucose to 5-hydroxymethylfurfural over SO₄²⁻/ZrO₂ and SO₄²⁻/ZrO₂–Al₂O₃ solid acid catalysts. *Catal Commun* 2009;10:1558–63.
- [363] Yang Y, Xiang X, Tong D, Hu C, Abu-Omar MM. One-pot synthesis of 5-hydroxymethylfurfural directly from starch over/ZrO₂–Al₂O₃ solid catalyst. *Bioresour Technol* 2012;116:302–6.
- [364] Asiashtiani A, Lee AF, Brown DR, Melero JA, Moralese G, Wilson K. Bifunctional SO₄/ZrO₂ catalysts for 5-hydroxymethylfurfural (5-HMF) production from glucose. *Catal Sci Technol* 2014;4:333–42.
- [365] Takagaki A, Ohara M, Nishimura S, Ebitani K. One-pot formation of furfural from xylose via isomerization and successive dehydration reactions over heterogeneous acid and base catalysts. *Chem Lett* 2010;39:838–40.
- [366] Fang Z, Zhang F, Zeng HY, Guo F. Production of glucose by hydrolysis of cellulose at 423 K in the presence of activated hydrotalcite nanoparticles. *Bioresour Technol* 2011;102:8017–21.
- [367] Takagaki A, Ohara M, Nishimura S, Ebitani K. A one-pot reaction for biorefinery: combination of solid acid and base catalysts for direct production of 5-hydroxymethylfurfural from saccharides. *Chem Commun* 2009;6276–8.
- [368] Ohara M, Takagaki A, Nishimura S, Ebitani K. Syntheses of 5-hydroxymethylfurfural and levoglucosan by selective dehydration of glucose using solid acid and base catalysts. *Appl Catal A Gen* 2010;383:149–55.
- [369] Shiroto M, Nishimura S, Ebitani K. One-pot synthesis of furfural from xylose using Al₂O₃–Ni–Al layered double hydroxide acid-base bi-functional catalyst and sulfonated resin. *Chem Lett* 2016;45:194–6.
- [370] Tuteja J, Nishimura S, Ebitani K. One-pot synthesis of furans from various saccharides using a combination of solid acid and base catalysts. *Bull Chem Soc Jpn* 2012;85:275–81.
- [371] Yue C, Rigoito MS, Hensen EJM. Glucose dehydration to 5-hydroxymethylfurfural by a combination of a basic zirconiosilicate and a solid acid. *Catal Lett* 2014;144:2121–8.
- [372] Son PA, Nishimura S, Ebitani K. Preparation of zirconium carbonate as water-tolerant solid base catalyst for glucose isomerization and one-pot synthesis of levulinic acid with solid acid catalyst. *Reac Kinet Mech Cat* 2014;111:183–97.
- [373] Pérez-Maqueda J, Arenas-Ligioiz I, López Ó, Fernández-Bolaños JG. Eco-friendly preparation of 5-hydroxymethylfurfural from sucrose using ion-exchange resins. *Chem Eng Sci* 2014;109:244–50.
- [374] Peng WH, Lee YY, Wu C, Wu KC-W. Acid–base bi-functionalized, large-pored mesoporous silica nanoparticles for cooperative catalysis of one-pot cellulose-to-HMF conversion. *J Mater Chem* 2012;22:23181–5.
- [375] Wang L, Wang H, Liu F, Zheng A, Zhang J, Sun Q, et al. Selective catalytic production of 5-hydroxymethylfurfural from glucose by adjusting catalyst wettability. *ChemSusChem* 2014;7:402–6.
- [376] Li H, Govind KS, Kotni R, Shunmugavel S, Riisager A, Yang S. Direct catalytic transformation of carbohydrates into 5-ethoxymethylfurfural with acid–base bifunctional hybrid nanospheres. *Energy Conv Manag* 2014;88:1245–51.
- [377] Hao W, Li W, Tang X, Zeng X, Sun Y, Liu S, et al. Catalytic transfer hydrogenation of biomass-derived 5-hydroxymethyl furfural to the building block 2, 5-bishydroxymethyl furan. *Green Chem* 2016;18:1080–8.
- [378] Jae J, Mahmoud E, Lobo RF, Vlachos DG. Cascade of liquid-phase catalytic transfer hydrogenation and etherification of 5-hydroxymethylfurfural to potential biodiesel components over Lewis acid zeolites. *ChemCatChem* 2014;6:508–13.
- [379] Lewis JD, Van de Vyver S, Crisci AJ, Gunther WR, Michaelis VK, Griffin RG, et al. A continuous flow strategy for the coupled transfer hydrogenation and etherification of 5-(hydroxymethyl)furfural using Lewis acid zeolites. *ChemSusChem* 2014;7:2255–65.
- [380] Song J, Zhou B, Zhou H, Wu L, Meng Q, Liu Z, et al. Porous zirconium–phytic acid hybrid: a highly efficient catalyst for Meerwein–Ponndorf–Verley reductions. *Angew Chem* 2015;127:9531–5.
- [381] Demma Carà P, Ciriminna R, Shiju NR, Rothenberg G, Pagliaro M. Enhanced heterogeneous catalytic conversion of furfuryl alcohol into butyl levulinate. *ChemSusChem* 2014;7:835–40.
- [382] Lu B, An S, Song D, Su F, Yang X, Guo Y. Design of organosulfonic acid functionalized organosilica hollow nanospheres for efficient conversion of furfural alcohol to ethyl levulinate. *Green Chem* 2015;17:1767–78.
- [383] Kaur N, Ali A. Lithium zirconate as solid catalyst for simultaneous esterification and transesterification of low quality triglycerides. *Appl Catal A Gen* 2015;489:193–202.
- [384] Rattanaphra D, Harvey A, Srinophakun P. Simultaneous conversion of triglyceride/free fatty acid mixtures into biodiesel using sulfated zirconia. *Top Catal* 2010;53:773–82.
- [385] Yan S, Salley SO, Ng KYS. Simultaneous transesterification and esterification of unrefined or waste oils over ZnO–La₂O₃ catalysts. *Appl Catal A Gen* 2009;353:203–12.
- [386] Lee HV, Juan JC, Taufiq-Yap YH. Preparation and application of binary acid–base CaO–La₂O₃ catalyst for biodiesel production. *Renew Energy* 2015;74:124–32.
- [387] Benvenuti F, Carlini C, Patrono P, Galletti AMR, Sbrana G, Massucci MA, et al. Heterogeneous zirconium and titanium catalysts for the selective synthesis of 5-hydroxymethyl-2-furaldehyde from carbohydrates. *Appl Catal A Gen* 2000;193:147–53.
- [388] Qi X, Guo H, Li L. Efficient conversion of fructose to 5-hydroxymethylfurfural catalyzed by sulfated zirconia in ionic liquids. *Ind Eng Chem Res* 2011;50:7985–9.
- [389] Moreau C, Durand R, Roux A, Tichit D. Isomerization of glucose into fructose in the presence of cation-exchanged zeolites and hydrotalcites. *Appl Catal A Gen* 2000;193:257–64.
- [390] Qu YS, Song YL, Huang CP, Zhang J, Chen BH. Alkaline ionic liquids as catalysts: a novel and green process for the dehydration of carbohydrates to give 5-hydroxymethylfurfural. *Ind Eng Chem Res* 2012;51:13008–13.
- [391] Zhao Q, Sun Z, Wang S, Huang G, Wang X, Jiang Z. Conversion of highly concentrated fructose into 5-hydroxymethylfurfural by acid–base bifunctional HPA nanocatalysts induced by choline chloride. *RSC Adv* 2014;4:63055–61.

- [392] Liu FJ, Kong WP, Qi CZ, Zhu LF, Xiao FS. Design and synthesis of mesoporous polymer-based solid acid catalysts with excellent hydrophobicity and extraordinary catalytic activity. *ACS Catal* 2012;2:565–72.
- [393] Li H, Saravananurugan S, Yang S, Riisager A. Direct transformation of carbohydrates to the biofuel 5-ethoxymethylfurfural by solid acid catalysts. *Green Chem* 2016;18:726–34.
- [394] Ruppert AM, Meeldijk JD, Kuipers BWM, Erné BH, Weckhuysen BM. Glycerol etherification over highly active CaO-based materials: new mechanistic aspects and related colloidal particle formation. *Chem Eur J* 2008;14:2016–24.
- [395] Calatayud M, Ruppert AM, Weckhuysen BM. Theoretical study on the role of surface basicity and Lewis acidity on the etherification of glycerol over alkaline earth metal oxides. *Chem Eur J* 2009;15:10864–70.
- [396] Sivaiah MV, Robles-Manuel S, Valange S, Barrault J. Recent developments in acid and base-catalyzed etherification of glycerol to polyglycerols. *Catal Today* 2012;198:305–13.
- [397] Gilkey MJ, Xu B. Heterogeneous catalytic transfer hydrogenation as an effective pathway in biomass upgrading. *ACS Catal* 2016;6:1420–36.
- [398] Weber N, Weitkamp P, Mukherjee KD. Fatty acid steryl, stanyl, and steroid esters by esterification and transesterification in vacuo using *Candida rugosa* lipase as catalyst. *J Agric Food Chem* 2001;49:67–71.
- [399] Roy I, Gupta MN. Non-thermal effects of microwaves on protease-catalyzed esterification and transesterification. *Tetrahedron* 2003;59:5431–6.
- [400] Alsalme A, Kozhevnikova EF, Kozhevnikov IV. Heteropoly acids as catalysts for liquid-phase esterification and transesterification. *Appl Catal A Gen* 2008;349:170–6.
- [401] Xu L, Wang Y, Yang X, Hu J, Li W, Guo Y. Simultaneous esterification and transesterification of soybean oil with methanol catalyzed by mesoporous $Ta_2O_5/SiO_2-[H_3PW_{12}O_{40}/R]$ (R:Me or Ph) hybrid catalysts. *Green Chem* 2009;11:314–17.
- [402] Srilatha K, Issariyakul T, Lingaiah N, Sai Prasad PS, Kozinski J, Dalai AK. Efficient esterification and transesterification of used cooking oil using 12-tungstophosphoric acid (TPA)/ Nb_2O_5 catalyst. *Energy Fuels* 2010;24:4748–55.
- [403] Garcia CM, Teixeira S, Marciniuk LL, Schuchardt U. Transesterification of soybean oil catalyzed by sulfated zirconia. *Bioresour Technol* 2008;99:6608–13.
- [404] Hoydonckx HE, De Vos DE, Chavan SA, Jacobs PA. Esterification and transesterification of renewable chemicals. *Top Catal* 2004;27:83–96.
- [405] Lien YS, Hsieh LS, Wu JCS. Biodiesel synthesis by simultaneous esterification and transesterification using oleophilic acid catalyst. *Ind Eng Chem Res* 2010;49:2118–21.
- [406] Boz N, Degirmenci N, Kalyon DM. Esterification and transesterification of waste cooking oil over Amberlyst 15 and modified Amberlyst 15 catalysts. *Appl Catal B: Environ* 2015;165:723–30.
- [407] Jiménez-Morales I, Santamaría-González J, Maireles-Torres P, Jiménez-López A. Calcined zirconium sulfate supported on MCM-41 silica as acid catalyst for ethanolation of sunflower oil. *Appl Catal B: Environ* 2011;103:91–8.
- [408] Tamilarasan S, Sahadevan R. Ultrasonic assisted acid base transesterification of algal oil from marine macroalgae *Caulerpa peltata*: optimization and characterization studies. *Fuel* 2014;128:347–55.
- [409] Ngo HL, Zafiroopoulos NA, Foglia TA, Samulski ET, Lin W. Efficient two-step synthesis of biodiesel from greases. *Energy Fuels* 2007;22:626–34.
- [410] Li Y, He D, Yuan Y, Cheng Z, Zhu Q. Influence of acidic and basic properties of ZrO_2 based catalysts on isosynthesis. *Fuel* 2002;81:1611–17.
- [411] López DE, Goodwin JG, Bruce DA, Furuta S. Esterification and transesterification using modified-zirconia catalysts. *Appl Catal A Gen* 2008;339:76–83.
- [412] Kim M, DiMaggio C, Yan S, Salley SO, Ng KYS. The synergistic effect of alcohol mixtures on transesterification of soybean oil using homogeneous and heterogeneous catalysts. *Appl Catal A Gen* 2010;378:134–43.
- [413] Pereo C, Bianchi D. Biomass upgrading through acid-base catalysis. *Chem Eng J* 2010;161:314–22.
- [414] Sun J, Zhu K, Gao F, Wang C, Liu J, Peden CHF, et al. Direct conversion of bio-ethanol to isobutene on nanosized $Zn_xZr_yO_z$ mixed oxides with balanced acid-base sites. *J Am Chem Soc* 2011;133:11096–9.
- [415] Nakajima T, Nameta H, Mishima S, Matsuzaki I, Tanabe K. A highly active and highly selective oxide catalyst for the conversion of ethanol to acetone in the presence of water vapour. *J Mater Chem* 1994;4:853–8.
- [416] Hutchings GJ, Johnston P, Lee DF, Williams CD. Acetone conversion to isobutene in high selectivity using zeolite β catalyst. *Catal Lett* 1993;21:49–53.
- [417] Tao LZ, Chai SH, Wang HP, Yan B, Liang Y, Xu BQ. Comparison of gas-phase dehydration of propane polyols over solid acid-base catalysts. *Catal Today* 2014;234:237–44.
- [418] Stošić D, Bennici S, Couturier JL, Dubois JL, Auroux A. Influence of surface acid-base properties of zirconia and titania based catalysts on the product selectivity in gas phase dehydration of glycerol. *Catal Commun* 2012;17:23–8.
- [419] Climent MJ, Corma A, De Frutos P, Iborra S, Noy M, Velty A, et al. Chemicals from biomass: synthesis of glycerol carbonate by transesterification and carbonylation with urea with hydrotalcite catalysts. The role of acid-base pairs. *J Catal* 2010;269:140–9.
- [420] Pérez-Barrado E, Pujol MC, Aguiló M, Llorca J, Cesteros Y, Díaz F, et al. Influence of acid-base properties of calcined MgAl and CaAl layered double hydroxides on the catalytic glycerol etherification to short-chain polyglycerols. *Chem Eng J* 2015;264:547–56.
- [421] Bobadilla LF, Penkova A, Romero-Sarria F, Centeno MA, Odriozola JA. Influence of the acid-base properties over NiSn/MgO-Al₂O₃ catalysts in the hydrogen production from glycerol steam reforming. *Int J Hydrogen Energy* 2014;39:5704–12.
- [422] Shiroitori M, Nishimura S, Ebihara K. One-pot synthesis of furfural derivatives from pentoses using solid acid and base catalysts. *Catal Sci Technol* 2014;4:971–8.
- [423] Elmekawy AA, Shiju NR, Rothenberg G, Brown DR. Environmentally benign bifunctional solid acid and base catalysts. *Ind Eng Chem Res* 2014;53:18722–8.
- [424] Lauwaert J, De Canck E, Esquivel D, Van Der Voort P, Thybaut JW, Marina GB. *Catal Today* 2015;246:35–45.
- [425] De S, Saha B, Luque R. Hydrodeoxygenation processes: advances on catalytic transformations of biomass-derived platform chemicals into hydrocarbon fuels. *Bioresour Technol* 2015;178:108–18.
- [426] Lee J, Kim YT, Huber GW. Aqueous-phase hydrogenation and hydrodeoxygenation of biomass-derived oxygenates with bimetallic catalysts. *Green Chem* 2014;16:708–18.
- [427] Slade JH, Knopf DA. Heterogeneous OH oxidation of biomass burning organic aerosol surrogate compounds: assessment of volatilisation products and the role of OH concentration on the reactive uptake kinetics. *Phys Chem Chem Phys* 2013;15:5898–915.
- [428] Li H, Zhang Q, Riisager A, Yang S. Catalytic valorization of cellulose and cellibiose with nanoparticles. *Curr Nanosci* 2015;11:1–14.
- [429] Zope BN, Hibbitts DD, Neurock M, Davis RJ. Reactivity of the gold/water interface during selective oxidation catalysis. *Science* 2010;330:74–8.
- [430] Silva B, Figueiredo H, Soares OSGP, Pereira MFR, Figueiredo JL, Lewandowska AE, et al. Evaluation of ion exchange-modified Y and ZSM5 zeolites in Cr(VI) biosorption and catalytic oxidation of ethyl acetate. *Appl Catal B: Environ* 2012;117–8:406–13.
- [431] Abad A, Concepción P, Corma A, García H. A collaborative effect between gold and a support induces the selective oxidation of alcohols. *Angew Chem Int Ed* 2005;44:4066–9.
- [432] Deng W, Zhang Q, Wang Y. Catalytic transformations of cellulose and cellulose-derived carbohydrates into organic acids. *Catal Today* 2014;234:31–41.
- [433] Zhang J, Li J, Tang Y, Lin L, Long M. Advances in catalytic production of bio-based polyester monomer 2,5-furandicarboxylic acid derived from lignocellulosic biomass. *Carbohydr Polym* 2015;130:420–8.
- [434] Cao Q, Dornan LM, Rogan L, Hughes NL, Muldoon MJ. Aerobic oxidation catalysis with stable radicals. *Chem Commun* 2014;50:4524–43.
- [435] Grasset FL, Katryniok B, Paul S, Nardello-Rataj V, Pera-Titus M, Clacens JM, et al. Selective oxidation of 5-hydroxymethylfurfural to 2,5-diformylfuran over intercalated vanadium phosphate oxides. *RSC Adv* 2013;3:9942–8.
- [436] Gong Y, Lin L. Oxidative decarboxylation of levulinic acid by silver(I)/persulfate. *Molecules* 2011;16:2714–25.
- [437] Besson M, Lahmer F, Gallezot P, Fuertes P, Flèche G. Catalytic oxidation of glucose on bismuth-promoted palladium catalysts. *J Catal* 1995;152:116–21.
- [438] Delidovich IV, Taran OP, Matvienko LG, Simonov AN, Simakova IL, Bobrovskaya AN, et al. Selective oxidation of glucose over carbon-supported Pd and Pt catalysts. *Catal Lett* 2010;140:14–21.
- [439] Besson M, Gallezot P. Selective oxidation of alcohols and aldehydes on metal catalysts. *Catal Today* 2000;57:127–41.
- [440] Sakurai H, Koga K, Kiuchi M. Gold nanoparticles deposited on Amberlyst-15: metal-acid bifunctional catalyst for cellobiose conversion to gluconic acid. *Catal Today* 2015;251:96–102.
- [441] Baatz C, Prüsse U. Preparation of gold catalysts for glucose oxidation by incipient wetness. *J Catal* 2007;249:34–40.
- [442] Witóńska I, Frajtak M, Karski S. Selective oxidation of glucose to gluconic acid over Pd–Te supported catalysts. *Appl Catal A Gen* 2011;401:73–82.
- [443] Amaniampong PN, Jia X, Wang B, Mushrif SH, Borgna A, Yang Y. Catalytic oxidation of cellobiose over TiO_2 supported gold-based bimetallic nanoparticles. *Catal Sci Technol* 2015;5:2393–405.
- [444] Prüsse U, Herrmann M, Baatz C, Decker N. Gold-catalyzed selective glucose oxidation at high glucose concentrations and oxygen partial pressures. *Appl Catal A Gen* 2011;406:89–93.
- [445] Rautiainen S, Lehtinen P, Vehkämäki M, Niemelä K, Kemell M, Heikkilä M, et al. Microwave-assisted base-free oxidation of glucose on gold nanoparticle catalysts. *Catal Commun* 2016;74:115–18.
- [446] Wojcieszak R, Cuccovia IM, Silva MA, Rossi LM. Selective oxidation of glucose to glucuronic acid by cesium-promoted gold nanoparticle catalyst. *J Mol Catal A Chem* 2016;doi:10.1016/j.molcata.2016.02.008.
- [447] Albert J, Wölfel R, Bösmann A, Wasserscheid P. Selective oxidation of complex, water-insoluble biomass to formic acid using additives as reaction accelerators. *Energy Environ Sci* 2012;5:7956–62.
- [448] Wölfel R, Taccardi N, Bosmann A, Wasserscheid P. Selective catalytic conversion of biobased carbohydrates to formic acid using molecular oxygen. *Green Chem* 2011;13:2759–63.
- [449] Li J, Ding DJ, Deng L, Guo QX, Fu Y. Catalytic air oxidation of biomass-derived carbohydrates to formic acid. *ChemSusChem* 2012;5:1313–18.
- [450] Niu M, Hou Y, Ren S, Wang W, Zheng Q, Wu W. The relationship between oxidation and hydrolysis in the conversion of cellulose in $NaVO_3-H_2SO_4$ aqueous solution with O_2 . *Green Chem* 2015;17:335–42.
- [451] Niu M, Hou Y, Ren S, Wu W, Marsh KN. Conversion of wheat straw into formic acid in $NaVO_3-H_2SO_4$ aqueous solution with molecular oxygen. *Green Chem* 2015;17:453–9.

- [452] Wang W, Niu M, Hou Y, Wu W, Liu Z, Liu Q, et al. Catalytic conversion of biomass-derived carbohydrates to formic acid using molecular oxygen. *Green Chem* 2014;16:2614–18.
- [453] Xu J, Zhang H, Zhao Y, Yang Z, Yu B, Xua H, et al. Heteropolyanion-based ionic liquids catalysed conversion of cellulose into formic acid without any additives. *Green Chem* 2014;16:4931–5.
- [454] Tang Z, Deng W, Wang Y, Zhu E, Wan X, Zhang Q, et al. Transformation of cellulose and its derived carbohydrates into formic and lactic acids catalyzed by vanadyl cations. *ChemSusChem* 2014;7:1557–67.
- [455] Zhang J, Sun M, Liu X, Han Y. Catalytic oxidative conversion of cellulosic biomass to formic acid and acetic acid with exceptionally high yields. *Catal Today* 2014;233:77–82.
- [456] Zhang J, Liu X, Sun M, Ma X, Han Y. Direct conversion of cellulose to glycolic acid with a phosphomolybdic acid catalyst in a water medium. *ACS Catal* 2012;2:1698–702.
- [457] Zhang J, Sun M, Han Y. Selective oxidation of glycerol to formic acid in highly concentrated aqueous solutions with molecular oxygen using V-substituted phosphomolybdic acids. *RSC Adv* 2014;4:35463–6.
- [458] Xu J, Zhao Y, Xu H, Zhang H, Yu B, Hao L, et al. Selective oxidation of glycerol to formic acid catalyzed by Ru(OH)₄/r-GO in the presence of FeCl₃. *Appl Catal B: Environ* 2014;154:5–267–73.
- [459] Kapkowski M, Bartczak P, Korczec M, Sitko R, Szade J, Balin K, et al. SiO₂-, Cu-, and Ni-supported Au nanoparticles for selective glycerol oxidation in the liquid phase. *J Catal* 2014;319:110–18.
- [460] Manas MG, Campos J, Sharnighausen LS, Lin E, Crabtree RH. Selective catalytic oxidation of sugar alcohols to lactic acid. *Green Chem* 2015;17:594–600.
- [461] Maris EP, Davis RJ. Hydrogenolysis of glycerol over carbon-supported Ru and Pt catalysts. *J Catal* 2007;249:328–37.
- [462] Maris EP, Ketchie WC, Murayama M, Davis RJ. Glycerol hydrogenolysis on carbon-supported PtRu and AuRu bimetallic catalysts. *J Catal* 2007;251:281–94.
- [463] Wang X, Song Y, Huang C, Liang F, Chen B. Lactic acid production from glucose over polymer catalysts in aqueous alkaline solution under mild conditions. *Green Chem* 2014;16:4234–40.
- [464] Biella S, Prati L, Rossi M. Selective oxidation of D-glucose on gold catalyst. *J Catal* 2002;206:242–7.
- [465] Ishida T, Kinoshita N, Okatsu H, Akita T, Takei T, Haruta M. Influence of the support and the size of gold clusters on catalytic activity for glucose oxidation. *Angew Chem Int Ed* 2008;47:9265–8.
- [466] Katryniok B, Kimura H, Skrzynińska E, Girardon JS, Fongarland P, Capron M, et al. Selective catalytic oxidation of glycerol: perspectives for high value chemicals. *Green Chem* 2011;13:1960–79.
- [467] Li H, Kotri R, Zhang Q, Shumugavel S, Yang S. Chemoselective oxidation of bio-glycerol with nano-sized metal catalysts. *Mini-Rev Org Chem* 2015;12:162–77.
- [468] Zhou CH, Zhao H, Tong DS, Wu LM, Yu WH. Recent advances in catalytic conversion of glycerol. *Catal Rev* 2013;55:369–453.
- [469] Dusselier M, Wouwe PV, Dewaele A, Makshina E, Sels BF. Lactic acid as a platform chemical in the biobased economy: the role of chemocatalysis. *Energy Environ Sci* 2013;6:1415–42.
- [470] Wang Y, Deng W, Wang B, Zhang Q, Wan X, Tang Z, et al. Chemical synthesis of lactic acid from cellulose catalysed by lead(II) ions in water. *Nat Commun* 2013;4:2141–7.
- [471] Wang FF, Liu CL, Dong WS. Highly efficient production of lactic acid from cellulose using lanthanide triflate catalysts. *Green Chem* 2013;15:2091–5.
- [472] Bermejo-Deval R, Assary RS, Nikolla E, Moliner M, Román-Leshkov Y, Hwang SJ, et al. Metalloenzyme-like catalyzed isomerizations of sugars by Lewis acid zeolites. *Proc Natl Acad Sci USA* 2012;109:9727–32.
- [473] Huo Z, Fang Y, Ren D, Zhang S, Yao G, Zeng X, et al. Selective conversion of glucose into lactic acid with transition metal ions in diluted aqueous NaOH solution. *ACS Sust Chem Eng* 2014;2:2765–71.
- [474] Mei N, Liu B, Zheng J, Lv K, Tang D, Zhang Z. A novel magnetic palladium catalyst for the mild aerobic oxidation of 5-hydroxymethylfurfural into 2,5-furandicarboxylic acid in water. *Catal Sci Technol* 2015;5:3194–202.
- [475] Vasiliu M, Jones AJ, Guynn K, Dixon DA. Prediction of the thermodynamic properties of key products and intermediates from biomass II. *J Phys Chem C* 2012;116:20738–54.
- [476] Tsanaktsis V, Vouvoudi E, Papageorgiou GZ, Papageorgiou DG, Chrissafis K, Bikiaris DN. Thermal degradation kinetics and decomposition mechanism of polyesters based on 2,5-furandicarboxylic acid and low molecular weight aliphatic diols. *J Anal Appl Pyrol* 2014;112:369–78.
- [477] Wilsens CHRM, Verhoeven JMGA, Noordover BAJ, Hansen MR, Auhl D, Rastogi S. Thermotropic polyesters from 2,5-furandicarboxylic acid and vanillic acid: synthesis, thermal properties, melt behavior, and mechanical performance. *Macromolecules* 2014;47:3306–16.
- [478] Wu B, Xu Y, Bu Z, Wu L, Li BG, Dubois P. Biobased poly(butylene 2,5-furandicarboxylate) and poly(butylene adipate-co-butylene 2,5-furandicarboxylate)s: from synthesis using highly purified 2,5-furandicarboxylic acid to thermo-mechanical properties. *Polymer (Guildf)* 2014;55:3648–55.
- [479] Wahlen J, Moens B, De Vos DE, Alsters PL, Jacobs PA. Titanium silicalite 1 (TS-1) catalyzed oxidative transformations of furan derivatives with hydrogen peroxide. *Adv Synth Catal* 2004;346:333–8.
- [480] Hansen TS, Sádaba I, García-Suárez EJ, Riisager A. Cu catalyzed oxidation of 5-hydroxymethylfurfural to 2,5-diformylfuran and 2,5-furandicarboxylic acid under benign reaction conditions. *Appl Catal A Gen* 2013;456:44–50.
- [481] Sheldon RA. Selective catalytic synthesis of fine chemicals: opportunities and trends. *J Mol Catal A Chem* 1996;107:75–83.
- [482] Smith MB, March J. March's advanced organic chemistry: reactions, mechanisms, and structure. 5th ed. New York: Wiley & Sons; 2000.
- [483] Vinke P, van Dama HE, van Bekkum H. Platinum catalyzed oxidation of 5-hydroxymethylfurfural. *Stud Surf Sci Catal* 1990;55:147–58.
- [484] Vinke P, van der Poel W, van Bekkum H. On the oxygen tolerance of noble metal catalysts in liquid phase alcohol oxidations the influence of the support on catalyst deactivation. *Stud Surf Sci Catal* 1991;59:385–94.
- [485] Gorbaney YY, Kegnæs S, Riisager A. Effect of support in heterogeneous ruthenium catalysts used for the selective aerobic oxidation of HMF in water. *Top Catal* 2011;54:1318–24.
- [486] Ståhlberg T, Eyjólfssdóttir E, Gorbaney YY, Sádaba I, Riisager A. Aerobic oxidation of 5-(hydroxymethyl)furfural in ionic liquids with solid ruthenium hydroxide catalysts. *Catal Lett* 2012;142:1089–97.
- [487] Gorbaney YY, Klitgaard SK, Woodley JM, Christensen CH, Riisager A. Gold-catalyzed aerobic oxidation of 5-hydroxymethylfurfural in water at ambient temperature. *ChemSusChem* 2009;2:672–5.
- [488] Casanova O, Iborra S, Corma A. Biomass into chemicals: aerobic oxidation of 5-hydroxymethyl-2-furfural into 2,5-furandicarboxylic acid with gold nanoparticle catalysts. *ChemSusChem* 2009;2:1138–44.
- [489] Zope BN, Davis SE, Davis RJ. Influence of reaction conditions on diacid formation during Au-catalyzed oxidation of glycerol and hydroxymethylfurfural. *Top Catal* 2012;55:24–32.
- [490] Gupta NK, Nishimura S, Takagaki A, Ebihara K. Hydrotalcite-supported gold-nanoparticle-catalyzed highly efficient base-free aqueous oxidation of 5-hydroxymethylfurfural into 2,5-furandicarboxylic acid under atmospheric oxygen pressure. *Green Chem* 2011;13:824–7.
- [491] Pasini T, Piccinini M, Blosi M, Bonelli R, Albonetti S, Dimitratos N, et al. Selective oxidation of 5-hydroxymethyl-2-furfural using supported gold-copper nanoparticles. *Green Chem* 2011;13:2091–9.
- [492] Wan X, Zhou C, Chen J, Deng W, Zhang Q, Yang Y, et al. Base-free aerobic oxidation of 5-hydroxymethyl-furfural to 2,5-furandicarboxylic acid in water catalyzed by functionalized carbon nanotube-supported Au-Pd alloy nanoparticles. *ACS Catal* 2014;4:2175–85.
- [493] Albonetti S, Lolli A, Morandi V, Migliori A, Lucarelli C, Cavani F. Conversion of 5-hydroxymethylfurfural to 2,5-furandicarboxylic acid over Au-based catalysts: optimization of active phase and metal-support interaction. *Appl Catal B: Environ* 2015;163:520–30.
- [494] Davis SE, Houk LR, Tamargo EC, Datye AK, Davis RJ. Oxidation of 5-hydroxymethylfurfural over supported Pt, Pd and Au catalysts. *Catal Today* 2011;160:55–60.
- [495] Saha B, Dutta S, Abu-Omar MM. Aerobic oxidation of 5-hydroxymethylfurfural with homogeneous and nanoparticulate catalysts. *Catal Sci Technol* 2012;2:79–81.
- [496] Lilga MA, Hallen RT, Gray M. Production of oxidized derivatives of 5-hydroxymethylfurfural (HMF). *Top Catal* 2010;53:1264–9.
- [497] Kröger M, Prüße U, Vorlop KD. A new approach for the production of 2,5-furandicarboxylic acid by *in-situ* oxidation of 5-hydroxymethylfurfural starting from fructose. *Top Catal* 2000;13:237–42.
- [498] Ribeiro ML, Schuchardt U. Cooperative effect of cobalt acetylacetone and silica in the catalytic cyclization and oxidation of fructose to 2,5-furandicarboxylic acid. *Catal Commun* 2003;4:83–6.
- [499] Saha B, Gupta D, Abu-Omar MM, Modak A, Bhaumik A. Porphyrin-based porous organic polymer-supported iron(III) catalyst for efficient aerobic oxidation of 5-hydroxymethyl-furfural into 2,5-furandicarboxylic acid. *J Catal* 2013;299:316–20.
- [500] Gao L, Deng K, Zheng J, Liu B, Zhang Z. Efficient oxidation of biomass derived 5-hydroxymethylfurfural into 2,5-furandicarboxylic acid catalyzed by Merrifield resin supported cobalt porphyrin. *Chem Eng J* 2015;270:444–9.
- [501] Siyo B, Schneider M, Pohl MM, Langer P, Steinfeldt N. Synthesis, characterization, and application of PVP-Pd NP in the aerobic oxidation of 5-hydroxymethylfurfural (HMF). *Catal Lett* 2014;144:498–506.
- [502] Saha R, Dhepe PL. Synthesis of 2,5-furandicarboxylic acid by the aerobic oxidation of 5-hydroxymethyl fufural over supported metal catalysts. *React Kinet Mech Cat* 2014;112:173–87.
- [503] Jain A, Jonnalagadda SC, Ramanujachary KV, Mugweru A. Selective oxidation of 5-hydroxymethyl-2-furful to furan-2,5-dicarboxylic acid over spinel mixed metal oxide catalyst. *Catal Commun* 2015;58:179–82.
- [504] Rass HA, Essayem N, Besson M. Selective aerobic oxidation of 5-HMF into 2,5-furandicarboxylic acid with pt catalysts supported on TiO₂- and ZrO₂-based supports. *ChemSusChem* 2015;7:1206–17.
- [505] Liu B, Ren Y, Zhang Z. Aerobic oxidation of 5-hydroxymethylfurfural into 2,5-furandicarboxylic acid in water under mild conditions. *Green Chem* 2015;17:1610–17.
- [506] Zhang Z, Zhen J, Liu B, Lv K, Deng K. Selective aerobic oxidation of the biomass-derived precursor 5-hydroxymethylfurfural to 2,5-furandicarboxylic acid under mild conditions over a magnetic palladium nanocatalyst. *Green Chem* 2015;17:1308–17.
- [507] Wang S, Zhang Z, Liu B. Catalytic conversion of fructose and 5-hydroxymethylfurfural into 2,5-furandicarboxylic acid over a recyclable Fe₃O₄-Co₃O₄ magnetite nanocatalyst. *ACS Sust Chem Eng* 2015;3:406–12.
- [508] Partenheimer W, Grushin VV. Synthesis of 2,5-diformylfuran and furan-2,5-dicarboxylic acid by catalytic air-oxidation of 5-hydroxymethylfurfural:

- unexpectedly selective aerobic oxidation of benzyl alcohol to benzaldehyde with metal/bromide catalysts. *Adv Synth Catal* 2001;343:102–11.
- [509] Navarro OC, Canós AC, Chornet SI. Chemicals from biomass: aerobic oxidation of 5-hydroxymethyl-2-furaldehyde into diformylfuran catalyzed by immobilized vanadyl-pyridine complexes on polymeric and organofunctionalized mesoporous supports. *Top Catal* 2009;52:304–14.
- [510] Carlini C, Patrono P, Raspolli Galletti AM, Sbrana G, Zima V. Selective oxidation of 5-hydroxymethyl-2-furaldehyde to furan-2,5-dicarboxaldehyde by catalytic systems based on vanadyl phosphate. *Appl Catal A Gen* 2005;289:197–204.
- [511] Nie J, Liu H. Aerobic oxidation of 5-hydroxymethylfurfural to 2,5-difomylfuran on supported vanadium oxide catalysts: structural effect and reaction mechanism. *Pure Appl Chem* 2012;84:765–77.
- [512] Nie J, Xie J, Liu H. Efficient aerobic oxidation of 5-hydroxymethylfurfural to 2,5-difomylfuran on supported Ru catalysts. *J Catal* 2013;301:83–91.
- [513] Xiang X, He L, Yang Y, Guo B, Tong D, Hu C. A one-pot two-step approach for the catalytic conversion of glucose into 2,5-difomylfuran. *Catal Lett* 2011;141:735–41.
- [514] Yang ZZ, Deng J, Pan T, Guo QX, Fu Y. A one-pot approach for conversion of fructose to 2,5-difomylfuran by combination of Fe₃O₄-SBA-SO₃H and K-OMS-2. *Green Chem* 2012;14:2986–9.
- [515] Takagaki A, Takahashi M, Nishimura S, Ebizaki K. One-pot synthesis of 2,5-difomylfuran from carbohydrate derivatives by sulfonated resin and hydrotalcite-supported ruthenium catalysts. *ACS Catal* 2011;1:1562–5.
- [516] Yadav GD, Sharma RV. Biomass derived chemicals: environmentally benign process for oxidation of 5-hydroxymethylfurfural to 2,5-difomylfuran by using nano-fibrous Ag-OMS-2-catalyst. *Appl Catal B: Environ* 2014;147:293–301.
- [517] Nie J, Xie J, Liu H. Activated carbon-supported ruthenium as an efficient catalyst for selective aerobic oxidation of 5-hydroxymethylfurfural to 2,5-difomylfuran. *Chin J Catal* 2013;34:871–5.
- [518] Jia X, Ma J, Wang M, Du Z, Lu F, Wang F, et al. Promoted role of Cu(NO₃)₂ on aerobic oxidation of 5-hydroxymethylfurfural to 2,5-difomylfuran over VOSO₄. *Appl Catal A Gen* 2014;482:231–6.
- [519] Le NT, Lakshmanan P, Cho K, Han Y, Kim H. Selective oxidation of 5-hydroxymethyl-2-furful into 2,5-difomylfuran over VO²⁺ and Cu²⁺ ions immobilized on sulfonated carbon catalysts. *Appl Catal A Gen* 2013;464:305–12.
- [520] Wang Y, Liu B, Huang K, Zhang Z. Aerobic oxidation of biomass-derived 5-(hydroxymethyl)furfural into 2,5-difomylfuran catalyzed by the trimetallic mixed oxide (Co–Ce–Ru). *Ind Eng Chem Res* 2014;53:1313–19.
- [521] Liu R, Chen J, Chen L, Guo Y, Zhong J. One-step approach to 2,5-difomylfuran from fructose by using a bifunctional and recyclable acidic polyoxometalate catalyst. *ChemPlusChem* 2014;79:1448–54.
- [522] Liu Y, Zhu L, Tang J, Liu M, Cheng R, Hu C. One-pot, one-step synthesis of 2,5-difomylfuran from carbohydrates over Mo-containing keggin heteropolyacids. *ChemSusChem* 2014;7:3541–7.
- [523] Nie J, Liu H. Efficient aerobic oxidation of 5-hydroxymethylfurfural to 2,5-difomylfuran on manganese oxide catalysts. *J Catal* 2014;316:57–66.
- [524] Chen J, Guo Y, Chen J, Song L, Chen L. One-step approach to 2,5-difomylfuran from fructose by proton- and vanadium-containing graphitic carbon nitride. *ChemCatChem* 2014;6:3174–81.
- [525] Antonyraj CA, Kim B, Kim Y, Shin S, Lee KY, Kim I, et al. Heterogeneous selective oxidation of 5-hydroxymethyl-2-furful (HMF) into 2,5-difomylfuran catalyzed by vanadium supported activated carbon in MIBK, extracting solvent for HMF. *Catal Commun* 2014;57:64–8.
- [526] Xu F, Zhang Z. Polyaniline-grafted VO(acac)₂: an effective catalyst for the synthesis of 2,5-difomylfuran from 5-hydroxymethylfurfural and fructose. *ChemCatChem* 2015;7:1470–7.
- [527] Sádaba I, Gorbaney YY, Kegnæs S, Putluru SSR, Berg RW, Riisager A. Catalytic performance of zeolite-supported vanadia in the aerobic oxidation of 5-hydroxymethylfurfural to 2,5-difomylfuran. *ChemCatChem* 2013;5:284–93.
- [528] Kompanets MO, Kushch OV, Litvinov YE, Pliekhov OL, Novikova KV, Novokhatko AO, et al. Oxidation of 5-hydroxymethylfurfural to 2,5-difomylfuran with molecular oxygen in the presence of *N*-hydroxyphthalimide. *Catal Commun* 2014;57:60–3.
- [529] Tong X, Sun Y, Bai X, Li Y. Highly efficient aerobic oxidation of biomass-derived 5-hydroxymethyl fufural to produce 2,5-difomylfuran in the presence of copper salts. *RSC Adv* 2014;4:44307–11.
- [530] Chen J, Zhong J, Guo Y, Chen L. Ruthenium complex immobilized on poly(4-vinylpyridine)-functionalized carbon-nanotube for selective aerobic oxidation of 5-hydroxymethylfurfural to 2,5-difomylfuran. *RSC Adv* 2015;5:5933–40.
- [531] Artz J, Mallmann S, Palkovits R. Selective aerobic oxidation of HMF to 2,5-difomylfuran on covalent triazine frameworks-supported Ru catalysts. *ChemSusChem* 2015;8:672–9.
- [532] Tao F, Cui Y, Yang P, Gong Y. One-pot, one-step, catalytic synthesis of 2,5-difomylfuran from fructose. *Russ J Phys Chem A* 2014;88:1091–6.
- [533] Laugel C, Estrine B, Le Bras J, Hoffmann N, Marinkovic S, Muzart J. NaBr/DMSO-induced synthesis of 2,5-difomylfuran from fructose or 5-(hydroxymethyl)furfural. *ChemCatChem* 2014;6:1195–8.
- [534] Liu B, Zhang Z, Lv K, Deng K, Duan H. Efficient aerobic oxidation of biomass-derived 5-hydroxymethylfurfural to 2,5-difomylfuran catalyzed by magnetic nanoparticle supported manganese oxide. *Appl Catal A Gen* 2014;472:64–71.
- [535] Karimi B, Mirzaei HM, Farhangi E. Fe₃O₄@SiO₂–TEMPO as a magnetically recyclable catalyst for highly selective aerobic oxidation of 5-hydroxymethylfurfural into 2,5-difomylfuran under metal- and halogen-free conditions. *ChemCatChem* 2014;6:758–62.
- [536] Zhang Z, Yuan Z, Tang D, Ren Y, Lv K, Liu B. Iron oxide encapsulated by ruthenium hydroxyapatite as heterogeneous catalyst for the synthesis of 2,5-difomylfuran. *ChemSusChem* 2014;7:3496–504.
- [537] Wang S, Zhang Z, Liu B, Li J. Environmentally friendly oxidation of biomass derived 5-hydroxymethylfurfural into 2,5-difomylfuran catalyzed by magnetic separation of ruthenium catalyst. *Ind Eng Chem Res* 2014;53:5820–7.
- [538] Du Z, Ma J, Wang F, Liu J, Xu J. Oxidation of 5-hydroxymethylfurfural to maleic anhydride with molecular oxygen. *Green Chem* 2011;13:554–7.
- [539] Lan J, Lin J, Chen Z, Yin G. Transformation of 5-hydroxymethylfurfural (HMF) to maleic anhydride by aerobic oxidation with heteropolyacid catalysts. *ACS Catal* 2015;5:2035–41.
- [540] Shi S, Guo H, Yin G. Synthesis of maleic acid from renewable resources: catalytic oxidation of furfural in liquid media with dioxygen. *Catal Commun* 2011;12:731–3.
- [541] Lan J, Chen Z, Lin J, Yin G. Catalytic aerobic oxidation of renewable furfural to maleic anhydride and furanone derivatives with their mechanistic studies. *Green Chem* 2014;16:4351–8.
- [542] Alonso-Fagñndez N, Granados ML, Mariscal R, Ojeda M. Selective conversion of furfural to maleic anhydride and furan with VO_x/Al₂O₃ catalysts. *ChemSusChem* 2012;5:1984–90.
- [543] Alonso-Fagñndez N, Agirrebal-Telleria I, Arias PL, Fierro JLG, Mariscal R, López Granados M. Aqueous-phase catalytic oxidation of furfural with H₂O₂: high yield of maleic acid by using titanium silicalite-1. *RSC Adv* 2014;4:54960–72.
- [544] Ghaznavi T, Neage C, Patience GS. Partial oxidation of D-xylose to maleic anhydride and acrylic acid over vanadyl pyrophosphate. *Biomass Bioenergy* 2014;71:285–93.
- [545] Taarning E, Nielsen IS, Egeblad K, Madsen R, Christensen CH. Chemicals from renewables: aerobic oxidation of furfural and hydroxymethylfurfural over gold catalysts. *ChemSusChem* 2008;1:75–8.
- [546] Menegazzo F, Fantinel T, Signoretto M, Pinna F, Manzoli M. On the process for furfural and HMF oxidative esterification over Au/ZrO₂. *J Catal* 2014;319:61–70.
- [547] Menegazzo F, Signoretto M, Pinna F, Manzoli M, Aina V, Cerrato G, et al. Oxidative esterification of renewable furfural on gold-based catalysts: which is the best support? *J Catal* 2014;309:241–7.
- [548] Menegazzo F, Signoretto M, Marchese D, Pinna F, Manzoli M. Structure–activity relationships of Au/ZrO₂ catalysts for 5-hydroxymethylfurfural oxidative esterification: effects of zirconia sulphation on gold dispersion, position and shape. *J Catal* 2015;326:1–8.
- [549] Podolean I, Kuncser V, Gheorghie N, Macovei D, Parvulescu VI, Coman SM. Ru-based magnetic nanoparticles (MNP) for succinic acid synthesis from levulinic acid. *Green Chem* 2013;15:3077–82.
- [550] Choudhary H, Nishimura S, Ebizaki K. Metal-free oxidative synthesis of succinic acid from biomass-derived furan compounds using a solid acid catalyst with hydrogen peroxide. *Appl Catal A Gen* 2013;458:55–62.
- [551] Wang Y, Vogelsgang F, Román-Leshkov Y. Acid-catalyzed oxidation of levulinate derivatives to succinates under mild conditions. *ChemCatChem* 2015;7:916–20.
- [552] Wu L, Dutta S, Mascal M. Efficient, chemical-catalytic approach to the production of 3-hydroxypropanoic acid by oxidation of biomass-derived levulinic acid with hydrogen peroxide. *ChemSusChem* 2015;8:1167–9.
- [553] Dutta S, Wu L, Mascal M. Efficient, metal-free production of succinic acid by oxidation of biomass-derived levulinic acid with hydrogen peroxide. *Green Chem* 2015;17:2335–8.
- [554] Gorbaney YY, Kegnæs S, Riisager A. Selective aerobic oxidation of 5-hydroxymethylfurfural in water over solid ruthenium hydroxide catalysts with magnesium-based supports. *Catal Lett* 2011;141:1752–60.
- [555] Ståhlberg T, Sørensen MG, Riisager A. Direct conversion of glucose to 5-(hydroxymethyl)furfural in ionic liquids with lanthanide catalysts. *Green Chem* 2010;12:321–5.
- [556] Nielsen IS, Taarning E, Egeblad K, Madsen R, Christensen CH. Direct aerobic oxidation of primary alcohols to methyl esters catalyzed by a heterogeneous gold catalyst. *Catal Lett* 2007;116:35–40.
- [557] Albonetti S, Pasini T, Lolli A, Blosi M, Piccinini M, Dimitratos N, et al. Selective oxidation of 5-hydroxymethyl-2-furful over TiO₂-supported gold–copper catalysts prepared from preformed nanoparticles: effect of Au/Cu ratio. *Catal Today* 2012;195:120–6.
- [558] Davis SE, Zope BN, Davis RJ. On the mechanism of selective oxidation of 5-hydroxymethylfurfural to 2,5-furandicarboxylic acid over supported Pt and Au catalysts. *Green Chem* 2012;14:143–7.
- [559] Yi G, Teong SP, Li X, Zhang Y. Purification of biomass-derived 5-hydroxymethylfurfural and its catalytic conversion to 2,5-furandicarboxylic acid. *ChemSusChem* 2014;7:2131–5.
- [560] Yi G, Teong SP, Zhang Y. The direct conversion of sugars into 2,5-furandicarboxylic acid in a triphasic system. *ChemSusChem* 2015;8:1151–5.
- [561] Amarasekara AS, Green D, McMillan E. Efficient oxidation of 5-hydroxymethylfurfural to 2,5-difomylfuran using Mn(III)-salen catalysts. *Catal Commun* 2008;9:286–8.
- [562] Ziach K, Obrocka-Hrycyna A, Jurczak J. Dynamic combinatorial libraries of 2,5-difomylfuran-derived macrocycles. *J Org Chem* 2014;79:10334–41.
- [563] Ma J, Du Z, Xu J, Chu Q, Pang Y. Efficient aerobic oxidation of 5-hydroxymethylfurfural to 2,5-difomylfuran, and synthesis of a fluorescent material. *ChemSusChem* 2011;4:51–4.

- [564] Halliday GA, Young JRJ, Grushin VV. One-pot, two-step, practical catalytic synthesis of 2,5-diformylfuran from fructose. *Org Lett* 2003;5:2003–5.
- [565] Centi G, Trifiro F, Ebner JR, Franchetti VM. Mechanistic aspects of maleic anhydride synthesis from C₄ hydrocarbons over phosphorus vanadium oxide. *Chem Rev* 1988;88:55–80.
- [566] Tóth B, Varga C, Bartha L. Olefin-maleic-anhydride copolymer based additives: a novel approach for compatibilizing blends of waste polyethylene and crumb rubber. *Waste Manage* 2015;38:65–71.
- [567] Liu D, Zhang X, Zhu L, Wu J, Lü X. Alternating ring-opening copolymerization of styrene oxide and maleic anhydride using asymmetrical bis-Schiff-base metal(III) catalysts. *Catal Sci Technol* 2015;5:562–71.
- [568] Guo H, Yin G. Catalytic aerobic oxidation of renewable furfural with phosphomolybdic acid catalyst: an alternative route to maleic acid. *J Phys Chem C* 2011;115:17516–22.
- [569] Casanova O, Iborra S, Corma A. Biomass into chemicals: one pot-base free oxidative esterification of 5-hydroxymethyl-2-furfural into 2,5-dimethylfuroate with gold on nanoparticulated ceria. *J Catal* 2009;265:109–16.
- [570] Pan T, Deng J, Xu Q, Zuo Y, Guo QX, Fu Y. Catalytic conversion of furfural into a 2,5-furandicarboxylic acid-based polyester with total carbon utilization. *ChemSusChem* 2013;6:47–50.
- [571] Ma J, Pang Y, Wang M, Xu J, Ma H, Nie X. The copolymerization reactivity of diols with 2,5-furandicarboxylic acid for furan-based copolyester materials. *J Mater Chem* 2012;22:3457–61.
- [572] Erhart AJE, Faaij APC, Patel MK. Replacing fossil based PET with biobased PEF: process analysis, energy and GHG balance. *Energy Environ Sci* 2012;5:6407–22.
- [573] Gomes M, Gandini A, Silvestre AJD, Reis B. Synthesis and characterization of poly(2,5-furan dicarboxylate)s based on a variety of diols. *J Polym Sci Part A Polym Chem* 2011;49:3759–68.
- [574] Ma J, Wang M, Du Z, Chen C, Gao J, Xu J. Synthesis and properties of furan-based imine-linked porous organic frameworks. *Polym Chem* 2012;3:2346–9.
- [575] Amarasekara AS, Green D, Williams LTD. Renewable resources based polymers: synthesis and characterization of 2,5-diformylfuran–urea resin. *Eur Polym J* 2009;45:595–8.
- [576] Narayanaswamy R, Ismail IS. Cosmetic potential of Southeast Asian herbs: an overview. *Phytochem Rev* 2015;14:419–28.
- [577] Markus H, Plomp AJ, Sandberg T, Nieminen V, Bitter JH, Murzin DY. Dehydrogenation of hydroxymatairesinol to oxomatairesinol over carbon nanofibre-supported palladium catalysts. *J Mol Catal A Chem* 2007;274:42–9.
- [578] Simakova OA, Murzina EV, Mäki-Arvela P, Leino AR, Campo BC, Kordas K, et al. Oxidative dehydrogenation of a biomass derived lignan-hydroxymatairesinol over heterogeneous gold catalysts. *J Catal* 2011;282:54–64.
- [579] Simakova OA, Smolentseva E, Estrada M, Murzina EV, Beloshapkin S, Willför SM, et al. From woody biomass extractives to health-promoting substances: selective oxidation of the lignan hydroxymatairesinol to oxomatairesinol over Au, Pd, and Au–Pd heterogeneous catalysts. *J Catal* 2012;291:95–103.
- [580] López M, Simakova OA, Murzina EV, Willför SM, Prosvirin I, Simakov A, et al. Gold particle size effect in biomass-derived lignin hydroxymatairesinol oxidation over Au/Al₂O₃ catalysts. *Appl Catal A Gen* 2015;504:248–55.
- [581] Ragauskas AJ, Beckham GT, Biddy MJ, Chandra R, Chen F, Davis MF, et al. Lignin valorization: improving lignin processing in the biorefinery. *Science* 2014;344:1246843.
- [582] Kang S, Li X, Fan J, Chang J. Hydrothermal conversion of lignin: a review. *Renew Sust Energy Rev* 2013;27:546–58.
- [583] Zhao Y, Xu Q, Pan T, Zuo Y, Fu Y, Guo QX. Depolymerization of lignin by catalytic oxidation with aqueous polyoxometalates. *Appl Catal A Gen* 2013;467:504–8.
- [584] Gao P, Li C, Wang H, Wang X, Wang A. Perovskite hollow nanospheres for the catalytic wet air oxidation of lignin. *Chin J Catal* 2013;34:1811–15.
- [585] Ma R, Xu Y, Zhang X. Catalytic oxidation of biorefinery lignin to value-added chemicals to support sustainable biofuel production. *ChemSusChem* 2015;8:24–51.
- [586] Chatel G, Rogers RD. Review: oxidation of lignin using ionic liquids – an innovative strategy to produce renewable chemicals. *ACS Sust Chem Eng* 2014;2:322–39.
- [587] Chenna NK, Jääskeläinen AS, Vuorinen T. Rapid and selective catalytic oxidation of hexenuronic acid and lignin in cellulosic fibers. *Ind Eng Chem Res* 2013;52:17744–9.
- [588] Yoshikawa T, Yagi T, Shinohara S, Fukunaga T, Nakasaka Y, Tago T, et al. Production of phenols from lignin via depolymerization and catalytic cracking. *Fuel Process Technol* 2013;108:69–75.
- [589] Toledano A, Serrano L, Labidi J. Organosolv lignin depolymerization with different base catalysts. *J Chem Technol Biotechnol* 2012;87:1593–9.
- [590] Climent MJ, Corma A, Iborra S. Conversion of biomass platform molecules into fuel additives and liquid hydrocarbon fuels. *Green Chem* 2014;16:516–47.
- [591] Larabi C, Maksoud WA, Szeto KC, Garron A, Arquilliere PP, Walter JJ, et al. Multifunctional heterogeneous catalyst for one step transformation of lignocellulosic biomass into low oxygenated hydrocarbons. *Appl Catal A Gen* 2015;495:162–72.
- [592] Dhepe PL, Fukuoka A. Cellulose conversion under heterogeneous catalysis. *ChemSusChem* 2008;1:969–75.
- [593] Dhepe PL, Fukuoka A. Cracking of cellulose over supported metal catalysts. *Catal Surv Asia* 2007;11:186–91.
- [594] Kamm B. Production of platform chemicals and synthesis gas from biomass. *Angew Chem Int Ed* 2007;46:5056–8.
- [595] Palkovits R, Tajvidi K, Procelewska J, Rinaldi R, Ruppert A. Hydrogenolysis of cellulose combining mineral acids and hydrogenation catalysts. *Green Chem* 2010;12:972–8.
- [596] Yan N, Zhao C, Luo C, Dyson PJ, Liu H, Kou Y. One-step conversion of cellobiose to C₆-alcohols using a ruthenium nanocluster catalyst. *J Am Chem Soc* 2006;128:8714–15.
- [597] Deng W, Liu M, Tan X, Zhang Q, Wang Y. Conversion of cellobiose into sorbitol in neutral water medium over carbon nanotube-supported ruthenium catalysts. *J Catal* 2010;271:22–32.
- [598] Ran M, Liu Y, Chu W, Liu Z, Borgna A. High dispersion of Ru nanoparticles supported on carbon nanotubes synthesized by water-assisted chemical vapor deposition for cellobiose conversion. *Catal Commun* 2012;27:69–72.
- [599] Ran M, Liu Y, Chu W, Borgna A. Enhanced conversion of cellobiose to sugar alcohols by controlled dispersion of ruthenium nanoparticles inside carbon nanotube channels. *Catal Lett* 2013;143:1139–44.
- [600] Luo C, Wang S, Liu H. Cellulose conversion into polyols catalyzed by reversibly formed acids and supported ruthenium clusters in hot water. *Angew Chem Int Ed* 2007;46:7636–9.
- [601] Liu QY, Liao YH, Wang TJ, Cai CL, Zhang Q, Tsubaki N, et al. One-pot transformation of cellulose to sugar alcohols over acidic metal phosphates combined with Ru/C. *Ind Eng Chem Res* 2014;53:12655–64.
- [602] Han JW, Lee H. Direct conversion of cellulose into sorbitol using dual-functionalized catalysts in neutral aqueous solution. *Catal Commun* 2012;19:115–18.
- [603] Liu M, Deng W, Zhang Q, Wang Y, Wang Y. Polyoxometalate-supported ruthenium nanoparticles as bifunctional heterogeneous catalysts for the conversions of cellobiose and cellulose into sorbitol under mild conditions. *Chem Commun* 2011;47:9717–19.
- [604] Xie X, Han J, Wang H, Zhu X, Liu X, Niu Y, et al. Selective conversion of microcrystalline cellulose into hexitols over a Ru/[Bmim]PW₁₂O₄₀ catalyst under mild conditions. *Catal Today* 2014;233:70–6.
- [605] Negoi A, Triantafyllidis K, Parvulescu VI, Coman SM. The hydrolytic hydrogenation of cellulose to sorbitol over M (Ru, Ir, Pd, Rh)-BEA-zeolite catalysts. *Catal Today* 2014;223:122–8.
- [606] Mishra DK, Dabbawala AA, Park JJ, Jhung SH, Hwang JS. Selective hydrogenation of D-glucose to D-sorbitol over HY zeolite supported ruthenium nanoparticles catalysts. *Catal Today* 2014;232:99–107.
- [607] Xi J, Zhang Y, Xia Q, Liu X, Ren J, Lu G, et al. Direct conversion of cellulose into sorbitol with high yield by a novel mesoporous niobium phosphate supported ruthenium bifunctional catalyst. *Appl Catal A Gen* 2013;459:52–8.
- [608] Reyes-Luyanda D, Flores-Cruz J, Morales-Pérez PJ, Encarnación-Gómez LG, Shi F, Voyles PM, et al. Bifunctional materials for the catalytic conversion of cellulose into soluble renewable biorefinery feedstocks. *Top Catal* 2012;55:148–61.
- [609] Wu Z, Ge S, Ren C, Zhang M, Yip A, Xu C. Selective conversion of cellulose into bulk chemicals over Bronsted acid-promoted ruthenium catalyst: one-pot vs. sequential process. *Green Chem* 2012;14:3336–43.
- [610] Liao Y, Liu Q, Wang T, Long J, Ma L, Zhang Q. Zirconium phosphate combined with Ru/C as a highly efficient catalyst for the direct transformation of cellulose to C₆ alditols. *Green Chem* 2014;16:3305–12.
- [611] Chen J, Wang S, Huang J, Chen L, Ma L, Huang X. Conversion of cellulose and cellobiose into sorbitol catalyzed by ruthenium supported on a polyoxometalate/metal–organic framework hybrid. *ChemSusChem* 2013;6:1545–55.
- [612] Fukuoka A, Dhepe PL. Catalytic conversion of cellulose into sugar alcohols. *Angew Chem Int Ed* 2006;45:5161–3.
- [613] Park DS, Yun D, Kim TY, Baek J, Yun YS, Yi J. A mesoporous carbon-supported Pt nanocatalyst for the conversion of lignocellulose to sugar alcohols. *ChemSusChem* 2013;6:2281–9.
- [614] Li J, Liu L, Liu Y, Li M, Zhu Y, Liu H, et al. Direct conversion of cellulose using carbon monoxide and water on a Pt–Mo₂C/C catalyst. *Energy Environ Sci* 2014;7:393–8.
- [615] Rodiansono R, Shimazu S. Effective production of sorbitol and mannitol from sugars catalyzed by Ni nanoparticles supported on aluminium hydroxide. *Bull Chem Reac Eng Catal* 2013;8:40–6.
- [616] Pang J, Wang A, Zheng M, Zhang Y, Huang Y, Chen X, et al. Catalytic conversion of cellulose to hexitols with mesoporous carbon supported Ni-based bimetallic catalysts. *Green Chem* 2012;14:614–17.
- [617] Van de Vyver S, Geboers J, Dusselier M, Schepers H, Vosch T, Zhang L, et al. Selective bifunctional catalytic conversion of cellulose over reshaped Ni particles at the tip of carbon nanofibers. *ChemSusChem* 2010;3:698–701.
- [618] Van de Vyver S, Geboers J, Schutwyser W, Dusselier M, Eloy P, Dornez E, et al. Tuning the acid/metal balance of carbon nanofiber-supported nickel catalysts for hydrolytic hydrogenation of cellulose. *ChemSusChem* 2012;5:1549–58.
- [619] Ji N, Zhang T, Zheng M, Wang A, Wang H, Wang X, et al. Direct catalytic conversion of cellulose into ethylene glycol using nickel-promoted tungsten carbide catalysts. *Angew Chem Int Ed* 2008;47:8510–13.
- [620] Pang J, Zheng M, Wang A, Zhang T. Catalytic hydrogenation of corn stalk to ethylene glycol and 1,2-propylene glycol. *Ind Eng Chem Res* 2011;50:6601–8.
- [621] Zhao G, Zheng M, Wang A, Zhang T. Catalytic conversion of cellulose to ethylene glycol over tungsten phosphide catalysts. *Chin J Catal* 2010;31:928–32.

- [622] Ji N, Zhang T, Zheng M, Wang A, Wang H, Wang X, et al. Catalytic conversion of cellulose into ethylene glycol over supported carbide catalysts. *Catal Today* 2009;147:77–85.
- [623] Zhang Y, Wang A, Zhang T. A new 3D mesoporous carbon replicated from commercial silica as a catalyst support for direct conversion of cellulose into ethylene glycol. *Chem Commun* 2010;46:862–4.
- [624] Tai Z, Zhang J, Wang A, Zheng M, Zhang T. Temperature-controlled phase-transfer catalysis for ethylene glycol production from cellulose. *Chem Commun* 2012;48:7052–4.
- [625] Tai Z, Zhang J, Wang A, Pang J, Zheng M, Zhang T. Catalytic conversion of cellulose to ethylene glycol over a low-cost binary catalyst of raney Ni and tungstic acid. *ChemSusChem* 2013;6:652–8.
- [626] Liu Y, Luo C, Liu H. Tungsten trioxide promoted selective conversion of cellulose into propylene glycol and ethylene glycol on a ruthenium catalyst. *Angew Chem Int Ed* 2012;51:3249–53.
- [627] Zheng M, Wang A, Ji N, Pang J, Wang X, Zhang T. Transition metal-tungsten bimetallic catalysts for the conversion of cellulose into ethylene glycol. *ChemSusChem* 2010;3:63–6.
- [628] Xi J, Ding D, Shao Y, Liu X, Lu G, Wang Y. Production of ethylene glycol and its monoether derivative from cellulose. *ACS Sust Chem Eng* 2014;2:2355–62.
- [629] Wang H, Zhu L, Peng S, Peng F, Yu H, Yang J. High efficient conversion of cellulose to polyols with Ru/CNTs as catalyst. *Renew Energy* 2012;37:192–6.
- [630] Deng W, Tan X, Fang W, Zhang Q, Wang Y. Conversion of cellulose into sorbitol over carbon nanotube-supported ruthenium catalyst. *Catal Lett* 2009;133:167–74.
- [631] Hattori H, Shishido T. Molecular hydrogen-originated protonic acid site as active site on solid acid catalyst. *Catal Surv Asia* 1997;1:205–13.
- [632] Lonergan WW, Vlachos DG, Chen JG. Correlating extent of Pt–Ni bond formation with low-temperature hydrogenation of benzene and 1,3-butadiene over supported Pt/Ni bimetallic catalysts. *J Catal* 2010;271:239–50.
- [633] Mu R, Fu Q, Xu H, Zhang H, Huang Y, Jiang Z, et al. Synergetic effect of surface and subsurface Ni species at Pt–Ni bimetallic catalysts for CO oxidation. *J Am Chem Soc* 2011;133:1978–86.
- [634] Rinaldi R, Porcari ADM, Rocha TC, Cassinelli WH, Ribeiro RU, Bueno JMC, et al. Construction of heterogeneous Ni catalysts from supports and colloidal nanoparticles—A challenging puzzle. *J Mol Catal A Chem* 2009;301:11–17.
- [635] De Jong KP, Geus JW. Carbon nanofibers: catalytic synthesis and applications. *Catal Rev* 2000;42:481–510.
- [636] Rodríguez-Reinoso F. The role of carbon materials in heterogeneous catalysis. *Carbon* 1998;36:159–75.
- [637] Tajvidi K, Hausoul PJ, Palkovits R. Hydrogenolysis of cellulose over Cu-based catalysts – Analysis of the reaction network. *ChemSusChem* 2014;7:1311–17.
- [638] Wang A, Zhang T. One-pot conversion of cellulose to ethylene glycol with multifunctional tungsten-based catalysts. *Acc Chem Res* 2013;46:1377–86.
- [639] Hu L, Lin L, Liu S. Chemoselective hydrogenation of biomass-derived 5-hydroxymethylfurfural into the liquid biofuel 2,5-dimethylfuran. *Ind Eng Chem Res* 2014;53:9969–78.
- [640] Dutta S, Maschal M. Novel pathways to 2,5-dimethylfuran via biomass-derived 5-(chloromethyl)furfural. *ChemSusChem* 2014;7:3028–30.
- [641] Nagpure AS, Venugopal AK, Lucas N, Manikandan M, Thirumalaiswamy R, Chilukuri S. Renewable fuels from biomass-derived compounds: Ru-containing hydrotalcites as catalysts for conversion of HMF to 2,5-dimethylfuran. *Catal Sci Technol* 2015;5:1463–72.
- [642] Qian Y, Zhu L, Wang Y, Lu X. Recent progress in the development of biofuel 2,5-dimethylfuran. *Renew Sust Energy Rev* 2015;41:633–46.
- [643] Saha B, Abu-Omar MM. Current technologies, economics, and perspectives for 2,5-dimethylfuran production from biomass-derived intermediates. *ChemSusChem* 2015;8:1133–42.
- [644] Roman-Leshkov Y, Barrett CJ, Liu ZY, Dumesic JA. Production of dimethylfuran for liquid fuels from biomass-derived carbohydrates. *Nature* 2007;447:982–5.
- [645] Upare PP, Hwang DW, Hwang YK, Lee UH, Hong DY, Chang JS. An integrated process for the production of 2,5-dimethylfuran from fructose. *Green Chem* 2015;17:3310–13.
- [646] Chidambaram M, Bell AT. A two-step approach for the catalytic conversion of glucose to 2,5-dimethylfuran in ionic liquids. *Green Chem* 2010;12:1253–62.
- [647] Wang J, Liu X, Hu B, Lu G, Wang Y. Efficient catalytic conversion of lignocellulosic biomass into renewable liquid biofuels via furan derivatives. *RSC Adv* 2014;4:31101–7.
- [648] Wang GH, Hilgert J, Richter FH, Wang F, Bongard HJ, Spliethoff B, et al. Platinum–cobalt bimetallic nanoparticles in hollow carbon nanospheres for hydrogenolysis of 5-hydroxymethylfurfural. *Nat Mater* 2014;13:293–300.
- [649] Zhu Y, Kong X, Zheng H, Ding G, Zhu Y, Li YW. Efficient synthesis of 2,5-dihydroxymethylfuran and 2,5-dimethylfuran from 5-hydroxymethylfurfural using mineral-derived Cu catalysts as versatile catalysts. *Catal Sci Technol* 2015;5:4208–17.
- [650] Yang P, Cui Q, Zu Y, Liu X, Lu G, Wang Y. Catalytic production of 2,5-dimethylfuran from 5-hydroxymethylfurfural over Ni/Co₃O₄ catalyst. *Catal Commun* 2015;66:55–9.
- [651] Nishimura S, Ikeda N, Ebitani K. Selective hydrogenation of biomass-derived 5-hydroxymethylfurfural (HMF) to 2,5-dimethylfuran (DMF) under atmospheric hydrogen pressure over carbon supported PdAu bimetallic catalyst. *Catal Today* 2014;232:89–98.
- [652] Zu Y, Yang P, Wang J, Liu X, Ren J, Lu G, et al. Efficient production of the liquid fuel 2,5-dimethylfuran from 5-hydroxymethylfurfural over Ru/Co₃O₄ catalyst. *Appl Catal B: Environ* 2014;146:244–8.
- [653] Nagpure AS, Lucas N, Chilukuri SV. Efficient preparation of liquid fuel 2,5-dimethylfuran from biomass-derived 5-hydroxymethylfurfural over Ru–NaY catalyst. *ACS Sust Chem Eng* 2015;3:2909–16.
- [654] Saha B, Bohn CM, Abu-Omar MM. Zinc-assisted hydrodeoxygenation of biomass-derived 5-hydroxymethylfurfural to 2,5-dimethylfuran. *ChemSusChem* 2014;7:3095–101.
- [655] Shi J, Wang Y, Yu X, Du W, Hou Z. Production of 2,5-dimethylfuran from 5-hydroxymethylfurfural over reduced graphene oxides supported Pt catalyst under mild conditions. *Fuel* 2016;163:74–9.
- [656] Huang YB, Chen MY, Yan L, Guo QX, Fu Y. Nickel-tungsten carbide catalysts for the production of 2,5-dimethylfuran from biomass-derived molecules. *ChemSusChem* 2014;7:1068–72.
- [657] Thanathanthanachon T, Rauchfuss TB. Efficient production of the liquid fuel 2,5-dimethylfuran from fructose using formic acid as a reagent. *Angew Chem Int Ed* 2010;49:6616–18.
- [658] De S, Dutta S, Saha B. One-pot conversions of lignocellulosic and algal biomass into liquid fuels. *ChemSusChem* 2012;5:1826–33.
- [659] Nakagawa Y, Tomishige K. Total hydrogenation of furan derivatives over silica-supported Ni–Pd alloy catalyst. *Catal Commun* 2010;12:154–6.
- [660] Alamillo R, Tucker M, Chia M, Pagán-Torres Y, Dumesic J. The selective hydrogenation of biomass-derived 5-hydroxymethylfurfural using heterogeneous catalysts. *Green Chem* 2012;14:1413–19.
- [661] Cai H, Li C, Wang A, Zhang T. Biomass into chemicals: one-pot production of furan-based diols from carbohydrates via tandem reactions. *Catal Today* 2014;234:59–65.
- [662] Yang Y, Du Z, Ma J, Lu F, Zhang J, Xu J. Biphasic catalytic conversion of fructose by continuous hydrogenation of HMF over a hydrophobic ruthenium catalyst. *ChemSusChem* 2014;7:1352–6.
- [663] Ohyama J, Esaki A, Yamamoto Y, Arai S, Satsuma A. Selective hydrogenation of 2-hydroxymethyl-5-furfural to 2,5-bis(hydroxymethyl)furan over gold sub-nano clusters. *RSC Adv* 2013;3:1033–6.
- [664] Chatterjee M, Ishizaka T, Kawanami H. Selective hydrogenation of 5-hydroxymethylfurfural to 2,5-bis(hydroxymethyl)furan using Pt/MCM-41 in an aqueous medium: a simple approach. *Green Chem* 2014;16:4734–9.
- [665] Yang W, Sen A. One-step catalytic transformation of carbohydrates and cellulosic biomass to 2,5-dimethyltetrahydrofuran for liquid fuels. *ChemSusChem* 2010;3:597–603.
- [666] Yépez A, Pineda A, García A, Romero AA, Luque R. Chemical transformations of glucose to value added products using Cu-based catalytic systems. *Phys Chem Chem Phys* 2013;15:12165–72.
- [667] Mitra J, Zhou X, Rauchfuss T. Pd/C-catalyzed reactions of HMF: decarbonylation, hydrogenation, and hydrogenolysis. *Green Chem* 2015;17:307–13.
- [668] Liu F, Audemar M, Vigier KDO, Clacens JM, Campo FD, Jérôme F. Combination of Pd/C and Amberlyst-15 in a single reactor for the acid/hydrogenating catalytic conversion of carbohydrates to 5-hydroxy-2,5-hexanedione. *Green Chem* 2014;16:4110–14.
- [669] Zhou H, Song J, Meng Q, He Z, Jiang Z, Zhou B, et al. Cooperative catalysis of Pt/C and acid resin for the production of 2,5-dimethyltetrahydrofuran from biomass derived 2,5-hexanedione under mild conditions. *Green Chem* 2016;18:220–5.
- [670] Jackson MA, Appell M, Blackburn JA. Hydrodeoxygenation of fructose to 2,5-dimethyltetrahydrofuran using a sulfur poisoned Pt/C catalyst. *Ind Eng Chem Res* 2015;54:7059–66.
- [671] Schlaef M. Selective deoxygenation of sugar polyols to α,ω -diols and other oxygen content reduced materials – A new challenge to homogeneous ionic hydrogenation and hydrogenolysis catalysis. *Dalton Trans* 2006;4645–53.
- [672] Tong X, Ma Y, Li Y. Biomass into chemicals: conversion of sugars to furan derivatives by catalytic processes. *Appl Catal A Gen* 2010;385:1–13.
- [673] Kong X, Zhu Y, Zheng H, Dong F, Zhu Y, Li Y-W. Switchable synthesis of 2,5-dimethylfuran and 2,5-dihydroxymethyltetrahydrofuran from 5-hydroxymethylfurfural over Raney Ni catalyst. *RSC Adv* 2014;4:60467–72.
- [674] Kang ES, Chae DW, Kim B, Kim YG. Efficient preparation of DHMF and HMFA from biomass-derived HMF via a Cannizzaro reaction in ionic liquids. *J Ind Eng Chem* 2012;18:174–7.
- [675] Dutta S, De S, Saha B. A brief summary of the synthesis of polyester building-block chemicals and biofuels from 5-hydroxymethylfurfural. *ChemPlusChem* 2012;77:259–72.
- [676] Grochowski MR, Yang W, Sen A. Mechanistic study of a one-step catalytic conversion of fructose to 2,5-dimethyltetrahydrofuran. *Chem Eur J* 2012;18:12363–71.
- [677] Luijckx GCA, Huck NPM, van Rantwijk F, Maat L, van Bekkum H. Ether formation in the hydrogenolysis of hydroxymethylfurfural over palladium catalysts in alcoholic solution. *Heterocycles* 2009;77:1037–44.
- [678] Kong X, Zhu Y, Zheng H, Li X, Zhu Y, Li YW. Ni nanoparticles inlaid nickel phyllosilicate as a metal-acid bifunctional catalyst for low-temperature hydrogenolysis reactions. *ACS Catal* 2015;5:5914–20.
- [679] Panagiotopoulou P, Martin N, Vlachos DG. Liquid-phase catalytic transfer hydrogenation of furfural over homogeneous Lewis acid-Ru/C catalysts. *ChemSusChem* 2015;8:2046–54.
- [680] Sharma RV, Das U, Sammynaiken R, Dalai AK. Liquid phase chemo-selective catalytic hydrogenation of furfural to furfuryl alcohol. *Appl Catal A Gen* 2013;454:127–36.
- [681] Yan K, Wu G, Lafleur T, Jarvis C. Production, properties and catalytic hydrogenation of furfural to fuel additives and value-added chemicals. *Renew Sust Energy Rev* 2014;38:663–76.

- [682] Zhang W, Zhu Y, Niu S, Li Y. A study of furfural decarbonylation on K-doped Pd/Al₂O₃ catalysts. *J Mol Catal A Chem* 2011;335:71–81.
- [683] Chuang IS, Maciel GE, Myers GE. Carbon-13 NMR study of curing in furfuryl alcohol resins. *Macromolecules* 1984;17:1087–90.
- [684] Burnette LW. The production of rubber from furfural. *Rubber Chem Technol* 1945;18:284–5.
- [685] Luo W, Liu J, Ma Y, Zhang B, Yang W. Preparation of polymer nanoparticles from renewable biobased furfuryl alcohol and maleic anhydride by stabilizer-free dispersion polymerization. *J Polym Sci Part A Polym Chem* 2012;50:3606–17.
- [686] Fam A, Eldridge A, Misra M. Mechanical characteristics of glass fibre reinforced polymer made of furfuryl alcohol bio-resin. *Mater Struct* 2014;47:1195–204.
- [687] Lange J-P, van de Graaf WD, Haan RJ. Conversion of furfuryl alcohol into ethyl levulinate using solid acid catalysts. *ChemSusChem* 2009;2:437–41.
- [688] Yao J, Wang H. Preparation of crystalline mesoporous titania using furfuryl alcohol as polymerizable solvent. *Ind Eng Chem Res* 2007;46:6264–8.
- [689] Dunlop AP, Peters JFN. The nature of furfuryl alcohol. *Ind Eng Chem* 1942;34:814–17.
- [690] Rao R, Dandekar A, Baker RTK, Vannice MA. Properties of copper chromite catalysts in hydrogenation reactions. *J Catal* 1997;171:406–19.
- [691] Nagaraja BM, Padmasri AH, Seetharamulu P, Hari Prasad Reddy K, David Raju B, Rama Rao KS. A highly active Cu-MgO-Cr₂O₃ catalyst for simultaneous synthesis of furfuryl alcohol and cyclohexanone by a novel coupling route – Combination of furfural hydrogenation and cyclohexanol dehydrogenation. *J Mol Catal A Chem* 2007;278:29–37.
- [692] Yan K, Liao J, Wu X, Xie X. A noble-metal free Cu-catalyst derived from hydrotalcite for highly efficient hydrogenation of biomass-derived furfural and levulinic acid. *RSC Adv* 2013;3:3853–6.
- [693] Nagaraja BM, Padmasri AH, David Raju B, Rama Rao KS. Vapor phase selective hydrogenation of furfural to furfuryl alcohol over Cu-MgO coprecipitated catalysts. *J Mol Catal A Chem* 2007;265:90–7.
- [694] Xu C, Zheng L, Liu J, Huang Z. Furfural hydrogenation on nickel-promoted Cu-containing catalysts prepared from hydrotalcite-like precursors. *Chin J Chem* 2011;29:691–7.
- [695] Chen X, Li H, Luo H, Qiao M. Liquid phase hydrogenation of furfural to furfuryl alcohol over Mo-doped Co-B amorphous alloy catalysts. *Appl Catal A Gen* 2002;233:13–20.
- [696] Li H, Luo H, Zhuang L, Dai W, Qiao M. Liquid phase hydrogenation of furfural to furfuryl alcohol over the Fe-promoted Ni-B amorphous alloy catalysts. *J Mol Catal A Chem* 2003;203:267–75.
- [697] Li H, Zhang S, Luo H. A Ce-promoted Ni-B amorphous alloy catalyst (Ni-Ce-B) for liquid-phase furfural hydrogenation to furfural alcohol. *Mater Lett* 2004;58:2741–6.
- [698] Li H, Chai W-M, Luo H-S, Li H-X. Hydrogenation of furfural to furfuryl alcohol over Co-B amorphous catalysts prepared by chemical reduction in variable media. *Chin J Chem* 2006;24:1704–8.
- [699] Vaidya PD, Mahajani VV. Kinetics of liquid-phase hydrogenation of furfuraldehyde to furfuryl alcohol over a Pt/C catalyst. *Ind Eng Chem Res* 2003;42:3881–5.
- [700] Kijeński J, Winiarek P, Paryjczak T, Lewicki A, Mikołajska A. Platinum deposited on monolayer supports in selective hydrogenation of furfural to furfuryl alcohol. *Appl Catal A Gen* 2002;233:171–82.
- [701] Merlo AB, Vetere V, Ruggera JF, Casella ML. Bimetallic PtSn catalyst for the selective hydrogenation of furfural to furfuryl alcohol in liquid-phase. *Catal Commun* 2009;10:1665–9.
- [702] Wei S, Cui H, Wang J, Zhuo S, Yi W, Wang L, et al. Preparation and activity evaluation of NiMoB/γ-Al₂O₃ catalyst by liquid-phase furfural hydrogenation. *China Particul* 2011;9:69–74.
- [703] Wu J, Shen Y, Liu C, Wang H, Geng C, Zhang Z. Vapor phase hydrogenation of furfural to furfuryl alcohol over environmentally friendly Cu–Ca/SiO₂ catalyst. *Catal Commun* 2005;6:633–7.
- [704] Sitthisa S, Resasco DE. Hydrodeoxygenation of furfural over supported metal catalysts: a comparative study of Cu, Pd and Ni. *Catal Lett* 2011;141:784–91.
- [705] Mironenko RM, Belskaya OB, Gulyaeva TI, Nizovskii AI, Kalinkin AV, Bukhtiyarov VI, et al. Effect of the nature of carbon support on the formation of active sites in Pd/C and Ru/C catalysts for hydrogenation of furfural. *Catal Today* 2015;249:145–52.
- [706] Perez RF, Fraga MA. Hemicellulose-derived chemicals: one-step production of furfuryl alcohol from xylose. *Green Chem* 2014;16:3942–50.
- [707] Nakagawa Y, Nakazawa H, Watanabe H, Tomishige K. Total hydrogenation of furfural over a silica-supported nickel catalyst prepared by the reduction of a nickel nitrate precursor. *ChemCatChem* 2012;4:1791–7.
- [708] Khairi S, Hara T, Ichikunia N, Shimazu S. Highly efficient and selective hydrogenation of unsaturated carbonyl compounds using Ni-Sn alloy catalysts. *Catal Sci Technol* 2012;2:2139–45.
- [709] Ordomsky VV, Schouten JC, van der Schaaf J, Nijhuis TA. Biphasic single-reactor process for dehydration of xylose and hydrogenation of produced furfural. *Appl Catal A Gen* 2013;451:6–13.
- [710] Zheng HY, Zhu YL, Teng BT, Bai ZQ, Zhang CH, Xiang HW, et al. Towards understanding the reaction pathway in vapour phase hydrogenation of furfural to 2-methylfuran. *J Mol Catal A Chem* 2006;246:18–23.
- [711] Sitthisa S, An W, Resasco DE. Selective conversion of furfural to methylfuran over silica-supported Ni-Fe bimetallic catalysts. *J Catal* 2011;284:90–101.
- [712] Lee WS, Wang Z, Zheng W, Vlachos DG, Bhan A. Vapor phase hydrodeoxygenation of furfural to 2-methylfuran on molybdenum carbide catalysts. *Catal Sci Technol* 2014;4:2340–52.
- [713] Lessard J, Morin J-F, Wehrung J-F, Magnin D, Chornet E. High yield conversion of residual pentoses into furfural via zeolite catalysis and catalytic hydrogenation of furfural to 2-methylfuran. *Top Catal* 2010;53:1231–4.
- [714] Panagiopoulou P, Martin N, Vlachos DG. Effect of hydrogen donor on liquid phase catalytic transfer hydrogenation of furfural over a Ru/RuO₂/C catalyst. *J Mol Catal A Chem* 2014;392:223–8.
- [715] Aliaga C, Tsung CK, Alayoglu S, Komvopoulos K, Yang P, Somorjai GA. Sum frequency generation vibrational spectroscopy and kinetic study of 2-methylfuran and 2,5-dimethylfuran hydrogenation over 7 nm platinum cubic nanoparticles. *J Phys Chem C* 2011;115:8104–9.
- [716] Biradar NS, Hengne AA, Biradar SN, Swami R, Rode CV. Tailoring the product distribution with batch and continuous process options in catalytic hydrogenation of furfural. *Org Process Res Dev* 2014;18:1434–42.
- [717] Mizugaki T, Togo K, Maeno Z, Mitsudome T, Jitsukawa K, Kaneda K. One-pot transformation of levulinic acid to 2-methyltetrahydrofuran catalyzed by Pt-Mo/H-beta in water. *ACS Sust Chem Eng* 2016;4:682–5.
- [718] Sitthisa S, Pham T, Prasomsri T, Sooknoi T, Mallinson RG, Resasco DE. Conversion of furfural and 2-methylpentanal on Pd/SiO₂ and Pd–Cu/SiO₂ catalysts. *J Catal* 2011;280:17–27.
- [719] Nagaraja BM, Siva Kumar V, Shasikala V, Padmasri AH, Sreedhar B, David Raju B, et al. A highly efficient Cu/MgO catalyst for vapour phase hydrogenation of furfural to furfuryl alcohol. *Catal Commun* 2003;4:287–93.
- [720] Rao RS, Baker RTK, Vannice MA. Furfural hydrogenation over carbon-supported copper. *Catal Lett* 1999;60:51–7.
- [721] Luo H, Li H, Zhuang L. Furfural hydrogenation to furfuryl alcohol over a novel Ni-Co-B amorphous alloy catalyst. *Chem Lett* 2001;5:404–5.
- [722] Lee S-P, Chen Y-W. Selective hydrogenation of furfural on Ni-P, Ni-B, and Ni–P–B ultrafine materials. *Ind Eng Chem Res* 1999;38:2548–56.
- [723] Gowda AS, Parkin S, Ladipo FI. Hydrogenation and hydrogenolysis of furfural and furfuryl alcohol catalyzed by ruthenium(II) bis(diimine) complexes. *Appl Organometal Chem* 2012;26:86–93.
- [724] Vorotnikov V, Mpourmpakis G, Vlachos DG. DFT study of furfural conversion to furan, furfuryl alcohol, and 2-methylfuran on Pd(111). *ACS Catal* 2012;2:2496–504.
- [725] Merat N, Godawa C, Gaset A. High selective production of tetrahydrofurfuryl alcohol: catalytic hydrogenation of furfural and furfuryl alcohol. *J Chem Technol Biotechnol* 1990;48:145–59.
- [726] Khan F-A, Vallat A, Süss-Fink G. Highly selective low-temperature hydrogenation of furfuryl alcohol to tetrahydrofurfuryl alcohol catalysed by montmorillonite-supported ruthenium nanoparticles. *Catal Commun* 2011;12:1428–31.
- [727] Tike MA, Mahajani VV. Kinetics of liquid-phase hydrogenation of furfuryl alcohol to tetrahydrofurfuryl alcohol over a Ru/TiO₂ catalyst. *Ind Eng Chem Res* 2007;46:3275–82.
- [728] Seo G, Chon H. Hydrogenation of furfural over copper-containing catalysts. *J Catal* 1981;67:424–9.
- [729] Zhu YL, Xiang HW, Li YW, Jiao HJ, Wu GS, Zhong B, et al. A new strategy for the efficient synthesis of 2-methylfuran and γ-butyrolactone. *New J Chem* 2003;27:208–10.
- [730] Zheng HY, Yang J, Zhu YL, Zhao GW. Synthesis of γ-butyrolactone and 2-methylfuran through the coupling of dehydrogenation and hydrogenation over copper-chromite catalyst. *React Kinet Catal Lett* 2004;82:263–9.
- [731] Yang J, Zheng HY, Zhu YL, Zhao GW, Zhang CH, Teng BT, et al. Effects of calcination temperature on performance of Cu-Zn-Al catalyst for synthesizing γ-butyrolactone and 2-methylfuran through the coupling of dehydrogenation and hydrogenation. *Catal Commun* 2004;5:505–10.
- [732] Dong F, Zhu Y, Zheng H, Zhu Y, Li X, Li Y. Cr-free Cu-catalysts for the selective hydrogenation of biomass-derived furfural to 2-methylfuran: the synergistic effect of metal and acid sites. *J Mol Catal A Chem* 2015;398:140–8.
- [733] Sitthisa S, Sooknoi T, Ma Y, Balbuena PB, Resasco DE. Kinetics and mechanism of hydrogenation of furfural on Cu/SiO₂ catalysts. *J Catal* 2011;277:1–13.
- [734] Shanmuganathan S, Natalia D, van den Wittenboer A, Kohlmann C, Greiner L, de María PD. Enzyme-catalyzed C–C bond formation using 2-methyltetrahydrofuran (2-MTHF) as (co)solvent: efficient and bio-based alternative to DMSO and MTBE. *Green Chem* 2010;12:2240–5.
- [735] Pace V, Hoyos P, Fernández M, Sinisterra JV, Alcántara AR. 2-Methyltetrahydrofuran as a suitable green solvent for phthalimide functionalization promoted by supported KF. *Green Chem* 2010;12:1380–2.
- [736] Pace V, Alcántara AR, Holzera W. Highly efficient chemoselective N-TBS protection of anilines under exceptional mild conditions in the eco-friendly solvent 2-methyltetrahydrofuran. *Green Chem* 2011;13:1986–9.
- [737] Cho A, Shin J, Takagaki A, Kikuchi R, Oyama ST. Ligand and ensemble effects in bimetallic NiFe phosphide catalysts for the hydrodeoxygenation of 2-methyltetrahydrofuran. *Top Catal* 2012;55:969–80.
- [738] Huber GW, Iborra S, Corma A. Synthesis of transportation fuels from biomass: chemistry, catalysts, and engineering. *Chem Rev* 2006;106:4044–98.
- [739] Liu X, Ünalw B, Jensen KF. Heterogeneous catalysis with continuous flow microreactors. *Catal Sci Technol* 2012;2:2134–8.
- [740] Fegyvernek I, Orha L, Láng G, Horváth IT. Gamma-valerolactone-based solvents. *Tetrahedron* 2010;66:1078–81.
- [741] Duan ZQ, Hu F. Highly efficient synthesis of phosphatidylserine in the eco-friendly solvent γ-valerolactone. *Green Chem* 2012;14:1581–3.
- [742] Luterbacher JS, Rand JM, Alonso DM, Han J, Youngquist JT, Maravelias CT, et al. Nonenzymatic sugar production from biomass using biomass-derived γ-valerolactone. *Science* 2014;343:277–80.

- [743] Yan K, Yang Y, Chai J, Lu Y. Catalytic reactions of gamma-valerolactone: a platform to fuels and value-added chemicals. *Appl Catal B: Environ* 2015;179:292–304.
- [744] Caretto A, Noé M, Selva M, Perosa A. Upgrading of biobased lactones with dialkylcarbonates. *ACS Sust Chem Eng* 2014;2:2131–41.
- [745] Derle SN, Parikh PA. Hydrogenation of levulinic acid and γ -valerolactone: steps towards biofuels. *Biomass Conv Bioref* 2014;4:293–9.
- [746] Wright WRH, Palkovits R. Development of heterogeneous catalysts for the conversion of levulinic acid to γ -valerolactone. *ChemSusChem* 2012;5:1657–67.
- [747] Horváth IT, Mehdi H, Fábos V, Boda L, Mika LT. γ -Valerolactone – A sustainable liquid for energy and carbon-based chemicals. *Green Chem* 2008;10:238–42.
- [748] Bond JQ, Alonso DM, Wang D, West RM, Dumesic JA. Integrated catalytic conversion of γ -valerolactone to liquid alkenes for transportation fuels. *Science* 2010;327:1110–14.
- [749] Alonso DM, Wettstein SG, Dumesic JA. Gamma-valerolactone, a sustainable platform molecule derived from lignocellulosic biomass. *Green Chem* 2013;15:584–95.
- [750] Abdelrahman OA, Heyden A, Bond JQ. Analysis of kinetics and reaction pathways in the aqueous-phase hydrogenation of levulinic acid to form γ -valerolactone over Ru/C. *ACS Catal* 2014;4:1171–81.
- [751] Serrano-Ruiz JC, West RM, Dumesic JA. Catalytic conversion of renewable biomass resources to fuels and chemicals. *Annu Rev Chem Biomol Eng* 2010;1:79–100.
- [752] Zhang J, Wu S, Li B, Zhang HD. Advances in the catalytic production of valuable levulinic acid derivatives. *ChemCatChem* 2012;4:1230–7.
- [753] Van de Vyver S, Thomas J, Geboers J, Keyzer S, Smet M, Dehaen W, et al. Catalytic production of levulinic acid from cellulose and other biomass-derived carbohydrates with sulfonated hyperbranched poly(arylene oxindole)s. *Energy Environ Sci* 2011;4:3601–10.
- [754] Weingarten R, Conner WC, Huber GW. Production of levulinic acid from cellulose by hydrothermal decomposition combined with aqueous phase dehydration with a solid acid catalyst. *Energy Environ Sci* 2012;5:7559–74.
- [755] Tominaga K, Mori A, Fukushima Y, Shimada S, Sato K. Mixed-acid systems for the catalytic synthesis of methyl levulinate from cellulose. *Green Chem* 2011;13:810–12.
- [756] Rackemann DW, Doherty WOS. The conversion of lignocellulosics to levulinic acid. *Biofuels Bioprod Bioref* 2011;5:198–214.
- [757] Runge T, Zhang C. Two-stage acid-catalyzed conversion of carbohydrates into levulinic acid. *Ind Eng Chem Res* 2012;51:3265–70.
- [758] Maldonado GMG, Assary RS, Dumesic J, Curtiss LA. Experimental and theoretical studies of the acid-catalyzed conversion of furfuryl alcohol to levulinic acid in aqueous solution. *Energy Environ Sci* 2012;5:6981–9.
- [759] Hu X, Song Y, Wu L, Gholizadeh M, Li C-Z. One-pot synthesis of levulinic acid/ester from C5 carbohydrates in a methanol medium. *ACS Sust Chem Eng* 2013;1:1593–9.
- [760] Cai H, Li C, Wang A, Xu G, Zhang T. Zeolite-promoted hydrolysis of cellulose in ionic liquid, insight into the mutual behavior of zeolite, cellulose and ionic liquid. *Appl Catal B: Environ* 2012;123–4:333–8.
- [761] Chamnankid B, Ratanatawanate C, Faungnawakij K. Conversion of xylose to levulinic acid over modified acid functions of alkaline-treated zeolite Y in hot-compressed water. *Chem Eng J* 2014;258:341–7.
- [762] Hengne AM, Rode CV. Cu-ZrO₂ nanocomposite catalyst for selective hydrogenation of levulinic acid and its ester to γ -valerolactone. *Green Chem* 2012;14:1064–72.
- [763] Tang X, Zeng X, Li Z, Hu L, Sun Y, Liu S, et al. Production of γ -valerolactone from lignocellulosic biomass for sustainable fuels and chemicals supply. *Renew Sust Energy Rev* 2014;40:608–20.
- [764] Upare PP, Lee JM, Hwang DW, Halligudi SB, Hwang YK, Chang JS. Selective hydrogenation of levulinic acid to γ -valerolactone over carbon-supported noble metal catalysts. *J Ind Eng Chem* 2011;17:287–92.
- [765] Yan Z, Lin L, Liu S. Synthesis of γ -valerolactone by hydrogenation of biomass-derived levulinic acid over Ru/C catalyst. *Energy Fuel* 2009;23:3853–8.
- [766] Sudhakar M, Lakshmi Kantam M, Jaya VS, Kishore R, Ramanujachary KV, Venugopal A. Hydroxyapatite as a novel support for Ru in the hydrogenation of levulinic acid to γ -valerolactone. *Catal Commun* 2014;50:101–4.
- [767] Moreno-Marrodán C, Barbaro P. Energy efficient continuous production of γ -valerolactone by bifunctional metal/acid catalysis in one pot. *Green Chem* 2014;16:3434–8.
- [768] Al-Shaal MG, Wright WRH, Palkovits R. Exploring the ruthenium catalysed synthesis of γ -valerolactone in alcohols and utilisation of mild solvent-free reaction conditions. *Green Chem* 2012;14:1260–3.
- [769] Yao Y, Wang Z, Zhao S, Wang D, Wu Z, Zhang M. A stable and effective Ru/polyethersulfone catalyst for levulinic acid hydrogenation to γ -valerolactone in aqueous solution. *Catal Today* 2014;234:245–50.
- [770] Raspolli Galletti AM, Antonetti C, De Luise V, Martinelli M. A sustainable process for the production of γ -valerolactone by hydrogenation of biomass-derived levulinic acid. *Green Chem* 2012;14:688–94.
- [771] Du X, Liu Y, Wang J, Cao Y, Fan K. Catalytic conversion of biomass-derived levulinic acid into γ -valerolactone using iridium nanoparticles supported on carbon nanotubes. *Chin J Catal* 2013;34:993–1001.
- [772] Deng J, Wang Y, Pan T, Xu Q, Guo QX, Fu Y. Conversion of carbohydrate biomass to γ -valerolactone by using water-soluble and reusable iridium complexes in acidic aqueous media. *ChemSusChem* 2013;6:1163–7.
- [773] Li W, Xie J-H, Lin H, Zhou QL. Highly efficient hydrogenation of biomass-derived levulinic acid to γ -valerolactone catalyzed by iridium pincer complexes. *Green Chem* 2012;14:2388–90.
- [774] Testa MI, Corbel-Demaily L, Parola VL, Venezia AM, Pinel C. Effect of Au on Pd supported over HMS and Ti doped HMS as catalysts for the hydrogenation of levulinic acid to γ -valerolactone. *Catal Today* 2015;257:291–6.
- [775] Yan K, Lafleur T, Liao J. Facile synthesis of palladium nanoparticles supported on multi-walled carbon nanotube for efficient hydrogenation of biomass-derived levulinic acid. *Nanopart Res* 2013;15:1906–12.
- [776] Yan K, Lafleur T, Wu G, Liao J, Ceng C, Xie X. Highly selective production of value-added γ -valerolactone from biomass-derived levulinic acid using the robust Pd nanoparticles. *Appl Catal A Gen* 2013;468:52–8.
- [777] Shimizu K, Kanno S, Kon K. Hydrogenation of levulinic acid to γ -valerolactone by Ni and MoO_x co-loaded carbon catalysts. *Green Chem* 2014;16:3899–903.
- [778] Mohan V, Venkateshwarlu V, Pramod CV, Raju BD, Rao KSR. Vapour phase hydrocyclisation of levulinic acid to γ -valerolactone over supported Ni catalysts. *Catal Sci Technol* 2014;4:1253–9.
- [779] Rong Z, Sun Z, Wang L, Lv J, Wang Y, Wang Y. Efficient conversion of levulinic acid into γ -valerolactone over Raney Ni catalyst prepared from melt-quenching alloy. *Catal Lett* 2014;144:1766–71.
- [780] Putrakumar B, Nagaraju N, Kumar VP, Charly KVR. Hydrogenation of levulinic acid to γ -valerolactone over copper catalysts supported on γ -Al₂O₃. *Catal Today* 2015;250:209–17.
- [781] Yan K, Chen A. Efficient hydrogenation of biomass-derived furfural and levulinic acid on the facely synthesized noble-metal-free Cu-Cr catalyst. *Energy* 2013;58:357–63.
- [782] Balla P, Perupuglu V, Vanama PK, Komandur VRC. Hydrogenation of biomass-derived levulinic acid to γ -valerolactone over copper catalysts supported on ZrO₂. *J Chem Technol Biotechnol* 2015;91:769–76.
- [783] Park JY, Kim MA, Lee SJ, Jung J, Jang HM, Upare PP, et al. Preparation and characterization of carbon-encapsulated iron nanoparticles and their catalytic activity in the hydrogenation of levulinic acid. *J Mater Sci* 2015;50:334–43.
- [784] Zhou H, Song J, Fan H, Zhang B, Yang Y, Hu J, et al. Cobalt catalysts: very efficient for hydrogenation of biomass-derived ethyl levulinate to γ -valerolactone under mild conditions. *Green Chem* 2014;16:3870–5.
- [785] Heeres H, Handana R, Chunai D, Rasrendra CB, Girisuta B, Heeres HJ. Combined dehydration/(transfer)-hydrogenation of C6-sugars (D-glucose and D-fructose) to γ -valerolactone using ruthenium catalysts. *Green Chem* 2009;11:1247–55.
- [786] Ding D, Wang J, Xi J, Liu X, Lu G, Wang Y. High-yield production of levulinic acid from cellulose and its upgrading to γ -valerolactone. *Green Chem* 2014;16:3846–53.
- [787] Molinari V, Antonietti M, Esposito D. An integrated strategy for the conversion of cellulosic biomass into γ -valerolactone. *Catal Sci Technol* 2014;4:3626–30.
- [788] Raspolli Galletti AM, Antonetti C, Ribechini E, Colombini MP, o Di Nasso NN, Bonari E. From giant reed to levulinic acid and gamma-valerolactone: a high yield catalytic route to valeric biofuels. *Appl Energy* 2013;102:157–62.
- [789] Hengne AM, Kamble SB, Rode CV. Single pot conversion of furfuryl alcohol to levulinic esters and γ -valerolactone in the presence of sulfonic acid functionalized ILs and metal catalysts. *Green Chem* 2013;15:2540–7.
- [790] Chia M, Dumesic JA. Liquid-phase catalytic transfer hydrogenation and cyclization of levulinic acid and its esters to γ -valerolactone over metal oxide catalysts. *Chem Commun* 2011;47:12233–5.
- [791] Tang X, Chen H, Hu L, Hao W, Sun Y, Zeng X, et al. Conversion of biomass to γ -valerolactone by catalytic transfer hydrogenation of ethyl levulinate over metal hydroxides. *Appl Catal B: Environ* 2014;147:827–34.
- [792] Tang X, Hu L, Sun Y, Zhao G, Hao W, Lin L. Conversion of biomass-derived ethyl levulinate into γ -valerolactone via hydrogen transfer from supercritical ethanol over a ZrO₂ catalyst. *RSC Adv* 2013;3:10277–84.
- [793] Song J, Wu L, Zhou B, Zhou H, Fan H, Yang Y, et al. A new porous Zr-containing catalyst with a phenate group: an efficient catalyst for the catalytic transfer hydrogenation of ethyl levulinate to γ -valerolactone. *Green Chem* 2015;17:1626–32.
- [794] Wang J, Jaenicke S, Chuah GK. Zirconium-Beta zeolite as a robust catalyst for the transformation of levulinic acid to γ -valerolactone via Meerwein-Ponndorf-Verley reduction. *RSC Adv* 2014;4:13481–9.
- [795] Yang Z, Huang YB, Guo QX, Fu Y. RANEY Ni catalyzed transfer hydrogenation of levulinic esters to γ -valerolactone at room temperature. *Chem Commun* 2013;49:5328–30.
- [796] Geboers J, Wang X, de Carvalho AB, Rinaldi R. Densification of biorefinery schemes by H-transfer with Raney Ni and 2-propanol: a case study of a potential avenue for valorization of alkyllevulinate to alkyl γ -hydroxypentanoates and γ -valerolactone. *J Mol Catal A Chem* 2014;388–9:106–15.
- [797] Amarasekara AS, Hasan MA. Pd/C catalyzed conversion of levulinic acid to γ -valerolactone using alcohol as a hydrogen donor under microwave conditions. *Catal Commun* 2015;60:5–7.
- [798] Deng L, Zhao Y, Li J, Fu Y, Liao B, Guo QX. Conversion of levulinic acid and formic acid into γ -valerolactone over heterogeneous catalysts. *ChemSusChem* 2010;3:1172–5.
- [799] Fábos V, Mika LT, Horváth IT. Selective conversion of levulinic and formic acids to γ -valerolactone with the Shvo catalyst. *Organometallics* 2014;33:181–7.
- [800] Ortiz-Cervantes C, García JJ. Hydrogenation of levulinic acid to γ -valerolactone using ruthenium nanoparticles. *Inorg Chim Acta* 2013;397:124–8.

- [801] Du XL, He L, Zhao S, Liu YM, Cao Y, He HY, et al. Hydrogen-independent reductive transformation of carbohydrate biomass into γ -valerolactone and pyrrolidone derivatives with supported gold catalysts. *Angew Chem* 2011;123:7961–5.
- [802] Du XL, Bi QY, Liu YM, Cao Y, Fan KN. Conversion of biomass-derived levulinic and formate esters into γ -valerolactone over supported gold catalysts. *ChemSusChem* 2011;4:1838–43.
- [803] Yuan J, Li SS, Yu L, Liu YM, Cao Y, He HY, et al. Copper-based catalysts for the efficient conversion of carbohydrate biomass into γ -valerolactone in the absence of externally added hydrogen. *Energy Environ Sci* 2013;6:3308–13.
- [804] Deng L, Li J, Lai DM, Fu Y, Guo QX. Catalytic conversion of biomass-derived carbohydrates into γ -valerolactone without using an external H₂ supply. *Angew Chem Int Ed* 2009;48:6529–32.
- [805] Amarasekara AS, Wriedt B, Edwards DLN. γ -Valerolactone from pyrolysis of calcium salts of levulinic-formic acid mixtures derived from cellulose. *Biomass Bioenergy* 2015;72:39–44.
- [806] Qi L, Horváth IT. Catalytic conversion of fructose to γ -valerolactone in γ -valerolactone. *ACS Catal* 2012;2:2247–9.
- [807] Alonso DM, Gallo JMR, Mellmer MA, Wettstein SG, Dumesic JA. Direct conversion of cellulose to levulinic acid and gamma-valerolactone using solid acid catalysts. *Catal Sci Technol* 2013;3:927–31.
- [808] Wettstein SG, Alonso DM, Chong Y, Dumesic JA. Production of levulinic acid and gamma-valerolactone (GVL) from cellulose using GVL as a solvent in biphasic systems. *Energy Environ Sci* 2012;5:8199–203.
- [809] Bui L, Luo H, Gunther WR, Román-Leshkov Y. Domino reaction catalyzed by zeolites with Bronsted and Lewis acid sites for the production of γ -valerolactone from furfural. *Angew Chem* 2013;125:8180–3.
- [810] Alonso DM, Wettstein SG, Mellmer MA, Gurbuz El, Dumesic JA. Integrated conversion of hemicellulose and cellulose from lignocellulosic biomass. *Energy Environ Sci* 2013;6:76–80.
- [811] Luo HY, Consoli DF, Gunther WR, Román-Leshkov Y. Investigation of the reaction kinetics of isolated Lewis acid sites in Beta zeolites for the Meerwein-Ponndorf-Verley reduction of methyl levulinate to γ -valerolactone. *J Catal* 2014;320:198–207.
- [812] Li H, Fang Z, Yang S. Direct conversion of sugars and ethyl levulinic acid into γ -valerolactone with superparamagnetic acid-base bifunctional ZrFeO_x nanocatalysts. *ACS Sust Chem Eng* 2015;4:236–46.
- [813] Li H, Fang Z, Yang S. Direct catalytic transformation of biomass derivatives into biofuel component γ -valerolactone with magnetic nickel-zirconium nanoparticles. *ChemPlusChem* 2016;81:135–42.
- [814] He J, Li H, Lu YM, Liu YX, Wu ZB, Hu DY, et al. Cascade catalytic transfer hydrogenation-cyclization of ethyl levulinic acid to γ -valerolactone with Al-Zr mixed oxides. *Appl Catal A Gen* 2016;510:11–19.
- [815] Ortiz-Cervantes C, Flores-Alamo M, García JJ. Hydrogenation of biomass-derived levulinic acid into γ -valerolactone catalyzed by palladium complexes. *ACS Catal* 2015;5:1424–31.
- [816] Xiao C, Goh TW, Qi Z, Goes S, Brashler K, Perez C, et al. Conversion of levulinic acid to gamma-valerolactone over few-layer graphene-supported ruthenium catalysts. *ACS Catal* 2016;6:593–9.
- [817] Selva M, Gottardo M, Perosa A. Upgrade of biomass-derived levulinic acid via Ru/C-catalyzed hydrogenation to γ -valerolactone in aqueous-organic-ionic liquids multiphase systems. *ACS Sust Chem Eng* 2013;1:180–9.
- [818] Michel C, Zaffran J, Ruppert AM, Matras-Michalska J, Jędrzejczyk M, Grams J, et al. Role of water in metal catalyst performance for ketone hydrogenation: a joint experimental and theoretical study on levulinic acid conversion into gamma-valerolactone. *Chem Commun* 2014;50:12450–3.
- [819] Bond JQ, Alonso DM, West RM, Dumesic JA. γ -Valerolactone ring-opening and decarboxylation over SiO₂/Al₂O₃ in the presence of water. *Langmuir* 2010;26:16291–8.
- [820] Lemonidou AA, López L, Manzer LE, Barteau MA. Dynamic microbalance studies of RhO_x/SiO₂ catalyst deactivation/regeneration for α -methylene γ -valerolactone synthesis. *Appl Catal A Gen* 2004;272:241–8.
- [821] Serrano-Ruiz JC, Dumesic JA. Catalytic routes for the conversion of biomass into liquid hydrocarbon transportation fuels. *Energy Environ Sci* 2011;4:83–99.
- [822] Yan K, Chen A. Selective hydrogenation of furfural and levulinic acid to biofuels on the ecofriendly Cu–Fe catalyst. *Fuel* 2014;115:101–8.
- [823] Bozell JJ, Moens L, Elliott DC, Wang Y, Neuenschwander GG, Fitzpatrick SW, et al. Production of levulinic acid and use as a platform chemical for derived products. *Resour Conserv Recy* 2000;28:227–39.
- [824] Du XL, Bi QY, Liu YM, Cao Y, He HY, Fan KN. Tunable copper-catalyzed chemoselective hydrogenolysis of biomass-derived γ -valerolactone into 1,4-pentanediol or 2-methyltetrahydrofuran. *Green Chem* 2012;14:935–9.
- [825] Upare PP, Lee JM, Hwang YK, Hwang DW, Lee JH, Halligudi SB, et al. Direct hydrocyclization of biomass-derived levulinic acid to 2-methyltetrahydrofuran over nanocomposite copper/silica catalysts. *ChemSusChem* 2011;4:1749–52.
- [826] Al-Shaal MG, Dzierbinski A, Palkovits R. Solvent-free γ -valerolactone hydrogenation to 2-methyltetrahydrofuran catalysed by Ru/C: a reaction network analysis. *Green Chem* 2014;16:1358–64.
- [827] Bond JQ, Wang D, Alonso DM, Dumesic JA. Interconversion between γ -valerolactone and pentenoic acid combined with decarboxylation to form butene over silica/alumina. *J Catal* 2011;281:290–9.
- [828] Voge HH, May NC. Isomerization equilibria among the *n*-butenes. *J Am Chem Soc* 1946;68:550–3.
- [829] Wang D, Hakim SH, Alonso DM, Dumesic JA. A highly selective route to linear alpha olefins from biomass-derived lactones and unsaturated acids. *Chem Commun* 2013;49:7040–2.
- [830] Kellucott AB, Salary R, Abdelrahman OA, Bond JQ. An examination of the intrinsic activity and stability of various solid acids during the catalytic decarboxylation of γ -valerolactone. *Catal Sci Technol* 2014;4:2267–9.
- [831] Gürbüz El, Alonso DM, Bond JQ, Dumesic JA. Reactive extraction of levulinic esters and conversion to γ -valerolactone for production of liquid fuels. *ChemSusChem* 2011;4:357–61.
- [832] Han J, Sen SM, Alonso DM, Dumesic JA, Maravelias CT. A strategy for the simultaneous catalytic conversion of hemicellulose and cellulose from lignocellulosic biomass to liquid transportation fuels. *Green Chem* 2014;16:653–61.
- [833] Buitrago-Sierra R, Serrano-Ruiz JC, Rodríguez-Reinoso F, Sepúlveda-Escribano A, Dumesic JA. Ce promoted Pd–Nb catalysts for γ -valerolactone ring-opening and hydrogenation. *Green Chem* 2012;14:3318–24.
- [834] Pham HN, Pagan-Torres YJ, Serrano-Ruiz JC, Wang D, Dumesic JA, Datye AK. Improved hydrothermal stability of niobia-supported Pd catalysts. *Appl Catal A Gen* 2011;397:153–62.
- [835] Sun P, Gao G, Zhao Z, Xia C, Li F. Stabilization of cobalt catalysts by embedding for efficient production of valeric biofuel. *ACS Catal* 2014;4:4136–42.
- [836] Palkovits R. Pentenoic acid pathways for cellulosic biofuels. *Angew Chem Int Ed* 2010;49:4336–8.
- [837] Lange JP, Price R, Ayoub P, Louis J, Petrus L, Clarke L, et al. Valeric biofuels: a platform of cellulosic transportation fuels. *Angew Chem Int Ed* 2010;49:4479–83.
- [838] Kon K, Onodera W, Shimizu K. Selective hydrogenation of levulinic acid to valeric acid and valeric biofuels by a Pt/HMFI catalyst. *Catal Sci Technol* 2014;4:3227–34.
- [839] Luo W, Deka U, Beale AM, van Eck ERH, Bruijninx PCA, Weckhuysen BM. Ruthenium-catalyzed hydrogenation of levulinic acid: influence of the support and solvent on catalyst selectivity and stability. *J Catal* 2013;301:175–86.
- [840] Pan T, Deng J, Xu Q, Xu Y, Guo QX, Fu Y. Catalytic conversion of biomass-derived levulinic acid to valerate esters as oxygenated fuels using supported ruthenium catalysts. *Green Chem* 2013;15:2967–74.
- [841] Chan-Thaw CE, Marelli M, Psaro R, Ravasio N, Zaccheria F. New generation biofuels: γ -valerolactone into valeric esters in one pot. *RSC Adv* 2013;3:1302–6.
- [842] Scotti N, Dangate M, Gervasini A, Evangelisti C, Ravasio N, Zaccheria F. Unraveling the role of low coordination sites in a Cu metal nanoparticle: a step toward the selective synthesis of second generation biofuels. *ACS Catal* 2014;4:2818–26.
- [843] Renz M. Ketonization of carboxylic acids by decarboxylation: mechanism and scope. *Eur J Org Chem* 2005;2005:979–88.
- [844] Alonso DM, Bond JQ, Serrano-Ruiz JC, Dumesic JA. Production of liquid hydrocarbon transportation fuels by oligomerization of biomass-derived C₉ alkenes. *Green Chem* 2010;12:992–9.
- [845] Serrano-Ruiz JC, Wang D, Dumesic JA. Catalytic upgrading of levulinic acid to 5-nonenone. *Green Chem* 2010;12:574–7.
- [846] Serrano-Ruiz JC, Braden DJ, West RM, Dumesic JA. Conversion of cellulose to hydrocarbon fuels by progressive removal of oxygen. *Appl Catal B: Environ* 2010;100:184–9.
- [847] Lange JP, Vesterling JZ, Haan RJ. Towards ‘bio-based’ Nylon: conversion of γ -valerolactone to methyl pentenoate under catalytic distillation conditions. *Chem Commun* 2007;3488–90.
- [848] Meeszen P, Vogt D, Keim W. Highly regioselective hydroformylation of internal, functionalized olefins applying PtSn complexes with large bite angle diphosphines. *J Organomet Chem* 1998;551:165–70.
- [849] Manzer LE. Catalytic synthesis of α -methylene- γ -valerolactone: a biomass-derived acrylic monomer. *Appl Catal A Gen* 2004;272:249–56.
- [850] Arasa M, Petrich RA, Mantecón A, Serra A. New thermosetting nanocomposites prepared from diglycidyl ether of bisphenol and γ -valerolactone initiated by rare earth triflate initiators. *Eur Polym J* 2010;46:15–13.
- [851] Raouf moghaddam S, Rood MTM, Buijze FKW, Drent E, Bouwman E. Catalytic conversion of γ -valerolactone to ϵ -caprolactam: towards Nylon from renewable feedstock. *ChemSusChem* 2014;7:1984–90.
- [852] Chalid M, Heeres HJ, Broekhuis AA. Ring-opening of γ -valerolactone with amino compounds. *J Appl Polym Sci* 2012;123:3556–64.
- [853] Huo W, Zhang C, Yuan H, Jia M, Ning C, Tang Y, et al. Vapor-phase selective hydrogenation of maleic anhydride to succinic anhydride over Ni/TiO₂ catalysts. *J Int Eng Chem* 2014;20:4140–5.
- [854] Huang Y, Ma Y, Cheng Y, Wang L, Li X. Active ruthenium catalysts prepared by *Cacumen Platycladi* leaf extract for selective hydrogenation of maleic anhydride. *Appl Catal A Gen* 2015;495:124–30.
- [855] Regenhardt SA, Trasarti AF, Meyer CL, Garrett TF, Marchi AJ. Selective gas-phase conversion of maleic anhydride to propionic acid on Pt-based catalysts. *Catal Commun* 2013;35:59–63.
- [856] Li M, Li G, Li N, Wang A, Dong W, Wang X, et al. Aqueous phase hydrogenation of levulinic acid to 1,4-pentanediol. *Chem Commun* 2014;50:1414–16.
- [857] Corbel-Demaily L, Ly BK, Minh P, Tapin B, Espeel C, Epron F, et al. Heterogeneous catalytic hydrogenation of biobased levulinic and succinic acids in aqueous solutions. *ChemSusChem* 2013;6:2388–95.

- [858] Braden DJ, Henao CA, Heltzel J, Maravelias CC, Dumesic JA. Production of liquid hydrocarbon fuels by catalytic conversion of biomass-derived levulinic acid. *Green Chem* 2011;13:1755–65.
- [859] Touchy AS, Siddiki SMAH, Kon K, Shimizu K. Heterogeneous Pt catalysts for reductive amination of levulinic acid to pyrrolidones. *ACS Catal* 2014;4:3045–50.
- [860] Ding G, Zhu Y, Zheng H, Chen H, Li Y. Vapour phase hydrogenolysis of biomass-derived diethyl succinate to tetrahydrofuran over CuO-ZnO/solid acid bifunctional catalysts. *J Chem Technol Biotechnol* 2011;86:231–7.
- [861] Zhao M, Yang X, Church TL, Harris AT. Novel CaO-SiO₂ sorbent and bifunctional Ni/Co-CaO/SiO₂ complex for selective H₂ synthesis from cellulose. *Environ Sci Technol* 2012;46:2976–83.
- [862] Shimura K, Yoshida H. Heterogeneous photocatalytic hydrogen production from water and biomass derivatives. *Energy Environ Sci* 2011;4:2467–81.
- [863] Takahashi T, Ueno K, Kai T. Vapor phase Beckmann rearrangement of cyclopentanone oxime over high silica HZSM-5 zeolites. *Micropor Mater* 1993;1:323–7.
- [864] Scognamiglio J, Jones L, Letizia CS, Api AM. Fragrance material review on cyclopentanone. *Food Chem Technol* 2012;50:5608–12.
- [865] Hronec M, Fulajtárová K, Liptaj T, Štolcová M, Prónayová N, Soták T. Cyclopentanone: a raw material for production of C₁₅ and C₁₇ fuel precursors. *Biomass Bioenergy* 2014;63:291–9.
- [866] Akashi T, Sato S, Takahashi R, Sodesawa T, Inui K. Catalytic vapor-phase cyclization of 1,6-hexanediol into cyclopentanone. *Catal Commun* 2003;4:411–16.
- [867] Dubkov KA, Panov GI, Starokon EV, Parmon VN. Non-catalytic liquid phase oxidation of alkenes with nitrous oxide. 2. Oxidation of cyclopentene to cyclopentanone. *React Kinet Catal Lett* 2002;77:197–205.
- [868] Hronec M, Fulajtárová K, Soták T. Highly selective rearrangement of furfuryl alcohol to cyclopentanone. *Appl Catal B: Environ* 2014;154:294–300.
- [869] Hronec M, Fulajtárová K. Selective transformation of furfural to cyclopentanone. *Catal Commun* 2012;24:100–4.
- [870] Zhou M, Zeng Z, Zhu H, Xiao G, Xiao R. Aqueous-phase catalytic hydrogenation of furfural to cyclopentanol over Cu-Mg-Al hydrotalcites derived catalysts: model reaction for upgrading of bio-oil. *J Energy Chem* 2014;23:91–6.
- [871] Yang Y, Du Z, Huang Y, Lu F, Wang F, Gao J, et al. Conversion of furfural into cyclopentanone over Ni–Cu bimetallic catalysts. *Green Chem* 2013;15:1932–40.
- [872] Hronec M, Fulajtárová K, Liptaj T. Effect of catalyst and solvent on the furan ring rearrangement to cyclopentanone. *Appl Catal A Gen* 2012;437-8:104–11.
- [873] Hronec M, Fulajtárová K, Mičušík M. Influence of furanic polymers on selectivity of furfural rearrangement to cyclopentanone. *Appl Catal A Gen* 2013;468:426–31.
- [874] Ohyama J, Kanao R, Esaki A, Satsuma A. Conversion of 5-hydroxymethylfurfural to a cyclopentanone derivative by ring rearrangement over supported Au nanoparticles. *Chem Commun* 2014;50:5633–6.
- [875] Chen X, Sun W, Xiao N, Yan Y, Liu S. Experimental study for liquid phase selective hydrogenation of furfuryl alcohol to tetrahydrofurfuryl alcohol on supported Ni catalysts. *Chem Eng J* 2007;126:5–11.
- [876] Zhang B, Zhu Y, Ding G, Zheng H, Li Y. Selective conversion of furfuryl alcohol to 1,2-pentanediol over a Ru/MnO_x catalyst in aqueous phase. *Green Chem* 2012;14:3402–9.
- [877] Mizugaki T, Yamakawa T, Nagatsu Y, Maeno Z, Mitsudome T, Jitsukawa K, et al. Direct transformation of furfural to 1,2-pentanediol using a hydrotalcite-supported platinum nanoparticle catalyst. *ACS Sust Chem Eng* 2014;2:2243–7.
- [878] Liu S, Amada Y, Tamura M, Nakagawa Y, Tomishige K. One-pot selective conversion of furfural into 1,5-pentanediol over a Pd-added Ir-ReO_x/SiO₂ bifunctional catalyst. *Green Chem* 2014;16:617–26.
- [879] Liu S, Amada Y, Tamura M, Nakagawa Y, Tomishige K. Performance and characterization of rhodium-modified Rh–Ir alloy catalyst for one-pot conversion of furfural into 1,5-pentanediol. *Catal Sci Technol* 2014;4:2535–49.
- [880] Xu W, Wang H, Liu X, Ren J, Wang Y, Lu G. Direct catalytic conversion of furfural to 1,5-pentanediol by hydrogenolysis of the furan ring under mild conditions over Pt/Co₂AlO₄ catalyst. *Chem Commun* 2011;47:3924–6.
- [881] Li F, Lu T, Chen B, Huang Z, Yuan G. Pt nanoparticles over TiO₂-ZrO₂ mixed oxide as multifunctional catalysts for an integrated conversion of furfural to 1,4-butandiol. *Appl Catal A Gen* 2014;478:252–8.
- [882] Nakagawa Y, Tamura M, Tomishige K. Catalytic materials for the hydrogenolysis of glycerol to 1,3-propanediol. *J Mater Chem A* 2014;2:6688–702.
- [883] Tuteja J, Choudhary H, Nishimura S, Ebitani K. Direct synthesis of 1,6-hexanediol from HMF over a heterogeneous Pd/ZrP catalyst using formic acid as hydrogen source. *ChemSusChem* 2014;7:96–100.
- [884] Mortensen PM, Grunwaldt JD, Jensema PA, Knudsen KG, Jensen AD. A review of catalytic upgrading of bio-oil to engine fuels. *Appl Catal A Gen* 2011;407:1–19.
- [885] Choudhary TV, Phillips CB. Renewable fuels via catalytic hydrodeoxygenation. *Appl Catal A Gen* 2011;397:1–12.
- [886] Xiu S, Shahbazi A. Bio-oil production and upgrading research: a review. *Renew Sust Energy Rev* 2012;16:4406–14.
- [887] Cheng K, Kang J, Huang S, You Z, Zhang Q, Ding J, et al. Mesoporous Beta zeolite-supported ruthenium nanoparticles for selective conversion of synthesis gas to C₅–C₁₁ isoparaffins. *ACS Catal* 2012;2:441–9.
- [888] Idem RO, Katikaneni SPR, Sethuraman R, Bakhshi NN. Production of C₄ hydrocarbons from modified Fischer-Tropsch synthesis over Co-Ni-ZrO₂/sulfated-ZrO₂ hybrid catalysts. *Energy Fuels* 2000;14:1072–82.
- [889] Sartipi S, Makkee M, Kapteijn F, Gascon J. Catalysis engineering of bifunctional solids for the one-step synthesis of liquid fuels from syngas: a review. *Catal Sci Technol* 2014;4:893–907.
- [890] Yu W, Tang Y, Mo L, Chen P, Lou H, Zheng X. One-step hydrogenation–esterification of furfural and acetic acid over bifunctional Pd catalysts for bio-oil upgrading. *Bioresour Technol* 2011;102:8241–6.
- [891] Yu W, Tang Y, Mo L, Chen P, Lou H, Zheng X. Bifunctional Pd/Al-SBA-15 catalyzed one-step hydrogenation–esterification of furfural and acetic acid: a model reaction for catalytic upgrading of bio-oil. *Catal Commun* 2011;13:35–9.
- [892] Lewis JD, Van de Vyver S, Crisci AJ, Gunther WR, Michaelis VK, Griffin RG, et al. A continuous flow strategy for the coupled transfer hydrogenation and etherification of 5-(hydroxymethyl)furfural using Lewis acid zeolites. *ChemSusChem* 2014;7:2255–65.
- [893] Zhang X, Wang T, Ma L, Wu C. Aqueous-phase catalytic process for production of pentane from furfural over nickel-based catalysts. *Fuel* 2010;89:2697–702.
- [894] Chen B, Li F, Huang Z, Yuan G. Tuning catalytic selectivity of liquid-phase hydrogenation of furfural via synergistic effects of supported bimetallic catalysts. *Appl Catal A Gen* 2015;500:23–9.
- [895] Huber GW, Dumesic JA. An overview of aqueous-phase catalytic processes for production of hydrogen and alkanes in a biorefinery. *Catal Today* 2006;111:119–32.
- [896] Davda RR, Shabaker JW, Huber GW, Cortright D, Dumesic JA. A review of catalytic issues and process conditions for renewable hydrogen and alkanes by aqueous-phase reforming of oxygenated hydrocarbons over supported metal catalysts. *Appl Catal B: Environ* 2005;56:171–86.
- [897] Kim YT, Dumesic JA, Huber GW. Aqueous-phase hydrodeoxygenation of sorbitol: a comparative study of Pt/Zr phosphate and PtArO_x/C. *J Catal* 2013;304:72–85.
- [898] de Beeck BO, Michie D, Geboers J, Holsbeek J, Morré E, Oswald S, et al. Direct catalytic conversion of cellulose to liquid straight-chain alkanes. *Energy Environ Sci* 2015;8:230–40.
- [899] Liu S, Tamura M, Nakagawa Y, Tomishige K. One-pot conversion of cellulose into n-hexane over the Ir-ReO_x/SiO₂ catalyst combined with HZSM-5. *ACS Sust Chem Eng* 2014;2:1819–27.
- [900] Sen SM, Alonso DM, Wettstein SG, Gürbüz El, Henao CA, Dumesic JA, et al. A sulfuric acid management strategy for the production of liquid hydrocarbon fuels via catalytic conversion of biomass-derived levulinic acid. *Energy Environ Sci* 2012;5:9690–7.
- [901] Zhao Y, Fu Y, Guo QX. Production of aromatic hydrocarbons through catalytic pyrolysis of γ-valerolactone from biomass. *Bioresour Technol* 2012;114:740–4.
- [902] Pupovac K, Palkovits R, Cu/MgAl₂O₄ as bifunctional catalyst for aldol condensation of 5-hydroxymethylfurfural and selective transfer hydrogenation. *ChemSusChem* 2013;6:2103–10.
- [903] Yati I, Yeom M, Choi JW, Choo H, Suh DJ, Ha JM. Water-promoted selective heterogeneous catalytic trimerization of xylose-derived 2-methylfuran to diesel precursors. *Appl Catal A Gen* 2015;495:200–5.
- [904] Liu D, Chen EYX. Integrated catalytic process for biomass conversion and upgrading to C₁₂ furan and alkane fuel. *ACS Catal* 2014;4:1302–10.
- [905] Liu D, Chen EYX. Diesel and alkane fuels from biomass by organocatalysis and metal-acid tandem catalysis. *ChemSusChem* 2013;6:2236–9.
- [906] Chheda JN, Dumesic JA. An overview of dehydration, aldol-condensation and hydrogenation processes for production of liquid alkanes from biomass-derived carbohydrates. *Catal Today* 2007;123:59–70.
- [907] Deduskošpan W, Faungnawakij K, Champreda V, Laosiripojana N. Hydrolysis/dehydration/aldol-condensation/hydrogenation of lignocellulosic biomass and biomass-derived carbohydrates in the presence of Pd/WO₃-ZrO₂ in a single reactor. *Bioresour Technol* 2011;102:2040–6.
- [908] Zákzeski J, Bruijnincx PCA, Jongerius AL, Weckhuysen BM. The catalytic valorization of lignin for the production of renewable chemicals. *Chem Rev* 2010;110:3552–99.
- [909] Liu H, Jiang T, Han B, Liang S, Zhou Y. Selective phenol hydrogenation to cyclohexanone over a dual supported Pd–Lewis acid catalyst. *Science* 2009;326:1250–2.
- [910] Deutsch KL, Shanks BH. Hydrodeoxygenation of lignin model compounds over a copper chromite catalyst. *Appl Catal A Gen* 2012;447-8:144–50.
- [911] Laskar DD, Tucker MP, Chen X, Helms GL, Yang B. Noble-metal catalyzed hydrodeoxygenation of biomass-derived lignin to aromatic hydrocarbons. *Green Chem* 2014;16:897–910.
- [912] Ji N, Wang X, Weidenthaler C, Spliethoff B, Rinaldi R. Iron(II) disulfides as precursors of highly selective catalysts for hydrodeoxygenation of dibenzyl ether into toluene. *ChemCatChem* 2015;7:960–6.
- [913] Wang X, Rinaldi R. A route for lignin and bio-oil conversion: dehydroxylation of phenols into arenes by catalytic tandem reactions. *Angew Chem Int Ed* 2013;52:11499–503.
- [914] Zhang W, Chen J, Liu R, Wang S, Chen L, Li K. Hydrodeoxygenation of lignin-derived phenolic monomers and dimers to alkane fuels over bifunctional zeolite-supported metal catalysts. *ACS Sust Chem Eng* 2014;2:683–91.
- [915] Corma A, Iborra S, Velty A. Chemical routes for the transformation of biomass into chemicals. *Chem Rev* 2007;107:2411–502.
- [916] Besson M, Gallezot P, Pinel C. Conversion of biomass into chemicals over metal catalysts. *Chem Rev* 2014;114:1827–70.

- [917] Straathof AJJ. Transformation of biomass into commodity chemicals using enzymes or cells. *Chem Rev* 2014;114:1871–908.
- [918] Asadieraghi M, Daud WMAW, Abbas HF. Heterogeneous catalysts for advanced bio-fuel production through catalytic biomass pyrolysis vapor upgrading: a review. *RSC Adv* 2015;5:22234–55.
- [919] Xuan J, Leung MKH, Leung DYC, Ni M. A review of biomass-derived fuel processors for fuel cell systems. *Renew Sust Energy Rev* 2009;13:1301–13.
- [920] Tominaga M, Shimazoe T, Nagashima M, Taniguchi I. Electrocatalytic oxidation of glucose at gold nanoparticle-modified carbon electrodes in alkaline and neutral solutions. *Electrochim Commun* 2005;7:189–93.
- [921] Yi Q, Yu W, Niu F. Novel nanoporous binary Au-Ru electrocatalysts for glucose oxidation. *Electroanal* 2010;22:556–63.
- [922] Ci S, Wen Z, Mao S, Hou Y, Cui S, He Z, et al. One-pot synthesis of high-performance Co/graphene electrocatalysts for glucose fuel cells free of enzymes and precious metals. *Chem Commun* 2015;51:9354–7.
- [923] Liu A, Ren Q, Xu T, Yuan M, Tang W. Morphology-controllable gold nanostructures on phosphorus doped diamond-like carbon surfaces and their electrocatalysis for glucose oxidation. *Sensor Actuat B: Chem* 2012;162:135–42.
- [924] Xia C, Ning W. A novel non-enzymatic electrochemical glucose sensor modified with FeOOH nanowire. *Electrochim Commun* 2010;12:1581–4.
- [925] Karczmarczyk A, Celebska A, Nogala W, Sashuk V, Chernyaeva O, Opallo M. Electrocatalytic glucose oxidation at gold and gold-carbon nanoparticulate film prepared from oppositely charged nanoparticles. *Electrochim Acta* 2014;117:211–16.
- [926] Shi Q, Diao G, Mu S. The electrocatalytic oxidation of glucose on the bimetallic Au-Ag particles-modified reduced graphene oxide electrodes in alkaline solutions. *Electrochim Acta* 2014;133:335–46.
- [927] Li R, Zhang J, Wang Z, Li Z, Liu J, Gu Z, et al. Novel graphene-gold nanohybrid with excellent electrocatalytic performance for the electrochemical detection of glucose. *Sensor Actuat B: Chem* 2015;208:421–8.
- [928] Jiang T, Yan L, Meng Y, Xiao M, Wu Z, Tsakarais P, et al. Glucose electrooxidation in alkaline medium: performance enhancement of PdAu/C synthesized by NH₃ modified pulse microwave assisted polyol method. *Appl Catal B: Environ* 2015;162:275–81.
- [929] Zhang S, Han L, Hou C, Li C, Lang Q, Han L, et al. Novel glucose sensor with Au@Ag heterogeneous nanorods based on electrocatalytic reduction of hydrogen peroxide at negative potential. *J Electroanal Chem* 2015;742:84–9.
- [930] Devadoss A, Sudhagar P, Das S, Lee SY, Terashima C, Nakata K, et al. Synergistic metal–metal oxide nanoparticles supported electrocatalytic graphene for improved photoelectrochemical glucose oxidation. *ACS Appl Mater Interfaces* 2014;6:4864–71.
- [931] Ma C, Xue W, Li J, Xing W, Hao Z. Mesoporous carbon-confined Au catalysts with superior activity for selective oxidation of glucose to gluconic acid. *Green Chem* 2013;15:1035–41.
- [932] Li Y, Niu X, Tang J, Lan M, Zhao H. A comparative study of nonenzymatic electrochemical glucose sensors based on Pt-Pd nanotube and nanowire arrays. *Electrochim Acta* 2014;130:1–8.
- [933] Brouzgou A, Yan LL, Song SQ, Tsakarais P. Glucose electrooxidation over Pd_xRh/C electrocatalysts in alkaline medium. *Appl Catal B: Environ* 2014;147:481–9.
- [934] Chen CC, Lin CL, Chen LC. Functionalized carbon nanomaterial supported palladium nano-catalysts for electrocatalytic glucose oxidation reaction. *Electrochim Acta* 2015;152:408–16.
- [935] Huo H, Xu Z, Zhang T, Xu C. Ni/CdS/TiO₂ nanotube array heterostructures for high performance photoelectrochemical biosensing. *J Mater Chem A* 2015;3:5882–8.
- [936] Long M, Tan L, Liu H, He Z, Tang A. Novel helical TiO₂ nanotube arrays modified by Cu₂O for enzyme-free glucose oxidation. *Biosens Bioelectron* 2014;59:243–50.
- [937] Li SJ, Xia N, Lv XL, Zhao MM, Yuan BQ, Pang H. A facile one-step electrochemical synthesis of graphene/NiO nanocomposites as efficient electrocatalyst for glucose and methanol. *Sensor Actuat B: Chem* 2014;190:809–17.
- [938] Wu J, Miao Y, Liang X, Yang Z, Yang Y, Ouyang R. Promotion effect of bismuth on nickel electrodeposition and its electrocatalysis to glucose oxidation. *Electroanal* 2014;26:856–63.
- [939] Gu Y, Liu Y, Yang H, Li B, An Y. Electrocatalytic glucose oxidation via hybrid nanomaterial catalyst of multi-wall TiO₂ nanotubes supported Ni(OH)₂ nanoparticles: optimization of the loading level. *Electrochim Acta* 2015;160:263–70.
- [940] Arvinte A, Sesay AM, Virtanen V. Carbohydrates electrocatalytic oxidation using CNT-NiCo-oxide modified electrodes. *Talanta* 2011;84:180–6.
- [941] Li L, Liang B, Shi J, Li F, Mascini M, Liu A. A selective and sensitive D-xylose electrochemical biosensor based on xylose dehydrogenase displayed on the surface of bacteria and multi-walled carbon nanotubes modified electrode. *Biosens Bioelectron* 2012;33:100–5.
- [942] Xu D, Luo L, Ding Y, Jiang L, Zhang Y, Ouyang X, et al. A novel nonenzymatic fructose sensor based on electrospun LaMnO₃ fibers. *J Electroanal Chem* 2014;727:21–6.
- [943] Jokic A, Ristic N, Jaksic MM, Spasojevic M, Krstajic N. Simultaneous electrolytic production of xylitol and xylonic acid from xylose. *J Appl Electrochem* 1991;21:321–6.
- [944] Aissa AA, Aider M. Electro-catalytic isomerization of lactose into lactulose: the impact of the electric current, temperature and reactor configuration. *Int Dairy J* 2014;34:213–19.
- [945] Kwon Y, Koper MTM. Electrocatalytic hydrogenation and deoxygenation of glucose on solid metal electrodes. *ChemSusChem* 2013;6:455–62.
- [946] Kwon Y, de Jong E, van der Waal JK, Koper MTM. Selective electrocatalytic oxidation of sorbitol to fructose and sorbose. *ChemSusChem* 2015;8:970–3.
- [947] Reichert E, Wintringer R, Volmer DA, Hempelmann R. Electro-catalytic oxidative cleavage of lignin in a protic ionic liquid. *Phys Chem Chem Phys* 2012;14:5214–21.
- [948] Lam CH, Lowe CB, Li Z, Longe KN, Rayburn JT, Caldwell MA, et al. Electrocatalytic upgrading of model lignin monomers with earth abundant metal electrodes. *Green Chem* 2015;17:601–9.
- [949] Vuyyuru KR, Strasser P. Oxidation of biomass derived 5-hydroxymethylfurfural using heterogeneous and electrochemical catalysts. *Catal Today* 2012;195:144–54.
- [950] Chadderton DJ, Xin L, Qi J, Qiu Y, Krishna P, More KL, et al. Electrocatalytic oxidation of 5-hydroxymethylfurfural to 2,5-furandicarboxylic acid on supported Au and Pd bimetallic nanoparticles. *Green Chem* 2014;16:3778–86.
- [951] Kwon Y, de Jong E, Raoufmoghaddam S, Koper MTM. Electrocatalytic hydrogenation of 5-hydroxymethylfurfural in the absence and presence of glucose. *ChemSusChem* 2013;6:1659–67.
- [952] Kwon Y, Birdja YY, Raoufmoghaddam S, Koper MTM. Electrocatalytic hydrogenation of 5-hydroxymethylfurfural in acidic solution. *ChemSusChem* 2015;8:1745–51.
- [953] Nilges P, Schröder U. Electrochemistry for biofuel generation: production of furans by electrocatalytic hydrogenation of furfurals. *Energy Environ Sci* 2013;6:2925–31.
- [954] Chu D, Hou Y, He J, Xu M, Wang Y, Wang S, et al. Nano TiO₂ film electrode for electrocatalytic reduction of furfural in ionic liquids. *J Nanopart Res* 2009;11:1805–9.
- [955] Li Z, Kelkar S, Lam CH, Luczek K, Jackson JE, Miller DJ, et al. Aqueous electrocatalytic hydrogenation of furfural using a sacrificial anode. *Electrochim Acta* 2012;64:87–93.
- [956] Zhao B, Chen M, Guo Q, Fu Y. Electrocatalytic hydrogenation of furfural to furfuryl alcohol using platinum supported on activated carbon fibers. *Electrochim Acta* 2014;135:139–46.
- [957] Wang F, Xu M, Wei L, Wei Y, Hu Y, Fang W, et al. Fabrication of La-doped TiO₂ film electrode and investigation of its electrocatalytic activity for furfural reduction. *Electrochim Acta* 2015;153:170–4.
- [958] Green SK, Lee J, Kim HJ, Tompsett GA, Kim WB, Huber GW. The electrocatalytic hydrogenation of furanic compounds in a continuous electrocatalytic membrane reactor. *Green Chem* 2013;15:1869–79.
- [959] Xin L, Zhang Z, Qi J, Chadderton DJ, Qiu Y, Warsko KM, et al. Electricity storage in biofuels: selective electrocatalytic reduction of levulinic acid to valeric acid or γ -valerolactone. *ChemSusChem* 2013;6:674–86.
- [960] Qiu Y, Xin L, Chadderton DJ, Qi J, Liang C, Li W. Integrated electrocatalytic processing of levulinic acid and formic acid to produce biofuel intermediate valeric acid. *Green Chem* 2014;16:1305–15.
- [961] Luo W, Bruijninck PCA, Weckhuysen BM. Selective, one-pot catalytic conversion of levulinic acid to pentanoic acid over Ru/H-ZSM5. *J Catal* 2014;320:33–41.
- [962] Yang Y, Gao G, Zhang X, Li F. Facile fabrication of composition-tuned Ru–Ni bimetallics in ordered mesoporous carbon for levulinic acid hydrogenation. *ACS Catal* 2014;4:1419–25.
- [963] Fashedemi OO, Ozoemena KI. Comparative electrocatalytic oxidation of ethanol, ethylene glycol and glycerol in alkaline medium at Pd-decorated FeCo@Fe/C core-shell nanocatalysts. *Electrochim Acta* 2014;128:279–86.
- [964] Yang L, Kinoshita S, Yamada T, Kanda S, Kitagawa H, Tokunaga M, et al. A metal–organic framework as an electrocatalyst for ethanol oxidation. *Angew Chem* 2010;122:5476–9.
- [965] Zheng JN, Lv JJ, Li SS, Xue MW, Wang AJ, Feng JJ. One-pot synthesis of reduced graphene oxide supported hollow Ag@Pt core–shell nanospheres with enhanced electrocatalytic activity for ethylene glycol oxidation. *J Mater Chem A* 2014;2:3445–51.
- [966] Ramulifho T, Ozoemena KI, Modibedi RM, Jafta CJ, Mathe MK. Electrocatalytic oxidation of ethylene glycol at palladium-bimetallic nanocatalysts (PdSn and PdNi) supported on sulfonate-functionalised multi-walled carbon nanotubes. *J Electroanal Chem* 2013;692:26–30.
- [967] Kim HJ, Lee J, Green SK, Huber GW, Kim WB. Selective glycerol oxidation by electrocatalytic dehydrogenation. *ChemSusChem* 2014;7:1051–6.
- [968] Wang H, Thia L, Li N, Ge X, Liu Z, Wang X. Pd nanoparticles on carbon nitride-graphene for the selective electro-oxidation of glycerol in alkaline solution. *ACS Catal* 2015;5:3174–80.
- [969] Hickey DP, McCamant MS, Giroud F, Sigman MS, Minteer SD. Hybrid enzymatic and organic electrocatalytic cascade for the complete oxidation of glycerol. *J Am Chem Soc* 2014;136:15917–20.
- [970] Wang J, Huang L, Yang R, Zhang Z, Wu J, Gao Y, et al. Recent advances in solid sorbents for CO₂ capture and new development trends. *Energy Environ Sci* 2014;7:3478–518.
- [971] Cole AJ, Mata L, Paul NA, de Nys R. Using CO₂ to enhance carbon capture and biomass applications of fresh water macroalgae. *GCB Bioen* 2014;6:637–45.
- [972] Inglis JL, MacLean BJ, Pryce MT, Vos JG. Electrocatalytic pathways towards sustainable fuel production from water and CO₂. *Coordin Chem Rev* 2012;256:2571–600.
- [973] Oh Y, Hu X. Organic molecules as mediators and catalysts for photocatalytic and electrocatalytic CO₂ reduction. *Chem Soc Rev* 2013;42:2253–61.

- [974] Kuhl KP, Hatsukade T, Cave ER, Abram DN, Kibsgaard J, Jaramillo TF. Electrocatalytic conversion of carbon dioxide to methane and methanol on transition metal surfaces. *J Am Chem Soc* 2014;136:14107–13.
- [975] Chen WF, Iyer S, Iyer S, Sasaki K, Wang CH, Zhu Y, et al. Biomass-derived electrocatalytic composites for hydrogen evolution. *Energy Environ Sci* 2013;6:1818–26.
- [976] Xie S, Zhai T, Li W, Yu M, Liang C, Gan J, et al. Hydrogen production from solar driven glucose oxidation over Ni(OH)_2 functionalized electroreduced-TiO₂ nanowire arrays. *Green Chem* 2013;15:2434–40.
- [977] Ni M, Leung DYC, Leung MKH. A review on reforming bio-ethanol for hydrogen production. *Int J Hydrogen Energy* 2007;32:3238–47.
- [978] Marr AC, Liu S. Combining bio- and chemo-catalysis: from enzymes to cells, from petroleum to biomass. *Trends Biotechnol* 2011;29:199–204.
- [979] Vennestrom PNR, Christensen CH, Pedersen S, Grunwaldt JD, Woodley JM. Next-generation catalysis for renewables: combining enzymatic with inorganic heterogeneous catalysis for bulk chemical production. *ChemCatChem* 2010;2:249–58.
- [980] Wongnate T, Sucharitakul J, Chaiyen P. Identification of a catalytic base for sugar oxidation in the pyranose 2-oxidase reaction. *Chembiochem* 2011;12:2577–86.
- [981] Leitner C, Neuhauser W, Volc J, Kulbe KD, Nidetzky B, Haltrich D. The Cetus process revisited: a novel enzymatic alternative for the production of aldose-free D-fructose. *Biocatal Biotransform* 1998;16:365–82.
- [982] Lee YC, Chen CT, Chiu YT, Wu KCW. An effective cellulose-to-glucose-to-fructose conversion sequence by using enzyme immobilized Fe₂O₃-loaded mesoporous silica nanoparticles as recyclable biocatalysts. *ChemCatChem* 2013;5:2153–7.
- [983] Ståhlberg T, Woodley JM, Riisager A. Enzymatic isomerization of glucose and xylose in ionic liquids. *Catal Sci Technol* 2012;2:291–5.
- [984] Lee YC, Dutta S, Wu KCW. Integrated, cascading enzyme-/chemocatalytic cellulose conversion using catalysts based on mesoporous silica nanoparticles. *ChemSusChem* 2014;7:3241–6.
- [985] Huang H, Denard CA, Alamillo R, Crisci AJ, Miao Y, Dumesic JA, et al. Tandem catalytic conversion of glucose to 5-hydroxymethylfurfural with an immobilized enzyme and a solid acid. *ACS Catal* 2014;4:2165–8.
- [986] Grande PM, Bergs C, Domínguez de María P. Chemo-enzymatic conversion of glucose into 5-hydroxymethylfurfural in seawater. *ChemSusChem* 2012;5:1203–6.
- [987] Boisen A, Christensen TB, Fu W, Gorbanev YY, Hansen TS, Jensen JS, et al. Process integration for the conversion of glucose to 2,5-furandicarboxylic acid. *Chem Eng Res Des* 2009;87:1318–27.
- [988] Krystof M, Pérez-Sánchez M, Domínguez de María P. Lipase-mediated selective oxidation of furfural and 5-hydroxymethylfurfural. *ChemSusChem* 2013;6:826–30.
- [989] Koopman F, Wierckx N, de Winde JH, Ruijssemaars HJ. Efficient whole-cell biotransformation of 5-(hydroxymethyl)furfural into FDCA, 2,5-furandicarboxylic acid. *Bioresour Technol* 2010;101:6291–6.
- [990] Boopathy R. Anaerobic biotransformation of furfural to furfuryl alcohol by a methanogenic archaeabacterium. *Int Biodeter Biodegr* 2009;63:1070–2.
- [991] Zhang Y, Han B, Ezeji TC. Biotransformation of furfural and 5-hydroxymethylfurfural (HMF) by *Clostridium acetobutylicum* ATCC 824 during butanol fermentation. *New Biotechnol* 2012;29:345–51.
- [992] Martin CH, Wu D, Prather KJ. Integrated bioprocessing for the pH-dependent production of 4-valerolactone from levulinic acid in *Pseudomonas putida* KT2440. *Appl Environ Microbiol* 2010;76:417–24.
- [993] Götz K, Liese A, Ansorge-Schumacher M, Hilterhaus L. A chemo-enzymatic route to synthesize (S)- γ -valerolactone from levulinic acid. *Appl Microbiol Biotechnol* 2013;97:3865–73.
- [994] Min K, Kim S, Yum T, Kim Y, Sang B-I, Um Y. Conversion of levulinic acid to 2-butaneone by acetoacetate decarboxylase from *Clostridium acetobutylicum*. *Appl Microbiol Biotechnol* 2013;97:5627–34.
- [995] Multer A, McGraw N, Hohn K, Vadlani P. Production of methyl ethyl ketone from biomass using a hybrid biochemical/catalytic approach. *Ind Eng Chem Res* 2013;52:56–60.
- [996] Grala A, Zieliński M, Dębowksi M, Dudek M. Effects of hydrothermal depolymerization and enzymatic hydrolysis of algae biomass on yield of methane fermentation process. *Pol J Environ Stud* 2012;21:361–6.
- [997] Ndoku JM, Suzuki W, Matsumoto K, Kobayashi H, Ooi T, Fukuoka A, et al. Polyhydroxyalkanoates production from cellulose hydrolysate in *Escherichia coli* LSS218 with superior resistance to 5-hydroxymethylfurfural. *J Biosci Bioeng* 2012;113:70–2.
- [998] Matsumoto K, Kobayashi H, Ikeda K, Komanoya T, Fukuoka A, Taguchi S. Chemo-microbial conversion of cellulose into polyhydroxybutyrate through ruthenium-catalyzed hydrolysis of cellulose into glucose. *Bioresour Technol* 2011;102:3564–7.
- [999] Lopez M, Fort S, Bizot H, Buléon A, Driguez H. Chemo-enzymatic synthesis of xyloglucano-oligosaccharides and their interactions with cellulose. *Carbohyd Polym* 2012;88:185–93.
- [1000] You C, Chen H, Myung S, Sathitsuksanoh N, Ma H, Zhang XZ, et al. Enzymatic transformation of nonfood biomass to starch. *Proc Natl Acad Sci USA* 2013;110:7182–7.
- [1001] Colmenares JC, Luque R. Heterogeneous photocatalytic nanomaterials: prospects and challenges in selective transformations of biomass-derived compounds. *Chem Soc Rev* 2014;43:765–78.
- [1002] Asghari FS, Yoshida H. Kinetics of the decomposition of fructose catalyzed by hydrochloric acid in subcritical water: formation of 5-hydroxymethylfurfural, levulinic, and formic acids. *Ind Eng Chem Res* 2007;46:7703–10.
- [1003] Girsuta B, Janssen LPBM, Heeres HJ. Kinetic study on the acid-catalyzed hydrolysis of cellulose to levulinic acid. *Ind Eng Chem Res* 2007;46:1696–708.
- [1004] Dutta S. Catalytic materials that improve selectivity of biomass conversions. *RSC Adv* 2012;2:12575–93.
- [1005] Zheng Y, Pan Z, Zhao R. Overview of biomass pretreatment for cellulosic ethanol production. *Int J Agric Biol* 2009;2:51–68.
- [1006] Hendriks ATWM, Zeeman G. Pretreatments to enhance the digestibility of lignocellulosic biomass. *Bioresour Technol* 2009;100:10–18.
- [1007] Guo F, Fang Z, Xu CC, Smith RL. Solid acid mediated hydrolysis of biomass for producing biofuels. *Prog Energy Combust Sci* 2012;38:672–90.
- [1008] Saritha M, Arora A, Lata. Biological pretreatment of lignocellulosic substrates for enhanced delignification and enzymatic digestibility. *Ind J Microbiol* 2012;52:122–30.
- [1009] Bak JS, Kim MD, Choi IG, Kim KH. Biological pretreatment of rice straw by fermenting with *Dichomitus squalens*. *New Biotechnol* 2010;27:424–34.
- [1010] Prajapati SK, Bhattachary A, Malik A, Vijay VK. Pretreatment of algal biomass using fungal crude enzymes. *Algal Res* 2015;8:8–14.
- [1011] Mosier N, Wyman C, Dale B, Elander R, Lee YY, Holtzapffe M, et al. Features of promising technologies for pretreatment of lignocellulosic biomass. *Bioresour Technol* 2005;96:673–86.
- [1012] Kärcher MA, Iqbal Y, Lewandowski I, Senn T. Comparing the performance of *Miscanthus x giganteus* and wheat straw biomass in sulfuric acid based pretreatment. *Bioresour Technol* 2015;180:360–4.
- [1013] Sun Y, Cheng JY. Hydrolysis of lignocellulosic materials for ethanol production: a review. *Bioresour Technol* 2002;83:1–11.
- [1014] de Almeida RM, Li JR, Nederlof C, O'Connor P, Makkee M, Moulijn JA. Cellulose conversion to isosorbide in molten salt hydrate media. *ChemSusChem* 2010;3:325–8.
- [1015] Okatova OV, Lavrenko PN, Cvetkov VN, Dautzenberg H, Philipp B. Viscometric and diffusion investigations in the cellulose/cadoxen/water system. *Acta Polym* 2003;40:297–301.
- [1016] Ramos LA, Frollini E, Heinze T. Carboxymethylation of cellulose in the new solvent dimethyl sulfoxide/tetrabutylammonium fluoride. *Carbohyd Polym* 2005;60:259–67.
- [1017] Song YB, Zhou JP, Zhang LN, Wu XJ. Homogenous modification of cellulose with acrylamide in NaOH/urea aqueous solutions. *Carbohyd Polym* 2008;73:18–25.
- [1018] Ishii D, Tatsumi D, Matsumoto T. Effect of solvent exchange on the supramolecular structure, the molecular mobility and the dissolution behavior of cellulose in LiCl/DMAC. *Carbohyd Res* 2008;343:919–28.
- [1019] Tadesse H, Luque R. Advances on biomass pretreatment using ionic liquids: an overview. *Energy Environ Sci* 2011;4:3913–29.
- [1020] Swatoski RP, Spear SK, Holbrey JD, Rogers RD. Dissolution of cellose with ionic liquids. *J Am Chem Soc* 2002;124:4974–5.
- [1021] Kamiya N, Matsushita Y, Hanaki M, Nakashima K, Narita M, Goto M, et al. Enzymatic *in-situ* saccharification of cellulose in aqueous-ionic liquid media. *Biotechnol Lett* 2008;30:1037–40.
- [1022] Jiang LQ, Fang Z, Zhao ZL, He F, Li HB. 2,3-Butanediol and acetoin production from enzymatic hydrolysis of ionic liquid-pretreated cellulose by *Paenibacillus polymyxa*. *Bioresources* 2015;10:1318–29.
- [1023] Jiang LQ, Fang Z, Li XK, Luo J, Fan SP. Combination of dilute acid and ionic liquid pretreatments of sugarcane bagasse for enzymatic saccharification. *Process Biochem* 2013;48:1942–6.
- [1024] Olivier-Bourbigou H, Magna L, Morvan D. Ionic liquids and catalysis: recent progress from knowledge to applications. *Appl Catal A Gen* 2010;373:1–56.
- [1025] Wang C, Wei Z, Wang L, Sun P, Wang Z. Assessment of bromide-based ionic liquid toxicity toward aquatic organisms and QSAR analysis. *Ecotox Environ Safe* 2015;115:112–18.
- [1026] Costa SPF, Pinto PCAG, Lapa RAS, Saraiva MLMFS. Toxicity assessment of ionic liquids with *Vibrio fischeri*: an alternative fully automated methodology. *J Hazard Mater* 2015;284:136–42.
- [1027] Deng Y, Beadham I, Ghavre M, Costa Gomes MF, Gathergood N, Husson P, et al. When can ionic liquids be considered readily biodegradable? Biodegradation pathways of pyridinium, pyrrolidinium and ammonium-based ionic liquids. *Green Chem* 2015;17:1479–91.
- [1028] Cheng YS, Chen KY, Chou TH. Concurrent calcium peroxide pretreatment and wet storage of water hyacinth for fermentable sugar production. *Bioresour Technol* 2015;176:267–72.
- [1029] da Costa JA, Marques JE, Gonçalves LRB, Rocha MVP. Enhanced enzymatic hydrolysis and ethanol production from cashew apple bagasse pretreated with alkaline hydrogen peroxide. *Bioresour Technol* 2015;179:249–59.
- [1030] Ahring BK, Biswas R, Ahmed A, Teller PJ, Uellendahl H. Making lignin accessible for anaerobic digestion by wet-explosion pretreatment. *Bioresour Technol* 2015;175:182–8.
- [1031] Ramadoss G, Muthukumar K. Influence of dual salt on the pretreatment of sugarcane bagasse with hydrogen peroxide for bioethanol production. *Chem Eng J* 2015;260:178–87.
- [1032] Zhou L, Yang X, Xu J, Shi M, Wang F, Chen C, et al. Depolymerization of cellulose to glucose by oxidation–hydrolysis. *Green Chem* 2015;17:1519–24.
- [1033] Wang YZ, Chen X, Wang Z, Zhao JF, Fan TT, Li DS, et al. Effect of low concentration alkali and ultrasound combination pretreatment on biogas production by stalk. *Adv Mat Res* 2011;383:3434–7.
- [1034] Diaz AB, de Souza Moretti MM, Bezerra-Bussoli C, Nunes CCC, Blandino A, da Silva R, et al. Evaluation of microwave-assisted pretreatment of

- lignocellulosic biomass immersed in alkaline glycerol for fermentable sugars production. *Bioresour Technol* 2015;185:316–23.
- [1035] Hu Z, Wen Z. Enhancing enzymatic digestibility of switchgrass by microwave-assisted alkali pretreatment. *Biochem Eng J* 2008;38:369–78.
- [1036] Ninomiya K, Kohori A, Tatsumi M, Osawa K, Endo T, Kakuchi R, et al. Ionic liquid/ultrasound pretreatment and *in-situ* enzymatic saccharification of bagasse using biocompatible cholinium ionic liquid. *Bioresour Technol* 2015;176:169–74.
- [1037] Nkemka VN, Murto M. Biogas production from wheat straw in batch and UASB reactors: the roles of pretreatment and seaweed hydrolysate as a co-substrate. *Bioresour Technol* 2013;128:164–72.
- [1038] Zheng Y, Zhao J, Xu F, Li Y. Pretreatment of lignocellulosic biomass for enhanced biogas production. *Prog Energy Combust Sci* 2014;42:35–53.
- [1039] Beck S, Bouchard J, Berry R. Dispersibility in water of dried nanocrystalline cellulose. *Biomacromolecules* 2012;13:1486–94.
- [1040] Wang Q, Liu S, Yang G, Chen J. Thermogravimetric kinetics of sugarcane bagasse pretreated by hot-water. *Bioresour Technol* 2013;129:676–9.
- [1041] Pu Y, Jiang N, Ragauskas AJ. Ionic liquid as a green solvent for lignin. *J Wood Chem Technol* 2007;27:23–33.
- [1042] Pińkowska H, Wółak Złocińska A. Hydrothermal decomposition of alkali lignin in sub- and supercritical water. *Chem Eng J* 2012;187:410–14.
- [1043] Azadi P, Farnood R. Review of heterogeneous catalysts for sub- and supercritical water gasification of biomass and wastes. *Int J Hydrogen Energy* 2011;36:9529–41.
- [1044] Bicker M, Kaiser D, Ott L, Vogel H. Dehydration of D-fructose to hydroxymethylfurfural in sub- and supercritical fluids. *J Supercrit Fluid* 2005;36:118–26.
- [1045] Fang Z, Xu C. Near-critical and supercritical water and their applications for biorefineries. Heidelberg Berlin: Springer-Verlag; 2014.
- [1046] Song J, Fan H, Ma J, Han B. Conversion of glucose and cellulose into value-added products in water and ionic liquids. *Green Chem* 2013;15:2619–35.
- [1047] Pinkert A, Goekse DF, Marsh KN, Pang S. Extracting wood lignin without dissolving or degrading cellulose: investigations on the use of food additive-derived ionic liquids. *Green Chem* 2011;13:3124–36.
- [1048] George A, Tran K, Morgan TJ, Benke PI, Berreco C, Lorente E, et al. The effect of ionic liquid cation and anion combinations on the macromolecular structure of lignins. *Green Chem* 2011;13:3375–85.
- [1049] Fang Z, Smith RL, Qi X. Production of biofuels and chemicals with ionic liquids. Heidelberg Berlin: Springer-Verlag; 2014.
- [1050] Zhang ZC. Catalytic transformation of carbohydrates and lignin in ionic liquids. *WIREs Energy Environ* 2013;2:655–72.
- [1051] Pinkert A, Marsh KN, Pang S, Staiger MP. Ionic liquids and their interaction with cellulose. *Chem Rev* 2009;109:6712–28.
- [1052] Marcotullio G, Jong WD. Chloride ions enhance furfural formation from D-xylene in dilute aqueous acidic solutions. *Green Chem* 2010;12:1739–46.
- [1053] Dutta S, De S, Alam MI, Abu-Omar MM, Saha B. Direct conversion of cellulose and lignocellulosic biomass into chemicals and biofuel with metal chloride catalysts. *J Catal* 2012;288:8–15.
- [1054] Hsu WH, Lee YY, Peng WH, Wu KCW. Cellulosic conversion in ionic liquids (ILs): effects of H_2O /cellulose molar ratios, temperatures, times, and different ILs on the production of monosaccharides and 5-hydroxymethylfurfural (HMF). *Catal Today* 2011;174:65–9.
- [1055] Brandt A, Ray MJ, To TQ, Leak DJ, Murphy RJ, Welton T. Ionic liquid pretreatment of lignocellulosic biomass with ionic liquid–water mixtures. *Green Chem* 2011;13:2489–99.
- [1056] Qi X, Watanabe M, Aida TM, Smith RL. Synergistic conversion of glucose into 5-hydroxymethylfurfural in ionic liquid–water mixtures. *Bioresour Technol* 2012;109:224–8.
- [1057] Govinda V, Attri P, Venkatesu P, Venkateswarlu P. Thermophysical properties of dimethylsulfoxide with ionic liquids at various temperatures. *Fluid Phase Equilib* 2011;304:35–43.
- [1058] Xiao S, Liu B, Wang Y, Fang Z, Zhang Z. Efficient conversion of cellulose into biofuel precursor 5-hydroxymethylfurfural in dimethyl sulfoxide–ionic liquid mixtures. *Bioresour Technol* 2014;151:361–6.
- [1059] Zhang Z, Liu B, Zhao Z. Conversion of fructose into 5-HMF catalyzed by $GeCl_4$ in DMSO and [Bmim]Cl system at room temperature. *Carbohyd Polym* 2012;88:891–5.
- [1060] Mushrif SH, Caratzoulas S, Vlachos DG. Understanding solvent effects in the selective conversion of fructose to 5-hydroxymethyl-furfural: a molecular dynamics investigation. *Phys Chem Chem Phys* 2012;14:2637–44.
- [1061] Tsilomelekis G, Josephson TR, Nikolakis V, Caratzoulas S. Origin of 5-hydroxymethylfurfural stability in water/dimethyl sulfoxide mixtures. *ChemSusChem* 2014;7:117–26.
- [1062] Wang H, Deng T, Wang Y, Qi Y, Hou X, Zhu Y. Efficient catalytic system for the conversion of fructose into 5-ethoxymethylfurfural. *Bioresour Technol* 2013;136:394–400.
- [1063] Beckerle K, Okuda J. Conversion of glucose and cellobiose into 5-hydroxymethylfurfural (HMF) by rare earth metal salts in N,N'-dimethylacetamide (DMA). *J Mol Catal A Chem* 2012;356:158–64.
- [1064] Vasudevan V, Mushrif SH. Insights into the solvation of glucose in water, dimethyl sulfoxide (DMSO), tetrahydrofuran (THF) and N,N'-dimethylformamide (DMF) and its possible implications on the conversion of glucose to platform chemicals. *RSC Adv* 2015;5:20756–63.
- [1065] Yang Y, Liu W, Wang N, Wang H, Song Z, Li W. Effect of organic solvent and Bronsted acid on 5-hydroxymethylfurfural preparation from glucose over $CrCl_3$. *RSC Adv* 2015;5:27805–13.
- [1066] Amarasekara AS, Williams LTD, Ebede CC. Mechanism of the dehydration of D-fructose to 5-hydroxymethylfurfural in dimethyl sulfoxide at 150 °C: an NMR study. *Carbohyd Res* 2008;343:3021–4.
- [1067] Qu Y, Huang C, Song Y, Zhang J, Chen B. Efficient dehydration of glucose to 5-hydroxymethylfurfural catalyzed by the ionic liquid, 1-hydroxyethyl-3-methylimidazolium tetrafluoroborate. *Bioresour Technol* 2012;121:462–6.
- [1068] Ren H, Girisuta B, Zhou Y, Liu L. Selective and recyclable depolymerization of cellulose to levulinic acid catalyzed by acidic ionic liquid. *Carbohyd Polym* 2015;117:569–76.
- [1069] Saravanamurugan S, Nguyen Van Buu O, Riisager A. Conversion of mono- and disaccharides to ethyl levulinate and ethyl pyranoside with sulfonic acid-functionalized ionic liquids. *ChemSusChem* 2011;4:723–6.
- [1070] Wang G, Zhang Z, Song L. Efficient and selective alcoholysis of furfuryl alcohol to alkyl levulinate catalyzed by double SO₃H-functionalized ionic liquids. *Green Chem* 2014;16:1436–43.
- [1071] Potvin J, Sorlien E, Hegner J, DeBoef B, Lucht BL. Effect of NaCl on the conversion of cellulose to glucose and levulinic acid via solid supported acid catalysis. *Tetrahedron Lett* 2011;52:5891–3.
- [1072] Ren H, Zhou Y, Liu L. Selective conversion of cellulose to levulinic acid via microwave-assisted synthesis in ionic liquids. *Bioresour Technol* 2013;129:616–19.
- [1073] Lai L, Zhang Y. The production of 5-hydroxymethylfurfural from fructose in isopropyl alcohol: a green and efficient system. *ChemSusChem* 2011;4:1745–8.
- [1074] Saha B, Abu-Omar MM. Advances in 5-hydroxymethylfurfural production from biomass in biphasic solvents. *Green Chem* 2014;16:24–38.
- [1075] Cai CM, Nagane N, Kumar R, Wyman CE. Coupling metal halides with a co-solvent to produce furfural and 5-HMF at high yields directly from lignocellulosic biomass as an integrated biofuels strategy. *Green Chem* 2014;16:3819–29.
- [1076] Mellmer MA, Gallo JMR, Alonso DM, Dumesic JA. Selective production of levulinic acid from furfuryl alcohol in THF solvent systems over H-ZSM-5. *ACS Catal* 2015;5:3354–9.
- [1077] Weingarten R, Rodriguez-Beuerman A, Cao F, Luterbacher JS, Alonso DM, Dumesic JA, et al. Selective conversion of cellulose to hydroxymethylfurfural in polar aprotic solvents. *ChemCatChem* 2014;6:2229–34.
- [1078] Cai CM, Zhang T, Kumar R, Wyman CE. THF co-solvent enhances hydrocarbon fuel precursor yields from lignocellulosic biomass. *Green Chem* 2013;15:3140–5.
- [1079] Yang Y, Hu CW, Abu-Omar MM. Conversion of carbohydrates and lignocellulosic biomass into 5-hydroxymethylfurfural using AlCl₃·6H₂O catalyst in a biphasic solvent system. *Green Chem* 2012;14:509–13.
- [1080] Yang Y, Hu CW, Abu-Omar MM. Synthesis of furfural from xylose, xylan, and biomass using AlCl₃·6H₂O in biphasic media via xylose isomerization to xylulose. *ChemSusChem* 2012;5:405–10.
- [1081] Shen Y, Sun J, Yi Y, Li M, Wang B, Xu F, et al. InCl₃-catalyzed conversion of carbohydrates into 5-hydroxymethylfurfural in biphasic system. *Bioresour Technol* 2014;172:457–60.
- [1082] Pholjaroen B, Li N, Wang Z, Wang A, Zhang T. Dehydration of xylose to furfural over niobium phosphate catalyst in biphasic solvent system. *J Energy Chem* 2013;22:826–32.
- [1083] Ordovsky VV, van der Schaaf J, Schouten JC, Nijhuis TA. Fructose dehydration to 5-hydroxymethylfurfural over solid acid catalysts in a biphasic system. *ChemSusChem* 2012;5:1812–19.
- [1084] Román-Leshkov Y, Chheda JN, Dumesic JA. Phase modifiers promote efficient production of hydroxymethylfurfural from fructose. *Science* 2006;312:1933–7.
- [1085] Ordovsky VV, van der Schaaf J, Schouten JC, Nijhuis TA. The effect of solvent addition on fructose dehydration to 5-hydroxymethylfurfural in biphasic system over zeolites. *J Catal* 2012;287:68–75.
- [1086] Okano T, Qiao K, Bao Q, Tomida D, Hagiwara H, Yokoyama C. Dehydration of fructose to 5-hydroxymethylfurfural (HMF) in an aqueous acetonitrile biphasic system in the presence of acidic ionic liquids. *Appl Catal A Gen* 2013;451:1–5.
- [1087] Román-Leshkov Y, Dumesic JA. Solvent effects on fructose dehydration to 5-hydroxymethylfurfural in biphasic systems saturated with inorganic salts. *Top Catal* 2009;52:297–303.
- [1088] Wang W, Ren J, Li H, Deng A, Sun R. Direct transformation of xylan-type hemicelluloses to furfural via SnCl₄ catalysts in aqueous and biphasic systems. *Bioresour Technol* 2015;183:188–94.
- [1089] Alonso DM, Wettstein SG, Bond JQ, Root TW, Dumesic JA. Production of biofuels from cellulose and corn stover using alkylphenol solvents. *ChemSusChem* 2011;4:1078–81.
- [1090] Mellmer MA, Sener C, Gallo JMR, Luterbacher JS, Alonso DM, Dumesic JA. Solvent effects in acid-catalyzed biomass conversion reactions. *Angew Chem Int Ed* 2014;53:11872–5.
- [1091] Mellmer MA, Alonso DM, Luterbacher JS, Gallo JMR, Dumesic JA. Effects of γ -valerolactone in hydrolysis of lignocellulosic biomass to monosaccharides. *Green Chem* 2014;16:4659–62.
- [1092] Zhang L, Yu H, Wang P, Li Y. Production of furfural from xylose, xylan and corn cob in gamma-valerolactone using FeCl₃·6H₂O as catalyst. *Bioresour Technol* 2014;151:355–60.
- [1093] Qi L, Yiu Mui F, Lo SW, Lui M, Akien GR, Horváth IT. Catalytic conversion of fructose, glucose, and sucrose to 5-(hydroxymethyl)furfural and levulinic and formic acids in γ -valerolactone as a green solvent. *ACS Catal* 2014;4:1470–7.

- [1094] Cui J, Tan J, Deng T, Cui X, Zheng H, Zhu Y, et al. Direct conversion of carbohydrates to γ -valerolactone facilitated by solvent effect. *Green Chem* 2015;17:3084–9.
- [1095] Caretto A, Perosa A. Upgrading of levulinic acid with dimethylcarbonate as solvent/reagent. *ACS Sust Chem Eng* 2013;1:989–94.
- [1096] Gao W, Li Y, Xiang Z, Chen K, Yang R, Argyropoulos DS. Efficient one-pot synthesis of 5-chloromethylfurfural (CMF) from carbohydrates in mild biphasic systems. *Molecules* 2013;18:7675–85.
- [1097] Kumari N, Olesen JK, Pedersen CM, Bols M. Synthesis of 5-bromomethylfurfural from cellulose as a potential intermediate for biofuel. *Eur J Org Chem* 2011;2011:1266–70.
- [1098] Zhang J, Wu R, Zhang G, Yao C, Zhang Y, Wang Y, et al. Recent studies on chemical engineering fundamentals for fuel pyrolysis and gasification in dual fluidized bed. *Ind Eng Chem Res* 2013;52:6283–302.
- [1099] Luo J, Fang Z, Smith RL. Ultrasound-enhanced conversion of biomass to biofuels. *Prog Energy Combust Sci* 2014;41:56–93.
- [1100] Rinaldi R, Schüth F. Design of solid catalysts for the conversion of biomass. *Energy Environ Sci* 2009;2:610–26.
- [1101] Mittelbach M, Schober S. The influence of antioxidants on the oxidation stability of biodiesel. *J Am Oil Chem Soc* 2003;80:817–23.
- [1102] Tanabe K, Misono M, Ono Y, Hattori H. New solid acids and bases: their catalytic properties. Amsterdam: Elsevier; 1989.
- [1103] Bruggink A, Schoevaart R, Kieboom T. Concepts of nature in organic synthesis: cascade catalysis and multistep conversions in concert. *Org Process Res Dev* 2003;7:622–40.
- [1104] Csicsery SM. Shape-selective catalysis in zeolites. *Zeolites* 1984;4:202–13.
- [1105] Taguchi A, Schüth F. Ordered mesoporous materials in catalysis. *Micropor Mesopor Mat* 2005;77:1–45.
- [1106] Schüth F, Schmidt W. Microporous and mesoporous materials. *Adv Mater* 2002;14:629–38.
- [1107] Wan Y, Yang HF, Zhao DY. Host–guest chemistry in the synthesis of ordered nonsiliceous mesoporous materials. *Acc Chem Res* 2006;39:423–32.
- [1108] Harada T, Ikeda S, Ng YH, Sakata T, Mori H, Torimoto T, et al. Rhodium nanoparticle encapsulated in a porous carbon shell as an active heterogeneous catalyst for aromatic hydrogenation. *Adv Funct Mater* 2008;18:2190–6.
- [1109] Guo F, Fang Z, Zhou T-J. Conversion of fructose and glucose into 5-hydroxymethylfurfural with lignin-derived carbonaceous catalyst under microwave irradiation in dimethyl sulfoxide–ionic liquid mixtures. *Bioresour Technol* 2012;112:313–18.
- [1110] Kubička D, Kikhtyanin O. Opportunities for zeolites in biomass upgrading – Lessons from the refining and petrochemical industry. *Catal Today* 2015;243:10–22.
- [1111] Zi G, Yan Z, Wang Y, Chen Y, Guo Y, Yuan F, et al. Catalytic hydrothermal conversion of carboxymethyl cellulose to value-added chemicals over metal–organic framework MIL-53(Al). *Carbohydr Polym* 2015;115:146–51.
- [1112] Chen J, Liu R, Guo Y, Chen L, Gao H. Selective hydrogenation of biomass-based 5-hydroxymethylfurfural over catalyst of palladium immobilized on amine-functionalized metal–organic frameworks. *ACS Catal* 2015;5:722–33.
- [1113] Chen J, Li K, Chen L, Liu R, Huang X, Ye D. Conversion of fructose into 5-hydroxymethylfurfural catalyzed by recyclable sulfonic acid-functionalized metal–organic frameworks. *Green Chem* 2014;16:2490–9.
- [1114] Schüth F, Sing KSW, Weitkamp J. Handbook of porous materials. Weinheim: Wiley-VCH; 2002.
- [1115] Ogihara Y, Smith RL, Inomata H, Ara K. Direct observation of cellulose dissolution in subcritical and supercritical water over a wide range of water densities (550–1000 kg/m³). *Cellulose* 2005;12:595–606.
- [1116] Okuhara T. Water-tolerant solid acid catalysts. *Chem Rev* 2002;102:3641–66.
- [1117] Lai DM, Deng L, Guo QX, Fu Y. Hydrolysis of biomass by magnetic solid acid. *Energy Environ Sci* 2011;4:3552–7.
- [1118] Gawande MB, Branco PS, Varma RS. Nano-magnetite (Fe_3O_4) as a support for recyclable catalysts in the development of sustainable methodologies. *Chem Soc Rev* 2013;42:3371–93.
- [1119] Shuttleworth PS, De Bruyn M, Parker HL, Hunt AJ, Budarin VL, Matharu AS, et al. Applications of nanoparticles in biomass conversion to chemicals and fuels. *Green Chem* 2014;16:573–84.
- [1120] Luque R, Menéndez JA, Arenillas A, Cot J. Microwave-assisted pyrolysis of biomass feedstocks: the way forward? *Energy Environ Sci* 2012;5:5481–8.
- [1121] Moseley JD, Kappe CO. A critical assessment of the greenness and energy efficiency of microwave-assisted organic synthesis. *Green Chem* 2011;13:794–806.
- [1122] Yin C. Microwave-assisted pyrolysis of biomass for liquid biofuels production. *Bioresour Technol* 2012;120:273–84.
- [1123] Chen WH, Tu YJ, Sheen HK. Disruption of sugarcane bagasse lignocellulosic structure by means of dilute sulfuric acid pretreatment with microwave assisted heating. *Appl Energ* 2011;88:2726–34.
- [1124] Lan W, Liu CF, Yue FX. Ultrasound-assisted dissolution of cellulose in ionic liquid. *Carbohydr Polym* 2011;86:672–7.
- [1125] Fang Z, Smith RL, Qi X. Production of biofuels and chemicals with microwave. Heidelberg Berlin: Springer-Verlag; 2015.
- [1126] Fang Z, Smith RL, Qi X. Production of biofuels and chemicals with ultrasound. Heidelberg Berlin: Springer-Verlag; 2015.
- [1127] Budarin VL, Shuttleworth PS, De Bruyn MD, Farmer TJ, Gronnow MJ, Pfaltzgraff L, et al. The potential of microwave technology for the recovery, synthesis and manufacturing of chemicals from bio-wastes. *Catal Today* 2015;239:80–9.
- [1128] Xie Q, Borges FC, Cheng Y, Wan Y, Li Y, Lin X, et al. Fast microwave-assisted catalytic gasification of biomass for syngas production and tar removal. *Bioresour Technol* 2014;156:291–6.
- [1129] Salema AA, Ani FN. Microwave induced pyrolysis of oil palm biomass. *Bioresour Technol* 2011;102:3388–95.
- [1130] Bu Q, Lei H, Ren S, Wang L, Zhang Q, Tang J, et al. Production of phenols and biofuels by catalytic microwave pyrolysis of lignocellulosic biomass. *Bioresour Technol* 2012;108:274–9.
- [1131] Mushtaq F, Mat R, Ani FN. A review on microwave assisted pyrolysis of coal and biomass for fuel production. *Renew Sust Energy Rev* 2014;39:555–74.
- [1132] Richel A, Laurent P, Watheler B, Watheler JP, Paquot M. Microwave-assisted conversion of carbohydrates. State of the art and outlook. *C R Chimie* 2011;14:224–34.
- [1133] Zhang Z, Zhao ZK. Solid acid and microwave-assisted hydrolysis of cellulose in ionic liquid. *Carbohydr Res* 2009;344:2069–72.
- [1134] Szabolcs Á, Molnár M, Díbó G, Mika IT. Microwave-assisted conversion of carbohydrates to levulinic acid: an essential step in biomass conversion. *Green Chem* 2013;15:439–45.
- [1135] Zhang Z, Zhao ZK. Microwave-assisted conversion of lignocellulosic biomass into furans in ionic liquid. *Bioresour Technol* 2010;101:1111–14.
- [1136] Qi X, Watanabe M, Aida TM, Smith RL. Fast transformation of glucose and di-/polysaccharides into 5-hydroxymethylfurfural by microwave heating in an ionic liquid/catalyst system. *ChemSusChem* 2010;3:1071–7.
- [1137] Yemis O, Mazza G. Acid-catalyzed conversion of xylose, xylan and straw into furfural by microwave-assisted reaction. *Bioresour Technol* 2011;102:7371–8.
- [1138] Koberg M, Cohen M, Ben-Amotz A, Gedanken A. Bio-diesel production directly from the microalgae biomass of *Nannochloropsis* by microwave and ultrasound radiation. *Bioresour Technol* 2011;102:4265–9.
- [1139] Patil PD, Gude VG, Mannarwamy A, Cooke P, Nirmalakhandan N, Lammers P, et al. Comparison of direct transesterification of algal biomass under supercritical methanol and microwave irradiation conditions. *Fuel* 2012;97:822–31.
- [1140] Rocha MVP, de Matos IJBL, de Lima LP, da Silva Figueiredo PM, Lucena IL, Fernandes FAN, et al. Ultrasound-assisted production of biodiesel and ethanol from spent coffee grounds. *Bioresour Technol* 2014;167:343–8.
- [1141] Veljković VB, Avramović JM, Stamenković OS. Biodiesel production by ultrasound-assisted transesterification: state of the art and the perspectives. *Renew Sust Energy Rev* 2012;16:1193–209.
- [1142] Zhang F, Fang Z, Wang YT. Biodiesel production directly from oils with high acid value by magnetic $Na_2SiO_3@Fe_3O_4/C$ catalyst and ultrasound. *Fuel* 2015;150:370–7.
- [1143] Subhadar PB, Gogate PR. Intensification of enzymatic hydrolysis of lignocellulose using ultrasound for efficient bioethanol production: a review. *Ind Eng Chem Res* 2013;52:11816–28.
- [1144] Karimi M, Jenkins B, Stroeve P. Ultrasound irradiation in the production of ethanol from biomass. *Renew Sust Energy Rev* 2014;40:400–21.



Hu Li is a postdoctoral fellow of Agricultural Engineering under supervision of Professor Zhen Fang, Nanjing Agricultural University, China. Dr. Li obtained his PhD [Co-supervisors: Professor Song Yang, Professor Zhen Fang (Chinese Academy of Sciences) and Associate Professor Anders Riisager (Technical University of Denmark)] from Center for R&D of Fine Chemicals, Guizhou University, China. His research focuses on the catalytic conversion of biomass into chemicals and biofuels with functional catalytic materials. Dr. Li has co-authored more than 30 peer-reviewed papers on biomass valorization. He is a guest editor of Current Organic Chemistry and an editorial board member of Frontiers in Applied Chemistry.



Zhen Fang is professor and leader of biomass group, Nanjing Agricultural University. He is the inventor of the “fast hydrolysis” process. He is listed in the “Most Cited Chinese Researchers” in energy for 2014 and 2015 (Elsevier-Scopus). Professor Fang specializes in thermal/biochemical conversion of biomass, nanocatalyst synthesis and its applications, and pretreatment of biomass for biorefineries. He obtained his PhDs from China Agricultural University (Biological and Agricultural Engineering, Beijing) and McGill University (Materials Engineering, Montreal). Professor Fang is Editor-in-Chief, Springer Book Series - *Biofuels and Biorefineries*; associate editor of *Bio-technology for Biofuels*, and is serving on editorial boards of major international journals in energy.



Richard L. Smith, Jr. is professor of Chemical Engineering, Graduate School of Environmental Studies, Research Center of Supercritical Fluid Technology, Tohoku University, Japan. Professor Smith has a strong background in physical properties and separations and obtained his PhD in chemical engineering from the Georgia Institute of Technology (USA). His research focuses on developing green chemical processes especially those that use water and carbon dioxide as the solvents in their supercritical state. He has expertise in physical property measurements and in separation techniques with ionic liquids and published has more than 200 scientific papers, patents, and reports in the field of chemical engineering. Professor Smith is the Asia regional editor for the *Journal of Supercritical Fluids* and has served on editorial boards of major international journals associated with properties and energy.



Song Yang is professor and director of Center for R&D of Fine Chemicals, Guizhou University, China. Professor Yang obtained his PhD from Guizhou University (with Professor Baoan Song). He accepted a post-doctoral position in the University of Texas Southwestern Medical Center at Dallas, USA. His research interests include the rational design of heterogeneous catalysts for biomass conversions, and the discovery of new antiviral agents. Professor Yang is an associate editor of RSC Advances and editorial board members of Current Nanoscience and Current Catalysis. He was appointed as Distinguished Professor of Cheung Kong Scholars Program in 2013, and has authored 12 patents and more than 100 scientific papers in international journals.